MOLECULAR PERTURBATIONS IN SYNUCLEINOPATHY DISORDERS: INSIGHTS FROM PRE-CLINICAL TO HUMAN NEUROPATHOLOGY

by

Paola Cristina Montenegro Larrea

A Dissertation

Submitted to the Faculty of Purdue University

In Partial Fulfillment of the Requirements for the degree of

Doctor of Philosophy

Medicinal Chemistry and Molecular Pharmacology (MCMP)

West Lafayette, Indiana

December 2018

THE PURDUE UNIVERSITY GRADUATE SCHOOL
STATEMENT OF COMMITTEE APPROVAL

Dr. Jean-Christophe Rochet, Chair

    Department of Medicinal Chemistry and Molecular Pharmacology

Dr. Jason Cannon

    Department of Health Sciences

Dr. Claudio Aguilar

    Department of Biology

Dr. Wanqing Liu

    Department of Medicinal Chemistry and Molecular Pharmacology

Approved by:

    Dr. Zhong-Yin Zhang

      Head of the Graduate Program

To my grandparents and my mother, eternal beacons that light my way.

ACKNOWLEDGMENTS

I also thank the outstanding pharmacy professional students, Brayden Strohmier and Sin Ying (Crystal) Ma, who trusted in me as your mentor and helped me with key experiments for my research. Former and current members from the Van Rijn lab: Dr. Richard VanRijn, Dr. Meridith Doyle, Dr. Nook Alongkronrusmee Terrance Chang and Mee Jung Ko, not only because of your guidance and advise, but also for your friendship. Members from the Cannon lab, especially to Dr. Sena Agim, for her invaluable mentorship and contribution to this research project; you were always there for me and became my solid foundation to continue growing as a scientist. Thank you so much!

I would like to thank my mother and brother, my little perfect family, for all the support and unconditional love. Despite the distance, you were always there right next to me. Also, I would like to thank my big family, aunts, uncles and cousins that always encourage me to keep going forward. Last, but not least, I would like to thank to my grandparents, Tito y Fabita, who always believed that I would proudly represent my country, Ecuador, with my hard work and positive attitude. I hope they knew that I did my best, and that I did it for them.

My greatest gratitude to my West Lafayette family, Adriano, Rafa, Christian, Xime, Joselyn, Tania, Varinia, Daniel, Mayarí, Diego, Kathy, Felipe, Marco, Monica, Matt, Shaminie, and Arpita. Each one of you guys helped me to keep my head in the game. You always extended your hand in the most fragile moments, and thanks to you I did not give up.

I would like to express my eternal gratitude to the person that means my reason, my home, my strength, and my example of success. Esteban Orellana, you encouraged me to meet my goals every day and you held me when I needed the most. Thanks to you I am where I am, and I am thrilled to continue this scientific adventure holding your hand. Thanks for all the love and encouragement, thanks for keeping me strong.

TABLE OF CONTENTS

LIST OF TABLES

LIST OF FIGURES

ABSTRACT

Author: Montenegro, Paola, C. PhD
Institution: Purdue University
Degree Received: December 2018
Title: Molecular Perturbations In Synucleinopathy Disorders: Insights From Pre-Clinical To
     Human Neuropathology
Committee Chair: Dr. Chris Rochet

Parkinson's disease (PD) is a devastating neurodegenerative disorder that affects 10 million people worldwide and is characterized by pronounced motor symptoms. Dementia with Lewy Bodies (DLB) involves both cognitive and motor deficits and affects ~1 million people in the United States. To date there is no cure for PD or DLB, and current treatments address only a subset of the symptoms that define these diseases. PD and DLB are 'synucleinopathies', defined as disorders involving the accumulation in patients' brains of Lewy bodies. Lewy bodies are cellular inclusions that consist largely of aggregated species of alpha-synuclein (aSyn), a presynaptic protein that exists as both cytosolic and membrane-bound forms. Pathophysiological findings suggest that aggregated aSyn is involved in neurodegeneration in PD and DLB. However, mechanisms by which aSyn forms neurotoxic aggregates, and neurotoxic processes that distinguish different synucleinopathies such as PD and DLB, are poorly understood. To address these gaps, we have (i) designed a protocol to establish a primary cell culture model that can recapitulate key neuropathological features of PD, (ii) examined effects of expressing aSyn variants in a rat model of PD, and (iii) examined the expression profiles of neuroprotective genes in PD and DLB brain specimens.

In the first part of my thesis, I describe the development of an optimized protocol to prepare primary midbrain and cortical cultures from rat embryonic brains for the study of PD and other synucleinopathies. The establishment of cellular models that simulate specific aspects of neuropathology can enable the characterization of molecular perturbations that lead to dopaminergic (DA) neuronal death. Our primary midbrain mixed culture model provides an outstanding opportunity to explore therapeutic strategies to rescue DA neurons from toxicity elicited by a range of PD-related insults. In addition, our primary cortical mixed cultures can be used to model cortical neuropathology in various CNS disorders including synucleinopathies.

A number of mutations in the gene that codes for aSyn are associated with familial, early-onset forms of PD. A major goal of my thesis research is to characterize neurotoxic effects of a recently discovered familial substitution, A53E. This mutant was chosen based on the rationale that the introduction of a negatively charged residue at position 53 could potentially interfere with aSyn-membrane interactions and favor A53E aggregation, as we described for other familial aSyn mutants. For the first time, we have reproduced the neurotoxicity of A53E seen in human patients by expressing the mutant protein in rat midbrain. Rats injected unilaterally in the substantia nigra (SN) with rAAV encoding A53E and another familial mutant, A53T, but not rAAV encoding WT aSyn or a vector-control ('stuffer') virus, exhibited a significant motor impairment. Immunohistochemical analysis at 14 weeks after the viral injection revealed that brain sections from aSyn-expressing rats exhibit key features reminiscent of neuropathology in human PD, including nigral dopaminergic neuron loss (confirmed by unbiased stereology), striatal terminal depletion, and aSyn inclusion formation. In addition, it was determined that WT aSyn and the A53E and A53T mutants invaded the non-injected substantia nigra, implying that expressed aSyn protein can spread throughout the brain in the rat rAAV-aSyn model. These results yield insights into the molecular basis for the neurotoxicity of A53E and shed light on a potential role for membrane-induced aSyn aggregation in PD pathogenesis in vivo, thus setting the stage for developing therapies to slow neurodegeneration in the brains of familial and idiopathic PD patients.

aSyn neurotoxicity varies with the expression of neuroprotective proteins, and misfolded aSyn affects cellular functions and gene expression. These observations suggest that differential gene expression patterns can inform us about similarities and differences in pathogenic mechanisms of different synucleinopathy disorders. A third phase of my thesis research was aimed at determining the expression levels of a panel of candidate neuroprotective genes in post-mortem brain samples from DLB and PD patients and age-matched controls (5 individuals in each group). mRNAs encoding the following proteins were quantified via qRT-PCR in homogenates prepared from the frontal cortex and the BA24 region encompassing the cingulate gyrus: DJ-1, a protein with antioxidant and chaperone activities; PGC1α, a master regulator of mitochondrial biogenesis and oxidative metabolism; MsrA, an antioxidant enzyme responsible for repairing oxidatively damaged proteins; and ATP13A2, a lysosomal protein involved in autophagy. In

addition to yielding new insights into differential gene expression patterns in cortex versus cingulate gyrus, the data revealed differences in mRNA expression levels in DLB versus non-DLB cortical tissue. Although levels of all four neuroprotective mRNAs were increased (or showed a trend towards being increased) in DLB cortex, Western blot analysis revealed that only the DJ-1 and PGC1α proteins showed a trend towards being up-regulated, whereas levels of ATP13A2 and MsrA were unchanged. These findings suggest that there is a failure to induce cellular antioxidant responses and lysosomal autophagy at the protein level in DLB cortex, and in turn this failure could contribute to neuropathology. Interestingly, analysis of the same panel of neuroprotective genes in PD cortical samples did not show significant differences in mRNA or protein levels compared to control samples, suggesting that different neuroprotective mechanisms are induced in DLB versus PD cortex. These studies shed light on brain-region specific changes in gene expression associated with different synucleinopathy disorders, and they set the stage for developing new diagnostic tests and therapeutic strategies.

CHAPTER 1.   INTRODUCTION

1.1. Synucleinopathy disorders overview

The term 'synucleinopathies' refers to a collection of neurological disorders characterized by the presence in patients' brains of cellular inclusions that consist largely of insoluble aggregated species of the presynaptic protein α-synuclein (aSyn)[1]. A defining feature of some synucleinopathy disorders, including Parkinson's disease (PD) and dementia with Lewy bodies (DLB), is the presence of neuronal aSyn-rich inclusions referred to as Lewy bodies. The brains of PD and DLB patients also typically contain Lewy neurites, defined as dystrophic processes enriched with aggregated aSyn[2]. In contrast, aSyn-rich inclusions are located in oligodendrocytes (and are referred to as 'glial cytoplasmic inclusions' (GCIs)) in the brains of patients with multiple system atrophy (MSA)[3]. Contributing to the overall spectrum of synucleinopathies, similar Lewy pathology has been found in several other diseases such as Alzheimer disease with Lewy bodies, neurodegeneration with brain iron accumulation type I, and pure autonomic failure[4]. Although all synucleinopathy disorders (by definition) have a shared property of abnormal aSyn accumulation, each of these syndromes has distinct clinical, etiological, and pathological features. Characteristic features of PD and DLB are outlined in the next section.

1.1.1. Parkinson's disease (PD)

PD is a multisystem CNS neurodegenerative disorder characterized by a progressive motor impairment and non-motor symptoms[5]. Worldwide 10 million people suffer from PD, a devastating neurodegenerative disorder that occurs with early or late onset, affecting patients between 40 and 80 years old. Described by James Parkinson as "the shaking palsy" over 200 years ago, to date there is no cure for PD. Important advances in diagnostic tests and symptomatic treatments have helped patients and their families improve their quality of life; nevertheless, none of these strategies can stop the disease. The complexity of PD etiology and pathophysiology makes it difficult to understand the exact origin of this disorder. Environmental interactions are considered risk factors for the development of PD[6]. It has been reported that individuals exposed throughout their lives to different pesticides or herbicides (e.g. rotenone and paraquat), traumatic brain

injury, nicotine, caffeine, opioid metabolites (i.e. 1-methyl-4-phenyl-1,2,3,6-tetrahydropyridine (MPTP)), methamphetamine and neurotoxic food derivatives (e.g. PhIP) developed PD at their elderly age[5–8]. All these neurotoxic compounds have been proven to alter vital cellular mechanisms such as mitochondrial electron transport[9] and proteasomal clearance[10], and these disruptions increase cellular oxidative stress, considered one of the main PD triggering factors[11] as outlined in greater detail below.

1.1.1.1. Symptoms

PD diagnosis is based mainly on the detection of a panel of motor symptoms, including bradykinesia (slowness of movement), shuffling when walking, loss of clear speaking, little or no facial expression, muscular rigidity, and resting tremor[12,13]. Concomitant with evident motor impairment, non-motor symptoms can compromise multiple body functions such as sleep-wake cycle regulation, cognitive behavior (e.g. memory retrieval, executive function, mood control), urogenital function, and olfactory funtion[5]. Multiple components of this complex symptomatology can be prevalent over the course of the patient's life, with progressively increasing disability and pain. By the time lateralized motor symptoms manifest in the patient, extensive damage is likely to have already occurred in one side of the brain. Therefore, clinical researchers are exploring the benefits of monitoring non-motor symptoms in families affected by PD in order to identify predictive markers that could provide an early diagnosis, thus potentially enabling the implementation of preventive measures[14].

1.1.1.2. Neuropathology

Dopaminergic (DA) neurons, localized in specific clusters extending from the brain stem into the forebrain, are mainly involved in modulating motor activity[15]. Progressive depletion of DA neurons in the *substantia nigra* (SN) causes the characteristic motor deficits found in PD[5]. Surviving nigral DA neurons, as well as neurons in other brain structures, develop Lewy bodies and Lewy neurites. The hallmark neuropathology of PD consists of a combination of DA neuronal loss together with the presence of Lewy pathology. At first clinical detection of motor symptoms, 80% of striatal DA nerve terminals have been depleted and 50% to 60% of nigral DA neurons have already been

lost[16]. However, studies in a non-human primate PD model suggest that a lesser degree of nigrostriatal degeneration is necessary to trigger motor deterioration[17]. DA neurons have been found to die in PD brains in a ventrolateral manner, first by retracting their axonal extensions from irrigated striatal areas and later decaying from surrounding regions to the center of the SN via a phenomenon called "the dying back process"[5]. Braak and colleagues[18] have hypothesized that Lewy neuropathology also first occurs before the manifestation of motor symptoms and spreads from the dorsal motor nucleus along a continuous pathological pathway towards cortical areas. Although conditions that trigger PD neuropathology remain uncertain, cumulative evidence strongly suggests that aSyn misfolding and aggregation play a major role in disease development[19].

PD cellular pathomechanisms include oxidative stress[11], mitochondrial dysfunction[20], and impairments in protein degradation mediated by the ubiquitin-proteasome system[21], events that play an important role in DA neurotoxicity[12]. Mitochondrial complex I deficits lead to oxidative stress, and it has been identified in peripheral cells and in post-mortem brain tissue of PD patients[22]. Two agents linked epidemiologically to elevated PD risk, rotenone and paraquat, are known to inhibit complex I (rotenone) or elicit oxidative stress (paraquat)[7]. Lysosomal dysfunction triggers a build-up of defective mitochondria by disrupting mitophagy, and mitochondrial defects result in perturbation of the endo-lysosomal pathway, leading to a vicious cycle underlying the cellular pathophysiology found in PD brain[23,24]. Inhibition of proteasome activity triggers the accumulation and aggregation of aSyn, contributing to Lewy body formations and neurotoxicity[21].

1.1.1.3. Diagnosis and Treatments

Thanks to neuropathological findings, it has been possible to standardize powerful imaging tests for the diagnostic of PD. For instance, presynaptic dopaminergic terminal functionality can be determined by positron emission tomography (PET) scans. PET scans of striatal brain region of PD patients reports a reduction in the signal of the radiotracer ^{18}F-labeled L-Dopa (^{18}F-DOPA) that binds to aromatic-L-amino-acid decarboxylase (AADC), dopamine transporter (DAT) and vesicular monamine

transporter (VMAT2)[25]. Besides ^{18}F-DOPA, more sensitive radiotracers such as ^{11}C-CFT (2β-carbomethoxy-3β-(4-fluorophenyl)tropane) that binds to DAT, are being investigated in order to improve PD PET imaging diagnostic[26].

Other techniques such as magnetic resonance imaging (MRI) or computed tomography (CT) scans can measure physical changes in the brain related to cognitive or motor deterioration[27]. Despite the accuracy of these tests, they are not practical for PD diagnosis prior to the onset of motor symptoms, an essential requirement for administering preventative measures. Hence, it is imperative to continue investigating mechanisms leading to the onset of neurodegeneration in order to have a sound basis for developing pre-symptomatic intervention strategies.

Multiple clinical trials and current FDA-approved drug treatments are focused on ameliorating the symptoms of PD[28–30]. In order to restore decreased levels of dopamine in the brain caused by the loss of DA neurons, the gold standard treatment is the administration of a mixture of levo-DOPA and carbidopa which effectively reduces the motor symptoms[31]. L-DOPA is a natural dopamine precursor that (in contrast to dopamine) can cross the blood brain barrier (BBB), but it can be metabolized to dopamine by aromatic-L-amino-acid decarboxylase (AACD) before reaching the brain[32]. AACD is an active enzyme in the brain, liver and intestine tract that can be inhibited by carbidopa, ensuring that L-DOPA is not converted to dopamine in the periphery[33]. This combinatory drug therapy reduced L-DOPA dose required for clinical response[33]. However, chronic L-DOPA/carbidopa treatment results in motor complications associated with a condition known as levodopa-induced dyskinesia, which includes exaggerated uncontrolled movements and neuropsychiatric side-effects[34]. Numerous clinical advances have been achieved in the dosage control of L-DOPA such that nowadays motor symptoms have been diminished significantly[31]. Developing treatments for non-motor symptoms is now the main focus in PD clinical research.

Recent strategies aimed at alleviating DA neuronal death include the use of drugs (i.e. isradipine[35], exenatide[36], nilotinib[37], inosine[38]) that are expected to work at the molecular

level via a range of protective mechanisms, including calcium channels antagonism, neurotrophic factors activation, tyrosine kinase-activation of autophagy and antioxidant activities enhancement. Gene therapy strategies may be effective in patients that suffer from aggressive familial PD, where the goal is to inhibit the expression of mutated genes (i.e. genes encoding mutant forms of GBA[39] or LRRK2[40]) that trigger PD pathology. Finally, intensive research efforts are focused on assessing the therapeutic potential of immunotherapy involving the use of vaccines and antibody infusions that target aSyn[41].

Surgical therapies such as deep brain stimulation (DBS) have led to effective symptomatic relief after the administration of CA-LE. DBS is an invasive procedure where electrodes are positioned in the brain nuclei (mainly in the ventral intermediate nucleus of the thalamus, subthalamic nucleus, or internal segment of the globus pallidus) in order to send electrical impulses that stimulate defective connections, reducing bradykinesia, rigidity, tremor, and gait difficulties[42].

The treatment options outlined above are highly varied due to the fact that not all PD patients have a positive response to a given form of therapy. PD medical research is changing gears in the search for treatments that can alleviate neurodegeneration (thus slowing disease progress) through the discovery of new druggable targets.

1.1.2. Dementia with Lewy Bodies (DLB)

DLB is a late-onset progressive dementia that commonly overlaps with clinical and neuropathological characteristics of Alzheimer's disease (AD)[1], leading to incorrect diagnosis that is only corrected after a post-mortem brain analysis[43]. DLB affects an estimated 1.4 million people in the United States and is particularly prevalent in people over 50 years old[44]. It is the second most common form of dementia after AD[45]. In a PD versus DLB incidence analysis it was determined that DLB occurred in 4 times fewer cases than PD, and that men were more frequently affected than women[46]. Despite the low incidence of DLB compared to PD, the number of research studies on DLB has increased in recent years because of the disease's high mortality risk in comparison with

other synucleinopathies[47]. Currently, there is no cure for DLB, and very little is known about patho-mechanisms behind the disease.

1.1.2.1. Symptoms

The abnormal accumulation of Lewy bodies in cortical regions of the brain in DLB patients is associated with cognitive impairment that includes declines in thinking, reasoning, and independent functioning, ultimately leading to interference with normal activities at home and in the workplaces[47]. DLB Lewy bodies can also spread into the midbrain SN, leading to a parkinsonism phenotype that includes hunched posture, muscular rigidity, and shuffling gait. As the disease progresses, visual hallucinations, delusions, sleep disruptions, and memory loss become more frequent[48]. A differential diagnosis of DLB and AD generally relies on the timing of memory loss onset, which manifests earlier in AD patients than in DLB patients when present. Additionally, DLB patients eventually develop motor deficits that are rare in AD patients[49]. Overall, the nature and temporal manifestation of symptoms distinguish DLB from other synucleinopathies and dementias.

1.1.2.2. Neuropathology

In DLB, as in other synucleinopathies, aSyn misfolding and fibrillization play a central pathogenic role[50]. aSyn is the major component of DLB Lewy bodies and Lewy neurites, defined as aggregated protein deposits in the cytoplasm and processes of neurons. Lewy bodies in DLB brains are widely spread throughout cortical regions of the brain and in late stages of the disease can be found in the brain stem and SN[1]. Cortical Lewy body lesions are associated with neocortical cholinergic deficits, resulting in a lowering of choline acetyltransferase levels in the temporal and parietal cortex. In turn, this cholinergic deficit is thought to be related to the characteristic cognitive decay in DLB patients[51]. Recent histological analysis suggests that alterations in lysosomal activity lead to a failure to degrade toxic aSyn species in DLB brains[52]. In several cases where DLB overlaps with AD, neuropathological features characteristic of AD (including amyloid plaques and neurofibrillary tangles) can be found along with Lewy pathology in patients' brains[43].

1.1.2.3. Diagnosis and Treatments

DLB diagnosis can be challenging because the symptoms are commonly confused with PD with dementia and AD[47]. Clinically, DLB is tentatively diagnosed when dementia symptoms appear within a year before the beginning of motor deficits. On the other hand, PD with dementia is clinically diagnosed when signs of cognitive decay occur one year after the parkinsonian symptoms[46,47]. In cases of DLB, imaging techniques are useful only when the dementia is accompanied with motor symptoms associated with DA neuronal death and a reduction of dopamine transporter uptake in the basal ganglia – a deficit that can be demonstrated by SPECT and PET scans[47]. MRI imaging has been helpful in analyzing the extent of pathology in the hippocampus, temporal lobe and putamen[47]. To date there is no conclusive test that can be used to diagnose DLB, and the disease is only confirmed upon post-mortem analysis of patients' brains. Finding an accurate DLB marker is imperative because some anti-parkinsonian or neuroleptic medications can exacerbate DLB symptoms[53]. Recently, it has been hypothesized that phosphorylated aSyn deposits in skin autonomic nerves could serve as diagnostic markers for DLB and other synucleinopathies[54].

Because DLB is a severe dementia, patients with this disorder need specialized, engaged, and informed care providers to help address major challenges associated with patients' cognitive dysfunction. Because DLB patients experience delirium and an inability to communicate, they are unable to explain their impairments. In cases of misdiagnosis, patients with DLB can be treated with dopaminergic therapies that affect cognitive functions and behaviour[53]. To avoid these side-effects, motor symptoms associated with DLB can be treated with non-pharmacological interventions that include exercise and cognitive training[55]. Pharmacological approaches are commonly used to treat cognitive symptoms, although these also have a risk of side-effects. Drugs such as rivastigmine[56], donepezil[57] and other cholinesterase inhibitors are used to improve global cognitive function, with limited success.

1.2. Pathological Similarities and differences between DLB and PD

Lewy neuropathology in DLB and PD is almost undistinguishable in late stages of the diseases, which in both cases reaches cortical and nigral areas in the brain[58]. The difference between these two brain diseases stands in the neuronal progression of Lewy pathology[59]. Studies of the progression of Lewy pathology suggest that in DLB the aSyn-rich structures extend from the amygdala[59], while PD Lewy pathology was defined by the Braak staging that define their origin at the lower brainstem[18]. However, the olfactory bulb is, mostly in DLB than PD, a region of interest in both diseases due to its proximity to limbic and neocortical regions which in are associated with cognitive impairment[60]. For this reason, it has been establish a staging theory for Lewy pathology progression for DLB that starts in the olfactory bulb and continues into the limbic system and neocortical areas, which differs from the PD Braak staging which does not accurately characterized all DLB cases[59,61].

Large phenotypical studies have determined a great variability among synucleinopathies. PD showed four main clinical phenotypes that increase in severity and Lewy pathology progression with age, meanwhile DLB showed three phenopical forms that overlap AD pahotlogy: pure DLB, DLB with AD and AD with amygdala Lewy bodies[58]. The pathological characterization of these diseases will help to establish a differential diagnosis between DLB, PD with dementia and AD. Senile plaques, sparse pathology and spongiform chamges, common severe AD pathology, can be present in DLB cases exarcerbating Lewy pathology and speeding its progression[47,59]

1.3. Alpha Synuclein (aSyn) presynaptic protein

The aSyn sequence was first reported at the end of the 1980's, when the protein was isolated from the electric organ of the Pacific electric ray (*Torpedo californica*). In this initial report, it was also determined that aSyn was a neuronal protein localized at presynaptic nerve terminals[62]. aSyn is a 140-residue protein encoded by the gene SNCA (acronym for SyNuClein, Alpha), and its molecular function is incompletely understood. The amino terminal sequence of aSyn is characterized by imperfect 6-residue repeats with a consensus sequence of KTKEGV, followed by a central hydrophobic region and a negatively charged highly acidic carboxy-terminal domain[63] (Fig. 1). aSyn is highly expressed in the nervous

system, specifically in presynaptic terminals, in close proximity to or in association with synaptic vesicles[1,63]; therefore, its function may be related to maintenance of the supply of synaptic vesicles and regulation of dopamine release in presynaptic sites[1]. aSyn is a natively unfolded monomeric protein in solution, but it can bind to lipid membranes through its amino-terminal portion, which adopts an alpha-helical structure upon associating with phospholipids[64–66]. Evidence suggests that aSyn may be a lipid-binding protein that regulates endocytosis and vesicle transport[63]. Apparently, unstructured monomers and helical oligomers of aSyn are present at equilibrium in a healthy neuron[67]. Emerging evidence determined that native cell-derived aSyn shows physiological α-helical tetramer structures when its bound to a membrane[68]. Physiologically functional multimeric membrane-bound aSyn promotes the assembly of the soluble NSF attachment protein receptor (SNARE) complex at the presynaptic plasma membrane[69]. Any destabilization of aSyn folded tetramer or membrane binding status originates aSyn misfolding and aggregation in PD[68,70]

Figure 1.1. Amino-acid sequence of aSyn. The blue-underlined region (residues 1-85) encompasses a series of imperfect six-residue repeats (KTK[E/Q]GV) shown in blue. The hydrophobic NAC segment (residues 61-95) is underlined in orange, and the unfolded C-terminal region (residues 96-140) is underlined in pink. Red letters indicate sites of familial substitutions (A30P, E46K, H50Q, G51D, A53E, A53T) [92]

1.3.1. aSyn in PD and DLB neuropathology

PD and DLB are related synucleinopathies characterized by aSyn aggregation in the form of Lewy bodies and Lewy neurites in neuronal systems[4]. Patients diagnosed with PD can develop mild or severe dementia, while DLB patients will reveal motor impairments with the progression of the disease. This evidence suggests that the sequential symptomatology that differentiates these two diseases may be related to how aSyn is being metabolized in the patients' brains[71]. Despite the fact that aSyn-rich inclusions can be found in the midbrains of DLB patients, these dense structures differ from inclusions found in PD brains in the way that the protein is internally distributed. 'Brain stem' Lewy

bodies are composed of a dense eosinophilic core of filamentous and granular material and a pale peripheral spherical halo. In contrast, 'cortical' Lewy bodies are less spherical structures without a distinctive core or halo, commonly reported as diffuse Lewy bodies[1].

Since the discovery of Lewy bodies by Dr. Friedrich Lewy and Dr. Alois Alzheimer, these inclusions comprising fibrillar structures have been characterized in detail. A high level of immunoreactivity of aSyn has been detected in Lewy bodies from PD and DLB, suggesting that the molecular characteristics of this pathology are similar in both diseases[72]. Besides being enriched with aggregated aSyn, Lewy bodies stain for more than 30 proteins including ubiquitin and subunits of the keratin family[72].

The progressive neurodegeneration throughout the brains of PD patients has led investigators to propose that some kind of pathogen composed of misfolded fragments of aSyn infects peripheral locations (i.e. nasal or gastric routes) from where the neuropathology spreads to the brain[73]. Consistent with this hypothesis, it has been shown that aSyn uses a prion-like mechanism to propagate from cell to cell through the extracellular space[74]. Several questions related to aSyn prion-like transmission remain unsolved, such as i) whether truncated aSyn is able to modify endogenous protein species so they become toxic, ii) which are the intracellular transfer routes that aSyn uses, and iii) why specific areas in the brain are more vulnerable to the invasion of aggregated aSyn.

Overall clinical and neurological features of PD and DLB are similar, both of them characterized by parkinsonisms, cognitive impairment and intraneuronal aSyn inclusions[71]. The lack of consistent diagnostic markers commonly overlap PD and DLB with Alzheimer's disease[1]. Slight differences such as the timing of the onset of dementia and in some cases the absent of it[71], and the main localization of Lewy bodies in PD vs DLB brains[1] suggest that there might be differential mechanisms that rule each of these synucleinopathies. Currently there is a lack of understanding of the different cellular processes that lead to PD versus DLB pathology.

1.3.2. Molecular phenomena involved in aSyn aggregation

The binding of aSyn to lipid membranes involves a structural transition of the N-terminal portion of the protein to an α-helical conformation[70]. In vitro studies from our group have

shown that structural perturbations in aSyn can disrupt the interaction between the central hydrophobic region of the protein and phospholipids, thus promoting an 'exposed' conformation that favors Syn aggregation at membrane surfaces and vesicle permeabilization[75,76] (Fig. 2). Additional evidence from studies involving the expression in primary midbrain cultures of aSyn mutants with different propensities to undergo lipid-induced self-assembly suggests that aSyn aggregation at membrane surfaces plays a central role in neurotoxicity[75]. Another group has shown that oligomers formed during aSyn aggregation in the absence of membranes elicit enhanced neurotoxicity, potentially via a mechanism involving membrane disruption[77].
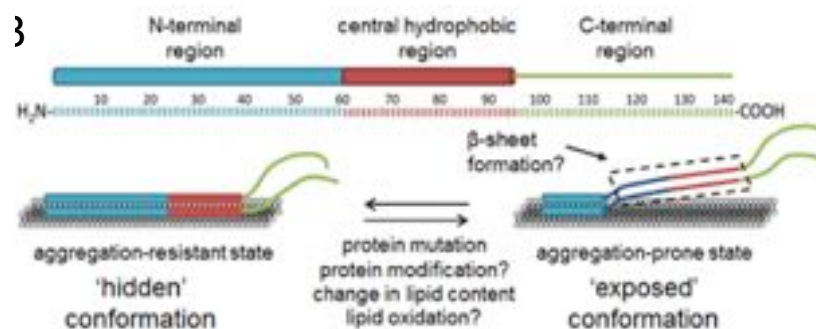
Figure 1.2. aSyn adopts interconverting α-helical conformations upon binding to phospholipid membranes. Model illustrating interconversion between two conformations of membrane-bound aSyn. (Top) Schematic of membrane-bound aSyn showing extension of the α-helix through the intrinsically aggregation-prone NAC domain. The N-domain (blue), NAC domain (red), and C-domain (green) are depicted above a map of the polypeptide chain. (Bottom) Various perturbations induce a shift from the 'hidden' conformation to the 'exposed' conformation. (Adapted from[78])

Post-translational modifications of the aSyn protein, including phosphorylation, ubiquitination, cross linking, truncations and nitration, seem to favor aSyn aggregation in PD[79,80]. In healthy conditions, only 4% of total aSyn is found to be phosphorylated at residue serine 129 (pSer129). In PD brain, 90% of aSyn is phosphorylated at Ser129, and thus pSer129-aSyn is accepted as a Lewy body marker in the synucleinopathy field[81]. Moreover, there are reports that pSer129 inhibits the membrane binding ability of aSyn, and this inhibitory effect could lead to changes in the protein's ability to aggregate at membrane surfaces[80].

1.3.3. Role of impaired protein clearance mechanisms in aSyn accumulation

Defects in lysosomal clearance mechanisms can contribute to the pathogenic accumulation of aSyn. As an example, the GBA gene codes for glucocerebrosidase (GCase), a lysosomal enzyme that breaks down abnormal glycolipid and protein deposits. Mutations in the GBA gene are associated with an increased risk of developing PD[82]. Pharmacological inhibition of GCase activity promotes accumulation of aSyn, demonstrating an interaction between defective lysosomal protein degradation and aSyn aggregation[83]. Furthermore, the reduced GCase activity can lead to an accumulation of its direct substrate glucosylceramide, which interacts with aSyn and promotes its oligomerization in a pathogenic loop[84].

The autophagy lysosomal pathway (ALP) and ubiquitin proteasome system (UPS) are preferred degradation mechanisms that modulate aSyn levels in the cell[85,86]. Failure in these proteolytic systems can lead to the accumulation aSyn oligomers.

The UPS is involved in the degradation of short-lived soluble proteins, whereas the ALP plays a key role in the elimination of bulky, longer-lived macromolecules. Together, the UPS and ALP contribute to an equilibrium between the synthesis, degradation, and secretion of proteins[86]. The presence of ubiquitinated aSyn inclusions in PD brains is an indication of UPS dysfunction, whereas the presence of dense proteinaceous structures reflects ALP impairment. Reports indicate that the expression of mutant aSyn and overexpression of WT aSyn inhibit proteasomal function by binding to both the 20S and 26S subunits[87,88]. Autophagic lysosomal function is disrupted by the accumulation of aSyn, which alters the balance between macroautophagy and chaperone-mediated autophagy (CMA)[89]. Macroautophagy involves the formation of a double membrane bound organelle, autophagosomes, plus the fusion with lysosomes to ensamble an autolysosome. Autolysosomes sequester organelles and cytoplasmic components in order to degrade them via lysosomal hydrolases[90]. CMA involves the selective targeting of proteins through specific sequence motifs to be lysosomal degraded with the assistance of the chaperone protein Hsc70[91]. aSyn impair autophagic pathways by different mechanisms that include (i) the disruption of autophagosomes precursors, omegasomes, by inhibition of Rab1a, (ii) inhibition of autophagosome-lysosome fusion, (iii) the

disruption of interaction between high mobility group box 1 (HMGB1) protein and beclin-1 that plays a role in autophagic induction, (iv) disfavoring the initiation of autophagy by the inhibition of JNK1, and (v) disruption the trafficking of lysosomal hydrolases imparing lysosomal degradation[92]. In all these cases the result is the accumulation of autophagic vacuoles with damaged molecules that can lead to neuronal degradation[86].

1.3.4. Role of aSyn in mitochondrial dysfunction and oxidative stress

aSyn has been studied extensively in terms of its potential subcellular pathogenic mechanisms that govern neurotoxicity in PD and other synucleinopathies. aSyn early oligomers may be involved in modulation of mitochondrial function in axons and presynaptic terminals[93]. Studies involving experimental models and the analysis of human PD brain specimens have shown that phenomena related to mitochondrial dysfunction such as the disruption of mitochondrial dynamics, bioenergetics defects, and complex I inhibition, all of which can lead to an increase in reactive oxygen species (ROS), are relevant pathomechanisms in PD and other synucleinopathies[94–97]. Direct interaction of overexpressed aSyn and mitochondria elicits a change in mitochondrial membrane curvature, leading to an increase in mitochondrial fragmentation that in turn provokes a deterioration of ER-mitochondria interactions, malfunction of the respiratory chain, and oxidative stress[20,98–100]. Accumulation of ROS induces oxidative damage of mtDNA, proteins, and lipids. β-sheet enriched aSyn oligomers and fibrils induce an increase in ROS levels and activate lipid peroxidation reactions, leading to aSyn modification and a further accumulation of toxic aSyn oligomers[101,102]. At the same time, cytosolic and mitochondrial Ca^{2+} and ROS levels are elevated as a result of oligomeric aSyn increasing the mitochondrial permeability transition pore (PTP), a perturbation that eventually results in increased mitochondrial swelling and neuronal death[20]. A recent study found that PTP was promoted by the selective oxidation of ATP synthase induced by oligomeric aSyn interaction. Interestingly, the study reported that the inhibition of aSyn oligomerzation prevented the induction of toxic PTP, determining that oligomeric aSyn alters cellular function in PD[103].

1.3.5. Familial PD-associated aSyn mutations implicated in protein aggregation

The association of SNCA gene mutations with familial PD[104] and the discovery of aSyn as a major component of Lewy bodies[105] are crucial observations supporting a role for aSyn in the etiology of PD. The protein has been found to be mutated in rare forms of familial autosomal-dominant PD[1,2]. Missense mutations (e.g. A30P, E46K, H50Q, G51D, A53E and A53T substitutions) (Fig. 1) and multiplications of the SNCA gene (triplication or duplication) cause a gain of toxic function that apparently promotes synucleinopathy pathology by favoring aSyn self-assembly and neurotoxicity[106,107]. It has been reported that some aSyn substitutions can cause structural disturbances of the protein, promoting the formation of high molecular weight oligomers that lead to the pathogenic fibrillar state by causing a decrease in the monomer:tetramer ratio[67]. Studies in our laboratory revealed that aSyn variants with the following three properties trigger dopaminergic (DA) cell death in a primary cell culture model of PD: i) a high propensity to adopt an 'exposed' membrane-bound conformation, with a short, lipid-bound N-terminal segment and unbound central and C-terminal segments; ii) an enhanced ability to undergo membrane-induced aggregation; and iii) a high propensity to elicit vesicle permeabilization[75,76].

1.4. Familial PD related genes (other than the aSyn gene): autosomal dominant and autosomal recessive mutations

Genetic cases account for just 10% of all PD patients, and they are commonly characterized by early age of onset and aggressive neuropathology[108]. Important progress in the investigation of sporadic PD has been guided by the identification of functional properties of proteins associated with PD genetic cases[5]. Besides the SNCA gene, several other genes with monogenic inheritance have been linked to familial PD. Defective proteins coded by PD-associated genes are mainly involved in the UPS and ALP systems, mitigation of oxidative stress, and mitochondrial function[12]. Familial pedigree analyses have led to the identification of gene mutations that vary from autosomal dominant (only one mutated allele is sufficient to cause the disease) to autosomal recessive (both alleles must be mutated in order to manifest the effect), located in 28 distinct chromosomal regions comprising at least 18 genes[108,109]. These genes have been identified by genetic linkage based on known

function of the coded protein or genome wide associations performed in large populations[108]. The complexity of PD genetics is not only a result of the existence of multiple genes associated with the disease, but also other complicating factors such as reduced or incomplete penetrance (skip generations) or variable expressivity (mild to severe phenotypes)[108]. Genes from only 6 chromosomal loci have been conclusively linked to familial PD, and they are located at various PARK loci[108]. Table 1 summarizes the genes that have been studied extensively because of their strong linkage to PD.

Table 1.1 Genes related with familial PD neuropathology			
GENE	MUTATION EFFECT	KEY ROLES	INHERITANCE
PARK2 / PARKIN	Loss of function	Mitophagy, protein ubiquitination, mitochondrial stability, antioxidant	Recessive
PARK5 / UCHL1	Loss of function	Autophagy, protein ubiquitination	Dominant
PARK6 / PINK1	Loss of function	Mitophagy, mitochondrial stability, antioxidant	Recessive
PARK7/DJ-1	Loss of function	Antioxidant, molecular chaperone	Recessive
PARK8 / LRRK2	Gain of function	Autophagy, protein phosphorylation	Dominant
PARK9 / ATP13A2	Loss of function	Lysosome activity regulation	Recessive

1.4.1. Genes associated with familial PD with autosomal-dominant inheritance.

The second most common gene associated with familial PD after SNCA is Leucine-rich repeat kinase 2 or LRRK2[40]. Patients carrying autosomal dominant mutations in LRRK2 manifest mild or late-onset PD with slow progression and no dementia. LRRK2 is a large 2527-residue protein widely expressed in the brain in association with the endoplasmic reticulum of DA neurons. The exact function of LRRK2 is unclear, but mutations in the LRRK2 gene have been shown to lead to perturbations in autophagy, cytoskeletal dynamics, kinase cascades, mitochondrial function, and vesicular trafficking[40]. Up to ~300 exonic variants of the LRRK2 gene have been identified, of which only a few are known to be pathogenic. The most common pathogenic mutation is the G2019S substitution, which seems to increase the LRRK2 kinase activity[110].

Another gene with high susceptibility for PD development is ubiquitin carboxy-terminal hydrolase L1 (UCHL1)[111]. UCHL1 is an enzyme expressed exclusively in neurons of the SN and is present in Lewy bodies[112,113]. The biological role of UCHL1 is related to modulation of ubiquitin-dependent proteolysis by recycling ubiquitin subunits through hydrolysis of peptide-ubiquitin bonds and processing ubiquitin precursors[114]. Mutations in UCHL1 are linked to defects in the ubiquitin proteolysis system[115]. The I93M substitution in UCHL1 leads to degeneration of DA neurons[116]. Further studies showed that mutated UCHL1 failed to ubiquitinate misfolded proteins which is associated to the cytoplasmic aggregation of misfolded aSyn in PD[117]. In addition I93M mutated UCHL1 interacts abnormally with members of CMA leading to autophagic activity inhibition which results in an increase of misfolded aSyn[118]. These observations support the role of UCHL1 in PD etiology and suggest that strategies aimed at enhancing UCHL1 function could be of therapeutic benefit in PD[111].

1.4.2. Genes associated with familial PD with autosomal-recessive inheritance.

Recessive mutations in the genes encoding the E3 ubiquitin ligase Parkin and the mitochondrial serine/threonine kinase PINK1, including point mutations, exon rearrangements, deletions, and duplications, are associated with juvenile- or early-onset forms of familial PD[108]. Parkin and PINK1 are functionally associated with mitochondrial autophagy (mitophagy)[119]. In health conditions, PINK1 protein, that is located in the mitochondria, is maintained at low levels in order to prevent mitophagy of healthy mitochondria. When mitochondria gets damaged by inhibition of complex I, loss of membrane potential, accumulation of misfolded proteins or mutated mitochondrial DNA, outer mitochondrial membrane gets depolarized activating the translocase of the outter membrane complex (TOM complex) that recruits PINK1 promoting its accumulation in the mitochondrial membrane[120]. Pink 1 phosphorilates ubiquitin and translocate cytosolic Parkin into the mitochrondria to activate its E3 ubiquitin ligase activity that in turn ubiquitinate outter mitochrondrial membrane proteins, targeting them for selective mitophagy of the damaged mitochrondria[121]. Parkin-mediated mitophagy requires the recruitment of downstream cytosolic autophagic factors such as p62 adaptor that will recruit autophagosomes to start uniquitinated mitochondrial proteins degradation[122]. On

the other side, PINK1 can independently recruit other autophagic factors, like optineurin and NDP52, to start parkin-independent autophagy of damaged mitochondria, which defines a model where PINK1 signals the beginning of autophagy of damaged mitochondria, and parkin amplifies the signal[123]. Mutations in PINK1 and parkin genes prevent the detection and clearance of defective mitochondria, thus promoting neuronal death[119].

1.4.3. DJ-1: an antioxidant chaperone protein

DJ-1 is a homodimer of 189-residue subunits expressed in almost all cells in the human body. A conserved C106 residue in DJ-1 sequence is considered as an oxidative stress sensor, which gets oxidized to cysteine sulfonic acid in response to oxidative stress[124]. The redox sensitivity of DJ-1 is considered an antioxidant property that activates a signaling cascade in response to mitochrondrial superoxides generation[125]. Studies performed in dopaminergic neurons derived from PD patients, carrying mutated DJ-1, identified a pathological cascade originated from mitochondrial oxidative stress leading to an accumulation of oxidized dopamine, reduced GCase activity, lysosomal dysfunction and eventual accumulation of aSyn[126]. Mitochondrial oxidative stress is exacerbated by elevated Ca^{2+} influx promoting the enzymatic signaling for the formation of free reactive oxygen species (ROS)[127]. Knockout DJ-1 mice showed down-regulated levels of uncoupling proteins UCP4 and UCP5, two proteins that regulate intracellular calcium movement[128], suggesting the role of DJ-1 in attenuating mitochondrial oxidative stress[125].

DJ-1 protein is also characterized as a glyoxalase, an enzyme that converts glyoxal (GO) or methylglyocal (MGO) to glycolic or lactic acid, respectively, in absence of glutathione[129]. GO and MGO are bioproducts from glucose oxidation, lipid peroxidation and DNA oxidation[130]. The interaction of GO and MGO with amino groups of proteins form reactive carbonyl stress compounds known as advanced glycation end products (AGEs), which have been related with the pathogenesis of PD[131]. It has been observed that AGEs are distributed in Lewy bodies, and induced apoptosis of cells mediated by oxidative stress[131]. DJ-1 is able to repair proteins from glycation and remove AGEs, a glyocalase activity that seems to be impaired in PD brans[129,132].

Deletion or missense mutations in the gene encoding DJ-1 have been found in several cases of familial PD, identifying it as a causative PD gene with recessive inheritance[133]. Notably, DJ-1 mutation L172Q found in a patient with early parkinsonism, showed links between low DJ-1 expression levels and Lewy body pathology suggesting a pathological pathway between DJ-1 and synucleinopalogy[134]. Experiment from our laboratory demonstrated that the over-expression of DJ-1 can prevent neuronal cell death in rat primary DA neuron cultures exposed to aSyn-A53T virus and other PD-related insults[135]. Recent *in vitro* experiments established that the physical interaction between DJ-1 and aSyn, and the reduction of aSyn dimetization and toxicity by DJ-1 overexpression constitute fundamental events in the neuroprotective mechanism of DJ-1, which is disrupted by DJ-1 mutations found in familial cases of PD[136].

Cumulative data put in evidence the neuroprotective potential of overexpresing DJ-1 in neurons and astrocytes, preventing dopaminergic neuronal death elicited by oxidative stress derived from toxic protein accumulation (e.g. aSyn aggregation) or oxidative damage elicited by PD-causing neurotoxicants (e.g. rotenone, MPTP or 6-OHDA)[137–140].

1.4.4. ATP13A2: a lysosomal protein involved in autophagy

ATP13A2 is a lysosomal P-type ATPase, encoded by PARK9 gene, involved in ALP-mediated degradation[141,142]. Evidence from cell culture studies suggests that ATP13A2 has a potential neuroprotective role as a regulator of aSyn metabolism, and, therefore, that lysosomal dysfunction caused by a deficiency of ATP13A2 contributes to the pathogenesis of synucleinophathies by promoting aSyn accumulation[142–144]. *In vivo* experiments evidenced that the lack of ATP13A2 exacerbated sensorymotor deficiency, promoted aSyn accumulation and endolysosomal dysfunction leading to dopaminergic neuronal death in animals overexpressing human aSyn[145–148]. Beside its role in the regulation of autophagy, other functions have been attributed to ATP13A2 including Mn^{2+} and Zn^{2+} metabolism and mitochondrial bioenergetics[149,150]. Loss-of-function mutations in PARK9, have been identified in patients with early-onset parkinsonism with dementia (Kufor-Rakeb syndrome)[151].

1.5. Additional proteins with potential neuroprotective effects in synucleinopathy diseases

1.5.1. PGC1α: a regulator of mitochondrial biogenesis and oxidative metabolism

Genome-wide expression analysis has led to the finding that the transcriptional co-activator PPARGCIA (PGC1α), a master regulator of mitochondrial biogenesis and oxidative metabolism, is down-regulated in PD brain[152]. Additionally, single nucleotide polymorphisms (SNPs) in PGC1α gene were found associated with risk of developing PD[153]. In human PD brains, under oxidative stress conditions, aSyn binds to the PGC1α gene promoter, provoking a transcriptional down-regulation of PGC1α that in turn results in mitochondrial dysfunction and aSyn oligomerization in a vicious cycle[154,155].

The major role of PCG1α is a transcriptional co-activation of multiple antioxidant pathways that modulate mitochondrial function and controls ATP homeostasis under oxidative stress[156]. The potential of PGC1α as PD therapeutic target is in constant investigation since enhancement of its transcriptional activity can cause unexpected effects[157]. Studies from our group demonstrated that over-expression of PGC1α in an *in vitro* primary midbrain culture model protected DA neurons from neurotoxicity elicited by the aSyn variant A53T and the toxic compound rotenone[152], suggesting that PGC1α could have neuroprotective activity against neuronal death. However, studies in an *in vivo* PD model demonstrated that the overexpression of PGC1α elicited down-regulation of genes involved in dopaminergic neurons maintenance, such as Pitx3 and Bdnf, and increased susceptibility to MPTP toxicity[157]. Even more, *in vitro* and *in vivo* experiments showed evidence that sustained expression of PGC1α increased mitochondrial biogenesis, basal respiration, and ATP production; however, higher levels of PGC1α led to dopamine depletion and dopaminergic neurons degeneration[157,158]. Furthermore, nigral neuronal neurons lacking the expression of PGC1α showed abnormal mitochondria and endoplasmatic reticulum plus severe degeneration elicited by human aSyn. The expression of PCG1α in the same PCG1α null neurons resulted in restoration of mitochondrial activity, dopaminergic cells viability and neuroportection against aSyn toxicity[159]. Far evidence highlights the neuroprotective benefits of PGC1α and the importance of maintain physiological levels of the transcriptional co-activator in order to control adverse effects.

Several strategies have confirmed that controlled expression of PGC1α can effectively protect dopaminergic neurons. Mechanistic *in vitro* studies determined that PGC1α regulate mitochondrial density in neurons, suggesting a therapeutic strategy that involved the up-regulation of PGC1α mitochondrial biogenesis activity in order to compensate the loss of mitochondria in neurodegenerative diseases[160]. A transgenic expression strategy employed the use of resveratrol to activate the expression of PGC1α in dopaminergic neurons enhancing the expression of mitochondrial antioxidants SOD2 and Trx2 and protecting neurons from MPTP toxicity[161,162]. These findings denote the great potential of PGC1α as a therapeutic target for PD.

1.5.2. MsrA: an antioxidant protein involved in the repair of oxidatively damaged proteins

Oxidative damage has a strong link to neurodegeneration in synucleinopathies[163]. In PD, surviving DA neurons experience failure of normal subcellular processes, including mitochondrial, lysosomal, and proteasomal function, ultimately leading to an imbalance between ROS levels and cellular antioxidant activities[96]. Oxidative stress promotes the formation of aSyn oligomers, and at the same time aSyn oligomers stimulate the production of ROS in a toxic cycle[20]. Methionine sulfoxide reductase A (MsrA) is an antioxidant protein that reduces protein-bound and -unbound methionine sulfoxide to methionine[164]. Upon exposure to ROS, aSyn undergoes oxidation at four methionine residues in aSyn (Met1, Met5, Met16, and Met27), yielding species with a high propensity to aggregate, particular in the presence of metal ions[165,166]. Oxidation of methionine residues in aSyn sequence decrease aSyn membrane affinity[167], and proteasomal degradation rate[168] which can be potentially implicated in lipid-induced aSyn aggregation. Repairing cellular machinery involve the anti-oxidant activity of MsrA that can selectively reduce oxidized methionine residues in aSyn[169]

Functional analyses performed in our lab have shown that overexpression of MsrA prevents DA neuronal cell death in rat primary midbrain cultures exposed to rotenone and aSyn-A53T virus, leading to the hypothesis that up-regulating MsrA can be

neuroprotective by reducing oxidatively damaged levels of aSyn[164]. *In vivo* studies showed that MsrA inhibits the development of motor defects promote by the expression of human aSyn, and that MsrA antioxidant system can be enhanced by dietary supplement S-methyl-L-cysteine (SMLC)[170]. Collectively these results classify the anti-oxidant activity of MsrA as a potential preventive therapy against brain disease that involve oxidative stress.

1.6. Genes associated with familial DLB

Conflicting clinical and neuropathological overlapping of DLB with PD with dementia (PDD) and AD often causes misdiagnosis that can only be defined in post-mortem autopsies, and also confirm that these disease may share the same molecular basis. Genetic studies may reveal unique DLB molecular pathological pathways, or will put in evidence common genetic profiles that connect DLB, PDD and AD. As matter of fact a recent genetic study confirmed APOE as a strong risk factor associated with the development of DLB, and SNCA and SCARB2 (commonly associated with PD[4,171]) were also associated with DLB[172]. These findings suggest that in addition to shared genetic factors with other dementias, DLB showed a unique profile that can reveal specific molecular etiology. Familial cases of DLB are very scarce and the disease presentation is heterogeneous within the family showing distinct DLB neuropathology but with variable parkinsonian symptoms[173]. From very few familia DLB studies, it was possible to determine one specific DLB locus (2q35-q36) but without the identification of pathogenic mutations[174]. Additional studies, focused on the synucleinopathy characteristic of DLB, found two amino acid subtitutions in β-synuclein gene (V70M and P123H) in familial cases of DLB[175]. Further analysis showed that P123H mutation produced neurodegeneration in mouse brain[176], suggesting that genetic alteration in β-synuclein may predispose the development of DLB.

1.6.1. Epigenetic modifications in PD versus DLB genes

Genetic similarities found between PD and DLB[177], but specific neuropathological differences indicate pathogenesis of PD and DLB is likely characterized by epigenetic events that perturb the expression of genes involved in controlling neuronal function and

survival[178]. In fact, different genes have been found to be differentially methylated in PD versus DLB. In addition to its impact on neuronal health, a differential expression pattern of key candidate genes could represent a unique pathological marker that could be used to distinguish among different synucleinopathies. For instance, it has been reported that SNCA gene is hypomethylated in both PD and DLB post-mortem brains, resulting in the overexpression of aSyn and its association with the translocation of DNA methyltranferase I from the nucleus into the cytosol, that directly impact overall DNA methylation[179]. As a result, two genes found up-regulated in PD (SEPW1 and PRKAR2A) showed methylation decay in both DLB and PD brains[179]. Transcriptome analysis of DLB post-mortem brains showed alteration in DNA methylation of genes related with synaptic function behavioral response, and circadian rhythm which are mechanisms correlated with cognitive decay in DLB patients[180,181]. Epigenome wide association studies failed to find DNA methylation differences in hallmark PD genes; however, altered methylation was found PARK16, GPNMB and STX1B, which are associated with risk of developing PD[182,183]. Neuroepigenomics may be considered a key approach to identify shared and unique neuroprotective proteins, which aberrant methylation may be causing neurodegeration in DLB and PD.

1.7. Synucleinopathy research models: strengths and weaknesses in replicating key neuropathological endpoints (mitochondrial dysfunction, oxidative stress, and impairment of lysosomal autophagy).

Understanding the molecular underpinnings of synucleinopathy diseases based on preclinical data is expected to lead to the discovery of novel and more effective therapies to slow down or even stop the toxic effects of aSyn. Studies involving the use of highly reproducible *in vitro* and *in vivo* models have yielded valuable insights into pathogenic cellular events that may represent potential therapeutic targets[184–186]. A reliable research model is characterized by its ability to replicate key pathophysiological events that are hallmarks of the disease. In complex and multisymptomatic disorders such as synucleinopathies, the selection of a research model depends on the objectives of the investigation. In general, two kinds of models have been proposed for the study of aSyn diseases, (i) neurotoxin-based and (ii) genetic[16]. Cellular and *in vivo* neurotoxin-based

models involving exposure to mitochondrial toxicants such as rotenone or MPTP successfully replicate selective dopaminergic neurodegeneration, specific mitochondrial complex I defects, and increased oxidative stress found in PD brains[9,135,187,188]. However, toxin-based models are not able to reproduce the entire neuropathogenic spectrum found in synucleinopathies[16]. For instance, limitations in the MPTP model are related with its acute mechanism of action that do not allow the chronic progressive neurodegeneration or the formation of aSyn aggregates[187,189]. In contrast, the rotenone PD model show advantages over the MPTP model since it is able to replicate neuronal cell death and aSyn inclusions formation, highlighting the link of rotenone exposure to high risk of developing PD[7]. Nevertheless, the rotenone model also show limitations in terms of low consistency in the percentage of animals that develop severe nigrostriatal lesions and the extent of the lesion[9]. Genetic models in which human WT, mutated aSyn or PD-linked genes are expressed *in vivo* or *in vitro* (including in human iPSC-derived neuronal cultures) successfully replicate DA neuronal death, the formation of aggregated aSyn Lewy body-like structures, progressive motor deficit and development of subcellular impairments including mitochondrial dysfunction, and lysosomal/proteasomal defects in surviving neurons[103,184,185,190,191,75]. Gene-based PD experimental models may be disadvantageous since an uncontrolled alteration of gene expression may lead to undesired secondary effects that can lead to the co-activations or attenuation of unknown genes or proteins that can be linked to PD-associated genes pathways[191]. from Unfortunately, there are no *in intro* or *in vivo* models considered as perfect replicas of all the synucleinopathy neuropathology. Thus, there are still gaps in our understanding of the connections among cellular dysfunction, aberrant aSyn aggregation, and neuronal death.

1.8. Thesis objectives

Our efforts during this thesis project were focused on the optimization of reliable *in vitro* and *in vivo* models that add new insights into aSyn-related defects in synucleinopathy disorders (and in particular PD and DLB), with the main objective of discovering new therapeutic targets.

In order to validate environmental neurotoxicants or genetic perturbations as potential causes of PD neuropathology, mechanistic studies must be performed in appropriate cellular models. During the last decade, efforts from our group (including research that I have carried out during my PhD studies) have led to the development of an optimized primary mixed-cell culture that recapitulates physiological conditions of the brain and has the biological complexity necessary to reproduce hallmark PD cellular events. The method is fast, straightforward, reproducible, and cost-effective and provides the opportunity to obtain large amounts of data from each experiment.

Data from extensive biochemical and cellular studies in our laboratory provided a strong premise for the idea that neighboring exposed aSyn conformers interact at the membrane surface, leading to aSyn aggregation coupled with membrane permeabilization and dopaminergic cell death in the midbrain. To address this hypothesis in an *in vivo* model, we analyzed the effects of over-expressing WT aSyn and two aSyn mutants, A53T and A53E, in rat midbrain. Because these mutants have different binding affinities for lipid vesicles[192,193], we infer that they could also have different propensities to aggregate at membrane surfaces and elicit membrane permeabilization[75,76]. Our studies of these two mutants in an *in vivo* model of PD will yield insights relevant to the role of membrane-induced aSyn aggregation and aSyn-mediated membrane permeabilization in neurodegeneration in the brains of PD patients.

aSyn neurotoxicity varies with the expression of neuroprotective proteins, and misfolded aSyn affects cellular functions and gene expression[178,179]. Therefore, it is critical to understand the expression patterns of neuroprotective genes/proteins that can play a role in modulating neuropathological pathways and the symptomatology of synucleinopathies. A focus of our research is to investigate the expression patterns of neuroprotective proteins that are predicted to be affected in both PD and DLB. Here we focused on the following panel of neuroprotective proteins: DJ-1, a protein with antioxidant and chaperone activities[194]; PGC1α, a master regulator of mitochondrial biogenesis and oxidative metabolism[154]; MsrA, an antioxidant enzyme responsible for repairing oxidatively damaged proteins[164]; and ATP13A2, a lysosomal protein involved in autophagy[143]. The objective of

this phase of my PhD research was to establish the expression profiles of these proteins in post-mortem brain samples from PD and DLB patients. This study of differential expression of proteins involved in cellular antioxidant responses, mitochondrial function, and lysosomal autophagy was designed to advance our understanding of mechanisms of neurodegeneration and neuroprotection in DLB and PD.

1.9. List of References

1.   Spillantini, M. G. & Goedert, M. The alpha-synucleinopathies: Parkinson's disease, dementia with Lewy bodies, and multiple system atrophy. *Ann. N. Y. Acad. Sci.* **920**, 16–27 (2000).

2.   Spillantini, M. G., Schmidt, M. L., Lee, V. M.-Y., Trojanowski, J. Q., Jakes, R. & Goedert, M. [alpha]-Synuclein in Lewy bodies. *Nature* **388**, 839–840 (1997).

3.   Nussbaum, R. L. Genetics of Synucleinopathies. *Cold Spring Harb. Perspect. Med.* **8**, a024109 (2018).

4.   Tagliafierro, L. & Chiba-Falek, O. Up-regulation of SNCA gene expression: implications to synucleinopathies. *Neurogenetics* **17**, 145–157 (2016).

5.   Poewe, W., Seppi, K., Tanner, C. M., Halliday, G. M., Brundin, P., Volkmann, J., Schrag, A.-E. & Lang, A. E. Parkinson disease. *Nat. Rev. Dis. Prim.* **3**, 17013 (2017).

6.   Cannon, J. R. & Greenamyre, J. T. The Role of Environmental Exposures in Neurodegeneration and Neurodegenerative Diseases. *Toxicol. Sci.* **124**, 225–250 (2011).

7.   Tanner, C. M., Kamel, F., Ross, G. W., Hoppin, J. A., Goldman, S. M., Korell, M., Marras, C., Bhudhikanok, G. S., Kasten, M., Chade, A. R., Comyns, K., Richards, M. B., Meng, C., Priestley, B., Fernandez, H. H. *et al.* Rotenone, Paraquat, and Parkinson's Disease. *Environ. Health Perspect.* **119**, 866–872 (2011).

8.   Callaghan, R. C., Cunningham, J. K., Sykes, J. & Kish, S. J. Increased risk of Parkinson's disease in individuals hospitalized with conditions related to the use of methamphetamine or other amphetamine-type drugs. *Drug Alcohol Depend.* **120**, 35–40 (2012).

9.   Cannon, J. R., Tapias, V., Na, H. M., Honick, A. S., Drolet, R. E. & Greenamyre, J. T. A highly reproducible rotenone model of Parkinson's disease. *Neurobiol. Dis.* **34**, 279–90 (2009).

10. Wang, X.-F., Li, S., Chou, A. P. & Bronstein, J. M. Inhibitory effects of pesticides on proteasome activity: Implication in Parkinson's disease. *Neurobiol. Dis.* **23**, 198–205 (2006).

11. Liu, Z., Zhou, T., Ziegler, A. C., Dimitrion, P. & Zuo, L. Oxidative Stress in Neurodegenerative Diseases: From Molecular Mechanisms to Clinical Applications. *Oxid. Med. Cell. Longev.* **2017**, 1–11 (2017).

12. Alexander, G. E. Biology of Parkinson's disease: pathogenesis and pathophysiology of a multisystem neurodegenerative disorder. *Dialogues Clin. Neurosci.* **6**, 259–80 (2004).

13. Bologna, M., Guerra, A., Paparella, G., Giordo, L., Alunni Fegatelli, D., Vestri, A. R., Rothwell, J. C. & Berardelli, A. Neurophysiological correlates of bradykinesia in Parkinson's disease. *Brain* **141**, 2432–2444 (2018).

14. Schapira, A. H. V., Chaudhuri, K. R. & Jenner, P. Non-motor features of Parkinson disease. *Nat. Rev. Neurosci.* **18**, 435–450 (2017).

15. Segura-Aguilar, J., Paris, I., Muñoz, P., Ferrari, E., Zecca, L. & Zucca, F. A. Protective and toxic roles of dopamine in Parkinson's disease. *J. Neurochem.* **129**, 898–915 (2014).

16. Dauer, W. & Przedborski, S. Parkinson's Disease. *Neuron* **39**, 889–909 (2003).

17. Tabbal, S. D., Tian, L., Karimi, M., Brown, C. A., Loftin, S. K. & Perlmutter, J. S. Low nigrostriatal reserve for motor parkinsonism in nonhuman primates. *Exp. Neurol.* **237**, 355–362 (2012).

18. Braak, H., Tredici, K. Del, Rüb, U., De Vos, R. A. I., Jansen Steur, E. N. H. & Braak, E. *Staging of brain pathology related to sporadic Parkinson's disease. Neurobiology of Aging* **24**, (2003).

19. Dijkstra, A. A., Voorn, P., Berendse, H. W., Groenewegen, H. J., Rozemuller, A. J. M., van de Berg, W. D. J. & Berg, W. D. J. van de. Stage-dependent nigral neuronal loss in incidental Lewy body and Parkinson's disease. *Mov. Disord.* **29**, 1244–1251 (2014).

20. Dolgacheva, L. P., Fedotova, E. I., Abramov, A. Y. & Berezhnov, A. V. Alpha-Synuclein and Mitochondrial Dysfunction in Parkinson's Disease. *Biochem. (Moscow), Suppl. Ser. A Membr. Cell Biol.* **12**, 10–19 (2018).

21. Bentea, E., Verbruggen, L. & Massie, A. The Proteasome Inhibition Model of Parkinson's Disease. *J. Parkinsons. Dis.* **7**, 31–63 (2017).

22. Keeney, P. M., Xie, J., Capaldi, R. A. & Bennett, J. P. Parkinson's Disease Brain Mitochondrial Complex I Has Oxidatively Damaged Subunits and Is Functionally Impaired and Misassembled. *J. Neurosci.* **26**, 5256–5264 (2006).

23. Plotegher, N. & Duchen, M. R. Crosstalk between Lysosomes and Mitochondria in Parkinson's Disease. *Front. Cell Dev. Biol.* **5**, 110 (2017).

24. Dehay, B., Martinez-Vicente, M., Caldwell, G. A., Caldwell, K. A., Yue, Z., Cookson, M. R., Klein, C., Vila, M. & Bezard, E. Lysosomal impairment in Parkinson's disease. *Mov. Disord.* **28**, 725–732 (2013).

25. Loane, C. & Politis, M. Positron emission tomography neuroimaging in Parkinson's disease. *Am. J. Transl. Res.* **3**, 323–41 (2011).

26. Huang, T., Wang, H., Tang, G., Liang, X., Shi, X. & Zhang, X. The Influence of Residual Nor-β-CFT in 11C CFT Injection on the Parkinson Disease Diagnosis. *Clin. Nucl. Med.* **37**, 743–747 (2012).

27. Mahlknecht, P., Hotter, A., Hussl, A., Esterhammer, R., Schocke, M. & Seppi, K. Significance of MRI in diagnosis and differential diagnosis of Parkinson's disease. *Neurodegener. Dis.* **7**, 300–18 (2010).

28. Fox, S. H., Katzenschlager, R., Lim, S.-Y., Barton, B., de Bie, R. M. A., Seppi, K., Coelho, M. & Sampaio, C. International Parkinson and movement disorder society evidence-based medicine review: Update on treatments for the motor symptoms of Parkinson's disease. *Mov. Disord.* **33**, 1248–1266 (2018).

29. Litvan, I., Kieburtz, K., Tröster, A. I. & Aarsland, D. Strengths and challenges in conducting clinical trials in Parkinson's disease mild cognitive impairment. *Mov. Disord.* **33**, 520–527 (2018).

30. Wong, J. K., Cauraugh, J. H., Ho, K. W. D., Broderick, M., Ramirez-Zamora, A., Almeida, L., Shukla, A. W., Wilson, C. A., de Bie, R. M., Weaver, F. M., Kang, N. & Okun, M. S. STN vs. GPi deep brain stimulation for tremor suppression in Parkinson disease: A systematic review and meta-analysis. *Parkinsonism Relat. Disord.* (2018). doi:10.1016/J.PARKRELDIS.2018.08.017

31. Espay, A. J., Pagan, F. L., Walter, B. L., Morgan, J. C., Elmer, L. W., Waters, C. H., Agarwal, P., Dhall, R., Ondo, W. G., Klos, K. J. & Silver, D. E. Optimizing extended-release carbidopa/levodopa in Parkinson disease. *Neurol. Clin. Pract.* **7**, 86–93 (2017).

32. Elroby, S. A. K., Makki, M. S. I., Sobahi, T. R. & Hilal, R. H. Toward the understanding of the metabolism of levodopa I. DFT investigation of the equilibrium geometries, acid-base properties and levodopa-water complexes. *Int. J. Mol. Sci.* **13**, 4321–39 (2012).

33. Nutt, J. G., Woodward, W. R. & Anderson, J. L. The effect of carbidopa on the pharmacokinetics of intravenously administered levodopa: The mechanism of action in the treatment of parkinsonism. *Ann. Neurol.* **18**, 537–543 (1985).

34. Olanow, C. W., Stern, M. B. & Sethi, K. The scientific and clinical basis for the treatment of Parkinson disease (2009). *Neurology* **72**, S1–S136 (2009).

35. Parkinson Study Group. Phase II safety, tolerability, and dose selection study of isradipine as a potential disease-modifying intervention in early Parkinson's disease (STEADY-PD). *Mov. Disord.* **28**, 1823–1831 (2013).

36. Aviles-Olmos, I., Dickson, J., Kefalopoulou, Z., Djamshidian, A., Ell, P., Soderlund, T., Whitton, P., Wyse, R., Isaacs, T., Lees, A., Limousin, P. & Foltynie, T. Exenatide and the treatment of patients with Parkinson's disease. *J. Clin. Invest.* **123**, 2730–2736 (2013).

37. Pagan, F., Hebron, M., Valadez, E. H., Torres-Yaghi, Y., Huang, X., Mills, R. R., Wilmarth, B. M., Howard, H., Dunn, C., Carlson, A., Lawler, A., Rogers, S. L., Falconer, R. A., Ahn, J., Li, Z. *et al.* Nilotinib Effects in Parkinson's disease and Dementia with Lewy bodies. *J. Parkinsons. Dis.* **6**, 503–517 (2016).

38. Schwarzschild, M. A., Ascherio, A., Beal, M. F., Cudkowicz, M. E., Curhan, G. C., Hare, J. M., Hooper, D. C., Kieburtz, K. D., Macklin, E. A., Oakes, D., Rudolph, A., Shoulson, I., Tennis, M. K., Espay, A. J., Gartner, M. *et al.* Inosine to Increase Serum and Cerebrospinal Fluid Urate in Parkinson Disease. *JAMA Neurol.* **71**, 141 (2014).

39. McEachern, K. A., Fung, J., Komarnitsky, S., Siegel, C. S., Chuang, W.-L., Hutto, E., Shayman, J. A., Grabowski, G. A., Aerts, J. M. F. G., Cheng, S. H., Copeland, D. P. & Marshall, J. A specific and potent inhibitor of glucosylceramide synthase for substrate inhibition therapy of Gaucher disease. *Mol. Genet. Metab.* **91**, 259–267 (2007).

40. Chen, J., Chen, Y. & Pu, J. Leucine-Rich Repeat Kinase 2 in Parkinson's Disease: Updated from Pathogenesis to Potential Therapeutic Target. *Eur. Neurol.* **79**, 256–265 (2018).

41. Schneeberger, A., Mandler, M., Mattner, F. & Schmidt, W. Vaccination for Parkinson's disease. *Parkinsonism Relat. Disord.* **18**, S11–S13 (2012).

42.   Perlmutter, J. S. & Mink, J. W. Deep brain stimulation. *Annu. Rev. Neurosci.* **29**, 229–57 (2006).

43.   Ubhi, K., Peng, K., Lessig, S., Estrella, J., Adame, A., Galasko, D., Salmon, D. P., Hansen, L. A., Kawas, C. H. & Masliah, E. Neuropathology of dementia with Lewy bodies in advanced age: A comparison with Alzheimer disease. *Neurosci. Lett.* **485**, 222–227 (2010).

44.   Kosaka, K. History and Latest Concepts of Lewy Body Disease and Dementia with Lewy Bodies. in *Dementia with Lewy Bodies* 3–9 (Springer Japan, 2017). doi:10.1007/978-4-431-55948-1_1

45.   Jellinger, K. A. Dementia with Lewy bodies and Parkinson's disease-dementia: current concepts and controversies. *J. Neural Transm.* **125**, 615–650 (2018).

46.   Savica, R., Grossardt, B. R., Bower, J. H., Boeve, B. F., Ahlskog, J. E. & Rocca, W. A. Incidence of Dementia With Lewy Bodies and Parkinson Disease Dementia. *JAMA Neurol.* **70**, 1396 (2013).

47.   McKeith, I. G., Boeve, B. F., Dickson, D. W., Halliday, G., Taylor, J.-P., Weintraub, D., Aarsland, D., Galvin, J., Attems, J., Ballard, C. G., Bayston, A., Beach, T. G., Blanc, F., Bohnen, N., Bonanni, L. *et al.* Diagnosis and management of dementia with Lewy bodies: Fourth consensus report of the DLB Consortium. *Neurology* **89**, 88–100 (2017).

48.   Mayo, M. C. & Bordelon, Y. Dementia with Lewy bodies. *Semin. Neurol.* **34**, 182–8 (2014).

49.   Marui, W., Iseki, E., Kato, M., Akatsu, H. & Kosaka, K. Pathological entity of dementia with Lewy bodies and its differentiation from Alzheimer's disease. *Acta Neuropathol.* **108**, 121–8 (2004).

50.   Hasegawa, M. Molecular Biology of Dementia with Lewy Bodies. in *Dementia with Lewy Bodies* 41–55 (Springer Japan, 2017). doi:10.1007/978-4-431-55948-1_4

51.   Perry, E. K., Haroutunian, V., Davis, K. L., Levy, R., Lantos, P., Eagger, S., Honavar, M., Dean, A., Griffiths, M. & McKeith, I. G. Neocortical cholinergic activities differentiate Lewy body dementia from classical Alzheimer's disease. *Neuroreport* **5**, 747–9 (1994).

52.   Gurney, R., Davidson, Y. S., Robinson, A. C., Richardson, A., Jones, M., Snowden, J. S. & Mann, D. M. A. Lysosomes, autophagosomes and Alzheimer pathology in dementia with Lewy body disease. *Neuropathology* **38**, 347–360 (2018).

53. Mosimann, U. P. & Mckeith, I. G. *Dementia with lewy bodies - diagnosis and treatment*. (2003).

54. Donadio, V., Incensi, A., Rizzo, G., Capellari, S., Pantieri, R., Stanzani Maserati, M., Devigili, G., Eleopra, R., Defazio, G., Montini, F., Baruzzi, A. & Liguori, R. A new potential biomarker for dementia with Lewy bodies. *Neurology* **89**, 318–326 (2017).

55. HAKOMORI, M., TOYODA, K., SUTOU, S., NOGUCHI, H. & TOMIMITSU, H. Advanced Dementia with Lewy Bodies Showing Remarkable Improvement of Activities of Daily Living by Interventions in the Recovery Rehabilitation Unit. *J. JAPANESE Assoc. Rural Med.* **65**, 1194–1200 (2017).

56. McKeith, I. G., Grace, J. B., Walker, Z., Byrne, E. J., Wilkinson, D., Stevens, T. & Perry, E. K. Rivastigmine in the treatment of dementia with Lewy bodies: preliminary findings from an open trial. *Int. J. Geriatr. Psychiatry* **15**, 387–92 (2000).

57. Mori, E., Ikeda, M., Kosaka, K. & Donepezil-DLB Study Investigators. Donepezil for dementia with Lewy bodies: A randomized, placebo-controlled trial. *Ann. Neurol.* **72**, 41–52 (2012).

58. Halliday, G. M., Holton, J. L., Revesz, T. & Dickson, D. W. Neuropathology underlying clinical variability in patients with synucleinopathies. *Acta Neuropathol.* **122**, 187–204 (2011).

59. Marui, W., Iseki, E., Nakai, T., Miura, S., Kato, M., Uéda, K. & Kosaka, K. Progression and staging of Lewy pathology in brains from patients with dementia with Lewy bodies. *J. Neurol. Sci.* **195**, 153–9 (2002).

60. Cersosimo, M. G. Propagation of alpha-synuclein pathology from the olfactory bulb: possible role in the pathogenesis of dementia with Lewy bodies. *Cell Tissue Res.* **373**, 233–243 (2018).

61. Frigerio, R., Fujishiro, H., Ahn, T.-B., Josephs, K. A., Maraganore, D. M., DelleDonne, A., Parisi, J. E., Klos, K. J., Boeve, B. F., Dickson, D. W. & Ahlskog, J. E. Incidental Lewy body disease: do some cases represent a preclinical stage of dementia with Lewy bodies? *Neurobiol. Aging* **32**, 857–63 (2011).

62. Maroteaux, L., Campanelli, J. T. & Scheller, R. H. Synuclein: a neuron-specific protein localized to the nucleus and presynaptic nerve terminal. *J. Neurosci.* **8**, 2804–15 (1988).

63. Goedert, M. Alpha-synuclein and neurodegenerative diseases. *Nat. Rev. Neurosci.* **2**, 492–501 (2001).

64. Paul H. Weinreb, Weiguo Zhen, ‡, Anna W. Poon, Kelly A. Conway, ‡ and & Peter T. Lansbury, J. *,. NACP, A Protein Implicated in Alzheimer's Disease and Learning, Is Natively Unfolded†. (1996). doi:10.1021/BI961799N

65. Davidson, W. S., Jonas, A., Clayton, D. F. & George, J. M. Stabilization of alpha-synuclein secondary structure upon binding to synthetic membranes. *J. Biol. Chem.* **273**, 9443–9 (1998).

66. Bussell, R. & Eliezer, D. A structural and functional role for 11-mer repeats in alpha-synuclein and other exchangeable lipid binding proteins. *J. Mol. Biol.* **329**, 763–78 (2003).

67. Dettmer, U., Newman, A. J., Luth, E. S., Bartels, T. & Selkoe, D. In vivo cross-linking reveals principally oligomeric forms of α-synuclein and β-synuclein in neurons and non-neural cells. *J. Biol. Chem.* **288**, 6371–85 (2013).

68. Bartels, T., Choi, J. G. & Selkoe, D. J. α-Synuclein occurs physiologically as a helically folded tetramer that resists aggregation. *Nature* **477**, 107–110 (2011).

69. Burré, J., Sharma, M. & Südhof, T. C. α-Synuclein assembles into higher-order multimers upon membrane binding to promote SNARE complex formation. *Proc. Natl. Acad. Sci.* **111**, E4274–E4283 (2014).

70. Bartels, T., Ahlstrom, L. S., Leftin, A., Kamp, F., Haass, C., Brown, M. F. & Beyer, K. The N-Terminus of the Intrinsically Disordered Protein α-Synuclein Triggers Membrane Binding and Helix Folding. *Biophys. J.* **99**, 2116–2124 (2010).

71. Irwin, D. J., Grossman, M., Weintraub, D., Hurtig, H. I., Duda, J. E., Xie, S. X., Lee, E. B., Van Deerlin, V. M., Lopez, O. L., Kofler, J. K., Nelson, P. T., Jicha, G. A., Woltjer, R., Quinn, J. F., Kaye, J. *et al.* Neuropathological and genetic correlates of survival and dementia onset in synucleinopathies: a retrospective analysis. *Lancet Neurol.* **16**, 55–65 (2017).

72. Wakabayashi, K., Tanji, K., Odagiri, S., Miki, Y., Mori, F. & Takahashi, H. The Lewy body in Parkinson's disease and related neurodegenerative disorders. *Mol. Neurobiol.* **47**, 495–508 (2013).

73. Braak, H., R b, U., Gai, W. P. & Del Tredici, K. Idiopathic Parkinson's disease: possible routes by which vulnerable neuronal types may be subject to neuroinvasion by an unknown pathogen. *J. Neural Transm.* **110**, 517–536 (2003).

74. Steiner, J. A., Quansah, E. & Brundin, P. The concept of alpha-synuclein as a prion-like protein: ten years after. *Cell Tissue Res.* **373**, 161–173 (2018).

75. Ysselstein, D., Joshi, M., Mishra, V., Griggs, A. M., Asiago, J. M., McCabe, G. P., Stanciu, L. A., Post, C. B. & Rochet, J.-C. Effects of impaired membrane interactions on α-synuclein aggregation and neurotoxicity. *Neurobiol. Dis.* **79**, 150–63 (2015).

76. Ysselstein, D., Dehay, B., Costantino, I. M., McCabe, G. P., Frosch, M. P., George, J. M., Bezard, E. & Rochet, J.-C. Endosulfine-alpha inhibits membrane-induced α-synuclein aggregation and protects against α-synuclein neurotoxicity. *Acta Neuropathol. Commun.* **5**, 3 (2017).

77. Winner, B., Jappelli, R., Maji, S. K., Desplats, P. A., Boyer, L., Aigner, S., Hetzer, C., Loher, T., Vilar, M., Campioni, S., Tzitzilonis, C., Soragni, A., Jessberger, S., Mira, H., Consiglio, A. *et al.* In vivo demonstration that alpha-synuclein oligomers are toxic. *Proc. Natl. Acad. Sci. U. S. A.* **108**, 4194–9 (2011).

78. Griggs, A. M., Ysselstein, D. & Rochet, J.-C. Role of Aberrant α-Synuclein–Membrane Interactions in Parkinson's Disease. *Bio-nanoimaging* 443–452 (2014). doi:10.1016/B978-0-12-394431-3.00039-0

79. Barrett, P. J. & Timothy Greenamyre, J. Post-translational modification of α-synuclein in Parkinson's disease. *Brain Res.* **1628**, 247–253 (2015).

80. Oueslati, A. Implication of Alpha-Synuclein Phosphorylation at S129 in Synucleinopathies: What Have We Learned in the Last Decade? (2016). doi:10.3233/JPD-160779

81. Fujiwara, H., Hasegawa, M., Dohmae, N., Kawashima, A., Masliah, E., Goldberg, M. S., Shen, J., Takio, K. & Iwatsubo, T. α-Synuclein is phosphorylated in synucleinopathy lesions. *Nat. Cell Biol.* **4**, 160–164 (2002).

82. Sidransky, E. & Lopez, G. The link between the GBA gene and parkinsonism. *Lancet Neurol.* **11**, 986–998 (2012).

83. Rocha, E. M., Smith, G. A., Park, E., Cao, H., Graham, A.-R., Brown, E., McLean, J. R., Hayes, M. A., Beagan, J., Izen, S. C., Perez-Torres, E., Hallett, P. J. & Isacson, O. Sustained Systemic Glucocerebrosidase Inhibition Induces Brain α-Synuclein Aggregation, Microglia and Complement C1q Activation in Mice. *Antioxid. Redox Signal.* **23**, 550–564 (2015).

84. Mazzulli, J. R., Xu, Y.-H., Sun, Y., Knight, A. L., McLean, P. J., Caldwell, G. A., Sidransky, E., Grabowski, G. A. & Krainc, D. Gaucher Disease Glucocerebrosidase and α-Synuclein Form a Bidirectional Pathogenic Loop in Synucleinopathies. *Cell* **146**, 37–52 (2011).

85. Tofaris, G. K., Kim, H. T., Hourez, R., Jung, J.-W., Kim, K. P. & Goldberg, A. L. Ubiquitin ligase Nedd4 promotes alpha-synuclein degradation by the endosomal-lysosomal pathway. *Proc. Natl. Acad. Sci. U. S. A.* **108**, 17004–9 (2011).

86. Xilouri, M., Brekk, O. R. & Stefanis, L. Alpha-synuclein and Protein Degradation Systems: a Reciprocal Relationship. *Mol. Neurobiol.* **47**, 537–551 (2013).

87. Tanaka, Y., Engelender, S., Igarashi, S., Rao, R. K., Wanner, T., Tanzi, R. E., Sawa, A., L. Dawson, V., Dawson, T. M. & Ross, C. A. Inducible expression of mutant alpha-synuclein decreases proteasome activity and increases sensitivity to mitochondria-dependent apoptosis. *Hum. Mol. Genet.* **10**, 919–926 (2001).

88. Snyder, H., Mensah, K., Theisler, C., Lee, J., Matouschek, A. & Wolozin, B. Aggregated and Monomeric α-Synuclein Bind to the S6′ Proteasomal Protein and Inhibit Proteasomal Function. *J. Biol. Chem.* **278**, 11753–11759 (2003).

89. Xilouri, M. & Stefanis, L. Autophagic pathways in Parkinson disease and related disorders. *Expert Rev. Mol. Med.* **13**, e8 (2011).

90. Parzych, K. R. & Klionsky, D. J. An Overview of Autophagy: Morphology, Mechanism, and Regulation. *Antioxid. Redox Signal.* **20**, 460–473 (2014).

91. Kaushik, S. & Cuervo, A. M. The coming of age of chaperone-mediated autophagy. *Nat. Rev. Mol. Cell Biol.* **19**, 365–381 (2018).

92. Asiago, J. M., Doyle, T. B., Mishra, V., Jacquet, A. de R. & Rochet, J.-C. CHAPTER 11. At the Intersection Between Mitochondrial Dysfunction and Lysosomal Autophagy: Role of PD-Related Neurotoxins and Gene Products. in 325–388 (2017). doi:10.1039/9781782622888-00325

93. Rocha, E. M., De Miranda, B. & Sanders, L. H. Alpha-synuclein: Pathology, mitochondrial dysfunction and neuroinflammation in Parkinson's disease. *Neurobiol. Dis.* **109**, 249–257 (2018).

94. Chen, H. & Chan, D. C. Mitochondrial dynamics-fusion, fission, movement, and mitophagy-in neurodegenerative diseases. *Hum. Mol. Genet.* **18**, R169–R176 (2009).

95. Heinz, S., Freyberger, A., Lawrenz, B., Schladt, L., Schmuck, G. & Ellinger-Ziegelbauer, H. Mechanistic Investigations of the Mitochondrial Complex I Inhibitor Rotenone in the Context of Pharmacological and Safety Evaluation. *Sci. Rep.* **7**, 45465 (2017).

96. Jenner, P. Oxidative stress in Parkinson's disease. *Ann. Neurol.* **53**, S26–S38 (2003).

97. Sanders, L. H. & Timothy Greenamyre, J. Oxidative damage to macromolecules in human Parkinson disease and the rotenone model. *Free Radic. Biol. Med.* **62**, 111–120 (2013).

98. Requejo-Aguilar, R. & Bolaños, J. P. Mitochondrial control of cell bioenergetics in Parkinson's disease. *Free Radic. Biol. Med.* **100**, 123–137 (2016).

99. Nakamura, K., Nemani, V. M., Azarbal, F., Skibinski, G., Levy, J. M., Egami, K., Munishkina, L., Zhang, J., Gardner, B., Wakabayashi, J., Sesaki, H., Cheng, Y., Finkbeiner, S., Nussbaum, R. L., Masliah, E. *et al.* Direct Membrane Association Drives Mitochondrial Fission by the Parkinson Disease-associated Protein α-Synuclein. *J. Biol. Chem.* **286**, 20710–20726 (2011).

100. Vicario, M., Cieri, D., Brini, M. & Calì, T. The Close Encounter Between Alpha-Synuclein and Mitochondria. *Front. Neurosci.* **12**, 388 (2018).

101. Ambaw, A., Zheng, L., Tambe, M. A., Strathearn, K. E., Acosta, G., Hubers, S. A., Liu, F., Herr, S. A., Tang, J., Truong, A., Walls, E., Pond, A., Rochet, J.-C. & Shi, R. Acrolein-mediated neuronal cell death and alpha-synuclein aggregation: Implications for Parkinson's disease. *Mol. Cell. Neurosci.* **88**, 70–82 (2018).

102. Deas, E., Cremades, N., Angelova, P. R., Ludtmann, M. H. R., Yao, Z., Chen, S., Horrocks, M. H., Banushi, B., Little, D., Devine, M. J., Gissen, P., Klenerman, D., Dobson, C. M., Wood, N. W., Gandhi, S. *et al.* Alpha-Synuclein Oligomers Interact with Metal Ions to Induce Oxidative Stress and Neuronal Death in Parkinson's Disease. *Antioxid. Redox Signal.* **24**, 376–391 (2016).

103. Ludtmann, M. H. R., Angelova, P. R., Horrocks, M. H., Choi, M. L., Rodrigues, M., Baev, A. Y., Berezhnov, A. V., Yao, Z., Little, D., Banushi, B., Al-Menhali, A. S., Ranasinghe, R. T., Whiten, D. R., Yapom, R., Dolt, K. S. *et al.* α-synuclein oligomers interact with ATP synthase and open the permeability transition pore in Parkinson's disease. *Nat. Commun.* **9**, 2293 (2018).

104. Polymeropoulos, M. H., Lavedan, C., Leroy, E., Ide, S. E., Dehejia, A., Dutra, A., Pike, B., Root, H., Rubenstein, J., Boyer, R., Stenroos, E. S., Chandrasekharappa, S., Athanassiadou, A., Papapetropoulos, T., Johnson, W. G. *et al.* Mutation in the alpha-synuclein gene identified in families with Parkinson's disease. *Science* **276**, 2045–7 (1997).

105. Baba, M., Nakajo, S., Tu, P. H., Tomita, T., Nakaya, K., Lee, V. M., Trojanowski, J. Q. & Iwatsubo, T. Aggregation of alpha-synuclein in Lewy bodies of sporadic Parkinson's disease and dementia with Lewy bodies. *Am. J. Pathol.* **152**, 879–84 (1998).

106. Spillantini, M. G. & Goedert, M. Synucleinopathies: past, present and future. *Neuropathol. Appl. Neurobiol.* **42**, 3–5 (2016).

107. Kasten, M. & Klein, C. The many faces of alpha-synuclein mutations. *Mov. Disord.* **28**, 697–701 (2013).

108. Klein, C. & Westenberger, A. Genetics of Parkinson's disease. *Cold Spring Harb. Perspect. Med.* **2**, a008888 (2012).

109. Lesage, S. & Brice, A. Parkinson's disease: from monogenic forms to genetic susceptibility factors. *Hum. Mol. Genet.* **18**, R48–R59 (2009).

110. Rubio, J. P., Topp, S., Warren, L., St. Jean, P. L., Wegmann, D., Kessner, D., Novembre, J., Shen, J., Fraser, D., Aponte, J., Nangle, K., Cardon, L. R., Ehm, M. G., Chissoe, S. L., Whittaker, J. C. *et al.* Deep sequencing of the *LRRK2* gene in 14,002 individuals reveals evidence of purifying selection and independent origin of the p.Arg1628Pro mutation in Europe. *Hum. Mutat.* **33**, 1087–1098 (2012).

111. Maraganore, D. M., Lesnick, T. G., Elbaz, A., Chartier-Harlin, M.-C., Gasser, T., Krüger, R., Hattori, N., Mellick, G. D., Quattrone, A., Satoh, J.-I., Toda, T., Wang, J., Ioannidis, J. P. A., de Andrade, M. & Rocca, W. A. UCHL1 is a Parkinson's disease susceptibility gene. *Ann. Neurol.* **55**, 512–521 (2004).

112. Lowe, J., McDermott, H., Landon, M., Mayer, R. J. & Wilkinson, K. D. Ubiquitin carboxyl-terminal hydrolase (PGP 9.5) is selectively present in ubiquitinated inclusion bodies characteristic of human neurodegenerative diseases. *J. Pathol.* **161**, 153–160 (1990).

113. Xia, Q., Liao, L., Cheng, D., Duong, D. M., Gearing, M., Lah, J. J., Levey, A. I. & Peng, J. Proteomic identification of novel proteins associated with Lewy bodies. *Front. Biosci.* **13**, 3850–6 (2008).

114. Healy, D. G., Abou-Sleiman, P. M. & Wood, N. W. Genetic causes of Parkinson?s disease: UCHL-1. *Cell Tissue Res.* **318**, 189–194 (2004).

115. Chung, K. K. ., Dawson, V. L. & Dawson, T. M. The role of the ubiquitin-proteasomal pathway in Parkinson's disease and other neurodegenerative disorders. *Trends Neurosci.* **24**, 7–14 (2001).

116. Setsuie, R., Wang, Y.-L., Mochizuki, H., Osaka, H., Hayakawa, H., Ichihara, N., Li, H., Furuta, A., Sano, Y., Sun, Y.-J., Kwon, J., Kabuta, T., Yoshimi, K., Aoki, S., Mizuno, Y. *et al.* Dopaminergic neuronal loss in transgenic mice expressing the Parkinson's disease-associated UCH-L1 I93M mutant. *Neurochem. Int.* **50**, 119–129 (2007).

117. Gong, B. & Leznik, E. The role of ubiquitin C-terminal hydrolase L1 in neurodegenerative disorders. *Drug News Perspect.* **20**, 365 (2007).

118. Kabuta, T., Furuta, A., Aoki, S., Furuta, K. & Wada, K. Aberrant interaction between Parkinson disease-associated mutant UCH-L1 and the lysosomal receptor for chaperone-mediated autophagy. *J. Biol. Chem.* **283**, 23731–8 (2008).

119. Pickrell, A. M. & Youle, R. J. The Roles of PINK1, Parkin, and Mitochondrial Fidelity in Parkinson's Disease. *Neuron* **85**, 257–273 (2015).

120. Jin, S. M. & Youle, R. J. PINK1- and Parkin-mediated mitophagy at a glance. *J. Cell Sci.* **125**, 795–9 (2012).

121. Kane, L. A., Lazarou, M., Fogel, A. I., Li, Y., Yamano, K., Sarraf, S. A., Banerjee, S. & Youle, R. J. PINK1 phosphorylates ubiquitin to activate Parkin E3 ubiquitin ligase activity. *J. Cell Biol.* **205**, 143–53 (2014).

122. Okatsu, K., Saisho, K., Shimanuki, M., Nakada, K., Shitara, H., Sou, Y., Kimura, M., Sato, S., Hattori, N., Komatsu, M., Tanaka, K. & Matsuda, N. p62/SQSTM1 cooperates with Parkin for perinuclear clustering of depolarized mitochondria. *Genes to Cells* **15**, no-no (2010).

123. Lazarou, M., Sliter, D. A., Kane, L. A., Sarraf, S. A., Wang, C., Burman, J. L., Sideris, D. P., Fogel, A. I. & Youle, R. J. The ubiquitin kinase PINK1 recruits autophagy receptors to induce mitophagy. *Nature* **524**, 309–314 (2015).

124. Kinumi, T., Kimata, J., Taira, T., Ariga, H. & Niki, E. Cysteine-106 of DJ-1 is the most sensitive cysteine residue to hydrogen peroxide-mediated oxidation in vivo in human umbilical vein endothelial cells. *Biochem. Biophys. Res. Commun.* **317**, 722–728 (2004).

125. Guzman, J. N., Sanchez-Padilla, J., Wokosin, D., Kondapalli, J., Ilijic, E., Schumacker, P. T. & Surmeier, D. J. Oxidant stress evoked by pacemaking in dopaminergic neurons is attenuated by DJ-1. *Nature* **468**, 696–700 (2010).

126. Burbulla, L. F., Song, P., Mazzulli, J. R., Zampese, E., Wong, Y. C., Jeon, S., Santos, D. P., Blanz, J., Obermaier, C. D., Strojny, C., Savas, J. N., Kiskinis, E., Zhuang, X., Krüger, R., Surmeier, D. J. *et al.* Dopamine oxidation mediates mitochondrial and lysosomal dysfunction in Parkinson's disease. *Science* **357**, 1255–1261 (2017).

127. Görlach, A., Bertram, K., Hudecova, S. & Krizanova, O. Calcium and ROS: A mutual interplay. *Redox Biol.* **6**, 260–71 (2015).

128. Ramsden, D. B., Ho, P. W.-L., Ho, J. W.-M., Liu, H.-F., So, D. H.-F., Tse, H.-M., Chan, K.-H. & Ho, S.-L. Human neuronal uncoupling proteins 4 and 5 (UCP4 and UCP5): structural properties, regulation, and physiological role in protection against oxidative stress and mitochondrial dysfunction. *Brain Behav.* **2**, 468–78 (2012).

129. Lee, J., Song, J., Kwon, K., Jang, S., Kim, C., Baek, K., Kim, J. & Park, C. Human DJ-1 and its homologs are novel glyoxalases. *Hum. Mol. Genet.* **21**, 3215–3225 (2012).

130. Thornalley, P. J., Langborg, A. & Minhas, H. S. Formation of glyoxal, methylglyoxal and 3-deoxyglucosone in the glycation of proteins by glucose. *Biochem. J.* **344 Pt 1**, 109–16 (1999).

131. Münch, G., Lüth, H. J., Wong, A., Arendt, T., Hirsch, E., Ravid, R. & Riederer, P. Crosslinking of alpha-synuclein by advanced glycation endproducts--an early pathophysiological step in Lewy body formation? *J. Chem. Neuroanat.* **20**, 253–7 (2000).

132. Richarme, G. & Dairou, J. Parkinsonism-associated protein DJ-1 is a bona fide deglycase. *Biochem. Biophys. Res. Commun.* **483**, 387–391 (2017).

133. Bonifati, V., Rizzu, P., Squitieri, F., Krieger, E., Vanacore, N., van Swieten, J. C., Brice, A., van Duijn, C. M., Oostra, B., Meco, G. & Heutink, P. DJ-1(PARK7), a novel gene for autosomal recessive, early onset parkinsonism. *Neurol. Sci.* **24**, 159–160 (2003).

134. Taipa, R., Pereira, C., Reis, I., Alonso, I., Bastos-Lima, A., Melo-Pires, M. & Magalhães, M. DJ-1 linked parkinsonism (PARK7) is associated with Lewy body pathology. *Brain* **139**, 1680–1687 (2016).

135. Liu, F., Nguyen, J. L., Hulleman, J. D., Li, L. & Rochet, J.-C. Mechanisms of DJ-1 neuroprotection in a cellular model of Parkinson's disease. *J. Neurochem.* **105**, 2435–2453 (2008).

136. Zondler, L., Miller-Fleming, L., Repici, M., Gonçalves, S., Tenreiro, S., Rosado-Ramos, R., Betzer, C., Straatman, K. R., Jensen, P. H., Giorgini, F. & Outeiro, T. F. DJ-1 interactions with α-synuclein attenuate aggregation and cellular toxicity in models of Parkinson's disease. *Cell Death Dis.* **5**, e1350 (2014).

137. Zhou, W., Zhu, M., Wilson, M. A., Petsko, G. A. & Fink, A. L. The oxidation state of DJ-1 regulates its chaperone activity toward alpha-synuclein. *J. Mol. Biol.* **356**, 1036–48 (2006).

138. De Miranda, B. R., Rocha, E. M., Bai, Q., El Ayadi, A., Hinkle, D., Burton, E. A. & Timothy Greenamyre, J. Astrocyte-specific DJ-1 overexpression protects against rotenone-induced neurotoxicity in a rat model of Parkinson's disease. *Neurobiol. Dis.* **115**, 101–114 (2018).

139. Paterna, J.-C., Leng, A., Weber, E., Feldon, J. & Büeler, H. DJ-1 and Parkin Modulate Dopamine-dependent Behavior and Inhibit MPTP-induced Nigral Dopamine Neuron Loss in Mice. *Mol. Ther.* **15**, 698–704 (2007).

140. Batelli, S., Invernizzi, R. W., Negro, A., Calcagno, E., Rodilossi, S., Forloni, G. & Albani, D. The Parkinson's Disease-Related Protein DJ-1 Protects Dopaminergic Neurons in vivo and Cultured Cells from Alpha-Synuclein and 6-Hydroxydopamine Toxicity. *Neurodegener. Dis.* **15**, 13–23 (2014).

141. Usenovic, M., Tresse, E., Mazzulli, J. R., Taylor, J. P. & Krainc, D. Deficiency of ATP13A2 leads to lysosomal dysfunction, α-synuclein accumulation, and neurotoxicity. *J. Neurosci.* **32**, 4240–6 (2012).

142. Dehay, B., Ramirez, A., Martinez-Vicente, M., Perier, C., Canron, M.-H., Doudnikoff, E., Vital, A., Vila, M., Klein, C. & Bezard, E. Loss of P-type ATPase ATP13A2/PARK9 function induces general lysosomal deficiency and leads to Parkinson disease neurodegeneration. *Proc. Natl. Acad. Sci.* **109**, 9611–9616 (2012).

143. Usenovic, M., Tresse, E., Mazzulli, J. R., Taylor, J. P. & Krainc, D. Deficiency of ATP13A2 leads to lysosomal dysfunction, α-synuclein accumulation, and neurotoxicity. *J. Neurosci.* **32**, 4240–6 (2012).

144. Gitler, A. D., Chesi, A., Geddie, M. L., Strathearn, K. E., Hamamichi, S., Hill, K. J., Caldwell, K. A., Caldwell, G. A., Cooper, A. A., Rochet, J.-C. & Lindquist, S. α-Synuclein is part of a diverse and highly conserved interaction network that includes PARK9 and manganese toxicity. *Nat. Genet.* **41**, 308–315 (2009).

145. Dirr, E. R., Ekhator, O. R., Blackwood, R., Holden, J. G., Masliah, E., Schultheis, P. J. & Fleming, S. M. Exacerbation of sensorimotor dysfunction in mice deficient in Atp13a2 and overexpressing human wildtype alpha-synuclein. *Behav. Brain Res.* **343**, 41–49 (2018).

146. Kett, L. R., Stiller, B., Bernath, M. M., Tasset, I., Blesa, J., Jackson-Lewis, V., Chan, R. B., Zhou, B., Di Paolo, G., Przedborski, S., Cuervo, A. M. & Dauer, W. T. -Synuclein-Independent Histopathological and Motor Deficits in Mice Lacking the Endolysosomal Parkinsonism Protein Atp13a2. *J. Neurosci.* **35**, 5724–5742 (2015).

147. Schultheis, P. J., Fleming, S. M., Clippinger, A. K., Lewis, J., Tsunemi, T., Giasson, B., Dickson, D. W., Mazzulli, J. R., Bardgett, M. E., Haik, K. L., Ekhator, O., Chava, A. K., Howard, J., Gannon, M., Hoffman, E. *et al.* Atp13a2-deficient mice exhibit neuronal ceroid lipofuscinosis, limited α-synuclein accumulation and age-dependent sensorimotor deficits. *Hum. Mol. Genet.* **22**, 2067–2082 (2013).

148. Daniel, G., Musso, A., Tsika, E., Fiser, A., Glauser, L., Pletnikova, O., Schneider, B. L. & Moore, D. J. α-Synuclein-induced dopaminergic neurodegeneration in a rat model of Parkinson's disease occurs independent of ATP13A2 (PARK9). *Neurobiol. Dis.* **73**, 229–243 (2015).

149. Park, J.-S., Koentjoro, B., Veivers, D., Mackay-Sim, A. & Sue, C. M. Parkinson's disease-associated human ATP13A2 (PARK9) deficiency causes zinc dyshomeostasis and mitochondrial dysfunction. *Hum. Mol. Genet.* **23**, 2802–15 (2014).

150. Tan, J., Zhang, T., Jiang, L., Chi, J., Hu, D., Pan, Q., Wang, D. & Zhang, Z. Regulation of Intracellular Manganese Homeostasis by Kufor-Rakeb Syndrome-associated ATP13A2 Protein. *J. Biol. Chem.* **286**, 29654–29662 (2011).

151. Ramirez, A., Heimbach, A., Gründemann, J., Stiller, B., Hampshire, D., Cid, L. P., Goebel, I., Mubaidin, A. F., Wriekat, A.-L., Roeper, J., Al-Din, A., Hillmer, A. M., Karsak, M., Liss, B., Woods, C. G. *et al.* Hereditary parkinsonism with dementia is caused by mutations in ATP13A2, encoding a lysosomal type 5 P-type ATPase. *Nat. Genet.* **38**, 1184–1191 (2006).

152. Zheng, B., Liao, Z., Locascio, J. J., Lesniak, K. A., Roderick, S. S., Watt, M. L., Eklund, A. C., Zhang-James, Y., Kim, P. D., Hauser, M. A., Grünblatt, E., Moran, L. B., Mandel, S. A., Riederer, P., Miller, R. M. *et al.* PGC-1α, a potential therapeutic target for early intervention in Parkinson's disease. *Sci. Transl. Med.* **2**, 52ra73 (2010).

153. Clark, J., Reddy, S., Zheng, K., Betensky, R. A. & Simon, D. K. Association of PGC-1alphapolymorphisms with age of onset and risk of Parkinson's disease. *BMC Med. Genet.* **12**, 69 (2011).

154. Siddiqui, A., Chinta, S. J., Mallajosyula, J. K., Rajagopolan, S., Hanson, I., Rane, A., Melov, S. & Andersen, J. K. Selective binding of nuclear alpha-synuclein to the PGC1alpha promoter under conditions of oxidative stress may contribute to losses in mitochondrial function: implications for Parkinson's disease. *Free Radic. Biol. Med.* **53**, 993–1003 (2012).

155. Eschbach, J., von Einem, B., Müller, K., Bayer, H., Scheffold, A., Morrison, B. E., Rudolph, K. L., Thal, D. R., Witting, A., Weydt, P., Otto, M., Fauler, M., Liss, B., McLean, P. J., Spada, A. R. La *et al.* Mutual exacerbation of peroxisome proliferator-activated receptor γ coactivator 1α deregulation and α-synuclein oligomerization. *Ann. Neurol.* **77**, 15–32 (2015).

156. Rohas, L. M., St-Pierre, J., Uldry, M., Jager, S., Handschin, C. & Spiegelman, B. M. A fundamental system of cellular energy homeostasis regulated by PGC-1. *Proc. Natl. Acad. Sci.* **104**, 7933–7938 (2007).

157. Clark, J., Silvaggi, J. M., Kiselak, T., Zheng, K., Clore, E. L., Dai, Y., Bass, C. E. & Simon, D. K. Pgc-1α Overexpression Downregulates Pitx3 and Increases Susceptibility to MPTP Toxicity Associated with Decreased Bdnf. *PLoS One* **7**, e48925 (2012).

158. Ciron, C., Lengacher, S., Dusonchet, J., Aebischer, P. & Schneider, B. L. Sustained expression of PGC-1 in the rat nigrostriatal system selectively impairs dopaminergic function. *Hum. Mol. Genet.* **21**, 1861–1876 (2012).

159. Ciron, C., Zheng, L., Bobela, W., Knott, G. W., Leone, T. C., Kelly, D. P. & Schneider, B. L. PGC-1α activity in nigral dopamine neurons determines vulnerability to α-synuclein. *Acta Neuropathol. Commun.* **3**, 16 (2015).

160. Wareski, P., Vaarmann, A., Choubey, V., Safiulina, D., Liiv, J., Kuum, M. & Kaasik, A. PGC-1α and PGC-1β Regulate Mitochondrial Density in Neurons. *J. Biol. Chem.* **284**, 21379–21385 (2009).

161. Mudò, G., Mäkelä, J., Liberto, V. Di, Tselykh, T. V., Olivieri, M., Piepponen, P., Eriksson, O., Mälkiä, A., Bonomo, A., Kairisalo, M., Aguirre, J. A., Korhonen, L., Belluardo, N. & Lindholm, D. Transgenic expression and activation of PGC-1α protect dopaminergic neurons in the MPTP mouse model of Parkinson's disease. *Cell. Mol. Life Sci.* **69**, 1153–1165 (2012).

162. St-Pierre, J., Drori, S., Uldry, M., Silvaggi, J. M., Rhee, J., Jäger, S., Handschin, C., Zheng, K., Lin, J., Yang, W., Simon, D. K., Bachoo, R. & Spiegelman, B. M. Suppression of Reactive Oxygen Species and Neurodegeneration by the PGC-1 Transcriptional Coactivators. *Cell* **127**, 397–408 (2006).

163. Giasson, B. I., Duda, J. E., Murray, I. V, Chen, Q., Souza, J. M., Hurtig, H. I., Ischiropoulos, H., Trojanowski, J. Q. & Lee, V. M. Oxidative damage linked to neurodegeneration by selective alpha-synuclein nitration in synucleinopathy lesions. *Science* **290**, 985–9 (2000).

164. Liu, F., Hindupur, J., Nguyen, J. L., Ruf, K. J., Zhu, J., Schieler, J. L., Bonham, C. C., Wood, K. V, Davisson, V. J. & Rochet, J.-C. Methionine sulfoxide reductase A protects dopaminergic cells from Parkinson's disease-related insults. *Free Radic. Biol. Med.* **45**, 242–55 (2008).

165. Glaser, C. B., Yamin, G., Uversky, V. N. & Fink, A. L. Methionine oxidation, α-synuclein and Parkinson's disease. *Biochim. Biophys. Acta - Proteins Proteomics* **1703**, 157–169 (2005).

166. Conway, K. A., Rochet, J. C., Bieganski, R. M. & Lansbury, P. T. Kinetic Stabilization of the alpha -Synuclein Protofibril by a Dopamine-alpha -Synuclein Adduct. *Science (80-.).* **294**, 1346–1349 (2001).

167. Maltsev, A. S., Chen, J., Levine, R. L. & Bax, A. Site-Specific Interaction between α-Synuclein and Membranes Probed by NMR-Observed Methionine Oxidation Rates. *J. Am. Chem. Soc.* **135**, 2943–2946 (2013).

168. Alvarez-Castelao, B., Goethals, M., Vandekerckhove, J. & Castaño, J. G. Mechanism of cleavage of alpha-synuclein by the 20S proteasome and modulation of its degradation by the RedOx state of the N-terminal methionines. *Biochim. Biophys. Acta - Mol. Cell Res.* **1843**, 352–365 (2014).

169. Binolfi, A., Limatola, A., Verzini, S., Kosten, J., Theillet, F.-X., Rose, H. M., Bekei, B., Stuiver, M., van Rossum, M. & Selenko, P. Intracellular repair of oxidation-damaged α-synuclein fails to target C-terminal modification sites. *Nat. Commun.* **7**, 10251 (2016).

170. Wassef, R., Haenold, R., Hansel, A., Brot, N., Heinemann, S. H. & Hoshi, T. Methionine Sulfoxide Reductase A and a Dietary Supplement S-Methyl-L-Cysteine Prevent Parkinson's-Like Symptoms. *J. Neurosci.* **27**, 12808–12816 (2007).

171. Alcalay, R. N., Levy, O. A., Wolf, P., Oliva, P., Zhang, X. K., Waters, C. H., Fahn, S., Kang, U. J., Liong, C., Ford, B., Mazzoni, P., Kuo, S., Johnson, A., Xiong, L., Rouleau, G. A. *et al.* SCARB2 variants and glucocerebrosidase activity in Parkinson's disease. *npj Park. Dis.* **2**, 16004 (2016).

172. Bras, J., Guerreiro, R., Darwent, L., Parkkinen, L., Ansorge, O., Escott-Price, V., Hernandez, D. G., Nalls, M. A., Clark, L. N., Honig, L. S., Marder, K., Van Der Flier, W. M., Lemstra, A., Scheltens, P., Rogaeva, E. *et al.* Genetic analysis implicates APOE, SNCA and suggests lysosomal dysfunction in the etiology of dementia with Lewy bodies. *Hum. Mol. Genet.* **23**, 6139–46 (2014).

173. Tsuang, D. W., DiGiacomo, L. & Bird, T. D. Familial occurrence of dementia with Lewy bodies. *Am. J. Geriatr. Psychiatry* **12**, 179–88 (2004).

174. Meeus, B., Nuytemans, K., Crosiers, D., Engelborghs, S., Peeters, K., Mattheijssens, M., Elinck, E., Corsmit, E., De Deyn, P. P., Van Broeckhoven, C. & Theuns, J. Comprehensive Genetic and Mutation Analysis of Familial Dementia with Lewy Bodies Linked to 2q35-q36. *J. Alzheimer's Dis.* **20**, 197–205 (2010).

175. Ohtake, H., Limprasert, P., Fan, Y., Onodera, O., Kakita, A., Takahashi, H., Bonner, L. T., Tsuang, D. W., Murray, I. V. J., Lee, V. M.-Y., Trojanowski, J. Q., Ishikawa, A., Idezuka, J., Murata, M., Toda, T. *et al.* Beta-synuclein gene alterations in dementia with Lewy bodies. *Neurology* **63**, 805–11 (2004).

176. Fujita, M., Sugama, S., Sekiyama, K., Sekigawa, A., Tsukui, T., Nakai, M., Waragai, M., Takenouchi, T., Takamatsu, Y., Wei, J., Rockenstein, E., LaSpada, A. R., Masliah, E., Inoue, S. & Hashimoto, M. A β-synuclein mutation linked to dementia produces neurodegeneration when expressed in mouse brain. *Nat. Commun.* **1**, 110 (2010).

177. Guerreiro, R., Escott-Price, V., Darwent, L., Parkkinen, L., Ansorge, O., Hernandez, D. G., Nalls, M. A., Clark, L., Honig, L., Marder, K., van der Flier, W., Holstege, H., Louwersheimer, E., Lemstra, A., Scheltens, P. *et al.* Genome-wide analysis of genetic correlation in dementia with Lewy bodies, Parkinson's and Alzheimer's diseases. *Neurobiol. Aging* **38**, 214.e7-214.e10 (2016).

178. Masliah, E., Dumaop, W., Galasko, D. & Desplats, P. Distinctive patterns of DNA methylation associated with Parkinson disease: identification of concordant epigenetic changes in brain and peripheral blood leukocytes. *Epigenetics* **8**, 1030–8 (2013).

179. Desplats, P., Spencer, B., Coffee, E., Patel, P., Michael, S., Patrick, C., Adame, A., Rockenstein, E. & Masliah, E. Alpha-synuclein sequesters Dnmt1 from the nucleus: a novel mechanism for epigenetic alterations in Lewy body diseases. *J. Biol. Chem.* **286**, 9031–7 (2011).

180. Humphries, C. E., Kohli, M. A., Nathanson, L., Whitehead, P., Beecham, G., Martin, E., Mash, D. C., Pericak-Vance, M. A. & Gilbert, J. Integrated Whole Transcriptome and DNA Methylation Analysis Identifies Gene Networks Specific to Late-Onset Alzheimer's Disease. *J. Alzheimer's Dis.* **44**, 977–987 (2015).

181. Liu, H.-C., Hu, C.-J., Tang, Y.-C. & Chang, J.-G. A pilot study for circadian gene disturbance in dementia patients. *Neurosci. Lett.* **435**, 229–233 (2008).

182. (IPDGC), I. P. D. G. C. & (WTCCC2), W. T. C. C. C. 2. A Two-Stage Meta-Analysis Identifies Several New Loci for Parkinson's Disease. *PLoS Genet.* **7**, e1002142 (2011).

183. Moore, K., McKnight, A. J., Craig, D. & O'Neill, F. Epigenome-Wide Association Study for Parkinson's Disease. *NeuroMolecular Med.* **16**, 845–855 (2014).

184. Singh Dolt, K., Hammachi, F. & Kunath, T. Modeling Parkinson's disease with induced pluripotent stem cells harboring α-synuclein mutations. *Brain Pathol.* **27**, 545–551 (2017).

185. Maries, E., Dass, B., Collier, T. J., Kordower, J. H. & Steece-Collier, K. The role of α-synuclein in Parkinson's disease: insights from animal models. *Nat. Rev. Neurosci.* **4**, 727–738 (2003).

186. Lopes, F. M., Bristot, I. J., da Motta, L. L., Parsons, R. B. & Klamt, F. Mimicking Parkinson's Disease in a Dish: Merits and Pitfalls of the Most Commonly used Dopaminergic In Vitro Models. *NeuroMolecular Med.* **19**, 241–255 (2017).

187. Smeyne, R. J. & Jackson-Lewis, V. The MPTP model of Parkinson's disease. *Mol. Brain Res.* **134**, 57–66 (2005).

188. Neely, M. D., Davison, C. A., Aschner, M. & Bowman, A. B. From the Cover: Manganese and Rotenone-Induced Oxidative Stress Signatures Differ in iPSC-Derived Human Dopamine Neurons. *Toxicol. Sci.* **159**, 366–379 (2017).

189. Dawson, T. M. & Dawson, V. L. Neuroprotective and neurorestorative strategies for Parkinson's disease. *Nat. Neurosci.* **5**, 1058–1061 (2002).

190. Kouroupi, G., Taoufik, E., Vlachos, I. S., Tsioras, K., Antoniou, N., Papastefanaki, F., Chroni-Tzartou, D., Wrasidlo, W., Bohl, D., Stellas, D., Politis, P. K., Vekrellis, K., Papadimitriou, D., Stefanis, L., Bregestovski, P. *et al.* Defective synaptic connectivity and axonal neuropathology in a human iPSC-based model of familial Parkinson's disease. *Proc. Natl. Acad. Sci.* **114**, E3679–E3688 (2017).

191. Lim, K.-L. & Ng, C.-H. Genetic models of Parkinson disease. *Biochim. Biophys. Acta - Mol. Basis Dis.* **1792**, 604–615 (2009).

192. Ghosh, D., Sahay, S., Ranjan, P., Salot, S., Mohite, G. M., Singh, P. K., Dwivedi, S., Carvalho, E., Banerjee, R., Kumar, A. & Maji, S. K. The Newly Discovered Parkinson's Disease Associated Finnish Mutation (A53E) Attenuates α-Synuclein Aggregation and Membrane Binding. *Biochemistry* **53**, 6419–6421 (2014).

193. Perrin, R. J., Woods, W. S., Clayton, D. F. & George, J. M. Interaction of Human α-Synuclein and Parkinson's Disease Variants with Phospholipids. *J. Biol. Chem.* **275**, 34393–34398 (2000).

194. Canet-Avilés, R. M., Wilson, M. A., Miller, D. W., Ahmad, R., McLendon, C., Bandyopadhyay, S., Baptista, M. J., Ringe, D., Petsko, G. A. & Cookson, M. R. The Parkinson's disease protein DJ-1 is neuroprotective due to cysteine-sulfinic acid-driven mitochondrial localization. *Proc. Natl. Acad. Sci. U. S. A.* **101**, 9103–8 (2004).

CHAPTER 2. OPTIMIZED PRIMARY MIDBRAIN AND CORTICAL CULTURES FOR THE STUDY OF PARKINSON'S DISEASE

2.1 Introduction

PD is characterized by selective loss of dopaminergic DA neurons in the *substantia nigra,* resulting in the destruction of neuronal connections with sensorimotor regions of the putamen in the basal ganglia and leading to the disease's hallmark motor impairment[1]. Understanding the molecular underpinnings of selective nigral DA neuronal loss is a major focus of research in the PD field. Multiple lines of evidence suggest that mutations in the aSyn gene, leading to amino acid substitutions (e.g. A53T) and over-expression as a result of gene multiplication play an important role in PD pathogenesis and Lewy body pathology[2]. PD diagnosis can only be confirmed during post-mortem examination, which only addresses end-stage consequences, making it difficult to determine the onset of the disease or to describe the progression of the pathophysiological mechanisms that lead to DA cell death.

In addition to being characterized by aSyn neuropathology, post-mortem PD brains show evidence of mitochondrial dysfunction and oxidative stress, two pathomechanisms implicated in the loss of DA neurons. Exposure to pesticides that elicit oxidative stress, such as rotenone and paraquat, is associated with a high risk of developing PD[3]. Rotenone, a natural occurring compound widely used as a pesticide and piscicide, readily crosses biological membranes including the blood brain barrier as a result of its high lipophilicity. Evidence from many studies indicate that rotenone is a strong inhibitor of mitochondrial complex I that interrupts the respiratory chain and causes an incomplete electron transfer, thus leading to a decrease in the efficiency of oxidative phosphorylation together with the formation of high levels of ROS[4]. Paraquat is a broad-spectrum herbicide that also triggers the production of ROS through a redox cyclin mechanism, increasing oxidative stress and inducing the aggregation of aSyn in DA neurons[5,6]. Human exposure to paraquat has been positively associated with the development of PD[3,7]. Paraquat is structurally similar to N-methyl-4-phenyl-1,2,3,6-tetrahydropyridine molecule (MPTP), an un-intentional by-product of the narcotic meperedine that inhibits mitochondrial complex I activity and has been shown to induce its associated with PD-related neuropathology in humans and rodents[3,7–9].

Establishing experimental neuronal models that reproduce the range of neuropathological endpoints observed in PD has been challenging due to the disease's great complexity. However, primary DA neuronal models have proven useful to investigate particular aspects of PD-related neuropathology. In the complex environment of the brain, and in mixed cell cultures that reproduce key features of this biological setting, astrocytes play a key role in protecting neurons from toxicity elicited by aSyn, rotenone or paraquat[10,11]. It has been associated that oxidative stress enhace aSyn aggregation[12], and the overexpression of hey neuroprotective pathways (e.g Nrf2 or GLP1R pathways) in astrocytes represent a potential target to develop PD therapies[11,13]   Both, rotenone and paraquat are metabolized in glial cells, where they are converted to molecules comparable to the MPTP active metabolite MPP$^+$ (1-methyl-4-phenylpyridinium), a molecule that triggers mitochondrial dysfunction via potent inhibition of complex I selectively in DA neurons[14,15]. These properties have led investigators to develop preclinical models involving the administration of aSyn-encoding DNAs, aSyn preformed fibrils, or toxicans (e.g. rotenone or paraquat) to model PD-related cellular phenomena such as mitochondrial and oxidative stress[6,16–18]. *In vivo* rodent models involving exposure to these insults have been extensively studied in order to characterize neurotoxic pathways activated bythese PD stresses and explore gene-enviroment interactions that result in PD-related pathology[3,19,20,21].

Cellular models of aSyn-, rotenone-, or paraquat-mediated neurodegeneration are also highly valuable to enable analyses of neurotoxic mechanisms and screens of neuroprotective candidates with a higher throughput than can be achieved *in vivo*.

Early cognitive dysfunction, hallucinations, and depression are all part of the panel of non-motor symptoms that also affect patients with PD and other synucleinopathies[22,23]. It has been reported that these non-motor symptoms are products of deficient levels of dopamine in cortical areas of the brain[22]. A majority of experimental models for the study of PD are focused on recapitulating neuropathological events happening in the midbrain. However, there are few cellular models design to enable the investigation of the role cortical neuron deficiencies in PD pathogenesis.

Here, we describe protocols that can be used to model key features of PD pathogenesis in cell culture. With our rat primary midbrain culture we were able to identify potential neuroprotective proteins, compounds and extracts that effectively reversed toxicity elicited by aSyn-A53T and PD-related neurotoxicants[24–27]. A second culture has been stablished from rat cortical tissue, thus opening windows of investigation not only into the pathology of PD, but also that of other diseases with a decay in cortical brain activities.

2.1.1 Need for an optimized protocol

Studies based on cellular PD models are necessary to accumulate data that permit a better understanding of the disease and support *in vivo* experimental strategies. Genetic and toxin-based cellular models that consistently replicate key PD neuropathological endpoints including mitochondrial damage, oxidative stress, protein clearance dysfunction, and aSyn toxicity, are highly valuable in ongoing efforts to identify disease-modifying therapies. Ideally, a cellular model of PD should also involve neuron-glia interactions in order to recapitulate endogenous neuroprotective activities that could pontentially be enhanced as a strategy to alleviate PD neurotoxicity.

Although our initial focus was on studies involving primary cultures derived from rat mesencephalon, we have used our optimized cell dissociation protocol to prepare cultures from other regions of the embryonic rat brain (e.g. neocortex) with minimal changes in cell density or plating format. Moreover, we have adapted our protocol to prepare primary midbrain and cortical astrocytes, thus enabling the characterization of astrocytic signaling mechanisms that lead to neurotoxicity (e.g. pro-inflammatory effects) or neuroprotection (e.g. antioxidant responses)[28]. Thus, our methods for preparing primary cell cultures are versatile and well-suited to addressing a broad range of questions central to the field of CNS diseases.

2.1.2 Published work using our protocol: neurotoxic effects of mutant aSyn, rotenone, paraquat, MG132, and heterocyclic amines

We have broadly used our rat primary midbrain cultures to replicate PD-like cellular pathology caused by genetic perturbations. In early studies, midbrain cultures were used to determine the effects of over-expressing the candidate neuroprotective proteins DJ-1[19], MsrA[25], and PGC1α[20], all three of which may incur a loss of function in PD, on DA neuron death elicited by the familial aSyn mutant, A53T. More recently, we used our midbrain culture model to demonstrate the protective activity of endosulfine-alpha (ENSA) against neurotoxicity elicited by two familial aSyn mutants, A30P and G51D16. ENSA is a cAMP regulated phosphoprotein that is down-regulated in neurodegenerative diseases18, has a high affinity for membrane-bound species of aSyn[17], and interferes with membrane-induced aSyn self-assembly and aSyn-mediated vesicle disruption[16].

Our primary midbrain culture model has also been used as a toxin-based model, yielding insight into potential environmental causes of sporadic PD. Rotenone, paraquat and MG132 are neurotoxicans used to model PD cellular impairments such as mitochondrial dysfunction, oxidative stress and proteasome inactivation that promote neuronal death[3,29]. Using our primary midbrain cultures, studies from our laboratory determined the great neuroprotective potential of proteins, such as DJ-1 or MsrA, inhibiting DA neuronal loss elicited rotenone, paraquat and MG132[24,25]. Additional studies determined the neuroprotective potential of dietary-derived compounds rich in anthocyanin and proanthocyanidin (e.g. blueberry, grape seeds, blackcurrant, and Chinese mulberry) and different polyphenols found in medicinal plants extracts (e.g. hibiscus, garlic cloves, red clover flowers, June berry) rescued dopaminergic neurons from mitochondrial deficit and neurotoxicity promoted by rotenone and paraquat[27,30,31] . Dietary intake of meats cooked at high temperatures can lead to exposure to heterocyclic amines (HCAs) which metabolites were shown to pass blood brain barrier (BBB)[32]. Recently, we have found that a number of HCAs, including PhIP (2-amino-1-methyl-6-phenylimidazo[4,5-b]pyridine), IQ (2-amino-3-methylimidazo[4,5-f]quinoline), MeIQ (2-amino-3,4-dimethylimidazo[4,5-f]quinoline), MeIQx (2-amino3,8-dimethylmidazo[4,5-f]quinoxaline), 4,8-DiMeIQx (2-amino-3,4,8 trimethylimidazo[4,5-f]quinoxaline),

harmane (PhIP,1-methyl-9H-pyrido[3,4-b]indole), norharmane (9H-pyrido[3,4-b]indole), and AaC (2-amino-9H-pyrido[2,3-b]indole), are selectively toxic to DA neurons in our primary midbrain cultures22,23. These examples highlight the value of testing candidate neuroprotective proteins for their effects on DA neuron death elicited by PD-related toxicants as a strategy to discover new PD targets.

It is of our great interest to discover candidate neuroprotective strategies that can ameliorate or stop neuronal death in PD. Using our midbrain primary mix-culture model we have contributed with valuable data to characterize different neuroprotective compounds, proteins and extracts against several PD-related insults. Strategies that rescued primary DA neurons from aSyn-A53T toxicity included treatments such as: (i) the genetic inhibition of Sirtuin2, a histone deacetylase that play a role in aging, that protected dopaminergic cells from aSyn-A53T toxicity through a mechanism that suggests a neuroprotective acitivity by tubulin acetylation[33], (ii) the use of selected compounds from a 115,000 library that proven to re-established ER-to-Glgi trafficking and mitochondrial damage elicited by aSyn[34], (iii) the use of N-aryl Benzimidazole (NAB) that reversed aSyn toxicity by a mechanism that promote endosomal transport dependent on E3 ubiquitin ligase named Rsp5/Nedd4, a ER-Golgi mechanism that is affected by aSyn toxity[35], and (iv) treatments with small molecules (eg. Drug-like phenyl-sulfonamide ELN484228 or Nortiptyline) that target aSyn to avoid its misfolding and aggregation at synaptic vesicles preventing membrane disruption[36,37]. Beyond finding neuroportective candidates, our primary mix-culture contributed to the discovery of acrolein as a PD susceptibility factor that promote selective DA neuronal cell death and aSyn aggregation[38], which can represent a novel therapeutic target that can ameliorate oxidative stress and lipid peroxidation in PD.

Current research involving our primary midbrain culture model is focused on characterizing the uptake of aSyn pre-formed fibrils (aSyn PFFs) and the PFF-mediated seeded aggregation of endogenous aSyn in midbrain and cortical primary neurons. Preliminary data from primary neurons transduced with adenovirus encoding aSyn-WT and treated with PFFs showed evidence of aSyn aggregation and propagation through the

cells body and neurites as a result of PFF uptake and aSyn-WT overexpression. Ongoing experiments aim to find small molecules and petides that interfere with membrane permeabilization *in vitro* and *in vivo*, mechanism that we hypothesize enhance prion-like spreading of aSyn aggregates. Our studies of aSyn PFF transmission in primary neuronal cultures are designed to yield insight into molecular mechanisms of aSyn prion-like propagation, thus setting the stage for discovering therapies to block the spread of aSyn neuropathology in PD.

2.2 Optimized Protocol

2.2.1 Materials

Plate and coverslip coating

- Poly-L-lysine hydrobromide; attachment factors: ≥70,000 MW (MP Biomedicals, cat. no. 0215017750)
- Rat tail Collagen Type I (Corning, cat. no. 354236)
- Cell culture plates (48-well, Falcon, cat. no. 353230; 96-well black plate, Corning, cat. no. 3720, Tissue culture treated culture dish D xH 150 mm x 25 mm, Corning, cat. no. 430599)
- 70% nitric acid (Fisher, cat. no. A483-212)
- Coverslips, thickness no.1, 8 mm diameter for 48-well-plates (ProSciTech, cat. no. G401-08)
- Sterile-filtered Milli-Q H_2O suitable for cell culture (Sigma, cat. no. W3500)

Dissection

- Sprague-Dawley pregnant rat at embryonic day 17 (E17) (Envigo)
- Solution I (Table 2.2)
- Tissue culture dishes, 100 x 20 mm style (Falcon, cat. no. 353003)
- Dissection tools (Fig. 2.1):
    - Standard pattern forceps (Fine Science tools (F.S.T.), cat. no. 11000-12 (Fig. 2.1A))
    - Standard pattern scissors (F.S.T., cat. no. 14101-14 (Fig. 2.1B))

o Fine angled scissors (F.S.T., cat. no. 14063-09 (Fig. 2.1C))

o Spring scissors Moria Dowell Straight (cutting edge, 10 mm) (F.S.T., cat. no. 15372-62 (Fig. 2.1D))

o Extra fine Graefe forceps serrate curved (F.S.T., cat. no. 11152-10 (Fig. 2.1E))

o Standard scalpel #3 (F.S.T., cat. no. 10003-12 (Fig. 2.1F))

o Blade #15 (F.S.T., cat. no. 10015-00 (Fig. 2.1G))
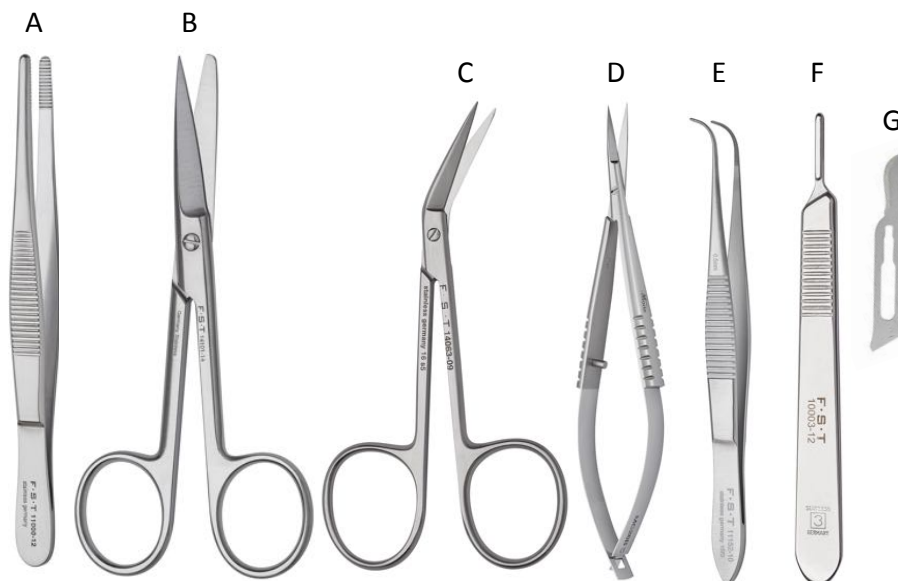
Figure 2.1. Dissection tools. A. Standard pattern forceps. B. Standard pattern scissors. C. Fine angled scissors. D. Spring scissors Moria Dowell Straight. E. Extra fine Graefe forceps serrate curved. F. Standard scalpel #3. G. Blade #15.

Cell culture preparation

- 12 to 15 midbrains or 3 cortices from E17 rat embryos

- Solution I (Table 2.2)

- Dubelcco's Modified Eagle Medium (DMEM) media (Table 2.2)

- Neurobasal media (Table 2.2)

- Trypsin from bovine pancreas (Sigma, cat. no. T8003)

- Deoxyribonuclease I (DNase), from bovine pancreas (Sigma, cat. no. D4527)

- Trypsin inhibitor, from glycine max soybean (Sigma, cat. no. T6522)

- Cytosine β-D-arabinofuranoside hydrochloride (AraC) (Sigma, cat. no. C6645)

- Sterile-filtered Milli-Q H_2O suitable for cell culture (Sigma, cat. no. W3500)

- Saline solution 0.9% (v/v)
- Cell strainer 70 μm (Falcon cat. no. 352350)
- 0.2 μm sterile syringe filter (Thermo Scientific, cat. no. 7262520)
- Cell culture-treated Falcon plates (48- and 96-well-plates), poly-L-lysine coated.
- Stericups (Millipore, cat. no. SCGPU02RE)

Cell treatments with virus or compound
- ViraPower Adenoviral Expression System (Invitrogen, cat. no K4930-00 and K4940-00)
- Adeno-X qPCR titration kit (Clontech, cat. no. 632252)
- DMEM or Neurobasal media (Table 2.2)
- Adenovirus encoding aSyn-A53T or β-galactosidase
- Rotenone (Sigma, cat no. R8875)
- Paraquat dichloride hydrate, PESTANAL analytical standard (Sigma, cat no. 36541)
- PhiP (2-Amino-1-methyl-6-phenylimidazo[4,5-b]pyridine) (Toronto Research Chemicals, cat. no. A617000)

Immunocytochemistry
- Paraformaldehyde (PFA) (Sigma, cat no. P6148)
- 1X PBS (Sigma, cat no. P5493)
- Regular fetal bovine serum (FBS) (Corning, cat. no. 35-011-CV)
- Primary and Secondary Antibodies (Table 2.1)
- 4', 6-diamidino-2-phenylindole (DAPI) (Sigma, cat. no. D9542)

Table 2.1. Antibodies			
Primary Antibodies			
Immunogen	**Host**	**Species Reactivity**	**Vendor**
Tyrosine Hydroxylase	Rabbit	Most Mammals	Phosphosolutions cat. no. 2025-T HRAB
Microtubule associated protein 2 (MAP2)	Chicken	Human, Rat, Mouse	Encor cat. no. CPCA-MAP2
Ionizing calcium binding adaptor molecule 1 (Iba1)	Rabbit	Mouse, Rat, Marmoset	Wako cat. no. NCNP24
Glial fibrillary acidic protein (GFAP)	Rabbit	Bovine, Canine, Human, Rat	Millipore cat. no. AB5804
Alpha-synuclein phosphoSerine129 EP1536Y (pSer129)	Rabbit	Mouse, Rat, Human	Abcam cat no. ab51253
Secondary Antibodies			
Fluorophore	**Host**	**Species Reactivity**	**Vendor**
IgG Alexa Fluor 488	Goat	Rabbit	ThermoFisher cat. no. A21034
IgG Alexa Fluor 488	Goat	Mouse	ThermoFisher cat. no. A32723
IgG Alexa Fluor 594	Goat	Chicken	ThermoFisher cat. no. A-11042
IgG Alexa Fluor 647	Goat	Chicken	ThermoFisher cat. no. A-21449

Instrumentation

- Vertical laminar flow hood
- Stereomicroscope (StemiDV4, Zeiss – Germany)
- Cytation 3 Cell Imaging Multi-Mode Reader (Biotek, Winooshi, VT)
- Inverted phase contrast microscope (OM900-T, Omano, USA)
- Dedicated cell culture incubator. Humidified atmosphere, 37 ºC, 5% CO_2
- Pipet-aid
- Hemocytometer

Miscellaneous

- 1.5 mL microcentrifuge tubes (Fisherbrand, cat. no. 05-408-129)
- 50 mL sterile conical tubes (Falcon, cat. no. 352098)
- 5 mL serological pipettes (Corning cat. no. CLS4487)

2.2.2   Preparation of media and solutions

! Caution - Work in a sterile laminar flow hood. Because all cell culture reagents are light sensitive, it is recommended to work with the hood lights turned off. Store solutions aliquots at -20 ºC up to a year, and culture media at 4 ºC up to 3 weeks.

- *Poly-L-lysine (10 mg/ mL stock)*: Add 3 mL of molecular grade water to the product vial containing 50 mg of poly-L-lysine. Allow poly-L-lysine to dissolve for 15 to 30 min. Add an additional 2 mL of molecular grade water into the vial, mix by pipetting, and sterilize by filtration using a 0.2 μm syringe filter. Prepare aliquots of 270 μL.
- *Trypsin (7.5 mg/mL stock)*: Dissolve 7.5 mg of trypsin in 1 mL of 0.9% (v/v) saline solution. Sterilize by filtration. Prepare aliquots of 40 μL.
- *DNase (4 mg/mL stock)*: In accordance with the quantity in the product vial, prepare a stock solution of 4 mg/mL by adding the appropriate volume of 0.9% (v/v) saline solution. Mix well, sterilize by filtration, and prepare 50 μL aliquots.
- *Trypsin inhibitor (2.7 mg/mL stock)*: Add 9 mL of 0.9% (v/v) saline solution to the product vial containing 25 mg of trypsin inhibitor. Mix by inverting more that 10 times. Sterilize by filtration, and prepare 450 μL aliquots.

- *AraC (40 mM stock)*: Carefully weigh 10.4 mg of AraC and dissolve in 929 μL of sterile-filtered H_2O. Sterilize by filtration, and prepare aliquots of 20 μL.

- *DMEM media*: Prepare 250 mL of DMEM media using the reagents listed in Table 2.2, as follows. Dissolve 2.6 g of DMEM and 0.74 g of sodium bicarbonate in Milli-Q H_2O in a beaker, adjust the pH to 7.2 using HCl, and add Milli-Q H_2O as needed so that the final volume of the solution is 200 mL. Add the following components to a 250 mL Stericup in the specified order (i.e. from lowest to highest volume to ensure proper mixing): 250 μL penicillin/streptomycin (100X), 25 mL FBS, 25 mL HS, and the pH-adjusted DMEM solution (200 mL). Mix and store at 4 °C. We recommend preparing fresh media for each animal

- *Neurobasal media (200 mL)*: Add the reagents listed in Table 2.2 to a 250 mL Stericup in the order of lowest to highest volume. Ensure proper mixing, and store at 4 °C.

- *Solution I* (Table 2.2): Dissolve glucose and BSA in Milli-Q H_2O in a beaker, adjust the pH to 7.3 using HCl, and add Milli-Q H_2O as needed so that the final volume of the solution is 90 mL. Add 10 mL of Solution I base (10X) followed by the 90 mL of glucose/BSA solution to a 250 mL Stericup, mix, and store at 4 °C. Solution I can be prepared 3 days before dissection and should be discarded after each use.

Table 2.2 Primary cell culture media and solutions				
Solution	**Components**	**Mass or Volume**	**Final Concentration**	**Vendor**
DMEM Media (pH 7.2) 250 mL	DMEM low glucose	2.6 g	1X	GIBCO Cat. No. 31-600-083
	Sodium bicarbonate	0.74 g	35.2 mM	SIGMA Cat. No S5761
	Fetal bovine serum (FBS) Premium (heat-inactivated)	25 mL	10% (v/v)	CORNING Cat. No. 35-016-CV
	Horse serum (HS)	25 mL	10% (v/v)	SIGMA Cat. No. H0146

Table 2.2 (Continued)				
	Penicillin/streptomycin (100X)	250 μL	0.1% (v/v)	GIBCO Cat. No. 15-140-122
Neurobasal Media (pH 7.2) 200 mL	Neurobasal medium	198 mL	99% (v/v)	GIBCO Cat. No. 21-103-049
	B-27 supplement	2 mL	2% (v/v)	GIBCO Cat No. A3582801
	GlutaMAX supplement	250 μL	0.25% (v/v)	GIBCO Cat No. 35-050-061
	Penicillin/streptomycin (100X)	200 μL	0.1% (v/v)	GIBCO Cat. No. 15-140-122
Solution 1 base (10X) 400 mL	Sodium chloride	40.28 g	1.85 M	SIGMA Cat. No. S7653
	Potassium chloride	2.4 g	80.5 mM	SIGMA Cat. No. P9333
	Sodium dihydrogen phosphate	0.83 g	17.5 mM	SIGMA Cat. No. 1.06370
	HEPES	35.26 g	370 mM	SIGMA Cat. No. H3375
Solution 1 (1X) 100 mL	Solution 1 base 10X	10 mL	1X	
(pH 7.3)	Glucose	0.26 g	14.5 mM	SIGMA Cat. No. D9434
	BSA	0.3 g	0.3% (w/v)	FISHER Cat. No. BP9703100

2.2.3   Preparation of coverslips and tissue culture plates

Treatment of coverslips with nitric acid – Timing: 24 h

Coverslips must be treated with nitric acid in order to remove the silicone coating that interferes with cell adherence to the glass surface. The acid also micro-etches the coverslip surface to promote cellular adhesion similar to that on a plastic substrate.

! Caution - Work in a fume hood, and do not use plastic containers.

1. In a heat-resistant glass beaker, empty an entire pack of 200 coverslips (Coverslips No.1, 0.8 mm for 48-well-plates). Wash the coverslips once with MilliQ H_2O. Decant the water, and add 70% (v/v) nitric acid, just enough to cover the coverslips. Cover the beaker with a glass lid.

2. Leave the coverslips fully immersed in 70% (v/v) nitric acid overnight in the fume hood. The next day, decant the nitric acid in a glass container, and wash the coverslips 6 times with Milli-Q H_2O, swirling very gently (10 min per wash). Remove the H_2O via aspiration with a vacuum line after each wash.

3. Cover the beaker with aluminum foil, and autoclave. Only open the autoclaved beaker in a laminar flow hood to keep the coverslips sterile.

Coating of plates and coverslips with poly-L-lysine – Timing: 1 h

The adherence of primary cells on a plastic plate depends on the nature of the plastic material and the surface coating. The best results are obtained with cell culture-treated 48- or 96-well plates from Falcon/Corning coated with poly-L-lysine. Similarly, primary cells adhere best to poly-L-lysine-coated glass coverslips (after treating the coverslips with nitric acid as outlined above).

1. Prepare a poly-L-lysine solution (40 µg/mL) in sterile-filtered H_2O. It is critical to stir the solution vigorously for at least 15 min in order to ensure complete dissolution.

2. Add a sufficient volume of the solution to cover the bottom of each well of the inner wells of the plate as illustrated in Fig. 2.2 (add sterile-filtered H_2O to the surrounding outer wells to prevent evaporation). Incubate the plate for at least 4 days at 37 °C before removing the poly-L-lysine for cell plating.

3. Where glass coverslips are needed, place each coverslip in the well of a multiwell plate using sterile forceps, and coat with poly-L-lysine as described above for at least 4 days at 37 °C.

4. On the day of cell culture preparation, wash the poly-L-lysine-coated plates, including both the inner (poly-L-lysine-coated) and the outer (uncoated) wells, with sterile-filtered H_2O. Store the plate at 37 °C prior to plating the cells.

Protocol workflow

Poly L lysine coating
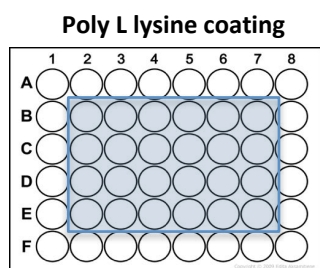
Only on inner wells of a multiwell plate.
Incubation at 37ºC for 3 days.

Dam dissection

E17 pregnant Sprague Dawley rat
euthanized by CO_2 exposure.

Fine dissection: midbrains isolation

2cm embryo   Whole brain   Midbrain
excision
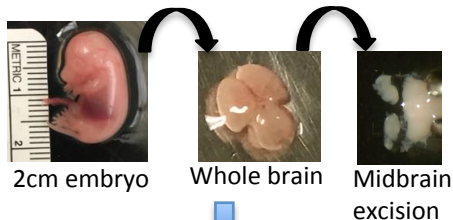
Mechanical and enzymatic cell dissociation

Incubation with trypsin at 37º C for 20 min)

Plating
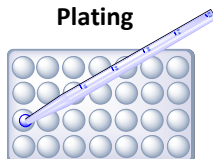
Cell suspension (54.5 x 10^4 cells/mL in
DMEM or Neurobasal media)
Growth of glial cells limited by treating
with AraC (20 µM, 37 ºC, 48 h) in the case
DMEM cultures.

Figure 2.2. Protocol workflow. Corning/Falcon tissue culture treated sterile plates, with or without coverslips (nitric acid-treated), are coated with poly-L-lysine and incubated at 37 °C for at least 3 days. Only inner wells (blue shading) are treated. It is important to fill the outer wells with water in order to maintain high humidity. An adult Sprague Dawley dam at embryonic day 17 (E17) is euthanized with exposure to CO_2 gas and embryos are harvested. Brains are extracted from 2 cm embryos, and midbrains are isolated with the assistance of a stereo microscope. Midbrains are mechanically and enzymatically dissociated using trypsin. Cells suspended in primary culture media are plated in wells of the treated multiwell plate.

2.2.4   Dissections

Dam dissection – Timing: 35 min

Dissection of the pregnant dam must be carried out inside a vertical laminar flow hood disinfected with ethanol, and all dissection tools must be autoclaved before starting the procedure. Our protocol was approved by the Purdue Animal Care and Use Committee.

1. Add 11 mL of solution I (Table 2.2) to each of two 10 cm dishes and 5 mL of solution I to a 50 mL conical tube .

2. Euthanize the pregnant dam using a CO_2 chamber with a two-step exposure: half influx (~6 L/min) for 2 min, followed by maximum influx (~12 L/min) for 3 min. Ensure that the rat is dead by confirming the loss of a withdrawal response to a toe pinch.

3. Start the rat dissection by making a horizontal incision in the lower abdomen using standard scissors. Cut the uterus membrane, and separate the embryos from the placenta using angled scissors. Transfer the embryos to a 10 cm dish containing solution I (Figs. 2.3A, B).

4. Remove each embryo from its surrounding amniotic sac by cutting with scissors (Figs. 2.3C-E).

5. Use fine spring scissors to cut the thin skull of each embryo along the entire length of the midline, and remove the brain. Transfer the brain to the second 10 cm dish containing solution I (Figs. 2.3F- H).
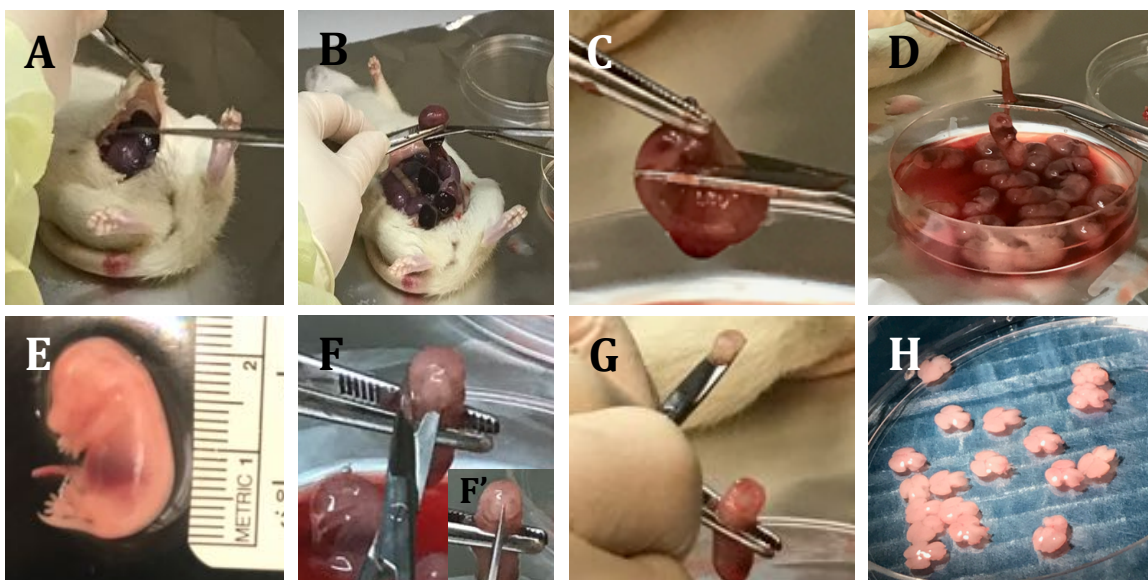
Figure 2.3. Procedure for collecting embryos from a pregnant dam. A. After cleaning the abdominal region with ethanol, the uterus is exposed by making an epidermal incision at the lower ventral portion of the abdomen. B. After opening the uterus walls, the embryos are separated from the placenta with a single cut between them. C-D. Forceps are used to hold the amniotic sac and gently push the the embryo out from the sac. E. 2 cm embryo is a typical size for E17 embryos, and variation in the embryo size may be indicative of an error in the pregnancy stage reported by the vendor. F. The embryo is held gently under the neck, and spring scissors are used to isolate the brain by: (i) cutting all the way through the base of the brain (F), and (ii) cutting the thin skull membrane through the mid dorsal region (F'). G. The whole brain is removed from the skull. H. The brains are transfered to fresh solution I (Table 2.2) for the subsequent fine dissection.

Fine dissection: midbrain isolation – *Timing: 35 min*

1. Place the brains with the dorsal side up on the stage of a stereomicroscope. Holding the hindbrain with forceps, gently fold each cortical hemisphere outward using a sterile scalpel blade to expose the midbrain (Figs. 2.4A, B).

2. Use a scalpel blade to separate the cortex from the midbrain following the tracings in Fig. 2.4C.

3. Again holding the hindbrain with forceps, remove the most anterior region of the midbrain, which contains the *substantia nigra* and part of the ventral tegmental area (Figs. 2.4D, E).

4. Remove the hindbrain from the remaining part of the midbrain (Fig. 2.4F).
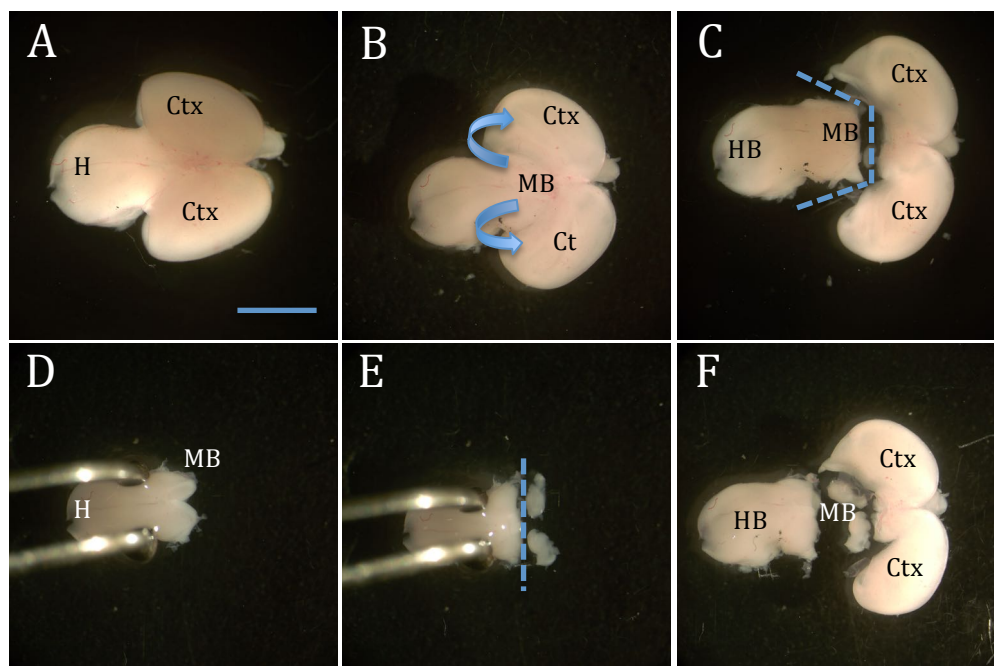
Figure 2.4. Steps for fine dissection of midbrains. A. The whole brain is positioned dorsally so that both hemispheres of the cortex (Ctx) are visible in front of the hindbrain (HB). B. The cortex hemispheres are gently opened towards the side (blue arrows), exposing the midbrain (MB). C. The cortex is removed from the remainder of the brain with three straight incisions (dashed blue lines) around the midbrain. D. The edges of the midbrain are trimmed to remove cortical tissue. E. The midbrain is excised from the hind brain with straight cuts (dashed blue line). F. Image showing embryonic rat brain sectioned into hindbrain, midbrain and cortex regions. The midbrain and cortex can be used for cell dissociation and plating. Images generated with a Leica MZFLIII stereo-microscope; scale bar in A: 5 mm.

2.2.5 Cell dissociation and plating– *Timing: 3 h*

1. Transfer the isolated midbrains into 50 mL conical tubes containing 5 mL of solution I.

2. Add 13.5 μL of trypsin (7.5 mg/ mL) to carry out enzymatic cell dissociation of 12 to 15 midbrains. With a 5 mL serological pipette fixed to an automatic pipet-aid set at fast release speed and medium intake peed, pipet up and down 15 times, making sure that the liquid is dispensed with some force against the inner wall of the conical tube in order to achieve a mechanical cell dissociation.

3. Incubate the tissue in a 37 °C water bath for 10 min.

4. Repeat the mechanical dissociation by pipetting 15 times, and incubate at 37 °C for another 10 min.

5. Repeat the mechanical dissociation, pipetting up and down 15 times.

6. Add 10 µL of DNase (4 mg/mL) and 200 µL of trypsin inhibitor (2.7 mg/mL). Mix by pipetting up and down. From this point, no additional cell dissociation will occur.

7. Centrifuge the samples at 180 x g (1,000 rpm) for 10 min. Decant the supernatant, and resuspend the pellet in 5 mL of solution I (10 mL for cortical tissue).

8. Transfer the sample to a new 50 mL conical tube by passing the liquid through a 70 µm cell strainer to filter out any remaining pieces of intact tissue. Wash the strainer with 2 mL of solution I in order to improve the yield.

9. Centrifuge the filtered cell suspension at 353 x g (1,400 rpm) for 6 min. Remove the supernatant by aspiration, and re-suspend the pellet in 5 mL of DMEM or Neurobasal media for midbrain cells or 10 mL of Neurobasal media for cortical cells.

10. Determine the cell yield by counting the cells using a hemocytometer, and adjust the volume of the cell suspension with media to achieve a concentration of 545,000 cells/mL.

11. Plate 170 µL or 330 µL of cell suspension (5.45×10^5 cells/ mL) in the inner wells of a 48- or 96-well plate, respectively, and fill the surrounding outer wells with sterile-filtered H_2O to prevent evaporation.

12. Place the plates at 37 °C in a cell culture incubator supplied with 5.5% (v/v) CO_2.

13. After 5 days, the cells should be attached to the bottom of the well or to the coverslip, and astrocytes should cover the entire surface.

14. To control the growth of astrocytes and microglia in cultures incubated in DMEM media, treat the cells with 17 to 20 µM AraC (the AraC concentration can be adjusted depending on the astrocyte density: 20 mM AraC at 90% confluence).

2.2.6   Pure primary cortical astrocytes culture

Neurons have low attachment affinity in presence of rat-tail collagen that in turn favors astrocytes attachment.

1. Coat cell culture dishes with 20 µg / ml rat-tail collagen diluted in 10 mL 0.02 N acetic acid. Allow coating for at least 30 min at 37 ºC.

2. Wash the cell culture dish with sterile MilliQ H_2O and plate the cortical cell suspension (prepared with the cell dissociation protocol).

3. Allow cells attachment for 48 h. Wash off neurons with periodical washes with fresh media every two days, for a total of 8 days after plating.

4. Use pure astrocytes culture or collect cell suspension in freezing media (DMEM + 5% DMSO). Store astrocytes at -80 ºC.

2.2.7 Cell treatments

Primary midbrain cultures are treated with neurotoxic or neuroprotective agents 7 to 10 days after plating.

Viral transduction – Timing: 72 h

For viral transductions, adenoviruses encoding aSyn variants (e.g. aSyn-A53T) or β-galactosidase (a control to exclude non-specific effects of viral transduction) are produced using the ViraPower Adenoviral Expression System, as described previously[24,39]. Adenoviral titers are determined using the AdenoX pPCR titration kit.

1. Thaw and maintain stock virus suspensions on ice.
2. Calculate the volume of stock virus suspension to add to the cells using the formula:

$$\text{volume} = \text{No. of cells x MOI/virus titer}$$

where MOI is the multiplicity of infection (number of viral particles per cell).

3. Pre-warm primary cell culture media. Prepare diluted virus suspension for each treatment in a 1.5 mL microcentrifuge tube, diluting the stock virus suspension into media to yield a minimum total volume of 300 µL or 200 µL for treatments carried out in 48- or 96-well plates, respectively. Mix gently by pipetting.

4. Remove the media from each well by aspiration, and replace with diluted virus suspension by gently pipetting the liquid against the inner wall of the well. This step should be carried out one well at a time to avoid drying out the cells.

5. Incubate the plate for 72 h.

6. Replace the treatment media with pre-warmed fresh primary cell culture media, and incubate for an additional 24 h.

Exposure to neurotoxic or neuroprotective compound – Timing: 24 to 96 h

Experiments that involve exposing the cultures to a neurotoxic or neuroprotective compound include a subset of wells treated with the corresponding vehicle as a negative control. Final concentrations are prepared in a way that DMSO or vehicles different than water (e.g. ethanol) are diluted 1000x in media.

1. Pre-warm primary cell culture media (DMEM or Neurobasal)
2. Prepare treatment media as follows:
    a. *Rotenone (1 mM stock):* Mix 0.04 g of rotenone in 1 mL 100% DMSO. Prepare 20ul aliquots and store at -80 ℃.
        i. Prepare an initial 100 μM rotenone dilution by adding 10 μL of 1mM rotenone to 990 μL strerile MilliQ H_2O .
        ii. Prepare treatment media 25 nM or 50 nM rotenone by adding 25 μL or 50 μL of 100 uM rotenone, respectively, into 10 mL DMEM or Neurobasal media.
    b. *Paraquat (10 mM)*: Always prepare fresh paraquat solution by adding 2mg of paraquat into 778 μL MilliQ H_2O.
        i. Prepare 2.5 μM paraquat treatment media by adding 2.5 μL of 10 mM paraquat into 10 mL DMEM or Neurobasal media.
    c. *PhiP (10 mM Stock, prepared at Dr. Jason Cannon Lab)* Mix 2.2 mg of PhiP in 1 mL 100% DMSO. Prepare 50 μL aliquots and store at -80 ℃.
        i. Prepare an initial 100 μM dilution by adding 10 μL of 10 mM PhiP to 90 μL of MilliQ H_2O.
        ii. Prepare 1 mM PhiP treatment media by adding 10 μL of 10 mM PhiP into 990 μL of DMEM or Neurobasal.
    d. Neuroprotective compounds (10 mM Stock) Aliquots prepared in DMSO and stored at -80 ℃.

       i. Prepare an initial 100 μM dilution by adding 10 μL of 10 mM compound to 90 μL of MilliQ H_2O.

       ii. Treatment media can be prepared by sequential dilutions of 10 mM compound in DMEM or Neurobasal until the desire concentration.

3. Aspirate old media and replace with treatment media.

   a. Rotenone, paraquat or PHIP treatment should be done no less than 24 h, and can be added after 72 h of viral treatment.

   b. Neuroprotective compounds treatment should be added together with viral treatment and reinforced after 72 h for a total of 96 h exposure.

  Immunocytochemistry (ICC)

! Caution - One must work efficiently, ensuring that the cells do not dry out during the staining procedure, to obtain high-quality ICC results. Shaking of microwell plates is not recommended because this could lead to lifting of the attached cells.

1. Decant the media from the plate. Wash the cells once by adding PBS to each well and immediately decanting the liquid.

2. Fix the cells by adding 300 μ L or 200 µL of PFA (4% v/v) to each well of a 48- or 96-well plate, respectively. Incubate for 20 min at room temperature in the dark.

3. Decant the PFA fixative, and wash once with PBS. Add blocking buffer (Table 2.3) to each well, and incubate at room temperature for 1 h (or longer) in the dark.

4. Decant the blocking buffer, and add a minimum volume of 100 μ L or 50 μ L of primary antibody solution to each well of a 48- or 96-well plate, respectively. Primary antibodies are diluted in PBS supplemented with BSA (1% w/v) as follows:

   a. For neuron viability analysis: rabbit anti-TH (1:1000) + chicken anti-MAP2 (1:2000).

   b. For combined neuron and glial cell analysis: (i) neurons and astrocytes: chicken anti-MAP2 (1:2000) + moue anti-GFAP (1:500); (ii) neurons and microglia: chicken anti-MAP2 (1:2000) + rabbit anti-IBA1 (1:100).

   c. For analyses of aSyn aggregation: rabbit anti-pSer129 (EP1536Y) (1:500) + chicken anti-MAP2 (1:2000)

5. Incubate overnight at 4ºC.

6. Decant primary antibody solution, and wash twice with PBS.

7. Add a minimum volume of 100 μ L or 50 μ L of secondary antibody solution to each well of a 48- or 96-well plate, respectively. Secondary antibodies are diluted in PBS supplemented with BSA (1% w/v) as follows:

    a. For neuron viability analysis: anti-rabbit IgG Alexa 488 (1:2000) + anti-chicken IgG Alexa 594 (1:2000).

    b. For combined neuron and glial cell analysis: (i) neurons and astrocytes: anti-chicken IgG Alexa 594 (1:2000) + anti-mouse IgG Alexa 488 (1:2000); (ii) neurons and microglia: anti-chicken IgG Alexa 594 (1:2000) + anti-rabbit IgG Alexa 488 (1:2000).

    c. For analyses of aSyn aggregation: anti-chicken IgG Alexa 647 (1:2000) + anti-rabbit IgG Alexa 488 (1:2000).

8. Incubate at room temperature for 1 h in the dark.

9. Decant secondary antibody solution, and wash three times with PBS.

10. Incubate with DAPI (500 nM in PBS) for 10 min. Wash twice with PBS (if necessary, the cells can be stored at this stage in PBS at 4ºC).

11. Acquire images using a plate reader. When using a Cytation 3 Cell Imaging Multi-Mode Reader equipped with a 4X objective, 16 and 12 images are generated for each well of a 48- or 96-well plate, respectively.

Table 2.3 ICC Buffers and Solutions

Solution	Components	Final Concentration	Vendor
Blocking Buffer	PBS	1X	SIGMA Cat. No. P5493
	BSA	1% (w/v)	Fisher brand Cat. No. BP9700
	Fetal Bovine Serum (FBS)	10% (v/v)	CORNING Cat. No. 35-011-CV
	Triton X-100	0.3% (v/v)	SIGMA Cat. No. X100
Primary and Secondary Antibody solutions	PBS	1X	SIGMA Cat. No. P5493
	BSA	1% (w/v)	Fisher brand Cat. No. BP9700

2.2.7.1   DA neuron counting

Images of primary midbrain cultures stained for MAP2 and TH are generated by the Cytation 3 Cell Imaging Multi-Mode Reader equipped with a 4X objective and scored for relative DA neuron viability as described before[24,39]. MAP2$^+$ and TH$^+$ primary neurons are counted by an investigator blinded to the experimental treatments. A total of 16 and 12 fields are analyzed from each well of a 48- or 96-well plate, respectively. Around 3000 or 2000 MAP2$^+$ neurons per well of a 48- or 96-well plates (respectively) are counted, and at least 3 biological replicates are carried out for each experiment. The data are expressed as the percentage of MAP2$^+$ neurons that also show immunoreactivity for TH.

2.2.7.2   Neurite length analysis

Neurite length analysis is performed on the same set of images as those used to assess relative DA cell viability[26,39]. Lengths of MAP2$^+$/TH$^+$ neurites are recorded for ~100 neurites extending from ~40 neurons (i.e. only neurons with an intact cell body) per well. Measurements are carried out by an investigator blinded to the experimental treatments using the Nikon NIS elements analysis software (Nikon Instruments), neurite lengths were calculated based on a calibration measurement that determine that each pixel correspond to 1.6 μm.

2.2.7.3   Glial cell counting

Images of primary midbrain or cortical cultures stained for the astrocytic marker GFAP or the microglial marker IBA1 4X are generated by the Cytation 3 Cell Imaging Multi-Mode Reader equipped with a 4X objective. Stitched images of entire wells (4x4 fields in a 48 well-plate or 3x4 fields in a 96 well-plate) are analyzed using the BioTek GEN 5 data analysis software. The intensity threshold is set to 5000 arbitrary units, and the diameter range of scored circular objects in the GFP (green) channel is set to 5 to 150 μm. Total cell numbers are plotted and analyzed for statistically significant differences among different treatment groups using GraphPad Prism software.

2.2.8   Troubleshooting

Table 2.4 Protocol Troubleshooting			
Procedure	Problem	Potential Reason	Solution
Cell culture	The cell yield is low.	1. The time taken for the dissection is excessive, leading to cell death during the procedure. 2. Cell dissociation is incomplete.	1. Keep track of the dissection time; the whole procedure should not take longer than 30 min. *2.* Increase the trypsin concentration and the number of times that the cell suspension is pipetted up and down.

Table 2.4 (Continued)			
	Cells die before attaching to the well.	1. The pH of the primary cell culture media is incorrect. 2. Reagents are expired or compromised. 3. Excessive force is used during pipetting.	1. Ensure that a carefully calibrated pH meter is used to adjust the media pH. 2. Do not use expired, discolored, or precipitated reagents. 3. Calibrate the pipettor to release at medium speed, and be sure to use a 5 ml serological pipette.
	Cells do not attach to the bottom of the well.	1. The poly-L-lysine solution is prepared incorrectly. 2. The surface of the plates or coverslips is incompatible with neuron adherence.	1. Ensure that the poly-L-lysine solution is stirred for at least 15 min, and/or increase the poly-L-lysine concentration. *2.* Neuron adherence depends on the nature of the plastic or glass surface. We recommend using Falcon/Corning products, and treating glass coverslips with nitric acid.
	Cells die after AraC treatment.	1. The AraC concentration is incorrect. 2. Astrocytes are treated with AraC too early.	1. Use a high-precision balance to weigh the AraC. 2. Verify that astrocytes cover 80% of the well surface before treating with AraC.
	Cells are contaminated.	1. The cells are exposed to non-sterile conditions.	1. All instruments, incubators, and tools required for the cell culture preparation must be properly sterilized and used exclusively for this protocol. Do not perform any other experiments nearby during the cell dissociation.

Table 2.4 (Continued)			
Viral transduction	Viruses encoding neurotoxic proteins fail to elicit neuronal death.	1. Viral titers are lower than expected.	*1.* Avoid freeze-thaw cycles of viral suspension, as these cycles can reduce the titer and infection efficiency. Prepare working viral dilutions, and avoid reusing any remaining diluted suspension.
ICC	The fluorescence signal is low or absent.	1. The cell permeabilization is insufficient. 2. The combination of primary and secondary antibodies is incorrect. The time taken for immunocytochemical staining is excessive, leading to drying of the cells.	1. Ensure that the volume of Triton X-100 introduced during the cell permeabilization is correct. 2. Ensure that the species specificity of the secondary antibody matches the species of the primary antibody host. 2. Use a multichannel pipette to reduce the staining time.
	Cells are lifted from the well surface.	3. 1. Excessive force is used during pipetting.	3. Gently pipet ICC solutions against the inner wall of the well so that the liquid flows gently on the cell layer.

2.3 Results

2.3.1 Characterization of rat primary midbrain cultures

To assess the cellular composition of our primary cultures obtained from embryonic rat midbrain, we routinely stain the cells for specific markers to detect different cell populations (Fig. 2.5A): i) MAP2, a protein that is expressed only in neuronal cells and is localized specifically in cell bodies and dendrites, constitutes an excellent marker of the neuronal subpopulation in mixed neuron-glia cultures; ii) TH, an enzyme involved in the biogenesis of the dopamine metabolic precursor L-DOPA, is expressed only in catecholaminergic neurons (i.e. DA neurons in the case of cultures derived from rat SNpc); iii) GFAP, a protein expressed in glial cells, particularly in astrocytes; and iv)

IBA1, a microglial marker broadly used in the analysis of neuroinflammatory responses by microglia activation[40]. The fact that all four of these cell populations are observed in our cultures highlights the complexity of this cellular model and underscores the suitability of these cultures for testing cellular events involving interactions among neurons and glial cells.

A dense, flat layer of astrocytes and microglia, consisting of between 4,000 and 6,000 cells per well (Fig. 2.5A,B), is typically observed in primary midbrain cultures grown in DMEM. Both glial cell populations support the spreading of neurons during the first 7 days of culture (Fig. 2.5C). DA neurons account for approximately 4 to 6% of MAP2$^+$ neurons in midbrain cultures prepared in DMEM (Fig. 2.5B).
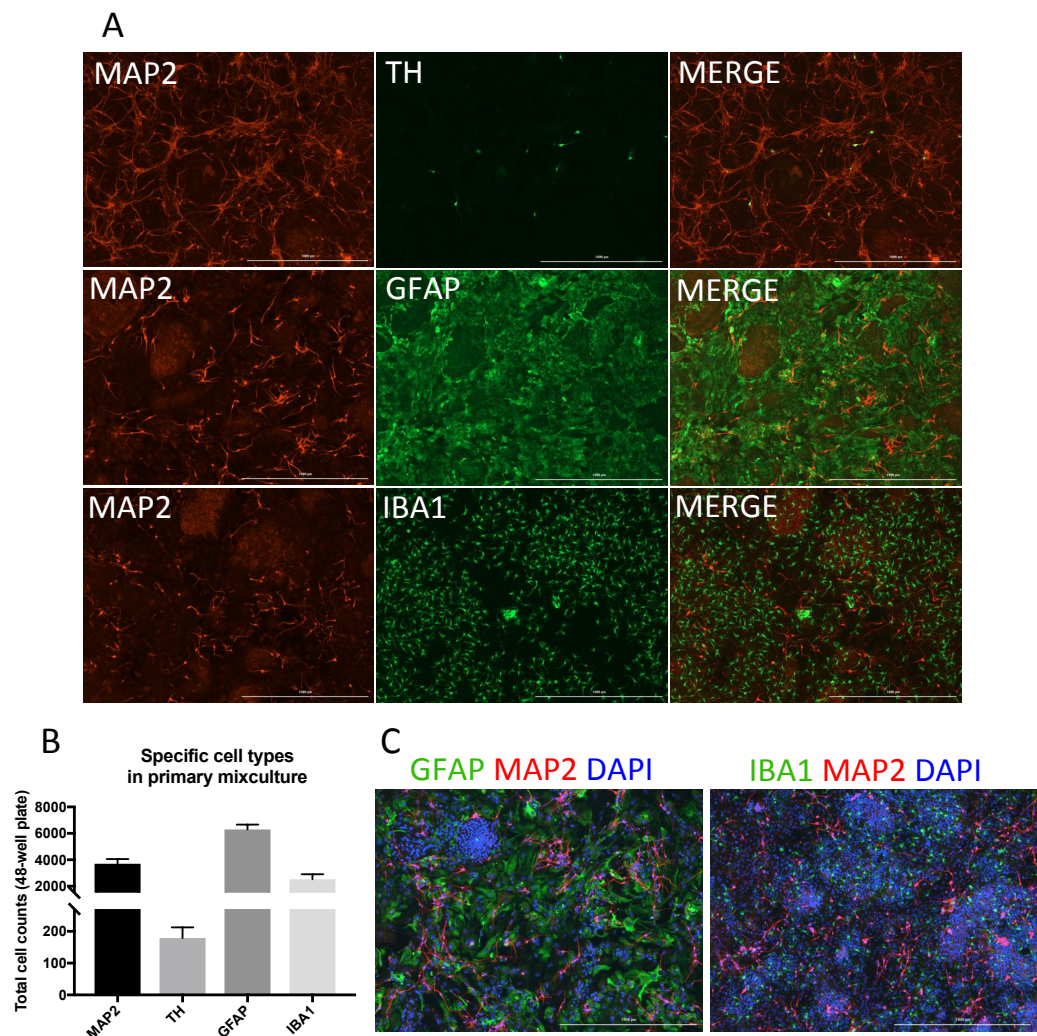
*Figure 2.5

*Figure 2.5. Characterization of rat primary midbrain cultures prepared in DMEM media. A. Representative images of primary midbrain cultures stained immunocytochemically for the following cell type-specific markers: MAP2, a neuronal marker; TH, a DA neuron-specific marker; GFAP, an astrocytes marker; and IBA1, a microglia marker. Merged images show the co-localization of MAP2 and TH (A), and the distribution of astrocytes (middle) or microglia (bottom) surrounding the neurons. B. Graph showing the mean number of cells of different types in untreated cultures grown in 48 well plates C. Representative images of primary midbrain cultures stained for MAP2 and GFAP (left), or MAP2 and IBA1 (right); nuclei in both images are stained with DAPI (blue). Images were taken with a Citation 3 Cell Imaging Multi-Mode Reader equipped with a 4x objective; green LED, 488 nm; red LED, 594 nm; blue LED, 330 nm; scale bar, 1000 μm.

Primary midbrain cultures prepared in Neurobasal media are characterized by MAP2$^+$/TH$^+$ neurons with very long neurites organized in an intricate network (Fig. 2.6A), abundant star-shaped astrocytes (Fig. 2.6B), and scarce microglia (Fig. 2.6C). In addition, cultures prepared in Neurobasal media have an increased ratio of neurons to glial cells as compared to cultures prepared in DMEM media. As published before[41], our Neurobasal + B27 serum free medium favored long term cultures with high neuronal survival and diminished glial cell population.
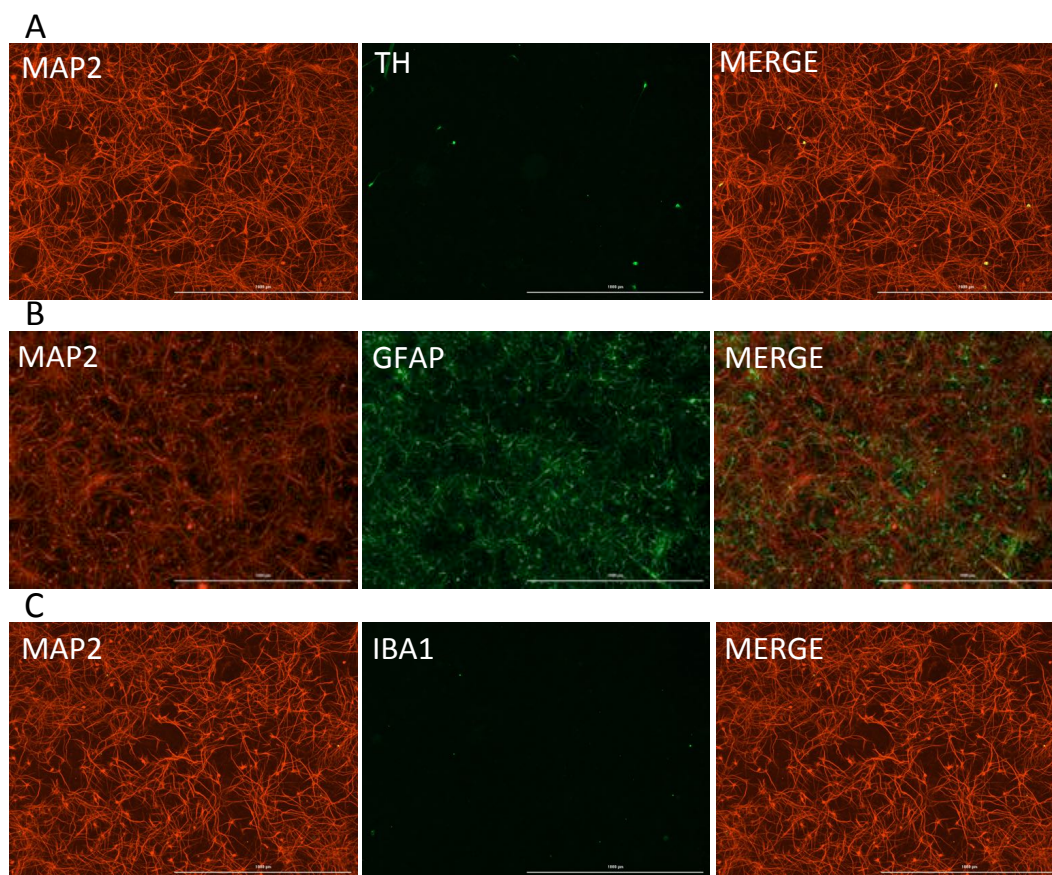
*Figure 2.6

*Figure 2.6. Characterization of rat primary midbrain cultures prepared in Neurobasal media. Representative images primary midbrain cultures stained immunocytochemically for the following cell type-specific markers: MAP2, a neuronal marker; TH, a DA neuron-specific marker; GFAP, an astrocytes marker; and IBA1, a microglia marker. Merged images show the co-localization of MAP2 and TH (A), and the distribution of astrocytes (B) or microglia (C) surrounding the neurons. B. Image of GFAP$^+$ astrocytes with characteristic star shape. Merged image shows the distribution of astrocytes with surrounding is showing neurons C. Microglia growth is not supported by Neurobasal media. Images were taken with a Citation 3 Cell Imaging Multi-Mode Reader equipped with a 4x objective; green LED, 488 nm; red LED, 594 nm; blue LED, 330 nm; scale bar, 1000 μm.

2.3.2   Characterization of rat primary cortical culture

Primary cultures obtained from embryonic rat cortices have similar features to primary midbrain primary cultures prepared in Neurobasal media: i) presence of a high density general neuronal population with long processes (Fig. 2.7A and B), ii) abundant star-shaped astrocytes (Fig. 2.7A) and iii) apparent absence of microglia cells populations (Fig. 2.7B).
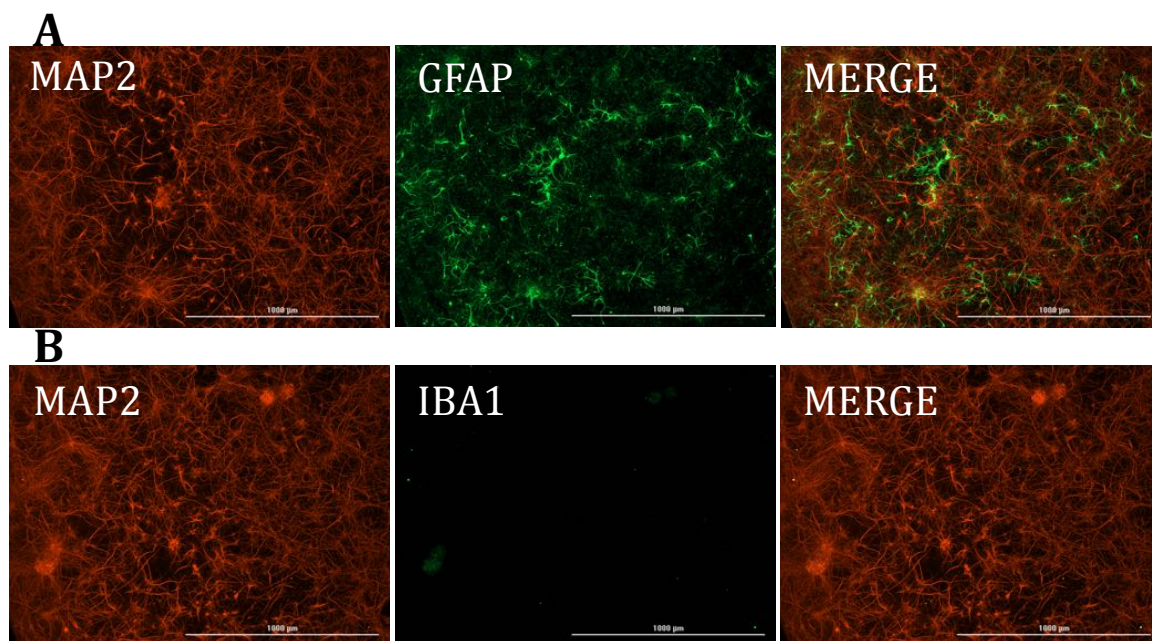
Figure 2.7. Characterization of rat primary cortical culture prepared in Neurobasal media. Representative images primary midbrain cultures stained immunocytochemically for the following cell type-specific markers: MAP2, a neuronal marker; GFAP, an astrocytes marker; and IBA1, a microglia marker. Merged images show the distribution of astrocytes (A) or microglia (B) surrounding the neurons. A. Image of GFAP$^+$ astrocytes with characteristic star shape GFAP. B. Microglia growth is not supported by Neurobasal media. Merged image shows the presence of MAP2$^+$ neurons. Images were taken with a Citation 3 Cell Imaging Multi-Mode Reader equipped with a 4x objective; green LED, 488 nm; red LED, 594 nm; blue LED, 330 nm; scale bar, 1000 μm.

2.4 Glial cell growth control: DMEM media supplemented with AraC versus Neurobasal media

Careful control of glial cell density is crucial to ensure proper glial/neuronal communication, a phenomenon that plays an important role in neuroprotective mechanisms.[42–44] Moreover, excessive growth of glial cells may result in the over-production of toxic bio-products, such as ROS, that could exacerbate oxidative stress and trigger cell death[45–48]. In order to control glial cell over-growth, DMEM cultures are treated with AraC, an anti-mitotic drug that target dividing glial cells and halts post-mitotic neurons. Primary midbrain cultures treated with AraC for 24 or 48 h show a time-dependent decrease in the density of astrocytes (Fig. 2.8A and B) and microglia (Fig. 2.8A and C), with little evidence of dose-dependence when comparing the effects of 17 versus 20 μM AraC. In contrast, the neuronal population is not affected by the AraC treatment (Fig. 2.8A and D).
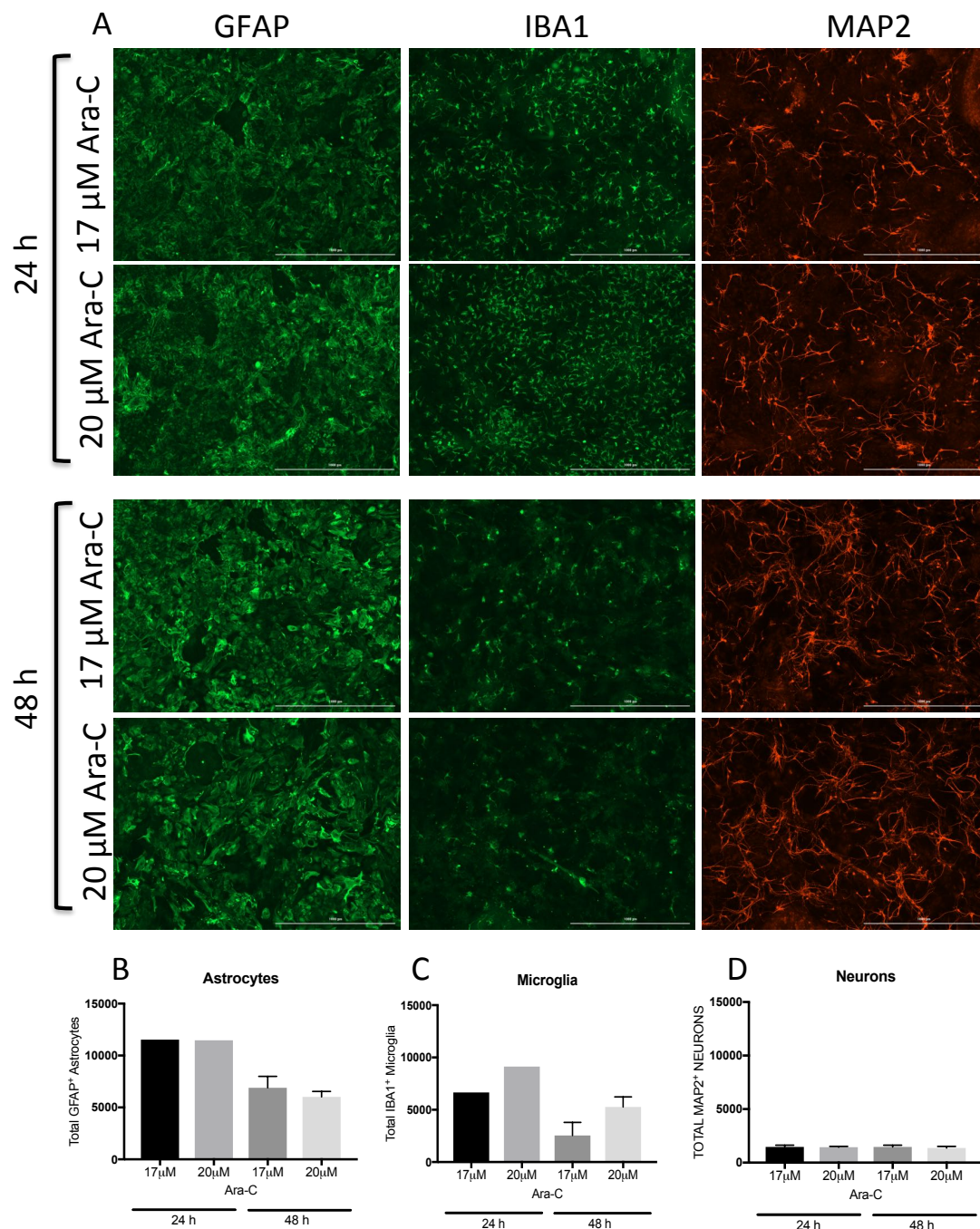
Figure 2.8. Effects of AraC treatment on the composition of rat primary midbrain cultures prepared in DMEM media. A. Representative immunofluorescence images of primary midbrain cultures showing the effects of treatment with AraC at two different concentrations (17 μM and 20 μM) for 24 h (top panel) and 48 h (bottom panel). B-D. Bar graphs showing total number of GFAP[+] astrocytes (B), Iba1^{+} microglia (C), and MAP2^{+} neurons (D), in cultures prepared in DMEM and treated with AraC at different concentrations for different times. The density of astrocytes and microglia can be controlled by adjusting the time of exposure to AraC, whereas the total number of neurons is not affected. (D). Images were taken with a Citation 3 Cell Imaging Multi-Mode Reader equipped with a 4x objective; green LED, 488 nm; red LED, 594 nm; blue LED, 330 nm; scale bar, 1000 μm.

Neurobasal cultures have the advantage of not requiring any intervention in order to control the glial cell population. The addition of B27 supplement to the Neurobasal media provides the conditions needed to produce cultures that are enriched with pre-natal neurons, have a reduced density of glial cells (0.5% of the whole cell population)[41], and are stable over 2 weeks. The microglial cell population is dramatically reduced in cultures prepared in Neurobasal media (Figs. 2.6 and 2.7) versus DMEM (Fig. 2.5).

We recommend that glial cell growth in DMEM cultures be controlled with a 48 h AraC treatment in order to obtain a balanced population of neuronal and glial cells, thus ensuring appropriate (potentially neuroprotective) communication among the different cell types and avoiding neurotoxicity that can result from glial cell over-growth. For cultures prepared in Neurobasal media, the number of astrocytes depends on the overall cell density, and thus one can modify the experimental conditions of these cultures just by altering the total number of cells plated.

2.4.1 Neurotoxic effects of PD-related insults in primary midbrain cultures

We define as 'PD-related insults' agents that elicit preferential toxicity to DA neurons in primary midbrain cultures, and thus recapitulate aspects of the neuropathology observed in PD patients' brains. As one approach, midbrain cultures are treated with rotenone, paraquat, or PhIP to establish toxin-based models characterized by mitochondrial dysfunction and oxidative stress[24,25,31,49–51]. Alternatively, the cultures are transduced with adenoviruses that code for human aSyn-A53T to recapitulate aSyn neurotoxicity in a genetic model. To control for non-specific toxic effects of viral transduction, a subset of cells are transduced with adenovirus coding for β-galactosidase ('LacZ'). For both the toxin-based and genetic models, neurotoxicity is measured in terms of relative DA neuron viability and the lengths of neurites extending from DA cell bodies. Representative images of cultures prepared in DMEM supplemented with AraC and subsequently exposed to rotenone, paraquat, or A53T adenovirus show evidence of preferential toxicity to DA neurons, as the number of DA cell bodies is reduced, and

neuronal extensions from surviving DA cell bodies are shortened (Fig. 2.9A). In comparison with the untreated control, midbrain cultures exposed to rotenone, paraquat, or A53T virus show a significant decrease in the percentage of TH$^+$ neurons (Fig. 2.9B) and in mean neurite lengths (Fig. 2.9C and D) [39,31].
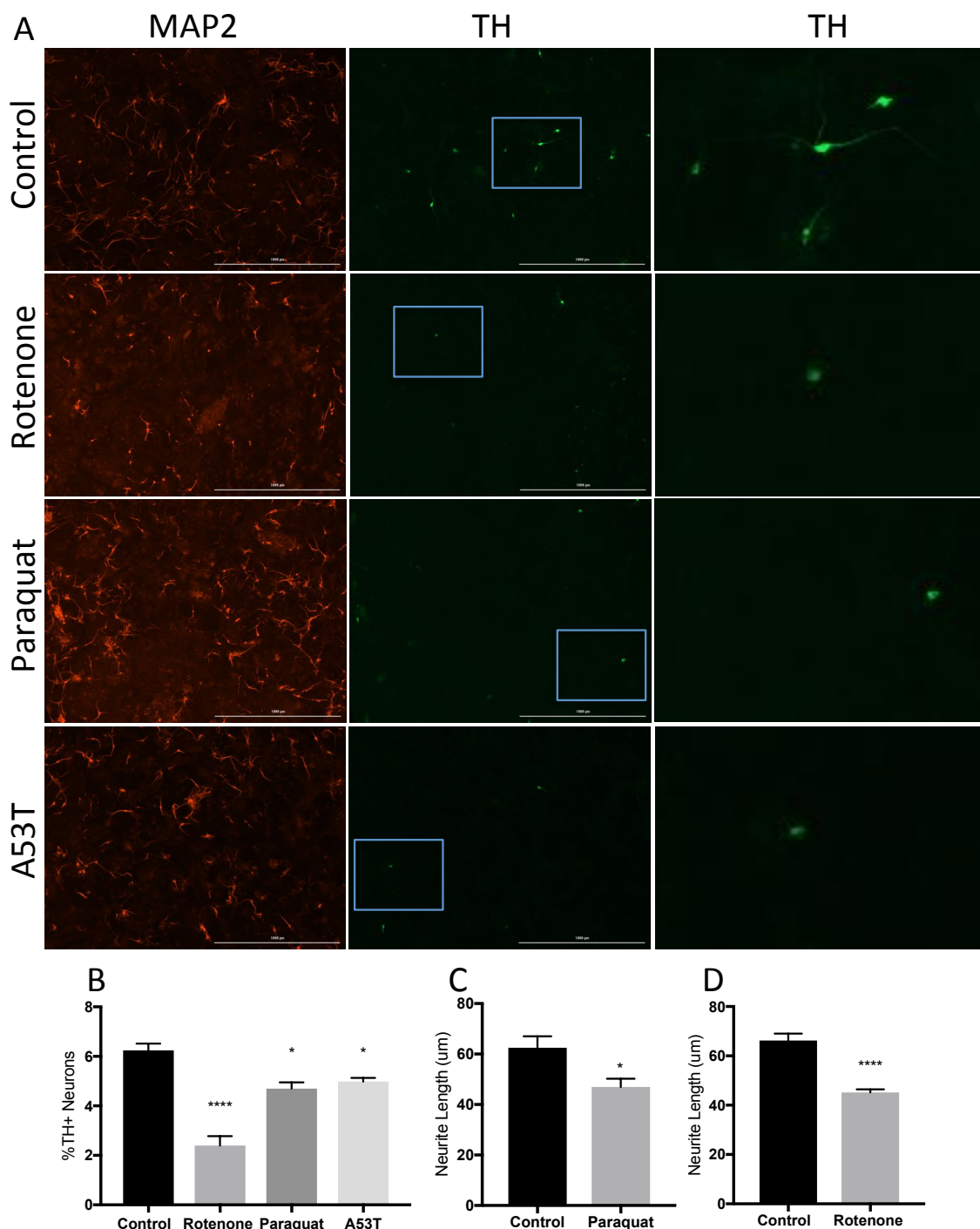
*Figure 2.9

*Figure 2.9. Neurotoxic effects of elicited by PD-related insults in DMEM cultures. Primary midbrain cultures (prepared in DMEM supplemented with 20 µM AraC) were exposed to rotenone (50 nM), paraquat (2.5 µM), or aSyn-A53T adenovirus (MOI = 10). Control cells were incubated in the absence of insult. The cultures were analyzed immunocytochemically with primary antibodies specific for MAP2 and TH. (A) Representative fluorescence micrographs showing the MAP2 stain (left column) or TH stain (middle column). The images in the right column are digitally magnified images showing the merged MAP2 and TH stains for the boxed regions in the corresponding middle panels. Images were taken with a Citation 3 Cell Imaging Multi-Mode Reader equipped with a 4x objective; green LED, 488 nm; red LED, 594 nm; blue LED, 330 nm; scale bar, 1000 µm. (B-D). Bar graphs showing relative DA neuron viability (B) and lengths of neurites extending from $MAP2^+$ / TH^+ neurons (C-D) in cultures subjected to different treatments. The data show that TH+ cell viability and the lengths of neurites extending from MAP2+/TH+ neurons are reduced in cultures exposed to PD-related insults compared to control cultures. The data are presented as the mean ± SEM, n = 5 or 10, *p < 0.05, ****p < 0.0001 versus untreated Control, one- way ANOVA followed by Tukey's multiple comparisons *post hoc* test. The data in B and D were subjected to a square root transformation.

Midbrain cultures prepared in Neurobasal media are distinguished by the presence of multiple long processes that extend from $MAP2^+$ and TH^+ cell bodies, forming intricate neurite networks (Fig. 2.10, 'Control'). The effects of PD-related insults on these neurite networks are slightly different in midbrain cultures prepared in Neurobasal media compared to DMEM media supplemented with AraC. Rotenone-treated Neurobasal cultures show a decrease in the lengths of processes extending from total ($MAP2^+$) neurons and dopaminergic (TH^+) neurons, as well as a dramatic reduction in the complexity of the overall neurite network (Fig. 2.10, 'Rotenone'). In contrast, images of Neurobasal cultures exposed to PhIP, Paraquat, or A53T adenovirus reveal no obvious change in the complexity of the overall neurite network, although one can find TH^+ neurons with shortened neurites or a reduction in the number of processes (Fig. 2.10, 'PhIP' or 'A53T'), similar to TH^+ neurons rotenone-treated cultures. Similarly, cultures prepared in Neurobasal media show a more pronounced loss of DA neurons when treated with rotenone compared to paraquat, PhIP or A53T adenovirus, whereas cultures prepared in DMEM supplemented with AraC show similar levels of DA cell death upon exposure to all four insults (Fig. 2.11).
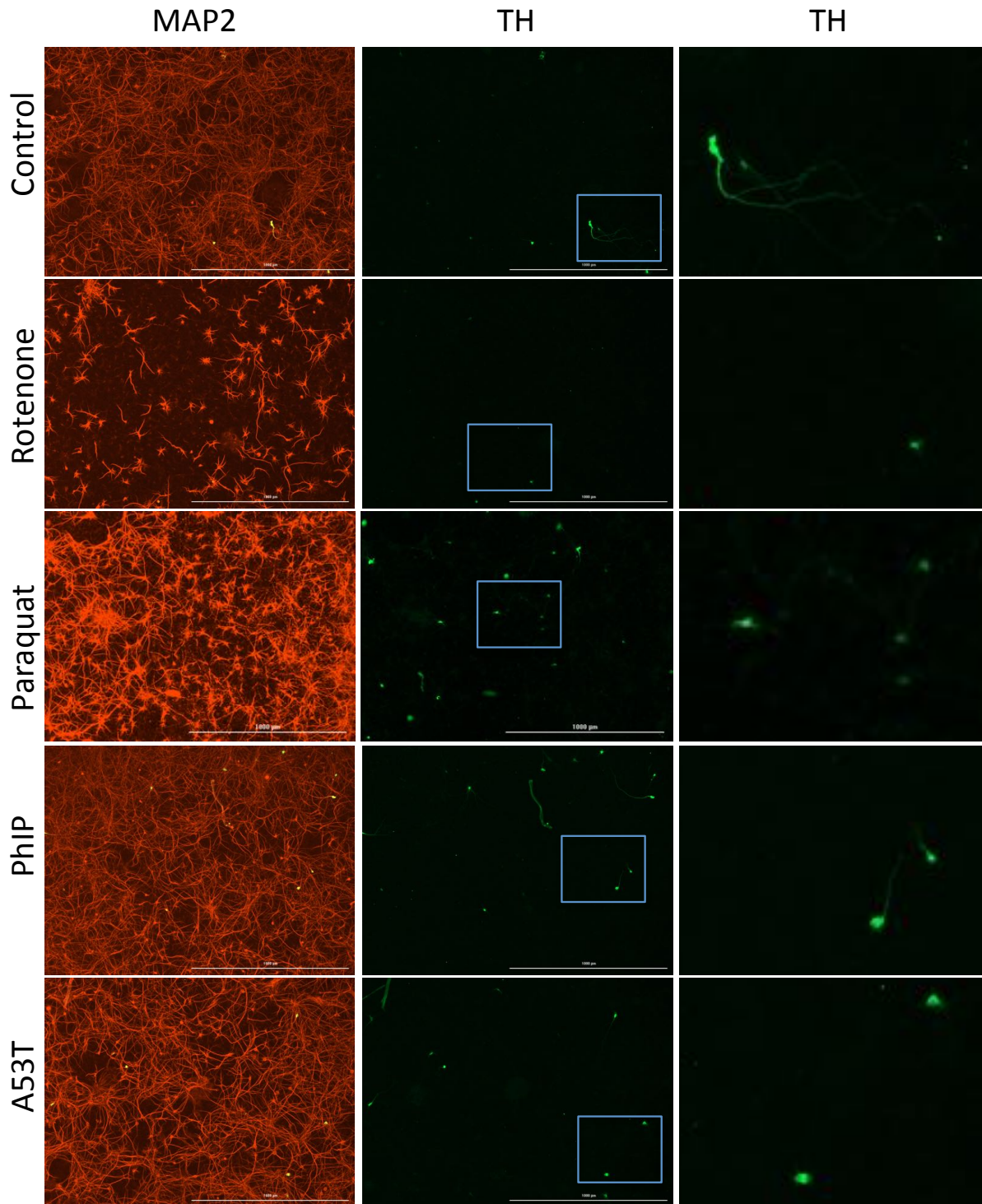
Figure 2.10. Neurotoxic effects of PD-related insults in Neurobasal cultures. Primary midbrain cultures were prepared in Neurobasal media and exposed to rotenone (50 nM), PhIP (1 µM), or aSyn-A53T adenovirus (MOI = 10). Control cells were incubated in the absence of insult. The cultures were analyzed immunocytochemically with primary antibodies specific for MAP2 and TH. Representative fluorescence micrographs are shown with MAP2 stain (left column) or TH stain (middle column). The images in the right column are digitally magnified images showing the merged MAP2 and TH stains for

the boxed regions in the corresponding middle panels. The images show a dramatic loss of MAP2$^+$ neurites in rotenone-treated cultures (left column) and an apparent decrease in the lengths of neurites extending from MAP2+/TH+ neurons in cultures exposed to PD-related insults compared to control cultures (right column). Images were taken with a Citation 3 Cell Imaging Multi-Mode Reader equipped with a 4x objective; green LED, 488 nm; red LED, 594 nm; blue LED, 330 nm; scale bar, 1000 μm.
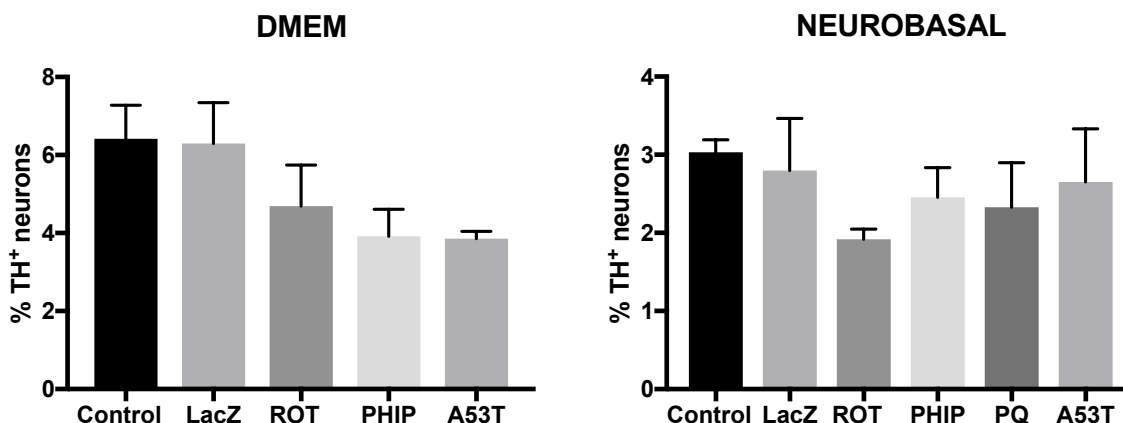
**Figure 2.11. A comparison of neurotoxic effects of PD-related insults in DMEM vs. Neurobasal cultures.** Primary midbrain cultures were prepared in DMEM media supplemented with 20 μM AraC (left) or Neurobasal media (right) and exposed to rotenone (25 nM), PhIP (1 μM), paraquat (2.5 μM), or aSyn-A53T adenovirus (MOI = 10). Additional cultures were untreated ('control') or transduced with adenovirus encoding the control protein β-galactosidase ('LacZ'). The cultures were analyzed immunocytochemically with primary antibodies specific for MAP2 and TH. Bar graphs show relative DA neuron viability in cultures subjected to different treatments. The data indicate that all four PD-related insults triggered a decrease in relative DA neuron viability in DMEM cultures, whereas only rotenone (but not paraquat, PhIP or A53T virus) elicited preferential DA cell death in Neurobasal cultures.

2.4.2 aSyn aggregation and prion-like spreading in primary midbrain cultures

The brains of patients with PD and other synucleinopathy disorders are characterized by the presence of aggregates (including Lewy bodies) enriched with aSyn phosphorylated at serine 129 (pSer129-aSyn), and evidence of prion-like spreading of aSyn pathology. Both of these neuropathological features are replicated in our primary midbrain culture model. Neurons in control cultures prepared in Neurobasal media show evidence of nuclear immunoreactivity when stained with the EP1536Y antibody specific for pSer129-aSyn (Fig. 2.12, 'Control'), consistent with previous reports[52,53]. In cultures transduced with adenovirus encoding WT human aSyn, we find that pSer129-aSyn immunoreactivity is increased in astrocytes, whereas no signal is detected in neurons (Fig. 2.12, 'WT-aSyn'). In cultures treated with both WT-aSyn PFFs and WT-aSyn adenovirus, pSer129-

aSyn signal is observed in both astrocytes and in the neuronal soma and processes (Fig. 2.12, 'WT + PFF'). Cultures treated with PFFs alone (Figure 2.13, 'PFF') showed absence of pSer129 immunoreactivity in neuronal processes, but small puncta was found in the intercellular space, suggesting that PFFs cellular uptake requires the presence of human WT aSyn expression.
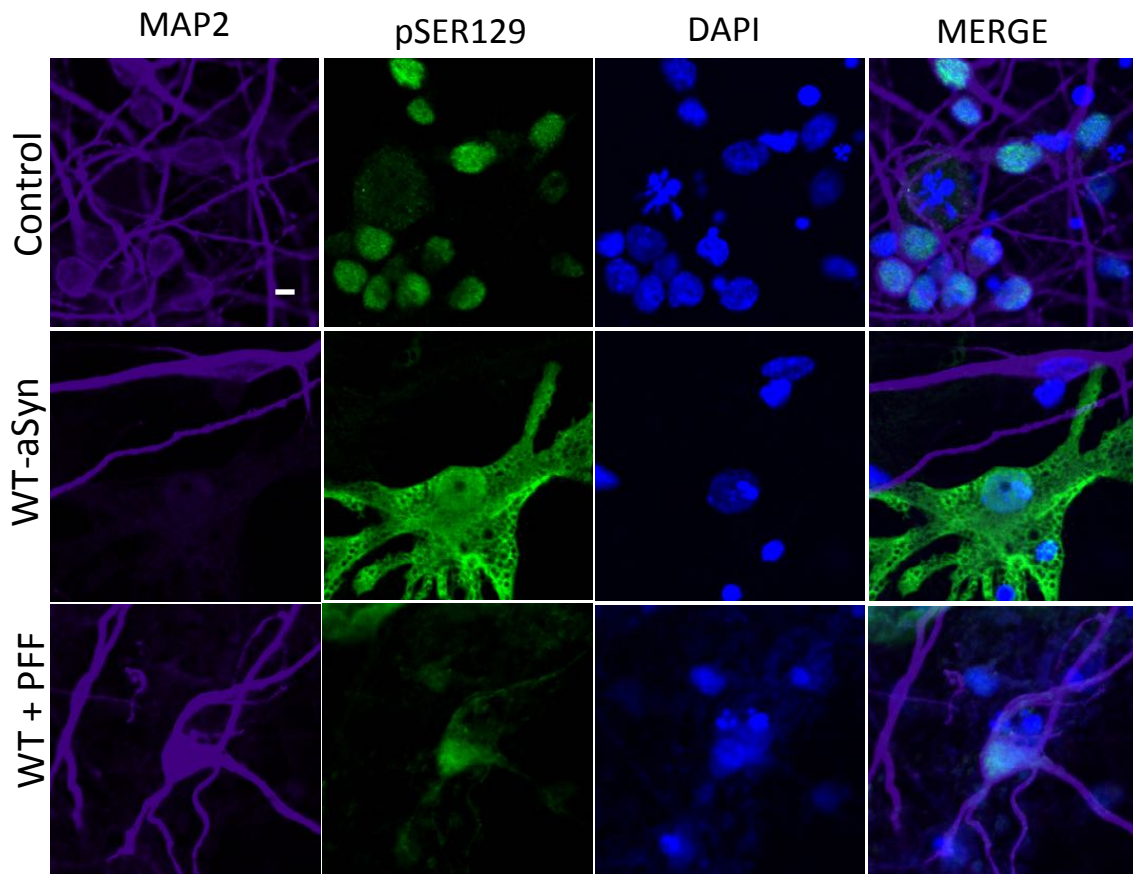
Figure 2.12. Evidence of aSyn PFF uptake and seeded aSyn aggregation in rat primary midbrain cultures. Primary midbrain cultures were simultaneously transduced with adenovirus encoding human WT aSyn and treated with PFFs derived from human WT aSyn for 72 h. The cultures were analyzed via confocal microscopy using a Nikon A1 confocal microscope equipped with 60X objective green LASER, 488 nm; far red LASER, 647 nm; blue LASER, 330 nm; scale bar, 10 μm, after staining with antibodies specific for pSer129 (clone EP1536Y; green) and MAP2 (purple). DAPI nuclear staining is shown in blue. pSer129[+] puncta in neuronal processes correspond to aSyn aggregates that likely formed as a result of PFF uptake PFF-mediated aggregation of cytosolic over-expressed human WT aSyn.
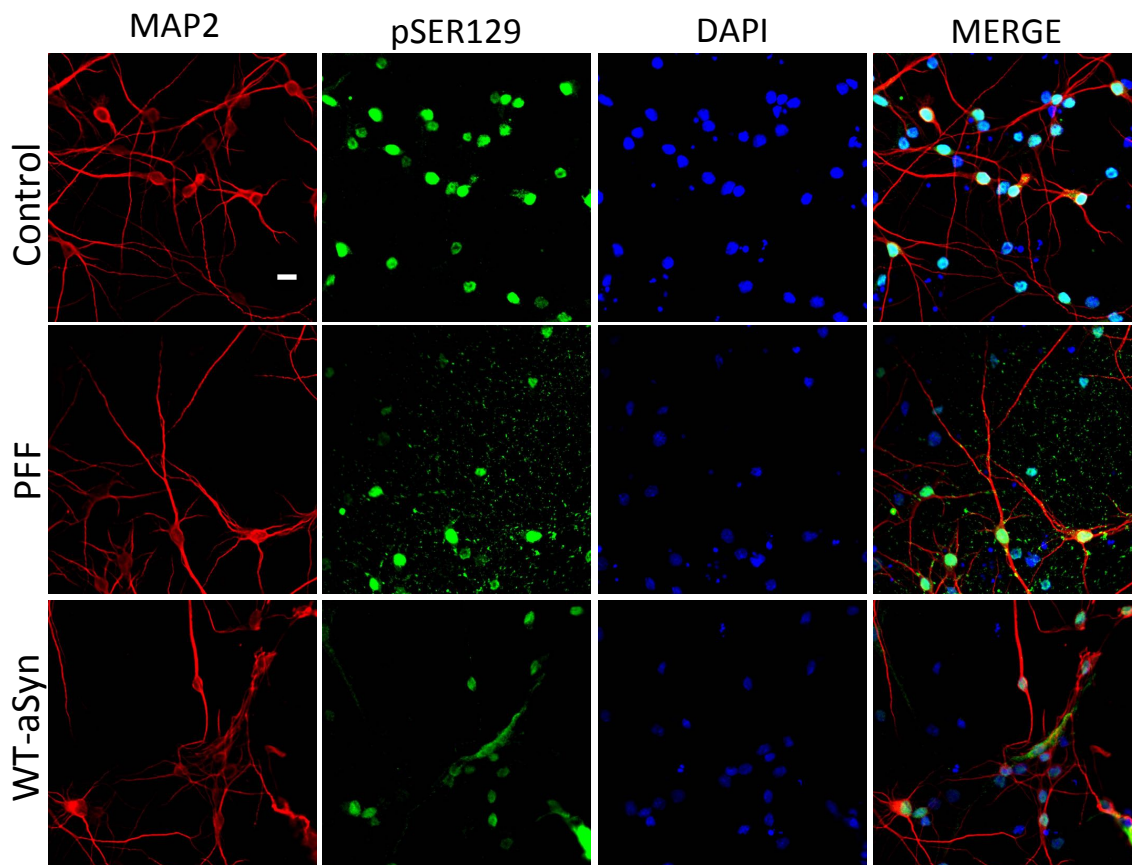
Figure 2.13. Evidence of WT-aSyn seeding is necessary for aSyn PFF uptake in rat primary midbrain cultures. Primary midbrain cultures were transduced with adenovirus encoding human WT aSyn or treated with PFFs derived from human WT aSyn for 72 h in separate experiments. The cultures were analyzed via confocal microscopy using a Nikon A1 confocal microscope equipped with 20X objective green LASER, 488 nm; red LASER, 594 nm; blue LASER, 330 nm; scale bar, 10 μm, after staining with antibodies specific for pSer129 (clone EP1536Y; green) and MAP2 (red). DAPI nuclear staining is shown in blue. pSer129[+] puncta in intercellular space correspond to aSyn PFF deposits outside the cells. Over-expressed human WT aSyn by itself did show evidence of cytosolic aSyn aggregates.

2.4.3   Antioxidant response from primary cortical astrocytes

Our protocol is able to establish pure primary cortical astrocytes cultures. Astrocitic cultures have been useful for the analysis of antioxidant response activation using a fluorescence-based reporter assay. We recently report a screen of plant extracts that activate NF-E2-related factor (Nrf2) antioxidant response[31,54]. Primary cortical astrocytes were transduced with a reported adenovirus encoding EGFP downstream of the SX2 enhancer and the HO-1 minimal promoter, two key elements in the activation of

antioxidant response elements (ARE)[55]. An increased detection of EGFP fluorescent signal suggests that the treatment increase binding of Nrf2 to ARE, activating the neuroprotective antioxidant pathway[54]. Details of these results can be found in de Rus, Rochet et al. 2017.

2.5 Discussion and Conclusion

2.5.1 Strengths and weaknesses of cellular PD models

Cell culture models can be used to recapitulate early stages of PD progression, allowing the characterization of molecular mechanisms involved in progressive neurodegeneration[56]. The use of immortalized neuronal models (e.g. PC12, SH-SY5Y, N27 cells) has been reasonably effective for the analysis of specific neuronal secretory or oncogenic pathways[57]. However, these cellular models have carcinogenic properties, such as the absence of a normal cellular aging process, that may be considered confounding factors in investigating the physiology of age-related neurodegenerative pathologies[56,57]. In specific cases, immortalized cell lines can be further differentiated into a neuron-like state[58]. However, this approach requires extensive manipulation that does not always yield a representative neuronal cell. Pure immortalized neuronal cell cultures lack the multiple cell types (e.g. neurons and glial cells) needed to model neurotoxic and neuroprotective mechanisms that occur in the brain.

Primary neuronal cultures have two key advantages as physiologically relevant models for the study of neurological diseases. First, they do not require extensive manipulation in order to achieve a state that reproduces key features of the central nervous system, including the presence of post-mitotic neurons in a controlled environment. Second, they consist of multiple cell types that are found in intact brains, including neurons astrocytes and microglia.

The preparation of primary cultures protocols can be expensive and time consuming, and can include excessive cell dissociation that may cause low yield or lack of consistency[32,31]. A majority of primary cultures are prepared from mouse embryos, which

can complicate the procedure since it will require the use of specialized equipment due to the size of the embryos[61]. Our rat-based protocol is characterized by a quick isolation of embryo brains, which ensures a high yield of primary cells. Here we describe a fast, straightforward, consistent and cost-effective protocol that results in an optimized primary mixed culture from rat embryos that approximates the physiological conditions of the midbrain and has the complexity necessary to reproduce hallmark PD cellular events.

2.5.2 Advantages of our primary cell culture models

Our protocol offers the opportunity to condition the cells depending on the investigation's objectives. The use of two different media formulation (DMEM and Neurobasal media) allows us to establish mixed cultures with different sensitivity levels to stress environments. On one hand, DMEM cultures allow the experimental control of glial cell growth, where astrocytic and microglial cells populations can be regulated in order to modulate the neuronal response to genetic and toxin-based PD insults. On the other hand, neurobasal cultures prevent the cultures from producing endogenous oxidative stress factors, which make it possible to evaluate the inherent toxicity elicited by different PD-related neurotoxic compounds or genes without confounds caused by endogenous ROS.

aSyn over-expression in primary midbrain cultures not treated with PFFs uptake leads to the formation of pSer129-aSyn$^+$ aggregates in astrocytes, but not in neurons, apparently because of the higher activity of the CMV reporter (which is responsible for driving aSyn expression from our adenoviral constructs) in the astrocytic cell population. The fact that neuronal pSer129-aSyn$^+$ aggregates are observed in cultures treated with both aSyn adenovirus and aSyn PFFs (but not in cultures treated with either agent individually) implies that virally expressed aSyn undergoes self-assembly in neurons via a seeding mechanism mediated by internalized PFFs.

Consistently, our primary midbrain culture treated with aSyn, PhIP, rotenone and paraquat showed between 30% and 50% reduction of TH$^+$ neurons. This range of neuronal loss provides an excellent margin where neuroprotection against PD-related

insults will be evident. Our protocol is a major contribution to the investigation of several aspects of PD cellular pathology, offering a unique experimental model that combines a range of orthogonal approaches (e.g. PD-related insults recapitulation, neuronal viability via cell counts and neurite length analysis, ROS sensitivity by modulation of glial cells numbers, expression analysis of PD-related proteins).

2.5.3 Assays of PD-related neurotoxicity or neuroprotection in primary midbrain cultures are highly dependent on the glial cell density.

The success of studies involving our primary midbrain culture model depends on the careful control of astrocytic and microglial cell density. Although a major advantage of our cultures is the fact that the neuronal population does not require the presence of an astrocytic feeder layer, it is nevertheless necessary to allow the growth of a sufficient number of supportive glial cells. Even a minor perturbation of the AraC treatment (e.g. a change in AraC concentration or incubation time) can lead to an increase or decrease in the number of astrocytes and microglia, in turn resulting in a change in neuron viability. For instance, we have noted that in DMEM cultured cells treated with a decreased concentration of AraC lead to a decreased in neurotoxicity of rotenone (data not shown). One way to avoid potential complications associated with AraC treatment is to conduct assays of neurotoxicity or neuroprotection in midbrain cultures prepared in Neurobasal media, where microglial cells are absent and the number of astrocytes depends on the overall cell plating density. Neurobasal cultures are particularly useful to monitor neurotoxicity elicited by rotenone or paraquat. Neurotoxic effects of rotenone in these cultures are surprising given the lack of microglia[62,63]. Astrocytes could play a role in mediating neurotoxicity through ROS production even in the absence of microglia.[64,65]

2.5.4 Rodent primary neuronal cultures vs. human iPSC-derived neurons

With no doubt, stem cells derived neurons can recapitulate important cellular events in PD and other neurological diseases, providing the outstanding opportunity to examine human-specific aspects of diseases and provide insights of genetic perturbations in neurotoxicity[66]. This feature is critical in PD-related studies because rodent DA neurons have shown to lack susceptibility to oxidative stress seen un their human counterparts[67]. However, iPSC-derived neurons are expensive models that require specialized techniques

for their preparation and must be maintained over extended time periods[66]. Another downside of iPSC-derived cultures is that astrocytes and neurons must be produced independently, and then they should be combined in a mixed culture[68], this requires additional optimization relative to what we have achieved with our rat primary cultures. Also, as of yet there is little information about how to prepare microglia from human iPSCs, and when this is feasible, then a 3rd cell type will have to be incorporated into the work flow of preparing iPSC-derived neuronal cultures[69]. One final disadvantage is that there are few examples of treatments that lead to robust DA neuronal death. In contrast, our primary neuronal culture is an economic and efficient alternative that offers feeder cells-free culture with a consistent range of neuronal loss response to PD-related insults, representing a unique model for different neuroprotective strategies. Accordingly, studies in rodent primary neuronal cultures can provide us with valuable preliminary data that can in turn be validated in iPSC-derived neuron models.

2.5.5   Primary cell culture model vs. *in vivo* model

Cellular and *in vivo* models can be considered complementary systems. An advantage of our primary cell culture model is that it can be used to characterize neurotoxic and neuroprotective mechanisms relating to specific areas in the brain, and even specific cell types, in a less complex environment than an *in vivo* model. Live imaging in the *substantia nigra* cannot be done in an intact brain, although cranial windows allow one to carry out these sorts of analyses in the more superficial cortical layers[70]. Live-cell imaging is uniquely feasible in primary cultures[71]; with the disadvantage that they are dissociated cultures that lack of intact circuitry or brain architecture. Combinatory outcomes from live-cell imaging in vivo and in primary cultures can elucidate mechanistic features that rule PD.

Another advantage of primary cell culture models is that they can be used to carry out a higher number of biological and technical replicates. Preliminary data obtained from experiments performed in primary cultures can be validated via *in vivo* studies, the design of which can be optimized according to information obtained from the preceding analyses in cell culture. For example, we recently characterized neurotoxic effects of the

familial aSyn mutant A53E (Ysselstein et al., unpublished data) and neuroprotective properties of the aSyn binding partner ENSA against aSyn neurotoxicity[26]. We have since validated A53E neurotoxicity in rats injected intranigrally with rAAV-aSyn (Chapter 3 of this thesis), and ENSA-mediated neuroprotection is now being investigated in the same *in vivo* model.

2.6   List of References

1.   Alexander, G. E. Biology of Parkinson's disease: pathogenesis and pathophysiology of a multisystem neurodegenerative disorder. *Dialogues Clin. Neurosci.* **6**, 259–80 (2004).

2.   Goedert, M. Alpha-synuclein and neurodegenerative diseases. *Nat. Rev. Neurosci.* **2**, 492–501 (2001).

3.   Tanner, C. M., Kamel, F., Ross, G. W., Hoppin, J. A., Goldman, S. M., Korell, M., Marras, C., Bhudhikanok, G. S., Kasten, M., Chade, A. R., Comyns, K., Richards, M. B., Meng, C., Priestley, B., Fernandez, H. H. *et al.* Rotenone, Paraquat, and Parkinson's Disease. *Environ. Health Perspect.* **119**, 866–872 (2011).

4.   Heinz, S., Freyberger, A., Lawrenz, B., Schladt, L., Schmuck, G. & Ellinger-Ziegelbauer, H. Mechanistic Investigations of the Mitochondrial Complex I Inhibitor Rotenone in the Context of Pharmacological and Safety Evaluation. *Sci. Rep.* **7**, 45465 (2017).

5.   Manning-Bog, A. B., McCormack, A. L., Li, J., Uversky, V. N., Fink, A. L. & Di Monte, D. A. The herbicide paraquat causes up-regulation and aggregation of alpha-synuclein in mice: paraquat and alpha-synuclein. *J. Biol. Chem.* **277**, 1641–4 (2002).

6.   McCormack, A. L., Atienza, J. G., Johnston, L. C., Andersen, J. K., Vu, S. & Di Monte, D. A. Role of oxidative stress in paraquat-induced dopaminergic cell degeneration. *J. Neurochem.* **93**, 1030–1037 (2005).

7.   Vaccari, C., El Dib, R. & de Camargo, J. L. V. Paraquat and Parkinson's disease: a systematic review protocol according to the OHAT approach for hazard identification. *Syst. Rev.* **6**, 98 (2017).

8.   Smeyne, R. J. & Jackson-Lewis, V. The MPTP model of Parkinson's disease. *Mol. Brain Res.* **134**, 57–66 (2005).

9.   Clark, J., Silvaggi, J. M., Kiselak, T., Zheng, K., Clore, E. L., Dai, Y., Bass, C. E. & Simon, D. K. Pgc-1α Overexpression Downregulates Pitx3 and Increases Susceptibility to MPTP Toxicity Associated with Decreased Bdnf. *PLoS One* **7**, e48925 (2012).

10.   Rathinam, M. L., Watts, L. T., Narasimhan, M., Riar, A. K., Mahimainathan, L. & Henderson, G. I. Astrocyte mediated protection of fetal cerebral cortical neurons from rotenone and paraquat. *Environ. Toxicol. Pharmacol.* **33**, 353–360 (2012).

11.   Gan, L., Vargas, M. R., Johnson, D. A. & Johnson, J. A. Astrocyte-Specific Overexpression of Nrf2 Delays Motor Pathology and Synuclein Aggregation throughout the CNS in the Alpha-Synuclein Mutant (A53T) Mouse Model. *J. Neurosci.* **32**, 17775–17787 (2012).

12.   Hashimoto, M., Hsu, L. J., Xia, Y., Takeda, A., Sisk, A., Sundsmo, M. & Masliah, E. Oxidative stress induces amyloid-like aggregate formation of NACP/alpha-synuclein in vitro. *Neuroreport* **10**, 717–21 (1999).

13.   Yun, S. P., Kam, T.-I., Panicker, N., Kim, S., Oh, Y., Park, J.-S., Kwon, S.-H., Park, Y. J., Karuppagounder, S. S., Park, H., Kim, S., Oh, N., Kim, N. A., Lee, S., Brahmachari, S. *et al.* Block of A1 astrocyte conversion by microglia is neuroprotective in models of Parkinson's disease. *Nat. Med.* **24**, 931–938 (2018).

14.   Dauer, W. & Przedborski, S. Parkinson's Disease. *Neuron* **39**, 889–909 (2003).

15.   de Rus Jacquet, A., Tambe, M. A. & Rochet, J.-C. Dietary Phytochemicals in Neurodegenerative Disease. in *Nutrition in the Prevention and Treatment of Disease* 361–391 (Elsevier, 2017). doi:10.1016/B978-0-12-802928-2.00018-7

16.   Sherer, T. B., Betarbet, R., Stout, A. K., Lund, S., Baptista, M., Panov, A. V, Cookson, M. R. & Greenamyre, J. T. An in vitro model of Parkinson's disease: linking mitochondrial impairment to altered alpha-synuclein metabolism and oxidative damage. *J. Neurosci.* **22**, 7006–15 (2002).

17.   Sanders, L. H. & Timothy Greenamyre, J. Oxidative damage to macromolecules in human Parkinson disease and the rotenone model. *Free Radic. Biol. Med.* **62**, 111–120 (2013).

18.   Volpicelli-Daley, L. A., Luk, K. C. & Lee, V. M.-Y. Addition of exogenous α-synuclein preformed fibrils to primary neuronal cultures to seed recruitment of endogenous α-synuclein to Lewy body and Lewy neurite–like aggregates. *Nat. Protoc.* **9**, 2135–2146 (2014).

19. Cannon, J. R., Tapias, V., Na, H. M., Honick, A. S., Drolet, R. E. & Greenamyre, J. T. A highly reproducible rotenone model of Parkinson's disease. *Neurobiol. Dis.* **34**, 279–90 (2009).

20. Ossowska, K., Wardas, J., Śmiałowska, M., Kuter, K., Lenda, T., Wierońska, J. M., Zięba, B., Nowak, P., Dąbrowska, J., Bortel, A., Kwieciński, A. & Wolfarth, S. A slowly developing dysfunction of dopaminergic nigrostriatal neurons induced by long-term paraquat administration in rats: an animal model of preclinical stages of Parkinson's disease? *Eur. J. Neurosci.* **22**, 1294–1304 (2005).

21. Johnson, M. E. & Bobrovskaya, L. An update on the rotenone models of Parkinson's disease: Their ability to reproduce the features of clinical disease and model gene–environment interactions. *Neurotoxicology* **46**, 101–116 (2015).

22. Schapira, A. H. V., Chaudhuri, K. R. & Jenner, P. Non-motor features of Parkinson disease. *Nat. Rev. Neurosci.* **18**, 435–450 (2017).

23. Spillantini, M. G. & Goedert, M. Synucleinopathies: past, present and future. *Neuropathol. Appl. Neurobiol.* **42**, 3–5 (2016).

24. Liu, F., Nguyen, J. L., Hulleman, J. D., Li, L. & Rochet, J.-C. Mechanisms of DJ-1 neuroprotection in a cellular model of Parkinson's disease. *J. Neurochem.* **105**, 2435–2453 (2008).

25. Liu, F., Hindupur, J., Nguyen, J. L., Ruf, K. J., Zhu, J., Schieler, J. L., Bonham, C. C., Wood, K. V, Davisson, V. J. & Rochet, J.-C. Methionine sulfoxide reductase A protects dopaminergic cells from Parkinson's disease-related insults. *Free Radic. Biol. Med.* **45**, 242–55 (2008).

26. Ysselstein, D., Dehay, B., Costantino, I. M., McCabe, G. P., Frosch, M. P., George, J. M., Bezard, E. & Rochet, J.-C. Endosulfine-alpha inhibits membrane-induced α-synuclein aggregation and protects against α-synuclein neurotoxicity. *Acta Neuropathol. Commun.* **5**, 3 (2017).

27. de Rus Jacquet, A., Timmers, M., Ma, S. Y., Thieme, A., McCabe, G. P., Vest, J. H. C., Lila, M. A. & Rochet, J.-C. Lumbee traditional medicine: Neuroprotective activities of medicinal plants used to treat Parkinson's disease-related symptoms. *J. Ethnopharmacol.* **206**, 408–425 (2017).

28. Niranjan, R. The Role of Inflammatory and Oxidative Stress Mechanisms in the Pathogenesis of Parkinson's Disease: Focus on Astrocytes. *Mol. Neurobiol.* **49**, 28–38 (2014).

29. Biasini, E., Fioriti, L., Ceglia, I., Invernizzi, R., Bertoli, A., Chiesa, R. & Forloni, G. Proteasome inhibition and aggregation in Parkinson's disease: a comparative study in untransfected and transfected cells. *J. Neurochem.* **88**, 545–53 (2004).

30. Strathearn, K. E., Yousef, G. G., Grace, M. H., Roy, S. L., Tambe, M. A., Ferruzzi, M. G., Wu, Q.-L., Simon, J. E., Lila, M. A. & Rochet, J.-C. Neuroprotective effects of anthocyanin- and proanthocyanidin-rich extracts in cellular models of Parkinson′s disease. *Brain Res.* **1555**, 60–77 (2014).

31. de Rus Jacquet, A., Tambe, M. A., Ma, S. Y., McCabe, G. P., Vest, J. H. C. & Rochet, J.-C. Pikuni-Blackfeet traditional medicine: Neuroprotective activities of medicinal plants used to treat Parkinson's disease-related symptoms. *J. Ethnopharmacol.* **206**, 393–407 (2017).

32. Teunissen, S. F., Vlaming, M. L. H., Rosing, H., Schellens, J. H. M., Schinkel, A. H. & Beijnen, J. H. Development and validation of a liquid chromatography–tandem mass spectrometry assay for the analysis of 2-amino-1-methyl-6-phenylimidazo[4,5-b]pyridine (PhIP) and its metabolite 2-hydroxyamino-1-methyl-6-phenylimidazo[4,5-b]pyridine (N-OH-PhIP) in plasma, urine, bile, intestinal contents, faeces and eight selected tissues from mice. *J. Chromatogr. B* **878**, 2353–2362 (2010).

33. Outeiro, T. F., Kontopoulos, E., Altmann, S. M., Kufareva, I., Strathearn, K. E., Amore, A. M., Volk, C. B., Maxwell, M. M., Rochet, J.-C., McLean, P. J., Young, A. B., Abagyan, R., Feany, M. B., Hyman, B. T. & Kazantsev, A. G. Sirtuin 2 Inhibitors Rescue -Synuclein-Mediated Toxicity in Models of Parkinson's Disease. *Science (80-.).* **317**, 516–519 (2007).

34. Su, L. J., Auluck, P. K., Outeiro, T. F., Yeger-Lotem, E., Kritzer, J. A., Tardiff, D. F., Strathearn, K. E., Liu, F., Cao, S., Hamamichi, S., Hill, K. J., Caldwell, K. A., Bell, G. W., Fraenkel, E., Cooper, A. A. *et al.* Compounds from an unbiased chemical screen reverse both ER-to-Golgi trafficking defects and mitochondrial dysfunction in Parkinson's disease models. *Dis. Model. Mech.* **3**, 194–208 (2010).

35. Tardiff, D. F., Jui, N. T., Khurana, V., Tambe, M. A., Thompson, M. L., Yeun Chung, C., Kamadurai, H. B., Tae Kim, H., Lancaster, A. K., Caldwell, K. A., Caldwell, G. A., Rochet, J.-C., Buchwald, S. L. & Lindquist, S. *Yeast reveal a "druggable" Rsp5/Nedd4 Network that Ameliorates α-Synuclein Toxicity in Neurons*.

36. Tóth, G., Gardai, S. J., Zago, W., Bertoncini, C. W., Cremades, N., Roy, S. L., Tambe, M. A., Rochet, J.-C., Galvagnion, C., Skibinski, G., Finkbeiner, S., Bova, M., Regnstrom, K., Chiou, S.-S., Johnston, J. *et al.* Targeting the Intrinsically Disordered Structural Ensemble of α-Synuclein by Small Molecules as a Potential Therapeutic Strategy for Parkinson's Disease. *PLoS One* **9**, e87133 (2014).

37. Collier, T. J., Srivastava, K. R., Justman, C., Grammatopoulous, T., Hutter-Paier, B., Prokesch, M., Havas, D., Rochet, J.-C., Liu, F., Jock, K., de Oliveira, P., Stirtz, G. L., Dettmer, U., Sortwell, C. E., Feany, M. B. *et al.* Nortriptyline inhibits aggregation and neurotoxicity of alpha-synuclein by enhancing reconfiguration of the monomeric form. *Neurobiol. Dis.* **106**, 191–204 (2017).

38. Ambaw, A., Zheng, L., Tambe, M. A., Strathearn, K. E., Acosta, G., Hubers, S. A., Liu, F., Herr, S. A., Tang, J., Truong, A., Walls, E., Pond, A., Rochet, J.-C. & Shi, R. Acrolein-mediated neuronal cell death and alpha-synuclein aggregation: Implications for Parkinson's disease. *Mol. Cell. Neurosci.* **88**, 70–82 (2018).

39. Ysselstein, D., Joshi, M., Mishra, V., Griggs, A. M., Asiago, J. M., McCabe, G. P., Stanciu, L. A., Post, C. B. & Rochet, J.-C. Effects of impaired membrane interactions on α-synuclein aggregation and neurotoxicity. *Neurobiol. Dis.* **79**, 150–63 (2015).

40. Frank, M. G., Baratta, M. V., Sprunger, D. B., Watkins, L. R. & Maier, S. F. Microglia serve as a neuroimmune substrate for stress-induced potentiation of CNS pro-inflammatory cytokine responses. *Brain. Behav. Immun.* **21**, 47–59 (2007).

41. Brewer, G. J., Torricelli, J. R., Evege, E. K. & Price, P. J. Optimized survival of hippocampal neurons in B27-supplemented neurobasal?, a new serum-free medium combination. *J. Neurosci. Res.* **35**, 567–576 (1993).

42. Gwak, Y. S., Hulsebosch, C. E. & Leem, J. W. Neuronal-Glial Interactions Maintain Chronic Neuropathic Pain after Spinal Cord Injury. *Neural Plast.* **2017**, 1–14 (2017).

43. Bruno, V., Sureda, F. X., Storto, M., Casabona, G., Caruso, A., Knopfel, T., Kuhn, R. & Nicoletti, F. The neuroprotective activity of group-II metabotropic glutamate receptors requires new protein synthesis and involves a glial-neuronal signaling. *J. Neurosci.* **17**, 1891–7 (1997).

44. HANSSON, E. & RÖNNBÄCK, L. Glial neuronal signaling in the central nervous system. *FASEB J.* **17**, 341–348 (2003).

45. Jenner, P. Oxidative stress in Parkinson's disease. *Ann. Neurol.* **53**, S26–S38 (2003).

46. Tjalkens, R. B., Streifel, K. M. & Moreno, J. A. CHAPTER 7. Neuroinflammation and Oxidative Stress in Models of Parkinson's Disease and Protein-Misfolding Disorders. in 184–209 (2017). doi:10.1039/9781782622888-00184

47. Lopez-Fabuel, I., Le Douce, J., Logan, A., James, A. M., Bonvento, G., Murphy, M. P., Almeida, A. & Bolaños, J. P. Complex I assembly into supercomplexes determines differential mitochondrial ROS production in neurons and astrocytes. *Proc. Natl. Acad. Sci. U. S. A.* **113**, 13063–13068 (2016).

48. Boje, K. M. & Arora, P. K. Microglial-produced nitric oxide and reactive nitrogen oxides mediate neuronal cell death. *Brain Res.* **587**, 250–256 (1992).

49. Strathearn, K. E., Yousef, G. G., Grace, M. H., Roy, S. L., Tambe, M. A., Ferruzzi, M. G., Wu, Q.-L., Simon, J. E., Lila, M. A. & Rochet, J.-C. Neuroprotective effects of anthocyanin- and proanthocyanidin-rich extracts in cellular models of Parkinson′s disease. *Brain Res.* **1555**, 60–77 (2014).

50. Griggs, A. M., Agim, Z. S., Mishra, V. R., Tambe, M. A., Director-Myska, A. E., Turteltaub, K. W., McCabe, G. P., Rochet, J.-C. & Cannon, J. R. 2-Amino-1-methyl-6-phenylimidazo[4,5-b]pyridine (PhIP) Is Selectively Toxic to Primary Dopaminergic Neurons In Vitro. *Toxicol. Sci.* **140**, 179–189 (2014).

51. Cruz-Hernandez, A., Agim, Z. S., Montenegro, P. C., McCabe, G. P., Rochet, J.-C. & Cannon, J. R. Selective dopaminergic neurotoxicity of three heterocyclic amine subclasses in primary rat midbrain neurons. *Neurotoxicology* **65**, 68–84 (2018).

52. Rutherford, N. J., Brooks, M. & Giasson, B. I. Novel antibodies to phosphorylated α-synuclein serine 129 and NFL serine 473 demonstrate the close molecular homology of these epitopes. *Acta Neuropathol. Commun.* **4**, 80 (2016).

53. Schell, H., Hasegawa, T., Neumann, M. & Kahle, P. J. Nuclear and neuritic distribution of serine-129 phosphorylated α-synuclein in transgenic mice. *Neuroscience* **160**, 796–804 (2009).

54. Johnson, J. A., Johnson, D. A., Kraft, A. D., Calkins, M. J., Jakel, R. J., Vargas, M. R. & Chen, P.-C. The Nrf2-ARE Pathway. *Ann. N. Y. Acad. Sci.* **1147**, 61–69 (2008).

55. Alam, J., Stewart, D., Touchard, C., Boinapally, S., Choi, A. M. & Cook, J. L. Nrf2, a Cap'n'Collar transcription factor, regulates induction of the heme oxygenase-1 gene. *J. Biol. Chem.* **274**, 26071–8 (1999).

56. Lopes, F. M., Bristot, I. J., da Motta, L. L., Parsons, R. B. & Klamt, F. Mimicking Parkinson's Disease in a Dish: Merits and Pitfalls of the Most Commonly used Dopaminergic In Vitro Models. *NeuroMolecular Med.* **19**, 241–255 (2017).

57. Bongarzone, E. R., Foster, L. M., Byravan, S., Verity, A. N., Landry, C. F., Schonmann, V., Amur-Umarjee, S. & Campagnoni, A. T. Conditionally Immortalized Neural Cell Lines: Potential Models for the Study of Neural Cell Function. *Methods* **10**, 489–500 (1996).

58. Forster, J. I., Köglsberger, S., Trefois, C., Boyd, O., Baumuratov, A. S., Buck, L., Balling, R. & Antony, P. M. A. Characterization of Differentiated SH-SY5Y as Neuronal Screening Model Reveals Increased Oxidative Vulnerability. *J. Biomol. Screen.* **21**, 496–509 (2016).

59. Kaneko, A. & Sankai, Y. Long-Term Culture of Rat Hippocampal Neurons at Low Density in Serum-Free Medium: Combination of the Sandwich Culture Technique with the Three-Dimensional Nanofibrous Hydrogel PuraMatrix. *PLoS One* **9**, e102703 (2014).

60. Walicke, P. A. Basic and acidic fibroblast growth factors have trophic effects on neurons from multiple CNS regions. *J. Neurosci.* **8**, 2618–27 (1988).

61. Weinert, M., Selvakumar, T., Tierney, T. S. & Alavian, K. N. Isolation, Culture and Long-Term Maintenance of Primary Mesencephalic Dopaminergic Neurons From Embryonic Rodent Brains. *J. Vis. Exp.* (2015). doi:10.3791/52475

62. Gao, H.-M., Hong, J.-S., Zhang, W. & Liu, B. Distinct role for microglia in rotenone-induced degeneration of dopaminergic neurons. *J. Neurosci.* **22**, 782–90 (2002).

63. Gao, H.-M., Liu, B. & Hong, J.-S. Critical role for microglial NADPH oxidase in rotenone-induced degeneration of dopaminergic neurons. *J. Neurosci.* **23**, 6181–7 (2003).

64. Chang, C. Y., Choi, D.-K., Lee, D. K., Hong, Y. J. & Park, E. J. Resveratrol Confers Protection against Rotenone-Induced Neurotoxicity by Modulating Myeloperoxidase Levels in Glial Cells. *PLoS One* **8**, e60654 (2013).

65. Goswami, P., Gupta, S., Joshi, N., Sharma, S. & Singh, S. Astrocyte activation and neurotoxicity: A study in different rat brain regions and in rat C6 astroglial cells. *Environ. Toxicol. Pharmacol.* **40**, 122–139 (2015).

66. Xiao, B., Ng, H. H., Takahashi, R. & Tan, E.-K. Induced pluripotent stem cells in Parkinson's disease: scientific and clinical challenges. *J. Neurol. Neurosurg. Psychiatry* **87**, 697–702 (2016).

67. Burbulla, L. F., Song, P., Mazzulli, J. R., Zampese, E., Wong, Y. C., Jeon, S., Santos, D. P., Blanz, J., Obermaier, C. D., Strojny, C., Savas, J. N., Kiskinis, E., Zhuang, X., Krüger, R., Surmeier, D. J. *et al.* Dopamine oxidation mediates mitochondrial and lysosomal dysfunction in Parkinson's disease. *Science* **357**, 1255–1261 (2017).

68. Maherali, N. & Hochedlinger, K. Guidelines and Techniques for the Generation of Induced Pluripotent Stem Cells. *Cell Stem Cell* **3**, 595–605 (2008).

69. Abud, E. M., Ramirez, R. N., Martinez, E. S., Healy, L. M., Nguyen, C. H. H., Newman, S. A., Yeromin, A. V., Scarfone, V. M., Marsh, S. E., Fimbres, C., Caraway, C. A., Fote, G. M., Madany, A. M., Agrawal, A., Kayed, R. *et al.* iPSC-Derived Human Microglia-like Cells to Study Neurological Diseases. *Neuron* **94**, 278–293.e9 (2017).

70. Yang, G., Pan, F., Parkhurst, C. N., Grutzendler, J. & Gan, W.-B. Thinned-skull cranial window technique for long-term imaging of the cortex in live mice. *Nat. Protoc.* **5**, 201–208 (2010).

71. Bains, M. & Heidenreich, K. A. Chapter 7 Live-Cell Imaging of Autophagy Induction and Autophagosome-Lysosome Fusion in Primary Cultured Neurons. *Methods Enzymol.* **453**, 145–158 (2009).

CHAPTER 3. EFFECTS OF THE A53E SUBSTITUTION ON ALPHA- SYNUCLEIN AGGREGATION AND NEUROTOXICITY IN PD MODELS

3.1 Introduction

The first aSyn mutation associated with early onset familial PD (encoding the A53T mutant form of the protein) was reported in 1997[1,2]. Subsequently, additional point mutations (e.g. mutations encoding the A30P[3], E46K[4], H50Q[5], and G51D[6] substitutions) and multiplications of the WT aSyn gene[7] were found to be linked to familial PD. Some substitution mutants (A30P, E46K and H50Q) were found to form oligomers or amyloid-like fribrils more rapidly than the wild-type protein[8–10]. Multiplication mutations were predicted to favor aSyn aggregation through mass action[11]

One of the subtituion mutatnts, G51D, did not form aggregates more rapidly than WT aSyn[12]. Previous studies were focused on aSyn self assembly in the absence of membranes, but aSyn in fact associates with phospholipids[13,14]. Evidence suggests that membranes can accelerate aSyn aggregation[15] Our studies of the A30P and G51D mutants (Fig 1.1) revealed that both mutants have an enhanced propensity to adopt an exposed conformation, leading to membrane-induced aggregation (a process closely associated with vesicle disruption) and neuronal toxicity[16,17].

3.1.1 A53E Substitution in PD

The A53E mutation was recently reported to be associated with early-onset PD[18]. The post-mortem brains of patients with this mutation were characterized by neuropathological features similar to those commonly observed in PD, DLB and MSA, with severe nigral degeneration and crescent-shaped Lewy pathology distributed in neuronal and glial cells from midbrain and cortical areas[18]. In one study, it was reported that A53E has delayed oligomerization and fibrillation kinetics when compared with the A53T variant[19]. Another group reported that A53E mutation influenced aSyn ability to aggregate and decreased its oligomerization in cellular models[20] The replacement of a

neutral alanine residue with a glutamate residue at the position 53 introduces a negative charge that could disrupt the amphipathic α-helical structure of membrane-bound aSyn, thus favoring the protein's adoption of an exposed structure with a high propensity to aggregate at the membrane surface[18,19]. Consistent with this idea, research carried out in our laboratory revealed that A53E variant has decreased affinity for lipid vescicles, and higher propensity to adopt an aSyn 'exposed' conformation and membrane-induced aggregation, effects that are correlated with increased dopaminergic neurons toxicity in a primary culture model (data non-published). In the set of studies described herein, we compared WT aSyn, A53E, and A53T in terms of their neuropathological effects in a rat aSyn over-expression model relevant to PD.

3.2   Materials and Methods

3.2.1   Materials

Stereotaxic surgery Materials

- Sprague-Dawley male rats, 3 months old (Envigo)
- Isoflurane Fluriso 250 mL (Vet One, cat no. 13985-528-60)
- F/air anesthesia gas filter (Am Bickford, cat. no. 80120F)
- Petrolatum Ophthalmic Ointment (Pharmaderm, cat. no. 37327)
- Betadine surgical scrub (Purdue Frederick Products, cat no. 19-027132)
- Surgery tools
    - Scalpel # 3 (Fine Science Tools (F.S.T.), cat. no. 10003-12)
    - Blade # 11 (F.S.T., cat. no 10011-00)
    - Cotton-tipped wooden-shaft sterile applicator (Puritan, cat. no. 25806)
    - 0.5 MM drill burr (World Precision Instrument, cat. no. 501855)
    - Hamilton Glass Syringe 10 µL, removable hypodermic needle (Hamilton, cat. no. 80314)
    - Crile-Wood needle holder (F.S.T., cat. no. 12003-15)
    - Narrow pattern Forceps (F.S.T., cat. no. 11002-12)
- Sterile Bone Wax (Med Vet International, cat. no. BW25X12)
- Microsurgical needle with suture nylon thread attached (F.S.T. cat. no 12051-08)

- Ketoprofen (Ketofen) 1 mg/mL (Zoetis, cat. no 4390L)

Stereotaxic surgery Equipment

- Isoflurane anesthesia system Tec 3 EX with 2 L induction box (Vetamac, serial no. SAS2273)
- Rat stereotaxic frame, single manipulator, 18 deg Ear Bars (World Precision Instrument, cat. no 502612)
- Electrical hair shaver
- Bone micro-drill system for Brain Surgery
- Nano-injection system
- Heating Pad

Cylinder test equipment

- Plexiglas transparent cylinder (20 cm diameter and 30 cm height).
- Red bulb light
- Digital Video-camera

Cardiac perfusion materials

- Paraformaldehyde (PFA) (Sigma, cat no. P6148)
- 1X PBS (Sigma, cat no. P5493)
- Pentobarbital sodium, Beuthanasia (50.9 mg/mL) (Merck, cat. no. 81-151148)
- Surgery tools
    - Standard pattern forceps (Fine Science tools (F.S.T.), cat. no. 11000-12)
    - Standard pattern scissors (F.S.T., cat. no. 14101-14)
    - Fine scissors-sharp (F.S.T., cat no 14060-09)
    - Vacutainer safety-lok blood collector 23G (BD, cat. no. 367283)
    - Friedman rongeur (F.S.T., cat. no. 16000-14)
    - Double-ended micro spatula (F.S.T. cat. no. 10091-12)
- Variable flow peristaltic pump (Fisherbrand, cat. no 13-876-1)
- 50 mL sterile conical tubes (Falcon, cat. no. 352098)

Brain Sectioning

- Frozen sliding microtome (ThermoScientific Microm HM430)
- Cryoprotectant in 0.1 M phosphate buffer
  - Sucrose crystalline (Fisher Chemicals, cat. no. S5-500)
  - Ethylene glycol (Fisher Chemicals, cat. no. E178-4)
- Dry Ice
- Clear 24 multiple well plates (Corning, cat. no. 3738)

Immunohistochemistry

- 1X PBS (Sigma, cat no. P5493)
- Proteinase K solution 20 mg/mL (Invitrogen, cat. no. AM2548)
- Triton X-100 (Fisher BioReagents, cat. no. BP151-500)
- Normal Donkey Serum (Jackson ImmunoResearch, cat. no. 017-000-121)
- Primary and Secondary antibodies (Table 3.1)
- Vectastain Elite ABC system (Vector Laboratories, cat. no. PK-7200)
- DAB Peroxidase substrate kit (Vector Laboratories, cat. no. SK-4100)
- DPX Mountant (Electron Microscopy Sciences, cat. no. 13512)
- Non-permanent EMS-Mount (Electron Microscopy Sciences, cat. no. 17986-06)
- Coverslips 24x40-1 (Fisherbrand, cat. no. 12-545-87)
- Superfrost plus microscope slides (Fisherbrand, cat. no. 22-037-246)

Table 3.1. Antibodies			
Primary Antibodies			
Immunogen	**Host**	**Species Reactivity**	**Vendor**
Alpha-Synuclein SYN1	Mouse	Rat, Human	BD Biosciences cat. no. 610787
Alpha-Synuclein LB509	Mouse	Human	Abcam cat. no. ab27766

Table 3.1. (Continued)			
Tyrosine hydroxylase (TH)	Rabbit	Human, Rat, Mouse, Feline, Ferret, Squid, Drosophila, Mollusk	Millipore cat. no. AB152
Tyrosine hydroxylase (TH)	Sheep	Mammals, Rat, Mouse	Millipore cat. no. AB1542
Alpha-synuclein phosphoSerine129 EP1536Y (pSer129)	Rabbit	Mouse, Rat, Human	Abcam cat no. ab51253
Alpha-synuclein phosphoSerine129 81A (pSer129)	Mouse	Human, Mouse	Millipore cat. no MABN826
Polyubiquitinated conjugates (pUB)	Mouse	Species independent	ENZO cat. no BML-PW8805-0500
Secondary Antibodies			
	Host	**Species Reactivity**	**Vendor**
IgG Alexa Fluor 488	Donkey	Mouse	Jackson ImmunoResearch cat. no. 715-545-151
IgG Alexa Fluor 488	Donkey	Rabbit	Jackson ImmunoResearch cat. no. 711-165-152
IgG Cy3	Donkey	Rabbit	Jackson ImmunoResearch cat. no. 715-165-152
IgG Cy3	Donkey	Mouse	Jackson ImmunoResearch cat. no 715-165-151
IgG Cy3	Donkey	Sheep	Jackson ImmunoResearch cat. no 713-165-147
IRDye 800CM IgG	Donkey	Sheep	LI-COR cat. no. 925-32214
Biotin IgG	Donkey	Mouse	Jackson ImmunoResearch cat. no 715-065-151
Biotin IgG	Donkey	Rabbit	Jackson ImmunoResearch cat. no 711-065-152

Fractionation of rat brain tissue

- HEPES buffer Sucrose (Lysis buffer)
    - HEPES (Sigma, cat. no. H3375)

      ○ Sucrose crystalline (Fisher Chemicals, cat. no. S5-500)

      ○ Phenylmethylsulfonyl fluoride (PMSF) (Sigma, cat. no P7626)

      ○ Protease inhibitor cocktail (Sigma, cat. no. P8340)

- Pestle homogenizer

- 1.5 mL microcentrigure tubes

- Sonicator XL-2000 (QSONIC)

- Centrifuge

Western Blotting

- Acrylamide (Sigma, cat. no. A3553)

- Bisacrylamide (Sigma, cat. no. 294381)

- Primary and Secondary antibodies (Table 3.1)

- 1X PBS (Sigma, cat no. P5493)

- Tween 20 (Fisher BioReagents, cat. no. BP337-500)

- Immobilon-P PVDF Membrane 0.45 μm (Millipore, cat. no. IPFL00010)

- Dry milk powder

- Paraformaldehyde (PFA) (Sigma, cat no. P6148)

- BSA (Fisher BioReagents, cat. no. BP9703100)

- Methanol (Fisher Chemical, cat. no. A452-4)

- ECF substrate for Western Blotting (GE Healthcare Amersham, cat. no. RPN5785)

3.2.2 Adeno-associated viral vector production

Recombinant AAV2/9 (rAAV) vectors were produced by the Viral Vector Facility of the Bezard laboratory (Bordeaux, France) as described before[21]. The viruses rAAV-aSyn-WT, rAAV-aSyn-A53E, rAAV-aSyn-A53T, and rAAV-stuffer were prepared from the corresponding AAV expression plasmids AAV9-CMVie/SynP-synWT-WPRE, AAV9-CMVie/SynP-synA53T-WPRE, AAV9-CMVie/SynP-synA53E-WPRE, and AAV2/9-CMVie/hSynP-WPRE-pA (Stuffer), where 'stuffer' refers to the empty vector.

3.2.3 Animals and surgery

All procedures for working with animals were approved and conducted in accordance with guidelines set by the Purdue Animal Care and Use Committee (PACUC). Adult male Sprague Dawley rats weighing 300 to 350 g at the time of surgery were housed two per cage with *ad libitum* access to food and water in a 12 h light/dark cycle.

All surgical procedures were performed under general anesthesia involving inhalation of isoflurane (3% isoflurane, 97% O_2, 150 CC/min). Rats were placed in a stereotaxic frame, and a solution of recombinant adeno-associated virus (rAAV) (4×10^9 genome copies in a 2 µL volume) was injected above the right *substantia nigra* (SN) (at 5.2 mm posterior and 2.0 mm lateral to bregma, 8.0 mm ventral to dura) using a 10 µL Hamilton syringe fitted with a glass capillary. Viral vector solution was infused at a rate of 200 nL/min, and the needle was left in place for an additional 5 min before slowly being retracted. There were 4 groups of rats (injected with rAAV-aSyn-WT, rAAV-aSyn-A53E, rAAV-aSyn-A53T, or rAAV-stuffer), and 12 animals per group.

3.2.4 Limb use asymmetry (cylinder) test

Rats were examined for limb use asymmetry using the cylinder test every 2 weeks after the viral injection. Rats (8 to 12 per group) were placed inside a transparent cylinder (20 cm diameter and 30 cm height) (Fig. 3.2A), and a video camera placed above the cylinder was used to record the rat's forelimb placements on the inner cylinder wall during the animal's spontaneous rearings over a period of 5 min. An investigator blinded to the group identities used the camera's slow motion and frame-by-frame features to score instances of i) left forelimb placement in the absence of right forelimb use, ii) right forelimb placement in the absence of left forelimb use, and iii) placement of both forelimbs on the inner cylinder wall. The overall limb-use asymmetry ratio was calculated from these data using the following formula:

$$\text{asymmetry ratio} = \frac{\text{\# of ipsilateral paw placements - \# of contralateral paw placements}}{\text{total \# of paw placements}}$$

where 'ipsilateral' and 'contralateral' refer to the same or opposite side relative to the brain hemisphere receiving the viral injection.

3.2.5 Post-mortem processing

A subset of rats (8 per group) were killed by pentobarbital sodium overdose (50.9 mg/ml, 2 mL/Kg), and perfused transcardically with 1X PBS followed by 4% (w/v) PFA in PBS. Brains were removed quickly after death and post-fixed overnight in the same fixative, then cryoprotected in PBS containing 30% sucrose at 4 ºC until sectioning[21]. Coronal sections (40 μm thick) were prepared from the brains of perfused rats using a frozen sliding microtome (ThermoScientific Microm HM430). Sections were stored at -20 ºC in cryoprotectant (30% w/v sucrose and 30% v/v ethylene glycol in 0.1 M phosphate buffer) prior to immunohistochemistry (IHC). Another subset of animals (4 per group) were killed 14 weeks after viral injection by decapitation, and their brains were flash-frozen with liquid nitrogen and stored at -80 °C for subsequent biochemical analysis.

3.2.6 Immunohistochemistry

IHC was performed on free-floating sections. A subset of sections were treated with Proteinase K (20 μg/mL) for 10 min at 37 °C before immunostaining to determine the levels of aSyn aggregates resistant to protease digestion[22,23] Sections processed for stereological analysis were pretreated overnight with a solution of 1% (v/v) Triton X-100 in PBS.

For 3,3'-diaminobenzidine (DAB) staining, sections were quenched with 3% (v/v) H_2O_2 (10 min, 22 °C) and blocked with blocking solution (1X PBS supplemented with 0.3% (v/v) Triton X-100 (PBS-T) and 10% (v/v) normal donkey serum) for 90 min at 22 °C. Sections were then incubated in primary antibody solution (anti-human aSyn (LB509, 1:250), anti-aSyn pSer129 (EP1536Y, 1:250), or anti-TH (1:2000) prepared in PBS-T supplemented with 1% (v/v) normal donkey serum) overnight at 4 ºC. After washing with 1X PBS (6 x 10 min, 22 °C), the sections were incubated with biotin-conjugated secondary antibodies (1:200 in PBS-T supplemented with 1% (v/v) normal donkey serum)

for 1 h at 22 °C, washed with 1X PBS (3 x 10min, 22 ºC), and treated with avidin-biotin-peroxidase complex (ABC Elite KIT) for 30 min at 22 °C. The sections were stained using DAB as a chromogen (30 to 40 sec exposure), mounted, and sealed with a coverslip and mounting medium.

For fluorescence IHC, sections were blocked as outlined above and incubated in primary antibody solution (anti-human aSyn (LB509, 1:250), anti-aSyn pSer129 (EP1536Y, 1:250), anti-TH (1:2000), or anti-polyUbiquitin (1:250) prepared in PBS-T supplemented with 1% (v/v) normal donkey serum) overnight at 4 ºC. After washing with 1X PBS (6 x 10 min, 22 °C), the sections were incubated with secondary antibodies conjugated to Alexa fluor or IR dye (1:500 in PBS-T supplemented with 1% (v/v) normal donkey serum) for 1 h at 22 °C and washed with 1X PBS. Images were obtained using a Nikon A1 confocal microscopy system or a LI-COR Odyssey imaging system and analyzed using the NIS Elements and Image Studio software packages.

3.2.7   Unbiased stereology

The total number of TH-positive neurons in the SNpc region was determined using the optical fractionator principle[24]. Unbiased stereology optimization and cell counting performed by an investigator blinded to the experimental treatments using the Visiopharm stereology software. Every 6th section spanning the entire SN was included in the counting procedure[25]. After IHC procedure, The average final section thickness was 30 μm, with a guard height of 0.5 μm for the top and bottom surfaces of the section. Cells clearly staining positive for TH were counted using an optical dissector workflow with a 37 μm x 37 μm counting frame (height x width) and a sampling grid of 80.7 μm x 80.7 μm. The optical dissector was used to randomly count between 200 and 300 fields per section starting at the top left corner of a region of interest (ROI) drawn around the SNpc. Stereotaxic parameters were optimized using sections from 3 animals injected with rAAV-stuffer. The average coefficient of error for each SN region analyzed was between 0.04 and 0.1, considered acceptable as an indication of cell count accuracy[24].

3.2.8 Fractionation of rat brain tissue

The rat brain fractionation procedure (Fig. 3.1) was adapted from a previously published protocol[15]. Flash frozen SN (20 mg) was manually grinded using a pestle homogenizer in 500 μL of ice cold lysis buffer (4 mM HEPES, pH 7.4, 0.32 mM sucrose, 1X protease and phosphatase inhibitors). The homogenized sample was sonicated with a QSonica XL2000 sonicator probe set up at output wattage 3 (10 strokes, 5 sec each). The sonicated tissue was centrifuged at 900 x g for 10 min at 4 ℃. The pellet from this spin (P1, enriched with heavy membranes and nuclear material) was resuspended in 50 μL lysis buffer and stored at -80 ℃ until use. The supernatant from the first spin (S1, enriched with soluble cytosolic material) was centrifuged at 10,000 x g for 15 min at 4 ℃. The resulting supernatant (S2, enriched with cytosolic light membranes) was stored at -80 ℃ until use, whereas the pellet (P2, the crude synaptosomal fraction) was resuspended in 400 μL of lysis buffer and centrifuged at 10,000 x g for 15 min at 4 ℃. The resulting pellet (P2') was resuspended in 500 μL of milliQ H_2O to cause a hypoosmotic shock, sonicated at output wattage 3 (5 strokes, 5 sec each), and supplemented with 2 μL of 1 M HEPES (pH 7.4) to adjust the concentration of HEPES to 4 mM. Further lysis of P2' was performed by incubating the sample for 30 min at 4 ℃ with gentle agitation. The P2' suspension was then centrifuged at 20,000 x g for 20 min at 4 ℃, and the resulting supernatant (S3) was stored at -80 ℃. The pellet from this spin (P3, the synaptosomal membrane fraction) was resuspended in 50 μL of lysis buffer and stored at -80 ℃ until use.
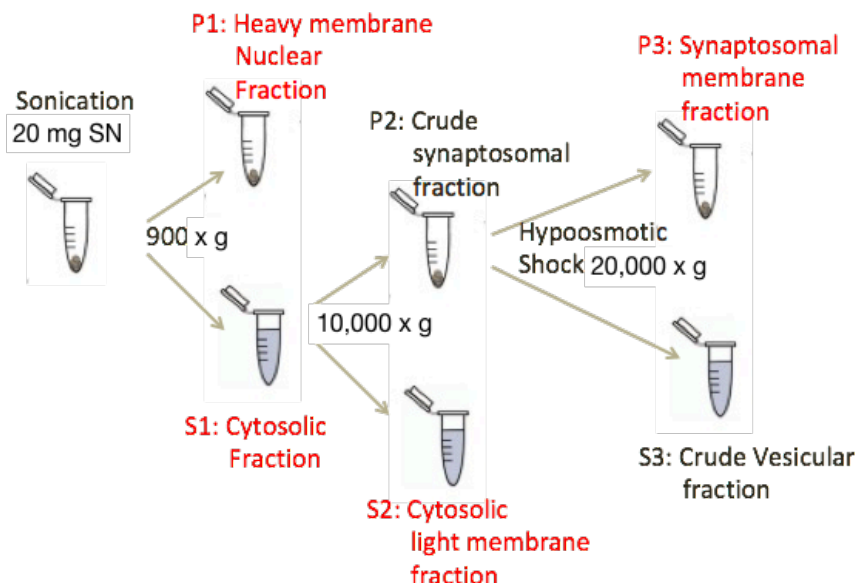
Figure 3.1. Schematic representation of rat brain fractionation procedure. Sequential centrifugation steps allow isolation of different subcellular fractions (See 'Materials and Methods' for details). Fractions indicated in red (S1, P1, S2, P3) were selected for Western blot analysis of membrane-associated aSyn.

3.2.9 Western blotting

Expression levels of total human aSyn and aSyn pSer129 in subcellular fractions obtained from samples of injected and intact rat SNpc were determined via Western blot analysis. The same volume from S1, P1, S2 and P3 fractions (10 uL of each) were combined with Laemmli buffer (final concentration, 60 mM Tris–HCl, pH 6.8, 2% (w/v) SDS, 10% (v/v) glycerol, 5% (v/v) β-mercaptoethanol, 0.01% (w/v) bromophenol blue), and the mixtures were boiled for 5 min (S1, S2, and P3) or heated at 70 ºC for 10 min (P1). Denatured proteins were separated via SDS-PAGE on a 15% (w/v) resolving gel and transferred to a PVDF membrane (pore size, 0.4 µm) at a voltage of 100 V for 1 h. The membrane was treated with 0.4% (w/v) PFA for 30 min at 22 ºC to crosslink the bound proteins. After blocking in 1X PBS supplemented with 5% tween 20 (PBS-T) and 10% (w/v) non-fat milk for 1 h at 22ºC, the membrane was washed with PBS-T and probed with primary antibody (anti-total aSyn (Syn1, 1:1500), anti-human aSyn (LB509, 1:1000), or anti-aSyn pSer129 (81A, 1:1000), prepared in PBS-T supplemented with 1% (w/v) BSA) overnight at 4 ºC. After washing in PBS-T, the membrane was probed with a secondary anti-mouse antibody conjugated to alkaline phosphatase (1/6000). To visualize the bands, the membrane was exposed to ECF substrate for 30 s, and images were acquired using an

Amersham Imager 600 RGB (GE Life Sciences, USA). Band densities were quantified using ImageJ software (NIH, Bethesda, MD).

3.2.10 Statistical Analysis

Behavioral data and mean fluorescence units from striatal terminals were analyzed by two way ANOVA followed by Tukey's multicomparison *post hoc* test. Outliers were identified and removed using the ROUT method. All statistical tests were carried out using GraphPad Prism 7.0

3.3 Results

3.3.1 Pilot Study: Short term expression of human aSyn in rat SN do not result in nigrostriatal lesion

Three months old male Sprague Dawley rats, 3 per group, were unilaterally stereotaxic injected in the SN with rAAV vectors encoding three aSyn variants: aSyn-WT, -A53T, and –A53E, and an empty rAAV vector control namely 'Stuffer. Three weeks after the viral injection, the rats were perfused with PFA, and the fixed brains were harvested in order to determine aSyn expression in SN and any aSyn toxicity-related striatal lesion. Coronal brain sections that contained the SNpc were co-stained for TH (to visualize nigral DA neurons) and human aSyn. Sections that contained the striatum were stained for TH to assess striatal DA nerve terminal density. Human aSyn was detected in DA neurons of the SNpc in the injected (but not the non-injected) hemisphere of rats infused with aSyn-encoding virus, whereas aSyn was absent from animals injected with rAAV-stuffer. Expression analysis data (data not shown) at this time point suggested that the level of expression of human aSyn was 1 fold higher from endogenous aSyn levels, however these results should be confirmed in replicate experiments. At this early time point, there was no evident loss of DA neurons or nerve terminals in the injected hemisphere versus the intact hemisphere for any of the treatment groups(Fig. 3.2). Moreover, no significant differences in nigral or striatal TH immunoreactivity were observed when comparing sections from animals injected with rAAV encoding the aSyn variants versus rAAV-stuffer (Fig. 3.3).
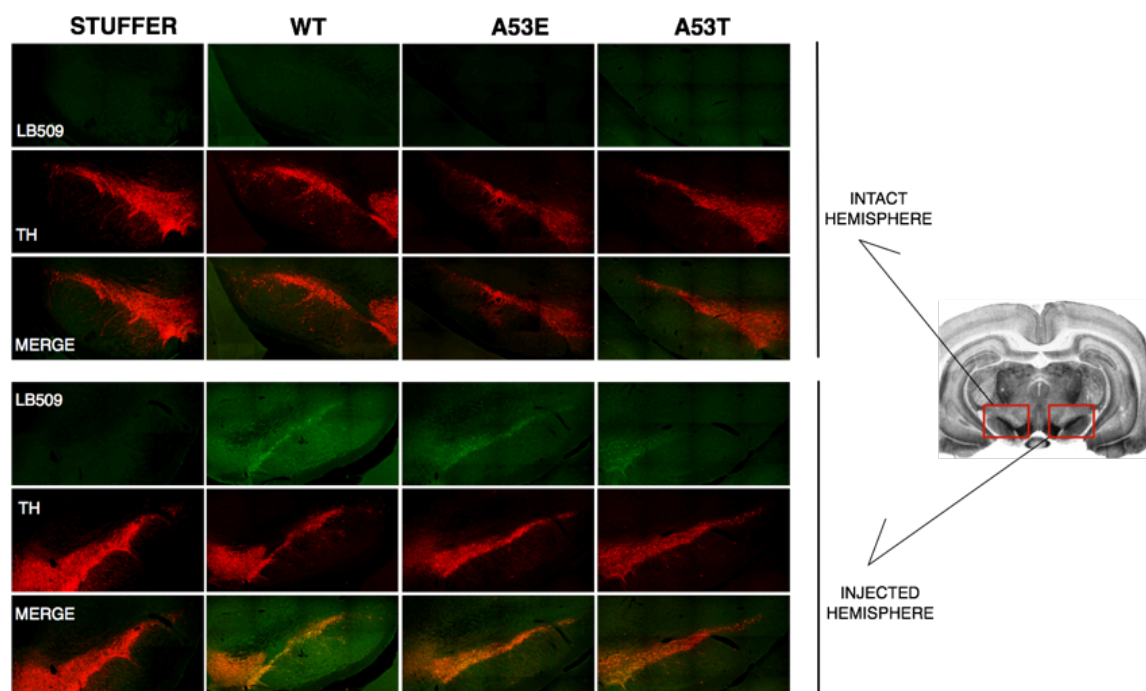
Figure 3.2. Pilot study: human aSyn expression in SN of rats stereotaxically injected only in the right hemisphere. Confocal microscopy images show nigral sections from the intact hemisphere (top set of panels) and the injected hemisphere (bottom set of panels) of rats transduced in the SN with rAAV-stuffer or -aSyn. The sections were stained for human aSyn (LB509, green laser) or TH (red laser) ('merge' panels show the overlap of the two stains). aSyn was only expressed in the injected SN of animals transduced with rAAV-aSyn (but not rAAV-stuffer), and there was considerable overlap between aSyn and TH immunoreactivity in this region. Images were taken using a NIKON A1 confocal system (4x3 large stitched images, 20X magnification) and analyzed with the NIS elements software. The reference SN section on the right was adapted from[26].

Figure 3.3. Animals transduced with rAAV-aSyn show no lesion in striatal dopaminergic terminals three weeks after the injection. <u>Left panel</u>: near-infrared scan of striatal sections stained for TH (green signal) (the numbers in red indicate striatal regions analyzed in terms of TH near-IR signal intensity in each of the samples). No lesion is evident in the intact side (Left – L) or the injected side (Right –R). <u>Right panel</u>: bar graph showing striatal TH signal for different groups of sections. The data show that there is no lesion in the injected hemisphere in any of the animals. Striatal sections were scanned using the LI-COR Odyssey system at IR800 scanning range. (n = 3 per group, 4 striatal sections per animal)

3.3.2   Rats expressing human A53E show a time-dependent increase in forelimb asymmetry.

Three months old male Sprague Dawley rats were unilaterally stereotaxic injected in SN with rAAV vectors encoding three aSyn variants: aSyn-WT, -A53T, and –A53E, and a control empty rAAV vector namely 'Stuffer. A total of 12 animals per group were characterized in terms of neurotoxic-related motor impairment, nigrostriatal lesions and membrane-induced aSyn aggregation. During a period spanning 14 weeks after the injection, the animals were tested for any deterioration of motor function using the limb use asymmetry (or 'cylinder') test (Fig. 3.4A). The results showed a trend towards increased use of the ipsilateral versus the contralateral forelimb (relative to the hemisphere of the injected SNpc) for animals injected with rAAV encoding the aSyn variants in comparison with the 'stuffer' control animals, which showed a balanced use of both forepaws during exploration of the cylinder walls. In the case of animals injected with rAAV-aSyn-WT, this apparent asymmetry did not become more pronounced during the 14-week analysis period (Fig. 3.4C). At week 12, a significant increase in the asymmetry ratio (suggestive of increased use of the forelimb controlled by the intact versus the lesioned SNpc) was observed for rats expressing the A53E mutant compared to control ('stuffer') animals (Fig. 3.4B). At week 14, a significant increase in the asymmetry ratio was observed for both A53E- and A53T-expressing rats compared to control animals (Fig. 3.4D).
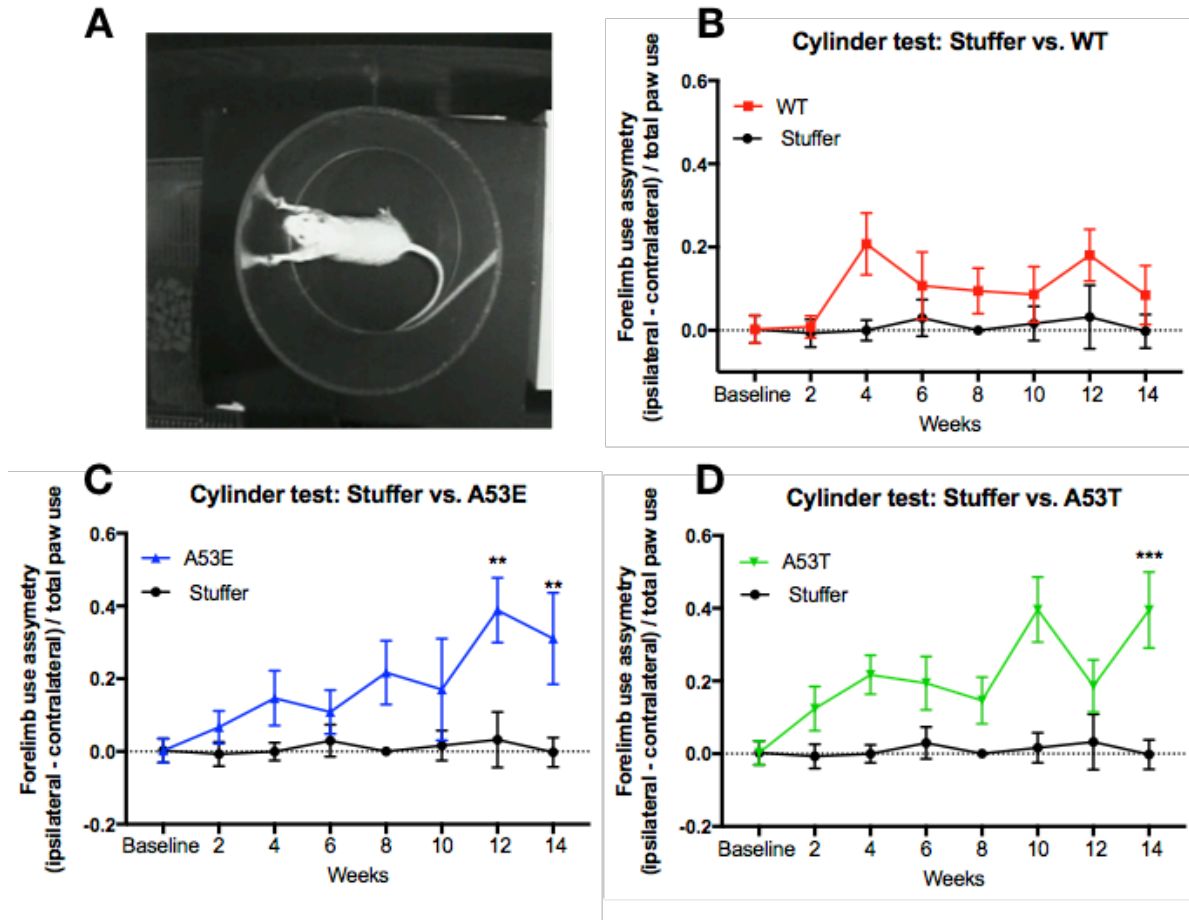
Figure 3.4. Data from the test show evidence of motor deficits associated with the expression of A53E or A53T in rat SN. Animals were stereotaxically injected with rAAV vectors encoding aSyn WT, A53T, or A53E or with stuffer (control) virus in the right SN. 14 weeks after the injection, rats were examined using the limb use asymmetry (cylinder) test. A. Image showing an overhead view of rat exploring the inner wall of a Plexiglas cylinder. B-D. Graphs of forelimb use asymmetry (calculated based on the number of times that the animals touched the cylinder wall with the ipsilateral, contralateral, or both forelimbs with respect to the lesioned side of the brain) plotted against the time after viral injection. The plots show comparisons of the data obtained for rats injected with rAAV-aSyn-WT (B), -A53E (C), or –A53T (D) versus rats infused with rAAV-stuffer. Data points are presented as the mean ± SEM, n = 12; **$p < 0.01$ A53E versus control, +++$p < 0.001$ A53T versus control, two-way ANOVA followed by Tukey's multiple comparison *post hoc* test. Outliers were identified and removed using the ROUT method (Q = 1%, a maximum of 3 outliers removed)

3.3.3 Expression of human A53E in rat SN results in PD-like neuropathology

3.3.3.1 Loss of striatal dopaminergic terminals

Fourteen weeks after the viral injection, striatal sections from 4 animals in each of the 4 groups (injected intranigrally with rAAV-stuffer, -aSyn-WT, -aSyn-A53T, or aSyn-A53E) were stained for TH to assess DA nerve terminal density. The results revealed a

significant reduction in the overall TH$^+$ fluorescence signal in striatal sections from the injected (but not the non-injected) hemisphere of animals infused with rAAV-aSyn-WT, -aSyn-A53T, or -aSyn-A53E (Fig 3.5). Rats injected with control virus (rAAV-stuffer) showed no lesion in the striatum. These results suggest that all three aSyn variants examined in our study elicited similar degrees of striatal DA nerve terminal depletion.
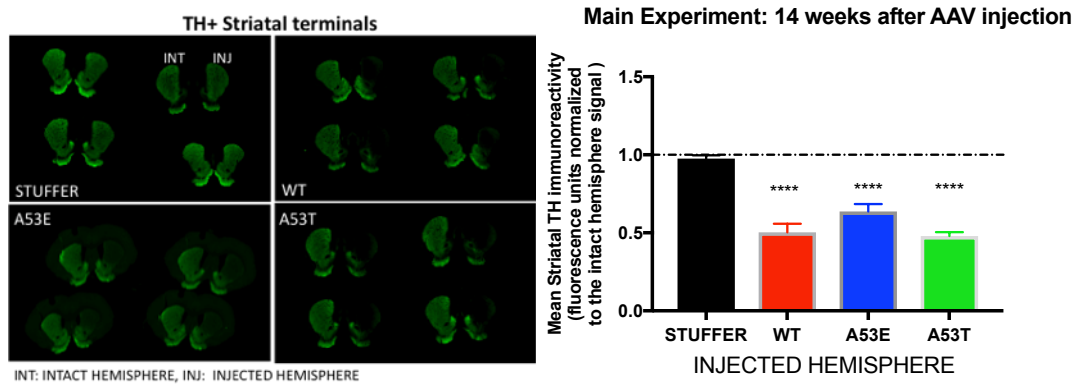
Figure 3.5. Expression of human aSyn-WT, -A53E or -A53T in rat SN leads to a loss of striatal DA terminals in the lesioned hemisphere. Rats were injected with rAAV-stuffer or rAAV-aSyn-WT, -A53E, or -A53T in the right SN, and striatal sections prepared from 4 animals per group at 14 weeks were stained for TH. Left panel: near-infrared scan of striatal sections showing TH signal (green). Severe lesions are evident in the injected side (INJ) of animals expressing WT, A53E and A53T. Right panel: bar graph showing striatal TH signal for different groups of sections. Transduction with rAAV ending aSyn variants, but not with rAAV-stuffer, leads to a decrease in a striatal TH fluorescence. Striatal sections were scanned using a LI-COR Odyssey system at IR800 scanning range. Data bars are presented as the mean ± SEM, n = 4; 4 striatal sections per animal ****p < 0.0001 versus control and versus intact side, two-way ANOVA followed by Turkey's multiple comparison *post hoc* test.

3.3.3.2 Loss of nigral dopaminergic neurons

Nigral sections obtained 14 weeks after the viral injection were co-stained for TH and human aSyn to visualize DA neurons and assess aSyn expression levels, respectively. The results showed evidence of robust human aSyn expression in TH$^+$ neurons in the injected (but not the non-injected) SNpc of animals transduced with rAAV-aSyn virus. Moreover, the overall nigral TH immunoreactivity appeared to be reduced in the injected versus the hemisphere of each section, as well as in the injected SNpc of rats transduced with rAAV-aSyn virus versus rAAV-stuffer virus. Quantification of TH$^+$ neurons via unbiased stereology revealed a trend towards DA neuron loss in the injected SNpc of animals infused with rAAV encoding WT or mutant aSyn, but not rAAV-

stuffer (Fig. 3.6). This suggestive trend will be confirmed via stereological analysis of sections prepared from the injected SNpc of 4 additional animals per group. Additional specific neuronal staining such as MAP2 or cresyl violet will be necessary to contrast and confirm the selective decrease of dopaminergic TH$^+$ neurons loss, and the potential depletion of other neurons types.
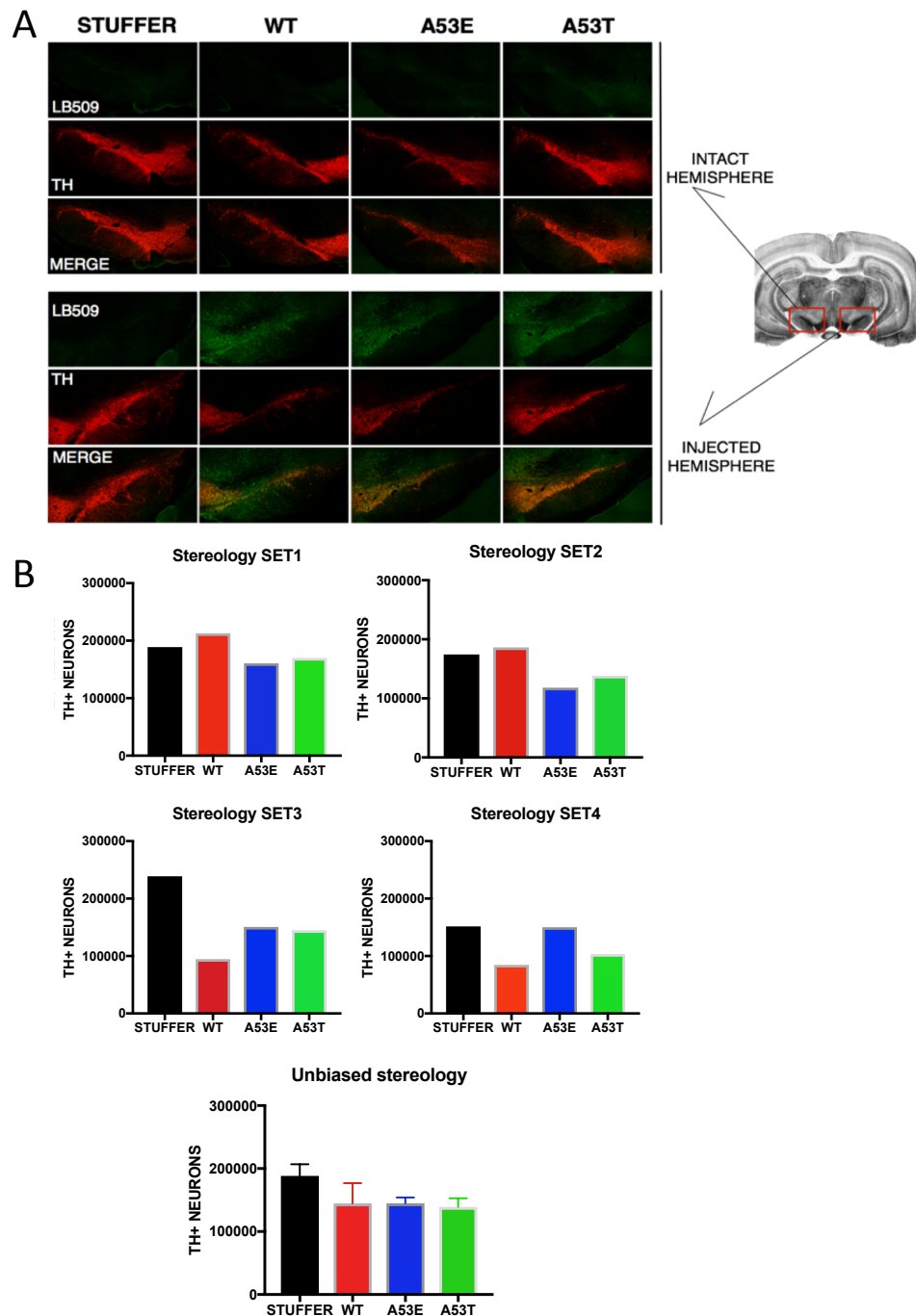
*Figure 3.6.

*Figure 3.6. Main study: Expression of human aSyn –WT, -A53E or –A53T in rat SN leads to nigral DA cell loss in the lesioned hemisphere. Rats were injected with rAAV-stuffer or with rAAV-aSyn-WT, -A53E, or A53T in the right SN, and nigral sections prepared from 4 animals per group at 14 weeks were stained for TH. A. Confocal microscopy images show nigral sections from the intact hemisphere (top set of panels) and the injected hemisphere (bottom set of panels) of rats transduced in the SN with rAAV-stuffer or -aSyn. The sections were stained for human aSyn (LB509, green laser) or TH (red laser) ('merge' panels show the overlap of the two stains). aSyn was only expressed in the injected SN of animals transduced with rAAV-aSyn (but not rAAV-stuffer), and there was considerable overlap between aSyn and TH immunoreactivity in this region. Images were taken using a NIKON A1 confocal system (4x3 large stitched images, 20X magnification) and analyzed with the NIS elements software. The reference SN section on the right was adapted from[26]. B. Bar graphs stereological data showing that transduction with the rAAV encoding the different aSyn variants (but not with rAAV-stuffer) leads to a loss of TH$^+$ neurons in the injected SN.

3.3.4 Evidence of Lewy-like neuropathology in rats injected with rAAV-aSyn

3.3.4.1 Proteinase K-resistant human aSyn inclusions

In order to detect aSyn aggregates, we stained sections prepared from the intact and injected SNpc regions of rAAV-transduced rats for human aSyn after proteinase K (PK) treatment. Because aSyn aggregates are resistant to PK digestion, treating brain sections with PK enhances the immunoreactivity of aSyn inclusions relative to the more diffuse stain observed for monomeric aSyn[27]. Abundant PK-resistant aSyn inclusions were found in neurons of the injected SNpc in animals infused with rAAV-aSyn-WT, -A53E, or -A53T, but not rAAV-stuffer (Fig 3.7, right panel). Interestingly, PK-resistant aSyn inclusions were also found in neurites and dotted structures of the intact SNpc in rats infused with aSyn virus (Fig. 3.7, middle panel), implying that the expressed human aSyn spread into the non-injected hemisphere.
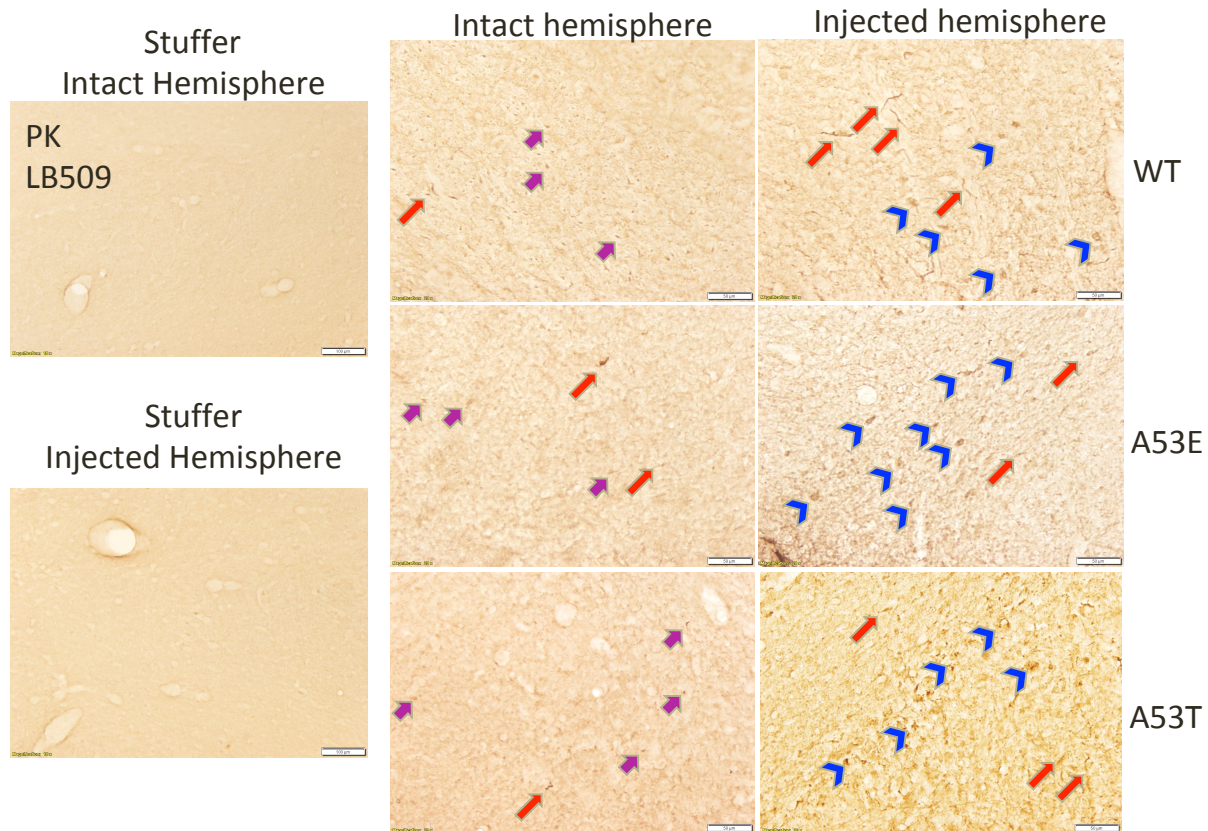
Figure 3.7. Expression of rAAV-aSyn-WT, -A53E, or –A53T leads to the formation of proteinase K-resistant aSyn aggregates in rat SN. The distribution of human aSyn in the intact and injected SN was examined via immunohistochemical analysis using a method involving proteinase K pre-treatment followed by the staining with the human aSyn-specific antibody LB509. Left column: images of intact and injected SN of control animals infused with rAAV-Stuffer showing a lack of human aSyn immunoreactivity. Center and right columns: Images of intact and injected SN or rats infused with rAAV-aSyn-WT (top), -A53E (middle), or –A53T (bottom) showing evidence of aSyn aggregation in both hemispheres. Lewy neurite-like structures (red arrows) and LB509^{+} dots (purple arrows) were found at low density in the intact side, suggesting (as one possibility) that misfolded aSyn may have spread from the injected hemisphere. Abundant Lewy body-like structures (blue arrowheads) and Lewy neurite-like structures (red arrows) were found in the injected SN. Images were taken at 20X magnification under bright-field illumination using an Olympus inverted microscope.

3.3.4.2 aSyn inclusions staining positive for pSer129

Phosphorylation of aSyn at serine 129 is a specific marker of aggregated aSyn in rodent or human brain[28,29]. As an additional approach to determine levels of nigral aSyn inclusions (as compared to staining for PK-resistant aSyn), we stained sections from the injected SNpc of rAAV-transduced rats for aSyn-pSer129 using the EP1536Y antibody. The results revealed aSyn-pSer129 immunoreactivity above background in the injected SNpc of rats infused with rAAV-aSyn-WT, -A53E, or -A53T, but not rAAV-stuffer

(Fig. 3.8). In general, nigral sections from animals injected with virus encoding WT or A53T aSyn were characterized by a more diffuse aSyn-pSer129 stain throughout the soma, as well as the presence of punctate cytoplasmic inclusions (Fig. 3.8, insets). In contrast, aSyn-pSer129$^+$ cells in sections from A53E-expressing animals generally showed a more intense, beaded staining pattern along the cell periphery.
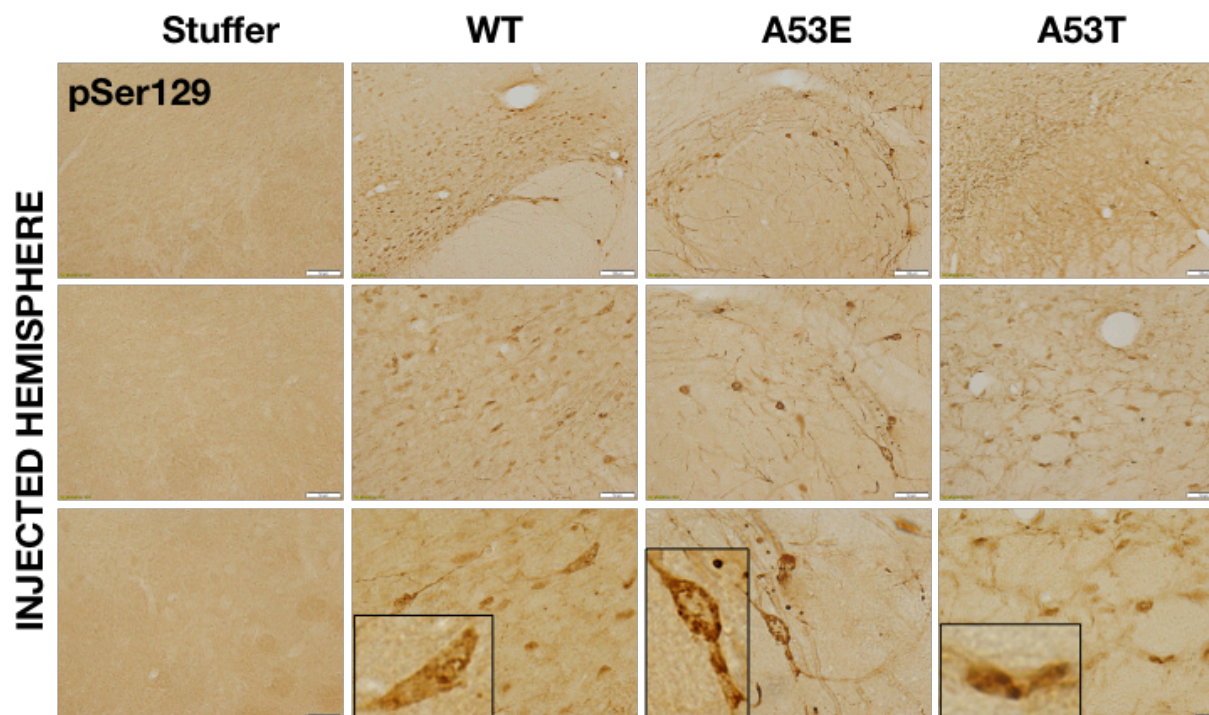
Figure 3.8. Expression of rAAV-aSyn-WT, - A53E, or –A53T leads to the formation of aSyn-pSer129$^+$ aggregates. Sections containing injected SN from animals infused with rAAV enconding human aSyn-WT, -A53E or -A53T or with rAAV-stuffer were stained with an antibody specific for aSyn-pSer129 (EP1536Y) and visualized with DAB. Images show evidence of pronounced pSer129 EP1536Y staining sections from rats overexpressing the aSyn variants, but not in rats infused with rAAV-stuffer. Images were taken at 10X, 20X and 40X magnification under bright-field illumination using an Olympus inverted microscope.

3.3.4.3 Polyubiquitinated conjugates in dopaminergic neurons

Another characteristic feature of Lewy bodies is the presence of polyubiquitin (polyUB) chains that presumably reflect failed attempts by neurons to eliminate defective proteins targeted for removal by the ubiquitin-proteasome system or lysosomal autophagy[30,31]. Accordingly, sections from the injected SNpc of rAAV-transduced rats were co-stained for aSyn-pSer129 (using the EP1536Y antibody) and polyUb conjugates. The results showed the presence of TH$^+$ neurons with overlapping aSyn-pSer129 and polyUB

immunoreactivity (both in the soma and in neurites) in the injected SNpc of rats infused with rAAV-aSyn-WT, -A53E, or -A53T, but not rAAV-stuffer (Fig. 3.9).
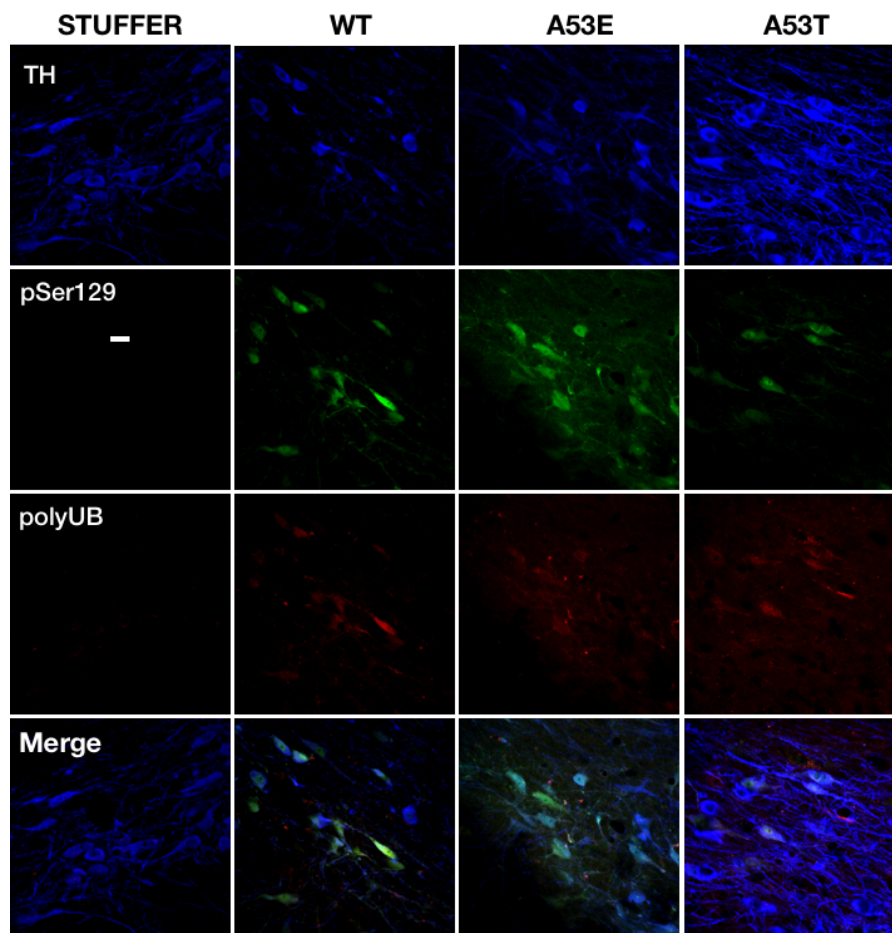
Figure 3.9. Expression of rAAV-aSyn-WT, - A53E, or –A53T leads to the formation of polyubiquitinated Lewy-like aggregates. Sections containing the injected SN from animals infused with rAAV encoding human aSyn-WT, A53E, A53T or or with rAAV-stuffer were co-stained with anitbodies specific for TH (blue), pSer129 (EP1536Y) (green), and polyuniquitinated conjugates (red), and analyzed via confocal microscopy. Merge images show the overlap of the tree stains. The images show evidence of Lewy-like structures in DA neurons. Images were taken at 60X magnification using a Nikon A1 confocal microscope; scale bar, 10 μm.

3.3.4.4   Evidence of membrane-induced aSyn aggregation in rat SN

To assess the subcellular distribution of aSyn in the brains of rats injected with rAAV-aSyn-WT, -A53E, or -A53T (or the control virus, rAAV-stuffer), the lesioned and intact SN regions from 3 animals per group were homogenized and fractionated via differential centrifugation, yielding the fractions illustrated in Fig. 3.1. Four of the recovered fractions were analyzed via Western blotting: S1, P1, S2 and P3. We found that the total aSyn (visualized by probing the blot with Syn1 as the primary antibody)

was present in all four fractions (Fig. 3.10A). Analysis of relative band intensities revealed a similar subcellular distribution of total aSyn (i.e. in general, similar aSyn levels in S1, P1, and S2 and a lower level in P3) when comparing the fractions obtained from the intact and injected SN within each group and across all four groups (Fig. 3.10B).
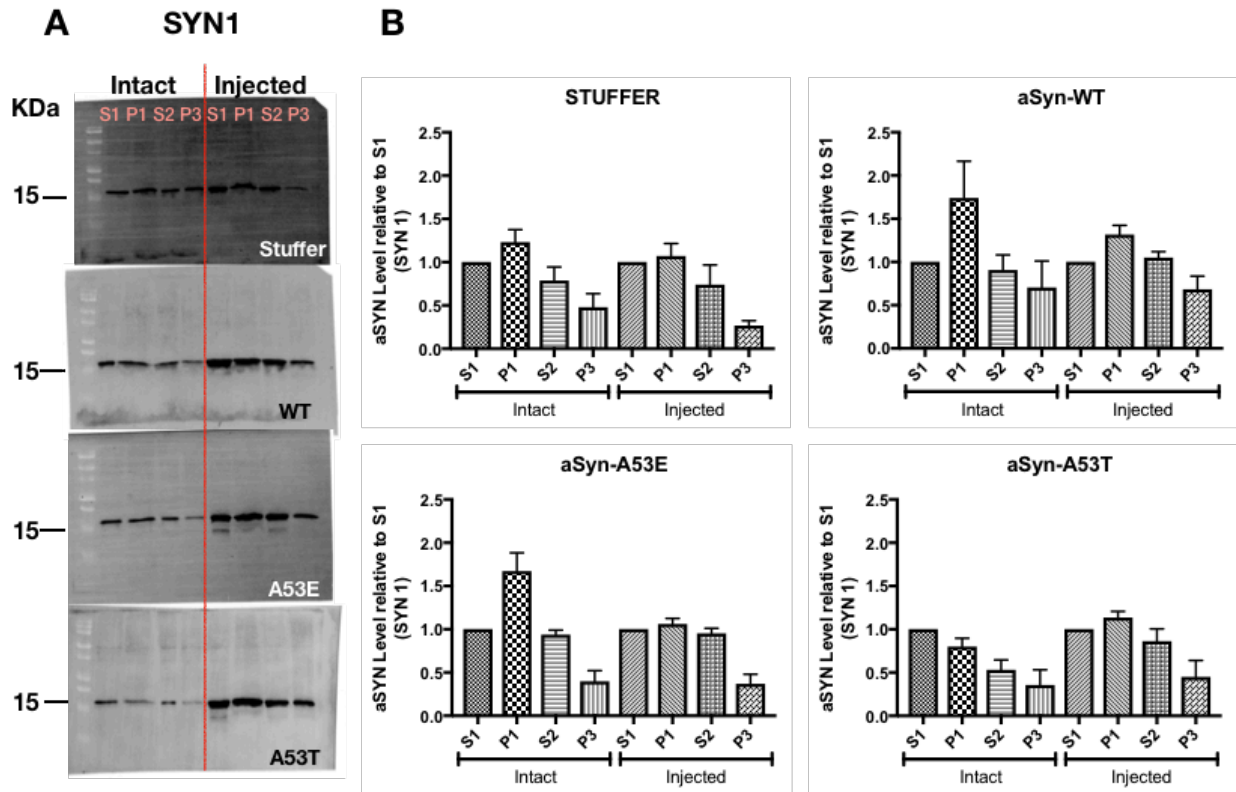
Figure 3.10. Total aSyn is present in multiple subcellular fractions in the SN of rats transduced with rAAV encoding different human aSyn variants. Subcellular fractions prepared from the intact and lesioned SN of rats receiving unilateral injections of rAAV-aSyn-WT, -A53E, or -A53T (or the control virus, rAAV-stuffer) were analyzed via Western blotting with a primary antibody specific for total aSyn (Syn1). A. Representative images of immunoblots showing aSyn expression in four isolated fractions (S1, P1, S2, and P3) from the intact and injected SN. B. Bar graphs showing the distribution of aSyn among the four fractions isolated from the intact and injected SN of rats infused with rAAV-stuffer or rAAV-aSyn-WT, -A53E, or -A53T. aSyn band intensities were determined via densitometric analysis and normalized within each set of four fractions ('intact' or 'injected') to the aSyn band intensity obtained for the corresponding S1 (cytosolic) fraction. N = 3 animals per group.

Western blot analysis of the same fractions using a primary antibody specific for human aSyn (LB509) revealed the presence of immunoreactivity in all four fractions obtained from the lesioned SNpc of rats transduced with rAAV-aSyn-WT, -A53E, or -A53T, but

not rAAV-stuffer, as expected (3.11, top panel). Data obtained via quantitation of the band intensities suggested that human aSyn-WT was present at higher levels in the cytosolic fractions (S1 and S2) than in the heavy membrane/nuclear fraction (P1), whereas A53E and A53T were more evenly distributed across all three fractions (Fig. 3.11, bottom panel). In turn, this observation implies that the familial aSyn mutants had a higher degree of association with cellular membranes in the lesioned SNpc than WT aSyn.

Remarkably, human aSyn immunoreactivity was also detected in the fractions obtained from the intact (non-lesioned) SNpc of at least one animal within each group of rats injected with rAAV-aSyn-WT, -A53E, or -A53T (Fig. 3.11, top panel), suggesting (as one possibility) that the expressed human aSyn variants had the ability to migrate from the injected SNpc to the nigral region in the opposite hemisphere. Pooled band intensity data implied that aSyn-A53E had a higher spreading propensity than aSyn-WT or -A53T (Fig 3.11, bottom panel), although additional controls are needed to confirm this finding (e.g. aSyn band intensities should be normalized to β-tubulin band intensities to correct for potential differences in levels of neuronal protein in homogenates prepared from different hemispheres and from different animals).

It is important to indicate that previous reports have shown that AAV9 viral vectors can use neuronal pathways to be transported into other areas in the brain[32], which suggest that aSyn spreading observed in this animals can be the result of AAV9 spreading.
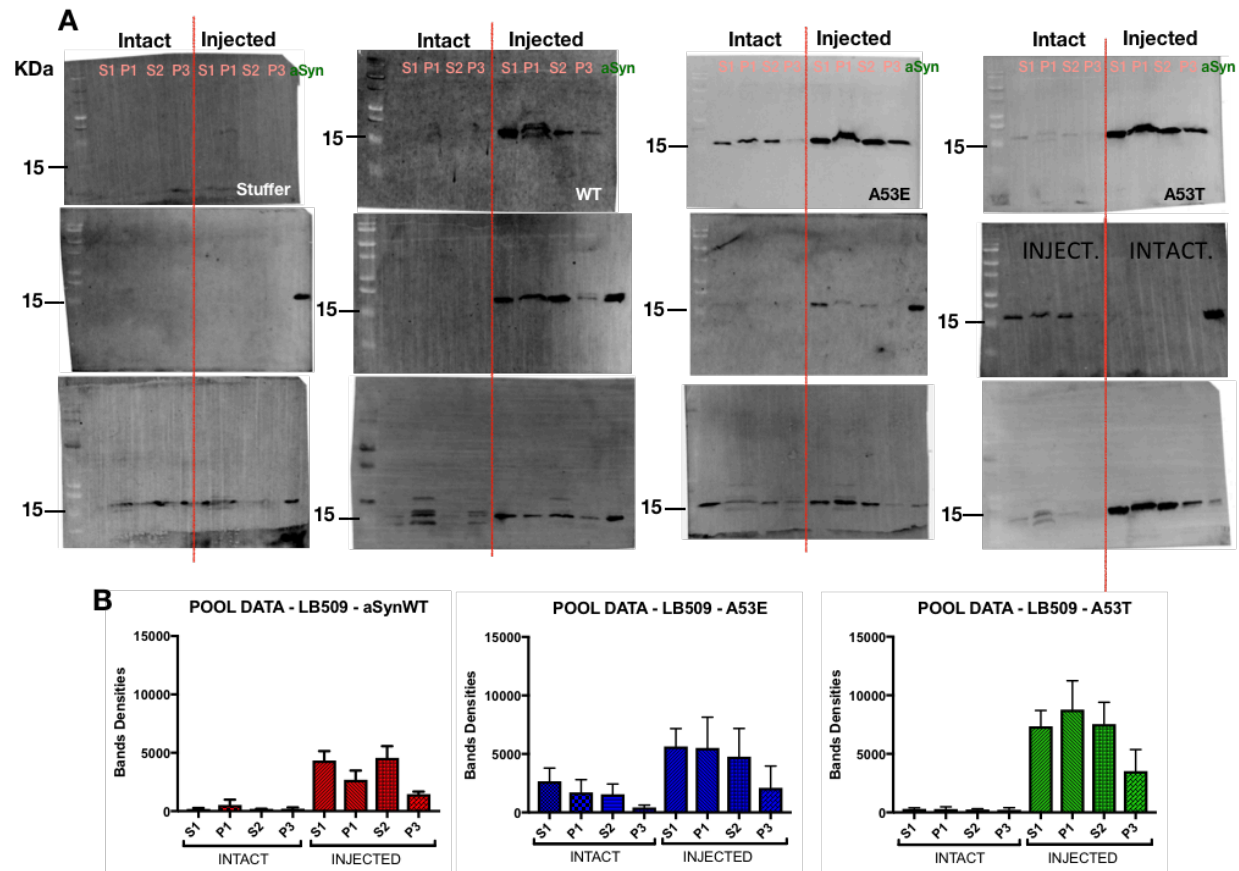
Figure 3.11. Human aSyn is present in multiple subcellular fractions in the SN of rats transduced with rAAV encoding different human aSyn variants. Subcellular fractions prepared from the intact and lesioned SN of rats receiving unilateral injections of rAAV-aSyn-WT, -A53E, or -A53T (or the control virus, rAAV-stuffer) were analyzed via Western blotting with a primary antibody specific for human aSyn (LB509). A. Images of immunoblots showing expression of the different human aSyn variants in four isolated fractions (S1, P1, S2, and P3) from the intact and injected SN. Last lane of middle and bottom images correcpond to 50ng of aSyn recombinant protein standard (green aSyn label). Lower-intensity aSyn bands were found in fractions from the intact hemisphere of at least one animal per group injected with rAAV-aSyn, suggesting a mild spreading of expressed aSyn protein from the injected side. Fractions obtained from the SN of animals injected with rAAV-stuffer did not show bands corresponding to human aSyn (dark dots in stuffer blot could correspond to blotting box primary antibody contamination). B. Bar graphs showing the distribution of human aSyn among the four fractions isolated from the intact and injected SN of rats infused with rAAV-aSyn-WT, -A53E, or -A53T. aSyn band intensities were determined via densitometric analysis. N = 3 animals per group.
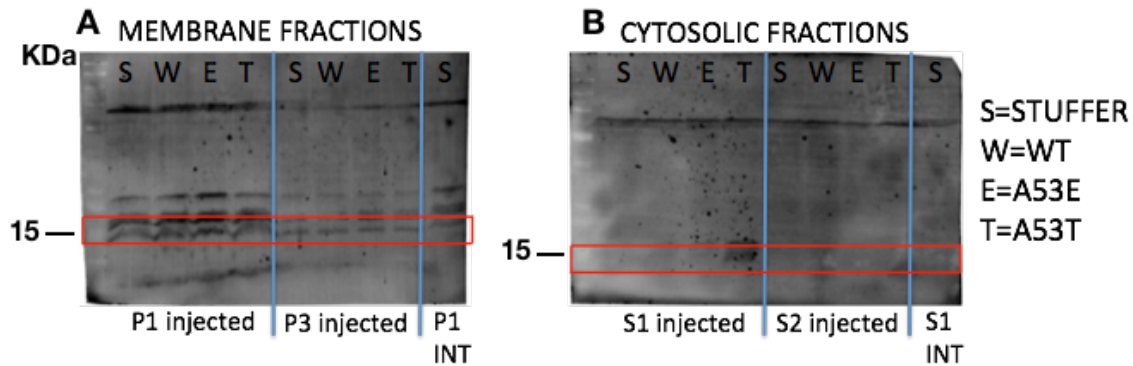
Figure 3.12. Aggregated (pSer129⁺) aSyn is primarily found in membrane-rich fractions isolated from the injected SN of rats infused with with rAAV-aSyn-WT, -A53E, or -A53T. Subcellular fractions prepared from the injected SN of rats receiving unilateral injections of rAAV-stuffer (S) or rAAV-aSyn-WT (W), -A53E (E), or -A53T (T) were analyzed via Western blotting with a primary antibody specific for aSyn-pSer129 (81A). (A) Immunoblot image showing the presence of aSyn-pSer129 in membrane-rich fractions P1 and P3. (B) Immunoblot image showing the absence of aSyn-pSer129 in cytosolic fractions S1 and S2 except for the S1 fraction obtained from the injected SN of a rat lesioned with rAAV-aSyn-A53T. The P1 and S1 fractions isolated from the intact SN of a rat infused with rAAV-stuffer ('P1 INT' (A) and 'S1 INT' (B)) were analyzed as negative controls.

Finally, the fractions obtained from the lesioned SNpc of rats transduced with rAAV-stuffer or rAAV-aSyn-WT, -A53E, or A53T were analyzed via Western blotting using a primary antibody specific for aSyn-pSer129 (81A) to determine the subcellular distribution of aggregated aSyn. aSyn-pSer129 immunoreactivity was detected to a greater extent in the P1 and P3 membrane fractions than in the cytosolic fractions, where aSyn-pSer129 was only present in the S1 fraction of a rat injected with rAAV-aSyn-A53T (Fig. 3.12). These data imply that aggregated (pSer129⁺) aSyn is associated with cellular membranes in rat SNpc, although additional quantitation and normalization, using total aSyn and human aSyn expression, is needed to compare levels of membrane-bound aSyn aggregates in the SNpc of rats expressing different aSyn variants.

3.4   Discussion and Conclusion

The neuropathological features shown by rats expressing human aSyn-A53E in this study were not significantly different from the neurotoxicity elicited by aSyn-WT and aSyn A53T. However, the earlier manifestation of motor impairment in the case of animals injected with rAAV-aSyn-A53E (week 12) compared to animals expressing aSyn-A53T (which showed motor deficits at week 14) or aSyn-WT (which did not exhibit significant forelimb use asymmetry up to the 14-week time point) implies that A53E was the most neurotoxic of the three aSyn variants. The more frequent use of the ipsilateral limb exhibited by A53E- and A53T-expressing animals is supported by the fact that nigrostriatal degeneration was only observed in the injected side, which is consistent with previously reported results by other groups that have characterized rAAV-aSyn rats[21,23,33–35]

Our finding that rats injected with rAAV-A53E or -A53T showed motor deficits at week 14, whereas animals infused with rAAV-aSyn-WT (on average) did not, is consistent with the earlier onset of PD symptoms in families that carry the A53E or A53T mutation[18,36], and aligns well with our observation that a subset of rats expressing WT aSyn showed evidence of a less pronounced loss of DA neurons in the injected SNpc compared to animals expressing either of the two familial mutants. In contrast, rats infused with rAAV-aSyn-WT, -A53E, or -A53T exhibited similar, pronounced reductions in striatal DA terminal depletion in the injected hemisphere, a finding that correlated poorly with our observation that only A53E- or A53T-expressing animals showed evidence of motor asymmetry. The absence of significant motor deficits, and the reduced loss of DA neurons cell bodies (despite the presence of severe striatal lesion) in aSyn-WT expressing animals are characteristics previously reported[37], and suggest a notably scenario where surviving cell bodies somehow can compensate for lack of striatal DA terminals. Overall, the more modest neuropathology elicited by aSyn-WT in our *in vivo* model allows us to conclude that this variant has lower intrinsic neurotoxicity *in vivo* compared to A53E or A53T. Future analysis of the fold of expression of human aSyn versus endogenous aSyn levels, in short and long term experiments, should be monitored in order to rule out any artifact results related with variable levels of expression of toxic aSyn variants.

Rats infused with rAAV encoding the aSyn variants showed a 40 to 50% striatal TH reduction and a 20 to 40% nigral DA cell loss. Analysis of the post-mortem brains of human PD patients has revealed that PD motor symptoms are associated with an ~80% depletion of striatal DA levels and a ~60% loss of nigral DA neurons[38]. Accordingly, our rat rAAV-aSyn model mimics the progressive striatal and nigral degeneration that occurs in the human disease, and presumably the degree of nigrostriatal pathology in this model would be similar to that observed in the brains of PD patients at a later experimental time point. The combination of severe striatal lesions and less extensive nigral DA cell death evident in the human aSyn-expressing rats represents a pattern commonly described as the 'dying back' process, a term that refers to the fact that the destruction of striatal terminals precedes the loss of nigral DA neurons in PD brain.

Neuronal bodies and processes of SNpc transduced with rAAV encoding each of the aSyn variants showed aSyn aggregates in the injected hemisphere. The fact that these inclusions stained positive for LB509, an antibody that has been reported to have high specificity for human aggregated aSyn[39], after proteinase K treatment, as well as for aSyn-pSer129 and polyUb, suggests that they were similar to Lewy bodies and Lewy neurites observed in the post-mortem brains of human PD patients[27,29,40]. The observation that Lewy-like inclusions were found in the intact hemisphere suggests that expressed aSyn spread from the injected SNpc to the nigral region on the opposite side, potentially via a rAAV migration from the point of injection into the opposite hemisphere. However, this idea is challenged by our pilot study data showing evidence of a high level of human aSyn expression only on the injected side 3 weeks after viral infusion. Future studies involving rats transduced with an rAAV-GFP vector will be conducted to rule out non-specific viral propagation as a cause for the appearance of aSyn immunoreactivity in both hemispheres in our rat model.

Variable patterns of expression of pSER129[+] inclusions found in aSyn-infused tissue could represent a formation of Lewy body-like structures in progress. Several neurons expressing the three variants of aSyn showed a general diffused cytosolic expression. We were able to detect similar annular or crescent-shaped structures previously reported in post-mortem brains expressing aSyn-A53E[18]. Our observation that A53E tended to form neuronal inclusions with a different morphology compared to those formed by aSyn-WT or-A53T in rat SNpc suggests that A53E undergoes self-assembly via a different mechanism or via the same mechanism but with altered kinetics compared to the other two variants. Each of these scenarios is consistent with evidence that recombinant A53E forms fibrils less rapidly than aSyn-WT or -A53T[19,41,42]

The idea that A53E could undergo self-assembly via a different mechanism compared to WT aSyn is supported by our evidence that A53E shows a trend towards having a higher propensity to form aggregates at membrane surface. Two key findings from our biochemical studies highlight the important role of aSyn-membrane interactions in PD-related neuropathology in vivo: (i) the injected SN of rats infused with rAAV-A53E or -A53T had higher relative levels of membrane-bound aSyn compared to animals transduced with rAAV encoding the less pathological WT protein; and (ii) pSer129[+] aSyn aggregates were more abundant in membrane fractions versus the cytosol. Future studies will be aimed at assessing the purity of the membrane and cytosolic fractions in order to exclude the possibility of cross contamination, as well as confirming the reproducibility of our findings. Another important goal will be to determine whether levels of membrane-associated pSer129[+] aggregates in the injected SNpc differ among rats expressing different aSyn variants. It is important to mention that commercial antibodies that detect aSyn pSer129 show different sensitivity[43]. From our experience we determined that pSer129 EP1536Y showed high specificity and sensitivity in tissue samples, whereas pSer129 81A showed high detection signal in protein samples transferred into western blot membranes. These observations suggest that the detection ability of these antibodies may be related with the structural conditions of the protein.

Overall, our *in vivo* PD model was found to mimic motor deficits and neuropathology characteristic of human PD patients. Accordingly, this model is suitable for examining the neuroprotective activities of candidate genes/proteins that may be effective in rescuing the toxic effects of aSyn variants. In particular, our rat model will enable us to validate therapeutic strategies that involve inducing the expression of candidate endogenous neuroprotective proteins (e.g. molecular chaperones or aSyn-interacting proteins that are down-regulated in PD[16]. These types of genetic strategies are attractive because they can lead to changes in multiple cellular pathways involved in neuronal defects, thereby slowing neurodegeneration and the progression of the disease.

3.5 List of References

1. Polymeropoulos, M. H., Lavedan, C., Leroy, E., Ide, S. E., Dehejia, A., Dutra, A., Pike, B., Root, H., Rubenstein, J., Boyer, R., Stenroos, E. S., Chandrasekharappa, S., Athanassiadou, A., Papapetropoulos, T., Johnson, W. G. *et al.* Mutation in the alpha-synuclein gene identified in families with Parkinson's disease. *Science* **276**, 2045–7 (1997).

2. Nussbaum, R. L. Genetics of Synucleinopathies. *Cold Spring Harb. Perspect. Med.* **8**, a024109 (2018).

3. Krüger, R., Kuhn, W., Müller, T., Woitalla, D., Graeber, M., Kösel, S., Przuntek, H., Epplen, J. T., Schols, L. & Riess, O. AlaSOPro mutation in the gene encoding α-synuclein in Parkinson's disease. *Nat. Genet.* **18**, 106–108 (1998).

4. Zarranz, J. J., Alegre, J., Gómez-Esteban, J. C., Lezcano, E., Ros, R., Ampuero, I., Vidal, L., Hoenicka, J., Rodriguez, O., Atarés, B., Llorens, V., Tortosa, E. G., del Ser, T., Muñoz, D. G. & de Yebenes, J. G. The new mutation, E46K, of α-synuclein causes parkinson and Lewy body dementia. *Ann. Neurol.* **55**, 164–173 (2004).

5. Appel-Cresswell, S., Vilarino-Guell, C., Encarnacion, M., Sherman, H., Yu, I., Shah, B., Weir, D., Thompson, C., Szu-Tu, C., Trinh, J., Aasly, J. O., Rajput, A., Rajput, A. H., Jon Stoessl, A. & Farrer, M. J. Alpha-synuclein p.H50Q, a novel pathogenic mutation for Parkinson's disease. *Mov. Disord.* **28**, 811–813 (2013).

6. Lesage, S., Anheim, M., Letournel, F., Bousset, L., Honoré, A., Rozas, N., Pieri, L., Madiona, K., Dürr, A., Melki, R., Verny, C. & Brice, A. G51D α-synuclein mutation causes a novel Parkinsonian-pyramidal syndrome. *Ann. Neurol.* **73**, 459–471 (2013).

7. Ross, O. A., Braithwaite, A. T., Skipper, L. M., Kachergus, J., Hulihan, M. M., Middleton, F. A., Nishioka, K., Fuchs, J., Gasser, T., Maraganore, D. M., Adler, C. H., Larvor, L., Chartier-Harlin, M.-C., Nilsson, C., Langston, J. W. *et al.* Genomic investigation of α-synuclein multiplication and parkinsonism. *Ann. Neurol.* **63**, 743–750 (2008).

8. Conway, K. A., Lee, S. J., Rochet, J. C., Ding, T. T., Williamson, R. E. & Lansbury, P. T. Acceleration of oligomerization, not fibrillization, is a shared property of both alpha-synuclein mutations linked to early-onset Parkinson's disease: implications for pathogenesis and therapy. *Proc. Natl. Acad. Sci. U. S. A.* **97**, 571–6 (2000).

9. Choi, W., Zibaee, S., Jakes, R., Serpell, L. C., Davletov, B., Anthony Crowther, R. & Goedert, M. Mutation E46K increases phospholipid binding and assembly into filaments of human α-synuclein. *FEBS Lett.* **576**, 363–368 (2004).

10. Ghosh, D., Mondal, M., Mohite, G. M., Singh, P. K., Ranjan, P., Anoop, A., Ghosh, S., Jha, N. N., Kumar, A. & Maji, S. K. The Parkinson's Disease-Associated H50Q Mutation Accelerates α-Synuclein Aggregation *in Vitro*. *Biochemistry* **52**, 6925–6927 (2013).

11. Rochet, J.-C., Hay, B. A. & Guo, M. Molecular Insights into Parkinson's Disease. in *Progress in molecular biology and translational science* **107**, 125–188 (2012).

12. Fares, M.-B., Ait-Bouziad, N., Dikiy, I., Mbefo, M. K., Jovi i , A., Kiely, A., Holton, J. L., Lee, S.-J., Gitler, A. D., Eliezer, D. & Lashuel, H. A. The novel Parkinson's disease linked mutation G51D attenuates in vitro aggregation and membrane binding of -synuclein, and enhances its secretion and nuclear localization in cells. *Hum. Mol. Genet.* **23**, 4491–4509 (2014).

13. Pirc, K. & Ulrih, N. P. α-Synuclein interactions with phospholipid model membranes: Key roles for electrostatic interactions and lipid-bilayer structure. *Biochim. Biophys. Acta - Biomembr.* **1848**, 2002–2012 (2015).

14. Lv, Z., Hashemi, M., Banerjee, S., Zagorski, K., Rochet, C. & Lyubchenko, Y. L. Phospholipid membranes promote the early stage assembly of α-synuclein aggregates. *bioRxiv* 295782 (2018). doi:10.1101/295782

15. Lee, H.-J., Choi, C. & Lee, S.-J. Membrane-bound -Synuclein Has a High Aggregation Propensity and the Ability to Seed the Aggregation of the Cytosolic Form. *J. Biol. Chem.* **277**, 671–678 (2002).

16. Ysselstein, D., Dehay, B., Costantino, I. M., McCabe, G. P., Frosch, M. P., George, J. M., Bezard, E. & Rochet, J.-C. Endosulfine-alpha inhibits membrane-induced α-synuclein aggregation and protects against α-synuclein neurotoxicity. *Acta Neuropathol. Commun.* **5**, 3 (2017).

17. Ysselstein, D., Joshi, M., Mishra, V., Griggs, A. M., Asiago, J. M., McCabe, G. P., Stanciu, L. A., Post, C. B. & Rochet, J.-C. Effects of impaired membrane interactions on α-synuclein aggregation and neurotoxicity. *Neurobiol. Dis.* **79**, 150–63 (2015).

18. Pasanen, P., Myllykangas, L., Siitonen, M., Raunio, A., Kaakkola, S., Lyytinen, J., Tienari, P. J., Pöyhönen, M. & Paetau, A. *A novel α-synuclein mutation A53E associated with atypical multiple system atrophy and Parkinson's disease-type pathology. Neurobiology of Aging* **35**, (2014).

19. Ghosh, D., Sahay, S., Ranjan, P., Salot, S., Mohite, G. M., Singh, P. K., Dwivedi, S., Carvalho, E., Banerjee, R., Kumar, A. & Maji, S. K. The Newly Discovered Parkinson's Disease Associated Finnish Mutation (A53E) Attenuates α-Synuclein Aggregation and Membrane Binding. *Biochemistry* **53**, 6419–6421 (2014).

20. Lázaro, D. F., Dias, M. C., Carija, A., Navarro, S., Madaleno, C. S., Tenreiro, S., Ventura, S. & Outeiro, T. F. The effects of the novel A53E alpha-synuclein mutation on its oligomerization and aggregation. *Acta Neuropathol. Commun.* **4**, 128 (2016).

21. Bourdenx, M., Dovero, S., Engeln, M., Bido, S., Bastide, M. F., Dutheil, N., Vollenweider, I., Baud, L., Piron, C., Grouthier, V., Boraud, T., Porras, G., Li, Q., Baekelandt, V., Scheller, D. *et al.* Lack of additive role of ageing in nigrostriatal neurodegeneration triggered by α-synuclein overexpression. *Acta Neuropathol. Commun.* **3**, 46 (2015).

22. Neumann, M., Kahle, P. J., Giasson, B. I., Ozmen, L., Borroni, E., Spooren, W., Müller, V., Odoy, S., Fujiwara, H., Hasegawa, M., Iwatsubo, T., Trojanowski, J. Q., Kretzschmar, H. A. & Haass, C. Misfolded proteinase K-resistant hyperphosphorylated alpha-synuclein in aged transgenic mice with locomotor deterioration and in human alpha-synucleinopathies. *J. Clin. Invest.* **110**, 1429–39 (2002).

23.   Volpicelli-Daley, L. A., Kirik, D., Stoyka, L. E., Standaert, D. G. & Harms, A. S. How can rAAV-α-synuclein and the fibril α-synuclein models advance our understanding of Parkinson's disease? *J. Neurochem.* **139**, 131–155 (2016).

24.   Oorschot, D. E. Total number of neurons in the neostriatal, pallidal, subthalamic, and substantia nigral nuclei of the rat basal ganglia: A stereological study using the cavalieri and optical disector methods. *J. Comp. Neurol.* **366**, 580–599 (1996).

25.   Cannon, J. R., Tapias, V., Na, H. M., Honick, A. S., Drolet, R. E. & Greenamyre, J. T. A highly reproducible rotenone model of Parkinson's disease. *Neurobiol. Dis.* **34**, 279–90 (2009).

26.   Paxinos, G. & Watson, C. *The rat brain in stereotaxic coordinates.*

27.   Tanji, K., Mori, F., Mimura, J., Itoh, K., Kakita, A., Takahashi, H. & Wakabayashi, K. Proteinase K-resistant α-synuclein is deposited in presynapses in human Lewy body disease and A53T α-synuclein transgenic mice. *Acta Neuropathol.* **120**, 145–154 (2010).

28.   Fujiwara, H., Hasegawa, M., Dohmae, N., Kawashima, A., Masliah, E., Goldberg, M. S., Shen, J., Takio, K. & Iwatsubo, T. α-Synuclein is phosphorylated in synucleinopathy lesions. *Nat. Cell Biol.* **4**, 160–164 (2002).

29.   Schell, H., Hasegawa, T., Neumann, M. & Kahle, P. J. Nuclear and neuritic distribution of serine-129 phosphorylated α-synuclein in transgenic mice. *Neuroscience* **160**, 796–804 (2009).

30.   Iwatsubo, T., Yamaguchi, H., Fujimuro, M., Yokosawa, H., Ihara, Y., Trojanowski, J. Q. & Lee, V. M. Purification and characterization of Lewy bodies from the brains of patients with diffuse Lewy body disease. *Am. J. Pathol.* **148**, 1517–29 (1996).

31.   Gong, B. & Leznik, E. The role of ubiquitin C-terminal hydrolase L1 in neurodegenerative disorders. *Drug News Perspect.* **20**, 365 (2007).

32.   Cearley, C. N. & Wolfe, J. H. A Single Injection of an Adeno-Associated Virus Vector into Nuclei with Divergent Connections Results in Widespread Vector Distribution in the Brain and Global Correction of a Neurogenetic Disease. *J. Neurosci.* **27**, 9928–9940 (2007).

33. Van der Perren, A., Toelen, J., Casteels, C., Macchi, F., Van Rompuy, A.-S., Sarre, S., Casadei, N., Nuber, S., Himmelreich, U., Osorio Garcia, M. I., Michotte, Y., D'Hooge, R., Bormans, G., Van Laere, K., Gijsbers, R. *et al.* Longitudinal follow-up and characterization of a robust rat model for Parkinson's disease based on overexpression of alpha-synuclein with adeno-associated viral vectors. *Neurobiol. Aging* **36**, 1543–1558 (2015).

34. Kirik, D., Rosenblad, C., Burger, C., Lundberg, C., Johansen, T. E., Muzyczka, N., Mandel, R. J. & Björklund, A. Parkinson-like neurodegeneration induced by targeted overexpression of alpha-synuclein in the nigrostriatal system. *J. Neurosci.* **22**, 2780–91 (2002).

35. Gombash, S. E., Manfredsson, F. P., Kemp, C. J., Kuhn, N. C., Fleming, S. M., Egan, A. E., Grant, L. M., Ciucci, M. R., MacKeigan, J. P. & Sortwell, C. E. Morphological and Behavioral Impact of AAV2/5-Mediated Overexpression of Human Wildtype Alpha-Synuclein in the Rat Nigrostriatal System. *PLoS One* **8**, e81426 (2013).

36. Athanassiadou, A., Voutsinas, G., Psiouri, L., Leroy, E., Polymeropoulos, M. H., Ilias, A., Maniatis, G. M. & Papapetropoulos, T. Genetic Analysis of Families with Parkinson Disease that Carry the Ala53Thr Mutation in the Gene Encoding α-Synuclein. *Am. J. Hum. Genet.* **65**, 555–558 (1999).

37. Decressac, M., Mattsson, B. & Björklund, A. Comparison of the behavioural and histological characteristics of the 6-OHDA and α-synuclein rat models of Parkinson's disease. *Exp. Neurol.* **235**, 306–315 (2012).

38. Dauer, W. & Przedborski, S. Parkinson's Disease. *Neuron* **39**, 889–909 (2003).

39. Jakes, R., Crowther, R. A., Lee, V. M.-Y., Trojanowski, J. Q., Iwatsubo, T. & Goedert, M. Epitope mapping of LB509, a monoclonal antibody directed against human α-synuclein. *Neurosci. Lett.* **269**, 13–16 (1999).

40. Xia, Q., Liao, L., Cheng, D., Duong, D. M., Gearing, M., Lah, J. J., Levey, A. I. & Peng, J. Proteomic identification of novel proteins associated with Lewy bodies. *Front. Biosci.* **13**, 3850–6 (2008).

41. Mohite, G. M., Navalkar, A., Kumar, R., Mehra, S., Das, S., Gadhe, L. G., Ghosh, D., Alias, B., Chandrawanshi, V., Ramakrishnan, A., Mehra, S. & Maji, S. K. The Familial α-Synuclein A53E Mutation Enhances Cell Death in Response to Environmental Toxins Due to a Larger Population of Oligomers. (2018). doi:10.1021/acs.biochem.8b00321

42. Mohite, G. M., Kumar, R., Panigrahi, R., Navalkar, A., Singh, N., Datta, D., Mehra, S., Ray, S., Gadhe, L. G., Das, S., Singh, N., Chatterjee, D., Kumar, A. & Maji, S. K. Comparison of Kinetics, Toxicity, Oligomer Formation, and Membrane Binding Capacity of α-Synuclein Familial Mutations at the A53 Site, Including the Newly Discovered A53V Mutation. *Biochemistry* **57**, 5183–5187 (2018).

43. Delic, V., Chandra, S., Abdelmotilib, H., Maltbie, T., Wang, S., Kem, D., Hunter, |, Scott, J., Underwood, R. N., Liu, Z., Volpicelli-Daley, L. A. & West, A. B. Sensitivity and specificity of phospho-Ser129 a-synuclein monoclonal antibodies. doi:10.1002/cne.24468

CHAPTER 4.   CHANGES IN THE EXPRESSION OF CANDIDATE NEUROPROTECTIVE GENES IN SYNUCLEINOPATHIES

4.1   Introduction

Dementia with Lewy bodies (DLB) and Parkinson's disease (PD) are two synucleinopathies with strong clinical and pathological overlaps. Both CNS disorders are characterized by extensive aSyn neuropathology[1]. Even though in both diseases the presence of aSyn-rich Lewy bodies (LB) extends from the brain stem into cortical regions, in PD brains classical spherical brain stem LBs are prevalent, whereas in DLB brains irregular-shaped LBs are found in the limbic system and in neocortical areas[2]. PD Lewy bodies stain positive for disease-linked proteins in addition to aSyn, including DJ-1, LRRK2, parkin, and PINK-1, each of which is thought to play a role in cellular clearance processes such as autophagy and the ubiquitin-proteasome system[2]. Very little is known about any differences in gene expression that could account for differences in neuropathology between PD and DLB. Elucidating genetic mechanisms that differentiate DLB from PD could lead to the identification of molecular tools for more accurate diagnosis and to a more improved understanding of pathogenic mechanisms, setting the stage for the development of disease-modifying therapies.

4.1.1   Gene expression changes reported in DLB and PD: an overview

In addition to gene mutations, epigenetic modifications that regulate the expression of aSyn are likely a key element in the development of DLB and PD. PD patients' brains show hypomethylation of the SNCA promoter, enhancing the expression of the aSyn protein and thus leading to a toxic gain of function[3]. Interestingly, aSyn has been shown to have aberrant epigenetic activity in PD and DLB brains by sequestering DNA methyltransferase I (Dnmt1) from the nucleus, resulting in a global DNA hypomethylation affecting the expression of genes that have preiotropic effects through their regulation of multiple complex pathways, such as SEPW1 and PRKAR2A[4]. Additional epigenetic analyses revealed that an imbalance of Dnmt1 and other DNA methyltransferases in the nucleus can be associated with a pre-activation of apoptotic pathways involved in motor neuron death[5]. Another study revealed that the expression of

A53T and A30P mutations of aSyn in a neuroblastoma celluar system altered the expression of many other genes, leading to perturbations of mitochondrial, lysosomal, and proteasomal activities[6]. Defining the expression pattern of genes associated with these mechanisms in DLB and PD can lead to a better understanding of cellular pathways that are perturbed in these diseases, thus facilitating the identification of potential therapeutic targets.

4.1.2 Genes implicated in DLB and PD

As related synucleinopathies, DLB and PD have overlapping genetic variations that can be considered biomarkers of these two diseases. Mutations in a number of genes, including those encoding aSyn, LRRK2, GBA, Parkin, and PINK1, are associated with familial PD[7]. Of these, variations in the genes encoding aSyn, LRRK2, and GBA have also been found to modulate the risk of DLB[8]. For example, aSyn gene triplication is often associated with DLB[7]. In addition, the gene encoding apolipoprotein E (ApoE), implicated in modulating AD risk, has been recently identified as a strong genetic risk factor for DLB[9]. Although total tau and phosphorylated tau are useful biomarkers for distinguishing between cases of AD from DLB[10], inconclusive results were obtained when this strategy was used to distinguish between PD from DLB patients[10]. Collectively, the identification of genes that can serve as biomarkers of both DLB and PD supports the idea that this is overlap between the pathogenic mechanisms of these two diseases. It is imperative to identify new genetic markers that can form the basis of more conclusive diagnostic tests during pre-clinical stages of DLB and PD. Information about the role of these genes and their encoded proteins in pathogenesis could also set the stage for developing disease-specific therapeutic strategies.

4.1.3 Neuroprotective gene panel examined in this study: scientific premise

The overlapping pathophysiology of DLB with PD, PD with dementia, and AD makes it difficult to diagnose these diseases and to identify well-targeted therapies. Establishing a gene expression profile that can be considered a hallmark of DLB or PD would greatly contribute to the development of specific molecular diagnostics that could be used to

detect the disease in its early stages. Information about differences in mRNA levels in different brain regions (e.g. cortex vs. cingulate gyrus) from patients and control individuals could lead to an improved understanding of the role of brain region-specific genetic perturbations in disease pathogenesis. Moreover, functional studies involving genes that are abnormally expressed in synucleinopathies could yield insight into specific pathogenic mechanisms.

In this study, we characterized post-mortem brain samples from DLB and PD patients and non-diseased controls in terms of their expression levels of a panel of genes (and their encoded proteins) previously found to have neuroprotective effects in PD models, based on the premise that DLB and PD have overlapping pathogenic mechanisms[11]. Our rationale for this approach was that by comparing the expression profiles of candidate neuroprotective proteins in brain samples from DLB or PD patients versus non-diseased controls, we could potentially identify genetic perturbations associated with each disorder, a subset of which might be linked to one disorder but not the other. Here, we examined the expression levels of the following candidate neuroprotective proteins: DJ-1, a protein with antioxidant and chaperone activities[12]; PGC1α, a master regulator of mitochondrial biogenesis and oxidative metabolism[13]; MsrA, an antioxidant enzyme responsible for repairing oxidatively damaged proteins[14]; and ATP13A2, a lysosomal protein involved in autophagy[15].

4.2   Materials and Methods

4.2.1 Materials

Tissue Homogenization

- Microtube Homogenizer (Benchmark Scientific, BeadBug D1030)
- Zirconia/Silica beads (BioSpec products, cat. no. 11079110Z)

Quantitative reverse transcription polymerase chain reaction (qRT-PCR)

- E.Z.N.A Total RNA kit (Omega Bio-tek, cat. no. R6834-01)

- High-Capacity cDNA Reverse Transcription kit (Applied Biosystems, cat. no. 43-688-14)

- iTaq Universal SYBR Green Supermix (Bio-Rad, cat. no. 1725121)

- Vii7 Real-Time PCR system (ThermoFisher Scientific)

- DNA primers (Table 4.1)

Table 4.1. DNA Primers

Gene Target	Forward Sequence	Reverse Sequence
Human aSyn	ATG ACT GGG CAC ATT GGA AC	CCA CAG GAA GGA ATT CTG GA
Human DJ-1	GGA GAC GGT CAT CCC TGT A	GCT GGC ATC AGG ACA AAT
Human MsrA	GGC AAC AGA ACA GTC GAA CCT TT	GGT ACA CCA CTC GGA CGA CTT CT
Human PGC1α	CAG CCA ACA CTC AGC TAA GTT A	CGA GCA GGG ACG TCT TT
Human Park9	CGC TGT TCC CTT GAC ACT T	CAC CCA GGT TGG TGT TGA
Human GAPDH	GAA GGT GAA GGT CGG AGT CAA C	CAG AGT TAA AAG CAG CCC TGG T

Western Blotting

- RIPA buffer

    - Trizma Hydrochloride (Sigma, cat. no. T3253)

    - Sodium Chloride (Fisher Chemicals, cat.no. S271-500)

    - Sodium Dodecyl Sulfate (Sigma, cat. no. L3771)

    - Sodium deoxycholate (Sigma, cat.no. 1.06504)

    - Triton X-100 ((Fisher BioReagents, cat. no. BP151-500)

    - Phenylmethylsulfonyl fluoride (PMSF) (Sigma, cat. no P7626)

    - Protease inhibitor cocktail (Sigma, cat. no. P8340)

- Pierce BCA Protein Assay Kit (Thermo Scientific cat. no. 23225)

- Acrylamide (Sigma, cat. no. A3553)

- Bisacrylamide (Sigma, cat. no. 294381)

- Primary and Secondary antibodies (Table 4.2)

- 1X PBS (Sigma, cat no. P5493)

- Tween 20 (Fisher BioReagents, cat. no. BP337-500)

- Immobilon-P PVDF Membrane 0.45 μm (Millipore, cat. no. IPFL00010)

- Dry milk powder

- Paraformaldehyde (PFA) (Sigma, cat no. P6148)

- BSA (Fisher BioReagents, cat. no. BP9703100)

- Methanol (Fisher Chemical, cat. no. A452-4)

- ECF substrate for Western Blotting (GE Healthcare Amersham, cat. no. RPN5785)

Immunohistochemistry

- 1X PBS (Sigma, cat no. P5493)

- Trisodium citrate dihydrate (Sigma, cat. no S1804)

- Proteinase K solution 20 mg/mL (Invitrogen, cat. no. AM2548)

- Triton X-100 (Fisher BioReagents, cat. no. BP151-500)

- Normal Donkey Serum (Jackson ImmunoResearch, cat. no. 017-000-121)

- Primary and Secondary antibodies (Table 4.2)

- Vectastain Elite ABC system (Vector Laboratories, cat. no. PK-7200)

- DAB Peroxidase substrate kit (Vector Laboratories, cat. no. SK-4100)

- DPX Mountant (Electron Microscopy Sciences, cat. no. 13512)

- Non-permanent EMS-Mount (Electron Microscopy Sciences, cat. no. 17986-06)

- Coverslips 24x40-1 (Fisherbrand, cat. no. 12-545-87)

- Superfrost plus microscope slides (Fisherbrand, cat. no. 22-037-246)

Table 4.2. Antibodies

Primary Antibodies			
Immunogen	**Host**	**Species Reactivity**	**Vendor**
Alpha-Synuclein SYN1	Mouse	Rat, Human	BD Biosciences cat. no. 610787
Alpha-Synuclein LB509	Mouse	Human	Abcam cat. no. ab27766
Alpha-Synuclein	Sheep	Human, Rat	Millipore cat. no. AB5334P
DJ-1/Park7	Rabbit	Human	Neuromics cat. no. RA22132
Methionine sulfoxide reductase A	Rabbit	Human, Mouse, Rat, Cow	Abcam cat no. ab16803
ATP13A2	Rabbit	Human, Mouse	Novus cat. no. NB110-41486
PGC1α H-300	Rabbit	Human, Mouse, Rat	Santa Cruz cat. no. sc-13067
Alpha-synuclein phosphoSerine129 81A (pSer129)	Mouse	Human, Mouse	Millipore cat. no MABN826
Secondary Antibodies			
	Host	**Species Reactivity**	**Vendor**
IgG Alexa Fluor 488	Donkey	Rabbit	Jackson ImmunoResearch cat. no. 711-165-152
IgG Cy3	Donkey	Mouse	Jackson ImmunoResearch cat no 715-165-151
IgG Alexa Fluor 647	Goat	Mouse	Life Technologies cat. no. A20186
Biotin IgG	Donkey	Sheep	Jackson ImmunoResearch cat no 713-065-147
Biotin IgG	Donkey	Rabbit	Jackson ImmunoResearch cat no 711-065-152

4.2.2 Human Brain Samples

Brain samples from France were collected as part of a Brain Donation Program from the Brain Bank "GIE Neuro-CEB". Brain samples from Massachusetts General Hospital were collected in the Neuropathology Core at the Massachusetts Alzheimer's Disease Research Center. DLB, PD, and control (non-DLB or non-PD) samples from frontal cortex and Brodmann area 24 (BA24, which encompasses the cingulate and cerebral cortex including anterior cingulate gyrus) were collected from age-matched individuals

(Table 4.3) who provided consent in accordance with bioethics laws in France and in the
United States.

Tabla 4.3 Human brain samples demography					
France ID	SEX	AGE (years)	POST-MORTEM TIME	ASSOCIATED PATHOLOGY	DIAGNOSED NEUROPATHOLOGY
8790	M	85	21 h	AD – Braak stage 3	DLB
8177	M	81	nd	AD – Braak 6	DLB
4762	F	83	12 h	nd	DLB
7814	M	69	15 h	AD – Braak 6	DLB
5766	M	74	21 h	nd	DLB
8401	F	60	28 h	Ischemia	Control
6203	M	78	23 h	Severe amyloid angiopathy	Control
8866	M	84	15 h 30 m	nd	Control
4078	M	73	10 h	Craniophrayngioma	Control
8251	M	79	nd	Mild atrophy Braak 2	Control
MGH ID	SEX	AGE (years)	POST-MORTEM TIME	ASSOCIATED PATHOLOGY	DIAGNOSED NEUROPATHOLOGY
1297	F	80	nd	AD/DLB Braak 6	DLB
1435	F	65	10 h	Moderate amyloid angiopathy	DLB
1891	M	61	20 h	AD/DLB Braak 6	DLB
1491	M	79	14 h	AD/DLB Braak 5	DLB
1590	M	62	24 h	DLB Braak 5	DLB
1887	M	60	14 h	nd	Control
1821	M	92	nd	Mild hypertensive cerebrovascular changes	Control
1886	F	58	18 h	nd	Control
1901	M	54	6 h	Mild hypertensive cerebrovascular changes	Control
1879	M	94	17 h	Terminal hypoxic changes	Control
1165	M	83	10 h	nd	PD
1755	M	84	6 h	nd	PD
1825	M	80	13 h	nd	PD
1027	M	75	15 h	nd	PD
1264	F	66	nd	nd	PD
1816	M	63	10 h	nd	PD

France: GIE-Neuro-CEB, MGH: Massachusetts General Hospital, nd: no data provided.

4.2.3 Quantitative reverse transcription polymerase chain reaction (qRT-PCR)

qRT-PCR reactions were run on a Viia-7 high-throughput real-time PCR system with 300 nM primers that targeted specifically the cDNA products of DJ-1, MsrA, PGC1α, PARK9 (ATP13A2), aSyn, or GAPDH using the iTaq Universal SYBR Green Supermix (BioRad, USA). Cycle threshold (C_T) values were normalized using C_T values determined for the housekeeping gene GAPDH, and mRNA levels were determined via delta C_T analysis.

4.2.4 Analysis of brain tissue homogenates by Western blotting

Samples of frontal cortex or the BA24 region (20 mg of each) were homogenized in RIPA buffer (50 mM Tris HCl, pH 7.4, 150 mM NaCl, 0.1% (w/v) SDS, 0.5% (w/v) sodium deoxycholate, 1% (v/v) Triton X-100) supplemented with protease inhibitor cocktail and PMSF (1 mM). Homogenization steps included two 4,000 rpm cycles of 20 sec each using 0.1 mm zirconia beads and a Benchmark Scientific BeadBug microtube homogenizer. After a 30 min incubation on ice, the homogenates were cleared by centrifugation at 16,000 x g for 15 min at 4 °C. The protein concentration in the resulting supernatant was determined via BCA assay An aliquot of the supernatant from each sample (equivalent to 30 mg of protein) was combined with Laemmli buffer (final concentration, 60 mM TrisHCl, pH 6.8, 2% (w/v) SDS, 10% (v/v) glycerol, 5% (v/v) β-mercaptoethanol, 0.01% (w.v) bromophenol blue), and the mixture was boiled for 5 min. Denatured proteins were separated via SDS-PAGE on a 15% (w/v) resolving gel and transferred to a PVDF membrane (pore size, 0.45 μm). The membrane was treated with 0.4% (w/v) PFA for 30 min at 22 ºC to crosslink the bound proteins. After blocking in 1X PBS supplemented with 5% tween 20 (PBS-T) and 10% (w/v) non-fat milk for 1 h at 22ºC, the membrane was washed with PBS-T and probed with primary antibody (anti-human DJ-1 (DJ-1/Park7, 1:10000), anti-human MsrA (1:3000), anti- human ATP13A2 (1:500), anti-human PGC1α (H-300, 1:1000) and aSyn-total aSyn (SYN1, 1:1500) prepared in PBS-T supplemented with 1% (w/v) BSA) overnight at 4 ºC. After washing in PBS-T, the membrane was probed with a secondary anti-rabbit or anti-mouse antibody conjugated to alkaline phosphatase (1:6000). To visualize the bands, the membrane was exposed to ECF substrate for 30 s,

and images were acquired using an Amersham Imager 600 RGB (GE Life Sciences, USA). Band densities were quantified using ImageJ software (NIH, Bethesda, MD).

4.2.5 Immunohistochemistry (IHC)

IHC was performed on slide-mounted paraffinized frontal cortex sections from DLB and PD patients and non-diseased individuals. Deparafinization was performed by washing twice with Histoclear, and antigen retrieval was assessed by incubating with citrate buffer (10 mM sodium citrate, 0.05% (v/v) Tween-20, pH 6.0) for 20 min at 95 ºC, with or without a subsequent treatment with proteinase K (20 µg/mL) for 20 min at 37 °C. Sections were rinsed with PBS-T (1X PBS 0.3% (v/v) Triton-X100), between incubation periods. The sections were hydrated with gradual changes from 100% to 80% (v/v) ethanol into distilled water, incubated for 1 h at 22 °C with blocking solution (10% (v/v) normal donkey serum containing 0.3% (v/v) Triton X-100). Fluorescence IHC was performed using primary antibody specific for DJ-1 (DJ-1/PARK7, 1:500), MsrA (1:500), ATP13A2(1:500), PGC1α (H-300, 1:500), human aSyn (LB509, 1:300), or aSyn-pSer129 (81A, 1:300) diluted in PBS-T supplemented with 1% (v/v) normal donkey serum,.and treated overnight at 4 ºC. After washing, the sections were incubated with secondary antibody: biotinylated anti-mouse IgG (1:200 dilution); anti-rabbit Alexa 488, anti-mouse Cy3, and anti-mouse Alexa 647 (1:1000) for 1 h at 22 °C in PBS-T 1% (v/v) normal donkey serum. Confocal images using were taken with 488, 594, 647 lasers using the Nikon A1 confocal system.

For DAB-IHC, sections were treated with total-aSyn (1:1000) and DJ-1 (DJ-1/PARK7, 1:500) diluted in PBS-T supplemented with 1% (v/v) normal donkey serum, and treated overnight at 4 ºC. After washing, sections were incubated with avidin-biotin-peroxidase complex (ABC Elite, Vecto Laboratories, USA) for 30 min at 22 °C, and visualized using 3,3-diaminobenzidine (DAB) as a chromogen. Sections were sealed with a coverslip and mounting medium DPX. Bright field images were taken at 10X, 20X and 40X magnification using an Olympus inverted microscope.

4.2.6 Statistical Analysis

CT values from qRT-PCR were analyzed using a *t*-test for normally distributed data and Wilcoxon test for non-parametric data. Densitometry data from Western blots were analyzed via Mann-Whitney test for non-parametric data. All statistical tests were carried out using GraphPad Prism 7.0

4.3 Results

4.3.1 mRNA expression patterns of candidate neuroprotective genes in DLB brain

Expression levels of the candidate neuroprotective genes DJ-1, MsrA, PGC1α, and ATP13A2 (Park9) were analyzed in post-mortem brain samples from DLB patients and age matched (non-DLB) controls collected at the "GIE Neuro-CEB" brain bank (Bordeaux, France) and at the Massachusetts General Hospital ("Mass. General") Alzheimer Research Center (Charlestown, MA, USA) (Table 4.3). mRNA levels were determined from delta CT values (high ΔCT = low mRNA concentration) in two different brain regions: frontal cortex and the BA24 region encompassing the cingulate gyrus. As shown in Fig. 4.1, the results showed opposite trends between the two groups of samples. In the GIE Neuro-CEB samples, DJ-1 and PGC1α showed trends towards down-regulation, while ATP13A2 and MsrA showed significant down-regulation only in the frontal cortex of DLB patients in comparison to non-DLB cortex. In contrast, in the Mass. General samples, only PGC1α showed a trend towards up-regulation, while DJ-1, MsrA and ATP13A2 showed significant up-regulation only in the frontal cortex of DLB patients in comparison with non-DLB cortex. No significant differences were observed between the BA24 region of DLB patients and non-DLB controls in either set of samples. Overall, these results show significant trends towards altered expression in the cortex but not in the BA24 region.
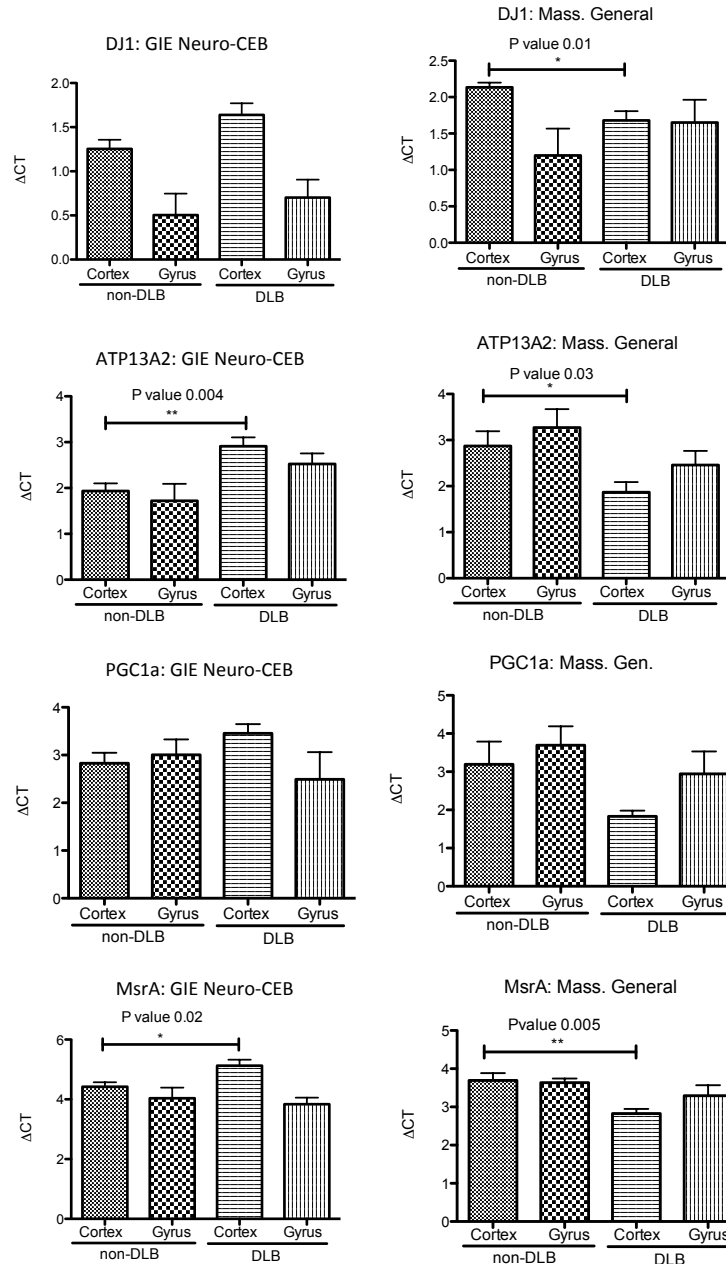
Figure 4.1. Expression profiles of candidate neuroprotective genes in two different sets of DLB samples. Samples of frontal cortex and the BA24 region (referred to in this figure as 'Gyrus') from DLB and age-matched non-DLB controls (6 g of each) were homogenized and examined for DJ-1, MsrA, PGC1α, and ATP13A2 mRNA levels via qRT-PCR (the analysis was carried out on a Vii7 Real-Time PCR system). Left panel: GIE Neuro-CEB cohort and right panel: Massachusetts Alzheimer's disease Research Center at the Massachusetts General Hospital (Mass. General). To compare gene expression levels, relative mRNA levels were assessed by determining ΔCT (Cycle Threshold of amplification) values using the housekeeping gene GAPDH as the reference. ΔCT values (CT target gene – CT reference gene) were plotted for samples from both cohorts. Note that the absolute amount of mRNA in each sample is inversely proportional to its ΔCT value (High ΔCT = low mRNA concentration). Mean +/- SEM; *t*-test for normally distributed data and Wilcoxon test for non-parametric data; *p≤0.05, **p≤0.01.

4.3.2 Levels of neuroprotective proteins in DLB brain

The Mass. General samples were analyzed via Western blotting to assess whether differences in mRNA levels observed when comparing cortical homogenates of DLB patients versus non-diseased controls led to corresponding changes in the expression levels of the encoded proteins. The Western blot data showed evidence of significant up-regulation of DJ-1 protein levels in DLB frontal cortex samples (Fig 4.2, top panel), consistent with the up-regulation of DJ-1 mRNA levels observed for this set of samples. Levels of PGC1α protein showed a trend towards being up-regulated in DLB frontal cortex, and this trend was consistent with a similar trend observed for PGC1α mRNA levels in the same samples. Interestingly, the Mass. General DLB cortical samples that showed evidence of significant up-regulation of ATP13A2 and MsrA mRNAs showed non-significant trends towards down-regulation of the encoded proteins. No significant differences in the levels of DJ-1, MsrA, or PGC1α protein were observed when comparing the BA24 region of DLB patients and non-diseased controls. Only ATP13A2 protein levels were found to be significantly different (down-regulated) in the BA24 region of DLB patients relative to controls.
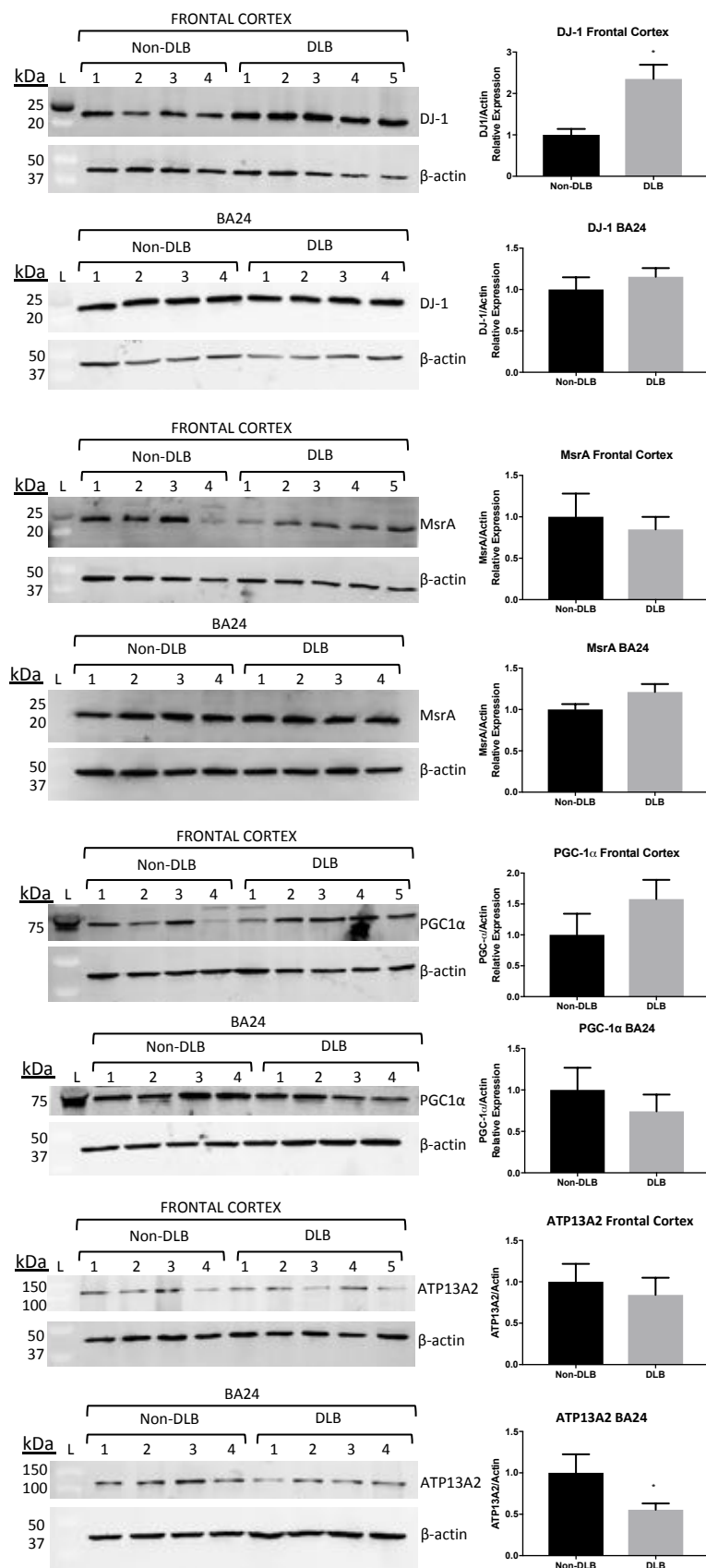
*Figure 4.2

*Figure 4.2. Levels of candidate neuroprotective proteins in DLB brain samples. Samples of frontal cortex and the BA24 region from DLB and age-matched non-DLB controls (10 mg of each) (Mass. General cohort) were homogenized and examined for DJ-1, MsrA, PGC1α, and ATP13A2 protein levels via Western blotting. Left panel: Images of Western blots probed for the different neuroprotective proteins and β-actin. Right panel: Bar graphs showing relative expression levels of neuroprotective proteins in each brain region determined via densitometric analysis of band intensities. Neuroprotective protein levels were normalized to the corresponding β-actin signal and divided by the mean value obtained for non-DLB control samples. The data are presented as the mean ± SEM, n = 4 or 5, *p < 0.05, Mann-Whitney test.

4.3.3 mRNA expression patterns of candidate neuroprotective genes in PD brain

Expression levels of the same panel of candidate neuroprotective genes were assessed in post-mortem brain samples from PD patients and age matched (non-PD) controls collected at the Mass General Alzheimer Research Center (Table 4.3). The results of qRT-PCR/delta-CT analysis (Fig. 4.3.) revealed no significant differences between levels of any of the candidate mRNAs when comparing the frontal cortex or BA24 region of PD patients versus non-PD controls. An interesting trend towards down-regulation of DJ-1 and ATP13A2 mRNAs was observed in cortical and BA24 samples from PD patients as compared to non-PD controls. Collectively, these data suggest that changes in the levels of candidate genes in the two specific brain regions analyzed may be a characteristic feature of DLB, but not of PD.
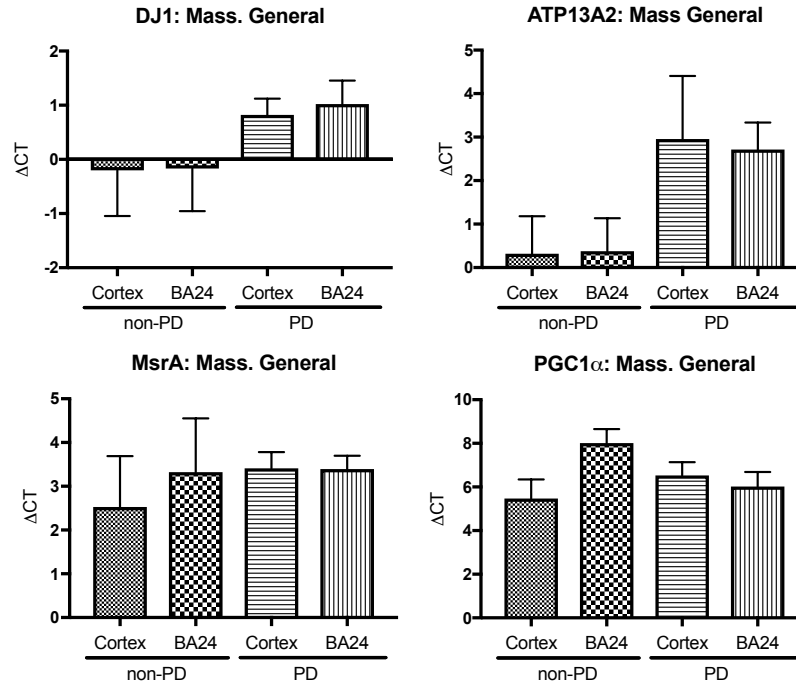
Figure 4.3. Expression profiles of candidate neuroprotective genes in PD brain samples. Samples of frontal cortex and the BA24 region from PD patients and age-matched non-PD controls (10 mg of each) were homogenized and examined for DJ-1, MsrA, PGC1α, and ATP13A2 mRNA levels via qRT-PCR (the analysis was carried out on 300 ng cDNA samples). To compare gene expression levels, relative mRNA levels were assessed by determining ΔCT values using the housekeeping gene GAPDH as the reference. Mean ± SEM; *t*-test for normally distributed data and Wilcoxon test for non-parametric data; non-significant differences.

4.3.4 Levels of neuroprotective proteins in PD brain

The Mass. General PD brain samples were also analyzed via Western blotting to assess the levels of the candidate neuroprotective proteins in brain samples from patients and non-PD controls. The data revealed no significant differences in the levels of any of the four proteins in the cortex or BA24 region of patients versus controls, consistent with the results obtained from analyses of the corresponding mRNA levels (Fig. 4.4). These findings further support the conclusion that changes in the expression levels of these four proteins in the cortex and limbic system are a characteristic feature of DLB, but not of PD.
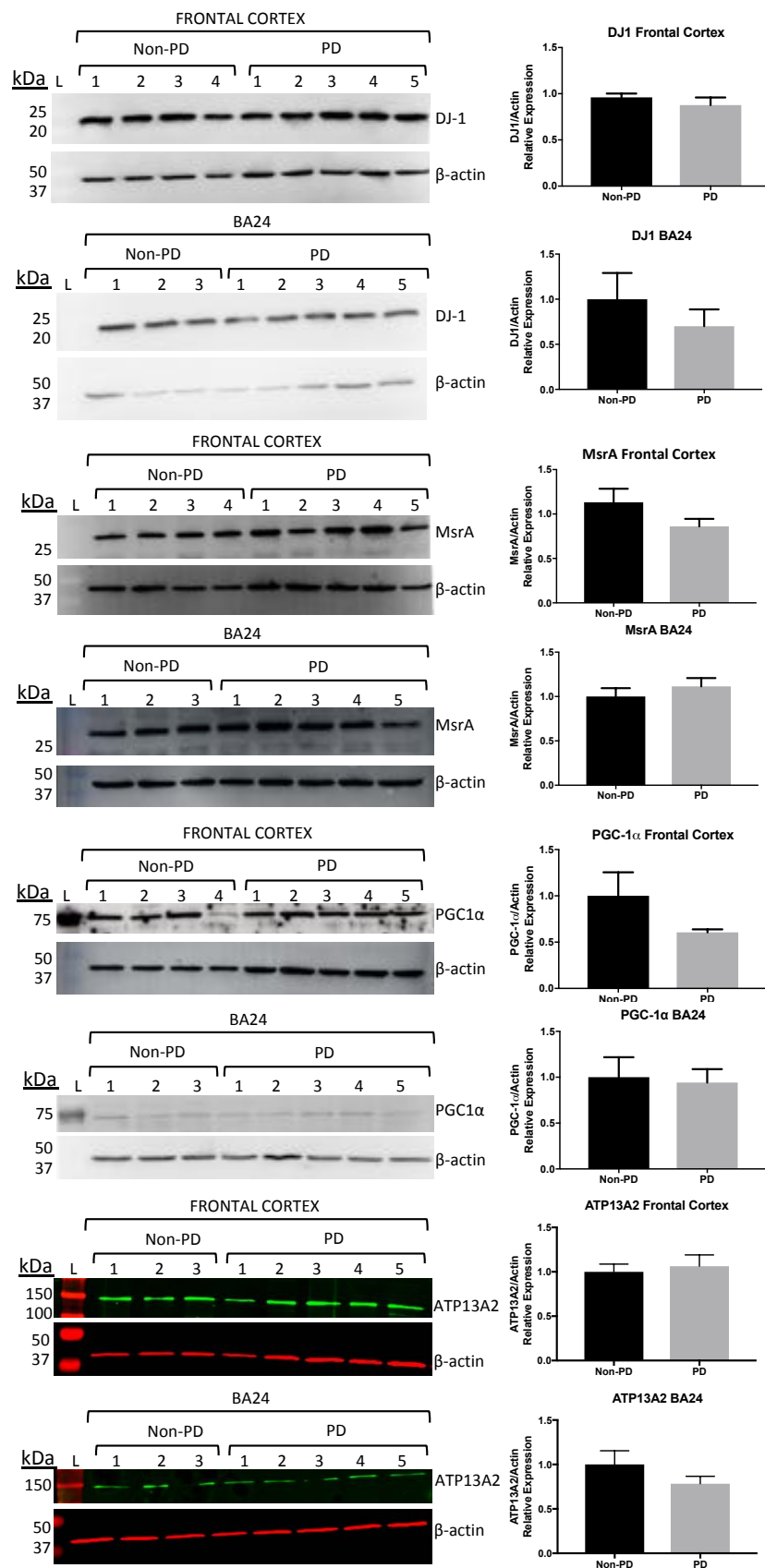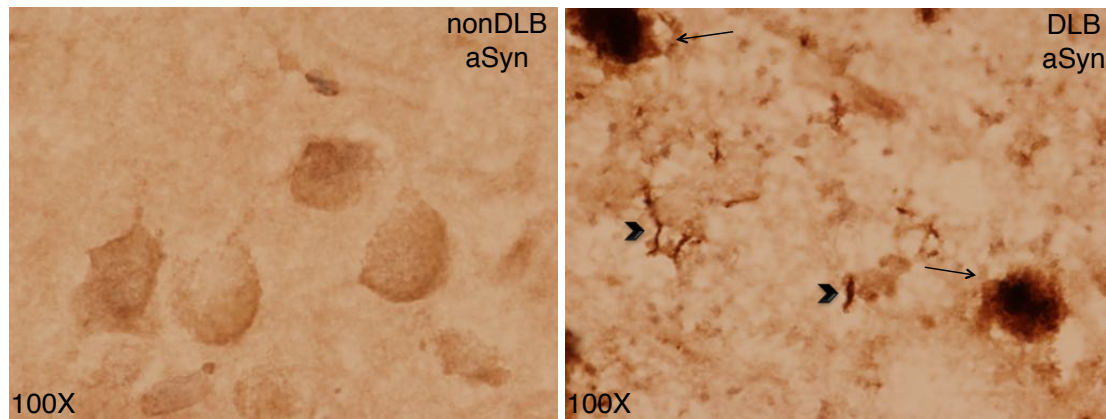
*Figure 4.4.

*Figure 4.4. Candidate neuroprotective proteins show no significant differences in expression in PD versus non-PD brain samples. Samples of frontal cortex and the BA24 region from PD patients and age-matched non-PD controls (10 mg of each) (Mass. General cohort) were homogenized and examined for DJ-1, MsrA, PGC1α and ATP13A2 protein levels via Western blotting. Left panel: Images of Western blots probed for the different neuroprotective proteins and β-actin. Right panel: Bar graphs showing relative expression levels of neuroprotective proteins in each brain region determined via densitometric analysis of band intensities. Neuroprotective protein levels were normalized to the corresponding β-actin signal and divided by the mean value obtained for non-PD control samples. The data are presented as the mean ± SEM, n = 3-5. Mann-Whitney test, non-significant differences.

4.3.5 Co-localization of candidate neuroprotective proteins with aggregated aSyn in DLB and PD brains

In the next phase of our study, post-mortem brains of DLB and PD patients were characterized in terms of aSyn neuropathology, and the potential impact of this pathology on the distribution of the four candidate neuroprotective proteins examined here. Sections of frontal cortex from DLB patients and age-matched, non-DLB controls were analyzed immunohistochemically using a primary antibody specific for human aSyn to confirm the presence of Lewy pathology. The sections were pretreated with PK treatment to selectively enhance immunoreactivity associated with aSyn aggregates, based on the premise that aggregated aSyn should be more resistant to PK digestion than the more diffuse, non-aggregated protein. In control (non-DLB) sections, only modest levels of neuronal aSyn staining were detected (Fig. 4.5, left). In contrast, round inclusions and thread-like structures characterized by a more intense aSyn immunoreactivity were observed in sections from DLB patients, suggesting that aSyn aggregates were recruited into structures with the appearance of classic Lewy bodies and Lewy neurites, respectively (Fig. 4.5, right).

Figure 4.5. Evidence of Lewy bodies and neurites in DLB cortex. aSyn immunoreactivity was examined in cortical sections from control individuals (non-DLB: left) and DLB patients (right) via immunohistochemical analysis using a method involving antigen retrieval with sequential sodium citrate and proteinase K treatments, followed by visualization of the stain with DAB. The images show evidence of aSyn aggregation, leading to the formation of Lewy bodies (thin arrows) and Lewy neurites (arrowheads), specifically in DLB cortex.

Based on our finding that DLB cortical sections had abundant aSyn neuropathology (Fig. 4.5), we hypothesized that aSyn might be up-regulated in DLB brain at the mRNA or protein level, thus favoring the protein's self-assembly. To address this hypothesis, cortical homogenates prepared from DLB patients and non-diseased controls were examined via qRT-PCR and Western blotting to assess aSyn mRNA and protein levels, respectively. The results indicated that levels of aSyn protein, but not aSyn mRNA, were increased in the cortex of DLB patients versus controls (Fig. 4.6.), suggesting that the observed aSyn neuropathology was driven by protein accumulation and post-translational modification rather than by an increase in transcription[16]. Additional analyses carried out on cortical homogenates prepared from PD patients, as well as from the BA24 region of DLB or PD patients and non-diseased controls, revealed no differences in levels of aSyn mRNA or protein among the different samples. Our observation that aSyn protein levels were not increased in PD cortex or BA24 region implies (as one possibility) that aSyn neuropathology may not have progressed to these brain regions in this cohort of patients.
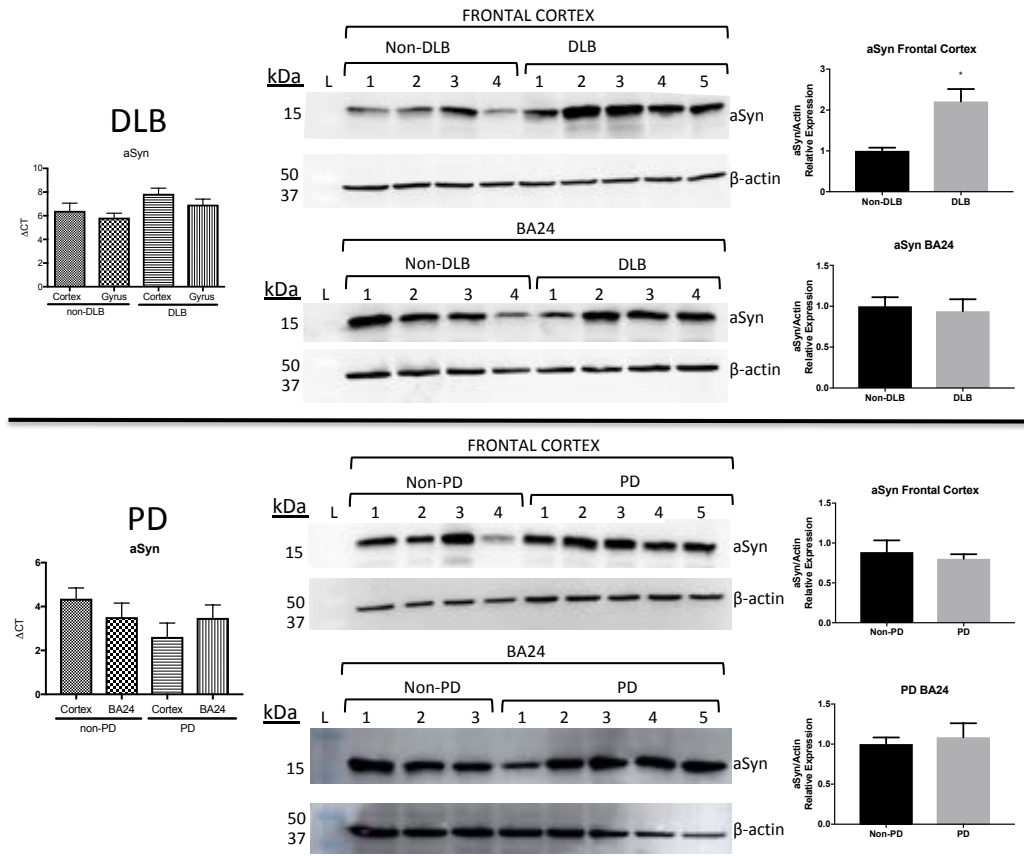
Figure 4.6. aSyn mRNA and protein levels in DLB and PD brains. Samples of frontal cortex and the BA24 region from DLB and PD patients and age-matched controls (Mass. General cohort) were homogenized and examined for levels of aSyn mRNA or protein. The mass of tissue homogenized was 10 mg for mRNA and protein analysis. Left panels: aSyn mRNA levels assessed via qRT-PCR by determining ΔCT values using the housekeeping gene GAPDH as the reference. Middle panel: Images of Western blots probed for human aSyn (LB509) and β-actin. Right panel: Bar graphs showing relative expression levels of aSyn in each brain region determined via densitometric analysis of band intensities. aSyn levels were normalized to the corresponding β-actin signal and divided by the mean value obtained for control samples. The data are presented as the mean ± SEM, n = 3-5, *p < 0.05, Mann-Whitney test.

Next, PK-treated cortical brain sections from DLB patients and non-DLB controls were stained for aSyn or DJ-1 in order to compare the two proteins in terms of their distribution in the diseased brain tissue. Stained sections from DLB patients (but not controls) were found to contain punctate structures with intense aSyn or DJ-1 immunoreactivity throughout the tissue (Fig. 4.7). These results suggested that aSyn and DJ-1 are both recruited into Lewy-like structures in DLB cortex.
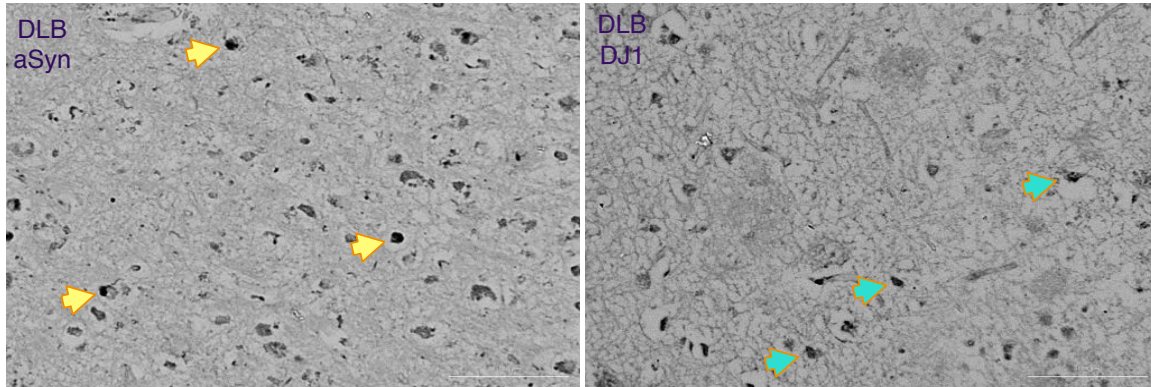
Figure 4.7. Evidence of aSyn and DJ-1 immunoreactivity associated with Lewy-like inclusions in DLB cortex. The distribution of aSyn and DJ-1 in cortical sections from DLB patients (Mass. General cohort) was examined via immunohistochemical analysis using a method involving antigen retrieval with sequential sodium citrate and proteinase K treatments, followed by visualization of the stain with DAB. The images show evidence of Lewy-like inclusions staining positive for aSyn (left, yellow arrows) or DJ-1 (right, green arrows) in DLB cortex. Images were taken with an automated Cytation 3 Cell Imaging Reader (BioTek) at 20X magnification under bright-field illumination.

Our observation that similar patterns of punctate immunoreactivity were observed in DLB cortical sections stained for aSyn or DJ-1 and visualized by DAB (Fig. 4.7) suggested that DJ-1 – and potentially other neuroprotective proteins – might be recruited into aSyn$^+$ aggregated structures in diseased brain tissue. To address this hypothesis, PK-treated cortical brain sections from DLB and PD patients were co-stained with antibodies specific for human aSyn (LB509) and DJ-1, MsrA, PGC1α, or ATP13A2 and imaged via confocal microscopy. The results indicated that human aSyn was co-localized with the candidate neuroprotective proteins in small punctate foci (DJ-1, ATP13A2) or larger inclusions (MsrA, PGC1α) in both DLB and PD sections (Fig. 4.8).
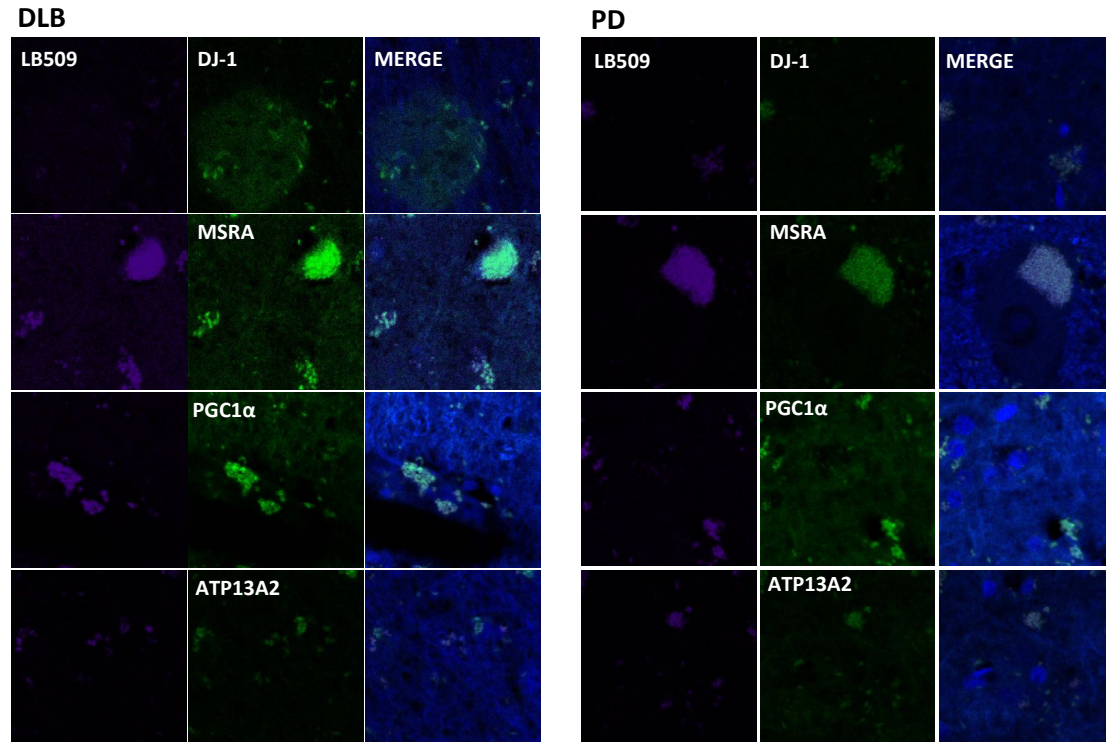
Figure 4.8. Neuroprotective proteins co-localize with aggregated (PK-resistant) human aSyn in cortical sections from DLB and PD brains. The distribution of human aSyn (LB509, purple signal) and DJ-1, MsrA, PGC1α, or ATP13A2 (green signal) was examined in PK-treated cortical sections from patients with DLB (left panels) or PD (right panels) (Mass. General cohort) via fluorescent immunohistochemical analysis. The images show co-localization of neuroprotective proteins with human aSyn in small puncta (DJ-1, ATP13A2) or larger inclusions (MsrA, PGC1α). Images were taken at 20X magnification using a Nikon A1 confocal microscope.

Next, we examined whether the candidate neuroprotective proteins were co-localized with aSyn-pSer129[+] aggregates in diseased brain tissue. Cortical brain sections from DLB and PD patients and from non-diseased controls were co-stained with antibodies specific for aSyn-pSer129 (81A) and DJ-1, MsrA, PGC1α, or ATP13A2 and imaged via confocal microscopy. The results indicated that the aSyn-pSer129 stain was very faint in control sections in comparison to DLB or PD sections, where punctate aSyn-pSer129 immunoreactivity was evident throughout the entire tissue (Fig. 4.9). DJ-1, MsrA, PGC1α, and ATP13A2 were found to co-localize with punctate structures that stained positive for aSyn-pSer129, further supporting the idea that the neuroprotective proteins might be recruited into structures containing aSyn aggregates in diseased brain tissue.
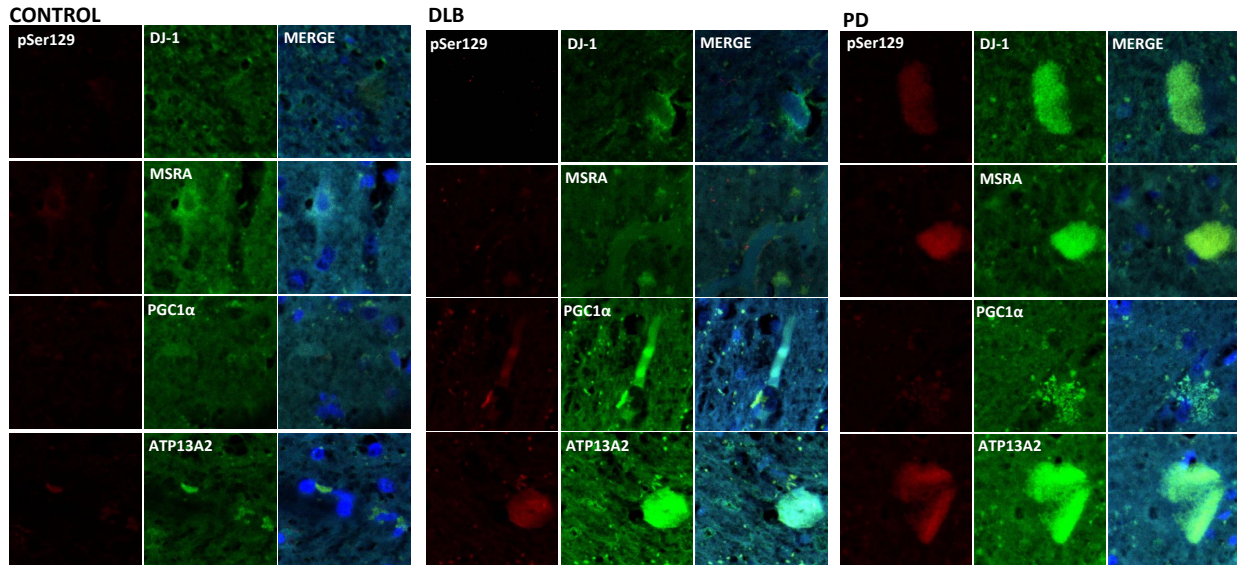
Figure 4.9. Neuroprotective proteins co-localize with aggregated (pSer129$^+$) aSyn in cortical sections from DLB and PD brains. The distribution of aSyn-pSer129 81A, (red signal) and DJ-1, MsrA, PGC1α, and ATP13A2 (green signal) was examined in cortical sections from non-diseased controls (left panels) or patients with DLB (middle panels) or PD (right panels) (Mass. General cohort) via fluorescent immunohistochemical analysis. The images show co-localization of neuroprotective proteins with human aSyn in small puncta or larger inclusions. Images were taken at 20X magnification using a Nikon A1 confocal microscope.

4.4   Discussion and Conclusion

A key result in our study was the demonstration that mRNAs encoding DJ-1, MsrA, and ATP13A2 were significantly up-regulated, and PGC1 mRNA levels showed a trend towards being increased, in cortical homogenates from DLB patients versus non-diseased controls in the Mass. General cohort (Table 4.4). This finding suggests that cellular factors involved in a range of neuroprotective mechanisms, including rescue of mitochondrial deficits, suppression of oxidative stress, repair of oxidatively damaged proteins, inhibition of protein aggregation, and lysosomal autophagy are activated in DLB cortex. The activation of these protective responses could potentially occur via the triggering of cellular signaling pathways by toxic phenomena characteristic of the diseased brain tissue, including ROS accumulation and aSyn neuropathology. A strategy that can prove the activation of subcellular mechanisms of protection could be by analyzing organelles integrity using specific markers, such us mitochondrial or lysosomal markers.

The fact that the increase in levels of neuroprotective mRNA in DLB cortex did not result in a corresponding up-regulation of the encoded proteins (aside from a non-significant trend towards an increase in levels of DJ-1 and PGC1α) could reflect a limitation in the power of our Western blotting method. Alternatively, the predicted increase in encoded neuroprotective proteins based on mRNA levels may have been offset by a loss of protein detectable via Western blotting through mechanisms such as enhanced protein degradation or aggregation as a result of post-translational modifications. In support of this idea, all four neuroprotective proteins were found to co-localize with Lewy bodies or Lewy neurites in DLB cortex, and we showed in previous studies that DJ-1 oxidation can promote the protein's misfolding and aggregation[17,18].

The evidence presented here that DJ-1 and ATP13A2 are detectable in Lewy bodies and other aSyn[+] aggregates is consistent with previous reports[19–22]. Moreover, our observation that MsrA and PGC1α co-localize with aggregated aSyn is a new finding. Some neuroprotective proteins may be sequestered into Lewy bodies as a result of their direct interaction with aggregated aSyn. For example, such interactions could be associated with a molecular chaperone function or with the repair of oxidatively damaged methionine residues in the case of DJ-1 and MsrA, respectively[14,23]. Alternatively, other proteins that are not known to interact directly with aSyn, including PGC1α and ATP13A2, may be recruited into Lewy bodies adventitiously (e.g. ATP13A2 may localize to Lewy bodies that have formed around lysosomes[20]).

In addition to the prefrontal cortex, the BA24 region is a key area of neuropathology in the brains of DLB patients[24]. The BA24 region includes most of the anterior cingulate gyrus, a component of the limbic system. Our data did not show significant changes in the expression of candidate neuroprotective proteins at the mRNA or protein level in the BA24 region from DLB patients, except for a significant decrease in ATP13A2 protein levels (Table 4.2). This finding suggests that DLB is characterized by molecular variability when comparing different brain regions, in this case the frontal cortex and the BA24 region encompassing the cingulate gyrus, and the neuropathology found in each

region may have different origins. In support of this interpretation, we found that aSyn protein levels were increased in the frontal cortex, but not the BA24 region, of DLB patients versus non-diseased controls. Additional support for this idea could be obtained by characterizing aSyn neuropathology in brain sections containing the BA24 region from this cohort of patients via IHC. Our observation that ATP13A2 protein levels were significantly reduced in the BA24 region of DLB patients relative to non-diseased controls is consistent with previously reported findings[19], and implies that a defect in lysosomal function (e.g. autophagy) could contribute to disease pathogenesis in the limbic system[15,20,25,26]. Our finding that ATP13A2 protein levels were decreased despite the fact that ATP13A2 mRNA levels were unchanged (and even showed a trend towards being increased) in the BA24 region of DLB patients versus non-diseased controls suggests that the ATP13A2 protein was down-regulated in the DLB BA24 region via a post-transcriptional mechanism.

Despite the fact that the frontal cortex is a site of neuropathology in PD brain[27], the up-regulation of neuroprotective mRNAs observed in DLB cortex from the Mass General cohort was not replicated in cortical samples from our cohort of PD patients. This finding highlights for the first time a difference in the induction of neuroprotective mechanisms in DLB versus PD cortex. A potential reason for this difference between our cohorts of DLB and PD patients is that the neuropathological features presumably involved in inducing the observed neuroprotective response in DLB cortex are absent in our PD cortical samples. Consistent with this idea, we found that the increase in aSyn protein levels observed in DLB cortex was not replicated in cortical homogenates from our cohort of PD patients, potentially because aSyn neuropathology had not progressed to the latest stage of the disease (Braak stage 6) in these individuals. Accordingly, it is possible that an up-regulation of neuroprotective mRNAs similar to that observed in DLB cortex occurs in more severely affected areas in PD brain, including the SN. This hypothesis could be addressed by examining nigral mRNA levels, as well as by characterizing aSyn neuropathology in cortical and nigral sections, from our cohort of PD patients. The results of these analyses could provide additional support for the concept that molecular perturbations in synucleinopathy diseases differ among different brain regions.

The absence of significant changes in neuroprotective genes and proteins in PD cortical samples versus the cortical genetic changes observed in DLB patients can be related with differences in the pathway of progression of Lewy pathology between DLB and PD. Our findings suggest that pathology in DLB reached fast and mainly cortical areas maybe using the olfactory bulb progression pathway[28,29]. While, PD samples that follow the brain stem progression pathway or Braak staging, will show neuropathology in mainly midbrain areas. These conclusions can be achieved by analyzing other areas in the brain in order to contrast genetic changes with Lewy pathology progression.

Additional insights about the analysis of altered gene expression in DLB brains can be the formation of different stains of aSyn fibrils, which can be generated by exposure to exogenous pathogens and has shown different neurotoxic phenotypes in different brain regions[30,31]. Also, the overlapping with AD pathology could play a role in differential gene expression[28], which can be analyzed by examining, via IHC, tau and Aβ deposits distribution together with neuroprotective genes.

The up-regulation of neuroprotective mRNAs observed in DLB cortex from the Mass General cohort was not replicated in cortical samples from the French cohort of DLB patients. This unexpected finding suggests that there were differences in cortical neuropathology between the two sets of DLB patients. These differences could be a result of hetereogeneity of neuropathology among the different cohorts, or they could reflect the fact that the disease progressed to different stages in the two sets of patients. Although in principle we could distinguish between these scenarios by examining aSyn levels and neuropathology in DLB cortex from the French cohort, unfortunately the cortical homogenates and sections needed for these types of analyses are unavailable. Additional studies with samples obtained from DLB and PD patients at different stages of disease progression could lead to the discovery of neuroprotective responses in brain regions that failed to show such responses in the current study, including the BA24 region in DLB patients and the frontal cortex in PD patients.

In summary, our study led to the finding that a panel of neuroprotective mRNAs are up-regulated (or show a trend towards being upregulated) in DLB cortex, and it yielded insight into disease pathways (e.g. mitochondrial dysfunction, autophagic impairment, protein oxidation and aggregation) that appear to be ineffectively countered because of a failure to produce the corresponding encoded neuroprotective proteins. Based on evidence that DJ-1[32], PGC1α[33], MsrA[14], and ATP13A2[34] alleviate neurodegeneration in PD and that they are not significantly up-regulated at the protein level in the brains of DLB or PD patients as reported here, increasing the expression of these proteins may be a viable therapeutic strategy for both synucleinopathy diseases. A goal of future studies will be to further characterize protective effects of these proteins against aSyn neurotoxicity in preclinical models of DLB and PD. Finally, the results reported here could contribute towards the determination of a DLB-specific genetic profile in post-mortem brain and perhaps also in peripheral biofluids (e.g. blood, CSF). Such a profile could be used for more accurate diagnosis and, in the case of biofluid markers, to monitor disease progression.

Table 4.4 Trends of expression of aSyn and neuroprotective genes in DLB and PD post- mortem brains (Mass. General cohort)

GENE	mRNA				Protein			
	DLB		PD		DLB		PD	
	FC	BA24	FC	BA24	FC	BA24	FC	BA24
aSYN	↓	=	↑	=	↑*	=	=	=
DJ-1	↑*	↓	↓	↓	↑	=	=	↓
MsrA	↑**	=	↓	=	=	↑	=	=
PGC1α	↑	=	=	=	↑	↓	↓	=
ATP13A2	↑*	↑	↓	↓	=	↓*	=	↓

4.5 List of references

1.   Nussbaum, R. L. Genetics of Synucleinopathies. *Cold Spring Harb. Perspect. Med.* **8**, a024109 (2018).

2. Wakabayashi, K., Tanji, K., Odagiri, S., Miki, Y., Mori, F. & Takahashi, H. The Lewy body in Parkinson's disease and related neurodegenerative disorders. *Mol. Neurobiol.* **47**, 495–508 (2013).

3. Jowaed, A., Schmitt, I., Kaut, O. & Wüllner, U. Methylation regulates alpha-synuclein expression and is decreased in Parkinson's disease patients' brains. *J. Neurosci.* **30**, 6355–9 (2010).

4. Desplats, P., Spencer, B., Coffee, E., Patel, P., Michael, S., Patrick, C., Adame, A., Rockenstein, E. & Masliah, E. Alpha-synuclein sequesters Dnmt1 from the nucleus: a novel mechanism for epigenetic alterations in Lewy body diseases. *J. Biol. Chem.* **286**, 9031–7 (2011).

5. Chestnut, B. A., Chang, Q., Price, A., Lesuisse, C., Wong, M. & Martin, L. J. Epigenetic regulation of motor neuron cell death through DNA methylation. *J. Neurosci.* **31**, 16619–36 (2011).

6. Baptista, M. J., O'Farrell, C., Daya, S., Ahmad, R., Miller, D. W., Hardy, J., Farrer, M. J. & Cookson, M. R. Co-ordinate transcriptional regulation of dopamine synthesis genes by alpha-synuclein in human neuroblastoma cell lines. *J. Neurochem.* **85**, 957–68 (2003).

7. Henchcliffe, C., Dodel, R. & Beal, M. F. Biomarkers of Parkinson's disease and Dementia with Lewy bodies. *Prog. Neurobiol.* **95**, 601–613 (2011).

8. Bonifati, V. Recent advances in the genetics of dementia with lewy bodies. *Curr. Neurol. Neurosci. Rep.* **8**, 187–9 (2008).

9. Bras, J., Guerreiro, R., Darwent, L., Parkkinen, L., Ansorge, O., Escott-Price, V., Hernandez, D. G., Nalls, M. A., Clark, L. N., Honig, L. S., Marder, K., Van Der Flier, W. M., Lemstra, A., Scheltens, P., Rogaeva, E. *et al.* Genetic analysis implicates APOE, SNCA and suggests lysosomal dysfunction in the etiology of dementia with Lewy bodies. *Hum. Mol. Genet.* **23**, 6139–46 (2014).

10. Parnetti, L., Tiraboschi, P., Lanari, A., Peducci, M., Padiglioni, C., D'Amore, C., Pierguidi, L., Tambasco, N., Rossi, A. & Calabresi, P. Cerebrospinal Fluid Biomarkers in Parkinson's Disease with Dementia and Dementia with Lewy Bodies. *Biol. Psychiatry* **64**, 850–855 (2008).

11. Jellinger, K. A. Dementia with Lewy bodies and Parkinson's disease-dementia: current concepts and controversies. *J. Neural Transm.* **125**, 615–650 (2018).

12. Canet-Avilés, R. M., Wilson, M. A., Miller, D. W., Ahmad, R., McLendon, C., Bandyopadhyay, S., Baptista, M. J., Ringe, D., Petsko, G. A. & Cookson, M. R. The Parkinson's disease protein DJ-1 is neuroprotective due to cysteine-sulfinic acid-driven mitochondrial localization. *Proc. Natl. Acad. Sci. U. S. A.* **101**, 9103–8 (2004).

13. Siddiqui, A., Chinta, S. J., Mallajosyula, J. K., Rajagopolan, S., Hanson, I., Rane, A., Melov, S. & Andersen, J. K. Selective binding of nuclear alpha-synuclein to the PGC1alpha promoter under conditions of oxidative stress may contribute to losses in mitochondrial function: implications for Parkinson's disease. *Free Radic. Biol. Med.* **53**, 993–1003 (2012).

14. Liu, F., Hindupur, J., Nguyen, J. L., Ruf, K. J., Zhu, J., Schieler, J. L., Bonham, C. C., Wood, K. V, Davisson, V. J. & Rochet, J.-C. Methionine sulfoxide reductase A protects dopaminergic cells from Parkinson's disease-related insults. *Free Radic. Biol. Med.* **45**, 242–55 (2008).

15. Usenovic, M., Tresse, E., Mazzulli, J. R., Taylor, J. P. & Krainc, D. Deficiency of ATP13A2 leads to lysosomal dysfunction, α-synuclein accumulation, and neurotoxicity. *J. Neurosci.* **32**, 4240–6 (2012).

16. Rochet, J.-C., Hay, B. A. & Guo, M. Molecular Insights into Parkinson's Disease. in *Progress in molecular biology and translational science* **107**, 125–188 (2012).

17. John D. Hulleman, ‡, Hamid Mirzaei, §,∇,#, Emmanuel Guigard, ‖,#, Kellie L. Taylor, ‡,#, Soumya S. Ray, ⊥, Cyril M. Kay, ‖, Fred E. Regnier, § and & Jean-Christophe Rochet*, ‡. Destabilization of DJ-1 by Familial Substitution and Oxidative Modifications: Implications for Parkinson's Disease†. (2007). doi:10.1021/BI7001778

18. Madian, A. G., Hindupur, J., Hulleman, J. D., Diaz-Maldonado, N., Mishra, V. R., Guigard, E., Kay, C. M., Rochet, J.-C. & Regnier, F. E. Effect of Single Amino Acid Substitution on Oxidative Modifications of the Parkinson's Disease-Related Protein, DJ-1. *Mol. Cell. Proteomics* **11**, M111.010892 (2012).

19. Murphy, K. E., Cottle, L., Gysbers, A. M., Cooper, A. A. & Halliday, G. M. ATP13A2 (PARK9) protein levels are reduced in brain tissue of cases with Lewy bodies. *Acta Neuropathol. Commun.* **1**, 11 (2013).

20. Dehay, B., Ramirez, A., Martinez-Vicente, M., Perier, C., Canron, M.-H., Doudnikoff, E., Vital, A., Vila, M., Klein, C. & Bezard, E. Loss of P-type ATPase ATP13A2/PARK9 function induces general lysosomal deficiency and leads to Parkinson disease neurodegeneration. *Proc. Natl. Acad. Sci.* **109**, 9611–9616 (2012).

21. Bandopadhyay, R., Kingsbury, A. E., Cookson, M. R., Reid, A. R., Evans, I. M., Hope, A. D., Pittman, A. M., Lashley, T., Canet-Aviles, R., Miller, D. W., McLendon, C., Strand, C., Leonard, A. J., Abou-Sleiman, P. M., Healy, D. G. *et al.* The expression of DJ-1 (PARK7) in normal human CNS and idiopathic Parkinson's disease. *Brain* **127**, 420–430 (2004).

22. Saito, Y., Miyasaka, T., Hatsuta, H., Takahashi-Niki, K., Hayashi, K., Mita, Y., Kusano-Arai, O., Iwanari, H., Ariga, H., Hamakubo, T., Yoshida, Y., Niki, E., Murayama, S., Ihara, Y. & Noguchi, N. Immunostaining of oxidized DJ-1 in human and mouse brains. *J. Neuropathol. Exp. Neurol.* **73**, 714–28 (2014).

23. Zhou, W., Zhu, M., Wilson, M. A., Petsko, G. A. & Fink, A. L. The oxidation state of DJ-1 regulates its chaperone activity toward alpha-synuclein. *J. Mol. Biol.* **356**, 1036–48 (2006).

24. McKeith, I. G., Boeve, B. F., Dickson, D. W., Halliday, G., Taylor, J.-P., Weintraub, D., Aarsland, D., Galvin, J., Attems, J., Ballard, C. G., Bayston, A., Beach, T. G., Blanc, F., Bohnen, N., Bonanni, L. *et al.* Diagnosis and management of dementia with Lewy bodies: Fourth consensus report of the DLB Consortium. *Neurology* **89**, 88–100 (2017).

25. Gusdon, A. M., Zhu, J., Van Houten, B. & Chu, C. T. ATP13A2 regulates mitochondrial bioenergetics through macroautophagy. *Neurobiol. Dis.* **45**, 962–972 (2012).

26. Kett, L. R., Stiller, B., Bernath, M. M., Tasset, I., Blesa, J., Jackson-Lewis, V., Chan, R. B., Zhou, B., Di Paolo, G., Przedborski, S., Cuervo, A. M. & Dauer, W. T. -Synuclein-Independent Histopathological and Motor Deficits in Mice Lacking the Endolysosomal Parkinsonism Protein Atp13a2. *J. Neurosci.* **35**, 5724–5742 (2015).

27. Horvath, J., Herrmann, F. R., Burkhard, P. R., Bouras, C. & Kövari, E. Neuropathology of dementia in a large cohort of patients with Parkinson's disease. *Parkinsonism Relat. Disord.* **19**, 864–868 (2013).

28.   Marui, W., Iseki, E., Nakai, T., Miura, S., Kato, M., Uéda, K. & Kosaka, K. Progression and staging of Lewy pathology in brains from patients with dementia with Lewy bodies. *J. Neurol. Sci.* **195**, 153–9 (2002).

29.   Cersosimo, M. G. Propagation of alpha-synuclein pathology from the olfactory bulb: possible role in the pathogenesis of dementia with Lewy bodies. *Cell Tissue Res.* **373**, 233–243 (2018).

30.   Kim, C., Lv, G., Lee, J. S., Jung, B. C., Masuda-Suzukake, M., Hong, C.-S., Valera, E., Lee, H.-J., Paik, S. R., Hasegawa, M., Masliah, E., Eliezer, D. & Lee, S.-J. Exposure to bacterial endotoxin generates a distinct strain of α-synuclein fibril. *Sci. Rep.* **6**, 30891 (2016).

31.   Peelaerts, W., Bousset, L., Van der Perren, A., Moskalyuk, A., Pulizzi, R., Giugliano, M., Van den Haute, C., Melki, R. & Baekelandt, V. α-Synuclein strains cause distinct synucleinopathies after local and systemic administration. *Nature* **522**, 340–344 (2015).

32.   Liu, F., Nguyen, J. L., Hulleman, J. D., Li, L. & Rochet, J.-C. Mechanisms of DJ-1 neuroprotection in a cellular model of Parkinson's disease. *J. Neurochem.* **105**, 2435–2453 (2008).

33.   Corona, J. C. & Duchen, M. R. PPARγ and PGC-1α as Therapeutic Targets in Parkinson's. *Neurochem. Res.* **40**, 308–316 (2015).

34.   Rochet, J.-C. New insights into lysosomal dysfunction in parkinson's disease: An emerging role for ATP13A2. *Mov. Disord.* **27**, 1092–1092 (2012).

CHAPTER 5. DISCUSSION

5.1   Summary of research

Understanding the pathological mechanisms of synucleinopathies can lead to the discovery of new drug targets that control the progression of neurodegeneration. This research project was aimed at investigating different molecular aspects of two major synucleinopathies, DLB and PD, in order to obtain insights into pathological mechanisms, as a first step towards identifying potential therapies that in combination could stop neuronal loss and Lewy pathology.

Current medications used for synucleinopathies are effective in controlling the immediate symptoms of synucleinopathy diseases, but there is no cure or therapy that can stop the underlying neurodegeneration. Intense efforts to find drugs or endogenous molecules that can stop neuronal death have led to the identification of compounds and proteins that could potentially improve neuronal viability. As part of this research, we established an optimized protocol for the preparation of primary neuronal cultures that can be used to test the efficacy and specificity of several compounds and proteins predicted to have neuroprotective activity against PD-related insults. Information about the ability of neuroprotective compounds and proteins to promote cell viability and neurite outgrowth will advance our understanding of mechanisms by which these agents attenuate neurodegeneration, as well as set the stage for further investigations of their neuroprotective activity *in vivo*.

The complexity of synuclein-related diseases seems to reflect the diverse neurotoxic mechanisms of aSyn[1]. Characterizing the effects of expressing aSyn mutants in *in vivo* PD models is a good strategy to establish a connection between behavioral impairments and neurotoxic mechanisms related to membrane-induced aSyn aggregation and aSyn-mediated membrane permeabilization. Here, we report the first investigation of the familial aSyn mutant A53E in an *in vivo* PD model. Key phenotypic outcomes of A53E-expressing rats, including the early emergence of behavioral impairment, the presence of severe striatal lesions, pronounced DA neuron death, and the presence of Lewy-body like pathology in

surviving neurons, highlight the neurotoxicity elicited by aSyn-A53E. Analysis of the distribution of A53E among different subcellular fractions provided clues about A53E association to cellular membranes and the protein's prion-like behavior involved in spreading to other parts of the brain. Previous reports indicated that A53E aggregation was delayed compared to WT and A53T[2], and that cultured A53E-expressing cells were sensitized to toxicity in the presence of PD-related insults due to an accumulation of aSyn-A53E oligomers[3]. Differences in the aggregation propensity of aSyn-A53E compared to aSyn-WT or -A53T may be reflected by the less compact nature of A53E Lewy body-like structures that could potentially result from the assembly of oligomers during early stages of Lewy body formation (and these less compact assemblies may be more toxic than Lewy bodies themselves[4]). Further investigation of the effects of A53E expression *in vivo* is necessary in order to understand the impact of this variant on other PD-related pathological outcomes such us neuroinflammation, glial cell activation, and the integrity of organelles such as Golgi bodies and mitochondria[5]. Our ongoing studies of aSyn-expressing rats could reveal potential therapeutic targets to stop neurotoxicity elicited not only by A53E, but also by other aSyn mutants found in familial PD.

The lack of specific molecular diagnostics that can distinguish DLB from PD is a major problem in developing strategies to prevent or treat these diseases. In general, both synucleinopathies are diagnosed when motor symptoms appear, a time at which neurodegeneration is already well advanced. Establishing a peripheral gene expression profile that differentiates DLB from PD could facilitate diagnosis, thereby making it feasible to implement strategies to delay the onset of neurodegeneration. In addition, analyzing the expression levels of neuroprotective proteins in DLB and PD could advance our understanding of cellular mechanisms affected in these diseases. Here, we present the first evidence of differences in genetic changes that occur in the brains of patients affected by these two related synucleinopathies. Strikingly, genes that are reported to have neuroprotective effects in PD or PD models (DJ-1, MsrA, PGC1α, and ATP13A2) were found to be up-regulated at the mRNA level in the frontal cortex of patients with DLB but not PD, suggesting that mechanisms of neuroprotection differ between these two synucleinopathies. These data set the stage for further expression analysis in other parts of

the brain, and also for studies aimed at elucidating neuroprotective mechanisms in a cellular DLB model. We believe that our expression studies in synucleinopathies will open windows of investigation to identify peripheral biomarkers and develop treatments for these diseases.

5.2   Future directions

5.2.1   Optimization of primary cultures for the study of cortical neuropathologies

Our lab is already testing our optimized primary cell culture protocol in order to establish suitable cultures for the investigation of cortical pathologies such as DLB or schizophrenia. Currently, we are exploring different ways to determine neuron viability in cultures exposed to neurotoxicants or to aSyn preformed fibrils. Our goal is to develop robust neurotoxicity assays in these cultures that can be used to test the pro-survival effects of candidate neuroprotective proteins and elucidate cortical signaling mechanisms that could be targeted for therapy.

5.2.2   Primary midbrain cultures from aSyn knockout rats

A goal of our future studies will be to develop an *in vitro* aSyn knockout model using our versatile primaries culture protocol. The loss of aSyn gene activity in an *in vitro* midbrain PD model would enable us to examine the neurotoxic effects of over-expressed aSyn variants in the absence of the endogenous rat protein and to address the role of aSyn in DA cell death elicited by other PD-related insults (e.g. environmental toxicants). Data obtained from experiments carried out in an aSyn knockout *in vitro* model would support future *in vivo* assays aimed at testing the role of aSyn in PD-related neurodegeneration triggered by different stresses.

5.2.3   Optimization of glial cell growth control

The complexity of synucleinopathies is evident in the diverse cellular pathology that characterizes these diseases. It is necessary to consider that neudegenerative disorders involve pathology in the complete cellular system found in the brain, and the tight

association and interaction of different types of brain cells play an important role in the development of CNS disorders. Our primary cell culture model offers the opportunity to modulate the density of glial cells that grow along with the neuronal population. Compounds such as Ara-C can be used to modulate the division rate of glial cells, thus balancing astrocytic, microglial, and neuronal populations. One problem is that glial cells are very sensitive to small changes in Ara-C concentrations, and small changes in the glial cell population can affect neurotoxic treatments that depend on compound metabolism mediated by glia. Currently, we are investigating different media formulations that can be used to control the overgrowth of glial cells, without affecting the neuronal population. In the future, we aim to develop flexible *in vitro* protocols that can be adjusted for different experimental requirements, thus expanding the range of investigations that can be undertaken to contribute to ongoing efforts to identify therapeutic targets for brain diseases.

5.2.4   Determine *in vivo* neuropathology of other aSyn variants

Our group[6] and others[7,8] found that aSyn familial mutations disrupt protein-membrane association, leading to enhanced aSyn aggregation and neurotoxicity. A30P and G51D are two aSyn mutants found not only in familial PD, but also in genetic cases of DLB and MSA[9–11]. The study of aSyn familial mutants such as A30P and G51D in our *in vivo* model will yield insight into the role of membrane-induced aSyn aggregation in the pathogenesis of several synucleinopathies. Our future experiments will focus on the characterization of neurotoxic effects caused by various familial aSyn mutants advance our understanding of the link between neuropathology and behavioral deficits. Moreover, optimized *in vivo* models involving the over-expression of different aSyn variants will serve as a powerful tool to test neuroprotective effects of small molecules and endogenous proteins.

5.2.5 Standardization of non-invasive imaging protocols that can be used to monitor the progression of neuropathology

Much of the information gathered to determine the causes of PD originates from end-point analysis of neuropathology in preclinical models and post-mortem analysis of human PD brains. Therefore, the exact origin and progressive neuropathological details of PD are still unclear. Studies of the progression of neuropathology and behavioral impairment in synucleinopathy disorders require non-invasive strategies that allow one to establish a connection between the beginning of neurodegeneration and behavioral decay. Diagnostic tests commonly used to determine the severity of disease in PD cases are useful to investigate aSyn-mediated neurodegeneration in preclinical models[12]. We propose to monitor neurodegeneration in our rat rAAV-aSyn model via positron emission tomography (PET) using a radiotracer that binds to the dopamine transporter (DAT) in order to perform non-invasive periodical evaluation of neuronal loss concomitant with behavioral tests[13]. This approach will allow us to (i) determine differences in the origin of neurodegeneration among different aSyn variants, and ii) screen neuroprotective compounds or proteins as potential therapies against aSyn toxicity.

5.2.6 Effects of candidate neuroprotective proteins against aSyn toxicity *in vivo*

A major focus of our laboratory is the discovery of potential neuroprotective proteins that can prevent aSyn-mediated neuronal death. Evidence from our group and others suggest that neurotoxic aSyn aggregation depend on aberrant interactions between aSyn and lipid membranes[6,14–17]. Endosulfine-alpha (ENSA), a cAMP-regulated phosphoprotein expressed in the CNS, interacts with aSyn at the surface of phospholipid membranes[18]. In addition, ENSA expression has been found to be down-regulated in some neurodegenerative diseases, including AD and DLB[15,19,20]. Recent studies from our group revealed neuroprotective effects of ENSA against toxicity elicited by the familial aSyn mutants A30P and G51D in primary midbrain cultures[15]. As a future direction, we propose *in vivo* experiments in order to validate ENSA as a target for PD therapy. Ongoing experiments aim to determine the neuroprotective effects of co-expressing ENSA in rats overexpressing human WT aSyn. An additional goal is to characterize

neuropathological outcomes related to ENSA down-regulation as observed in synucleinopathy disorders, in order to validate this protein as a target for PD treatment.

5.2.7 Determine effects of expressing candidate protective proteins against aSyn neurotoxicity

Previous studies from our group led to the characterization of neuroprotective effects of DJ-1, MsrA, PGC1α, and ATP13A2 against toxicity elicited by the familial aSyn mutant A53T[21–24]. Results from this thesis project indicate that these neuroprotective genes are expressed differently in the brains of patients affected by different synucleinopathies. Future studies are needed to determine the effects of neuroprotective genes against toxicity elicited by other aSyn familial mutants. We suggest the use of our optimized primary midbrain cultures as well as human iPSC-derived neurons as *in vitro* DLB and PD models to enable differentiation of the most effective neuroprotective mechanisms in each of these two synucleinopathies. Results from these experiments could lead to the identification of common therapeutic targets for neuropathology elicited by all known familial aSyn mutants.

5.3 List of References

1. Goedert, M. Alpha-synuclein and neurodegenerative diseases. *Nat. Rev. Neurosci.* **2**, 492–501 (2001).

2. Ghosh, D., Sahay, S., Ranjan, P., Salot, S., Mohite, G. M., Singh, P. K., Dwivedi, S., Carvalho, E., Banerjee, R., Kumar, A. & Maji, S. K. The Newly Discovered Parkinson's Disease Associated Finnish Mutation (A53E) Attenuates α-Synuclein Aggregation and Membrane Binding. *Biochemistry* **53**, 6419–6421 (2014).

3. Mohite, G. M., Navalkar, A., Kumar, R., Mehra, S., Das, S., Gadhe, L. G., Ghosh, D., Alias, B., Chandrawanshi, V., Ramakrishnan, A., Mehra, S. & Maji, S. K. The Familial α-Synuclein A53E Mutation Enhances Cell Death in Response to Environmental Toxins Due to a Larger Population of Oligomers. (2018). doi:10.1021/acs.biochem.8b00321

4. Winner, B., Jappelli, R., Maji, S. K., Desplats, P. A., Boyer, L., Aigner, S., Hetzer, C., Loher, T., Vilar, M., Campioni, S., Tzitzilonis, C., Soragni, A., Jessberger, S., Mira, H., Consiglio, A. *et al.* In vivo demonstration that alpha-synuclein oligomers are toxic. *Proc. Natl. Acad. Sci. U. S. A.* **108**, 4194–9 (2011).

5. Lázaro, D. F., Dias, M. C., Carija, A., Navarro, S., Madaleno, C. S., Tenreiro, S., Ventura, S. & Outeiro, T. F. The effects of the novel A53E alpha-synuclein mutation on its oligomerization and aggregation. *Acta Neuropathol. Commun.* **4**, 128 (2016).

6. Ysselstein, D., Joshi, M., Mishra, V., Griggs, A. M., Asiago, J. M., McCabe, G. P., Stanciu, L. A., Post, C. B. & Rochet, J.-C. Effects of impaired membrane interactions on α-synuclein aggregation and neurotoxicity. *Neurobiol. Dis.* **79**, 150–63 (2015).

7. Lee, H.-J., Choi, C. & Lee, S.-J. Membrane-bound -Synuclein Has a High Aggregation Propensity and the Ability to Seed the Aggregation of the Cytosolic Form. *J. Biol. Chem.* **277**, 671–678 (2002).

8. Flagmeier, P., Meisl, G., Vendruscolo, M., Knowles, T. P. J., Dobson, C. M., Buell, A. K. & Galvagnion, C. Mutations associated with familial Parkinson's disease alter the initiation and amplification steps of α-synuclein aggregation. *Proc. Natl. Acad. Sci.* **113**, 10328–10333 (2016).

9. Kiely, A. P., Asi, Y. T., Kara, E., Limousin, P., Ling, H., Lewis, P., Proukakis, C., Quinn, N., Lees, A. J., Hardy, J., Revesz, T., Houlden, H. & Holton, J. L. α-Synucleinopathy associated with G51D SNCA mutation: a link between Parkinson's disease and multiple system atrophy? *Acta Neuropathol.* **125**, 753–769 (2013).

10. Jie Li, ‡,§, Vladimir N. Uversky, *,‡,§,‖ and & Anthony L. Fink*, §. Effect of Familial Parkinson's Disease Point Mutations A30P and A53T on the Structural Properties, Aggregation, and Fibrillation of Human α-Synuclein†. (2001). doi:10.1021/BI010616G

11. Meeus, B., Theuns, J. & Van Broeckhoven, C. The Genetics of Dementia With Lewy Bodies. *Arch. Neurol.* **69**, 1113–1118 (2012).

12. Wang, J., Zuo, C. T., Jiang, Y. P., Guan, Y. H., Chen, Z. P., Xiang, J. De, Yang, L. Q., Ding, Z. T., Wu, J. J. & Su, H. L. 18F-FP-CIT PET imaging and SPM analysis of dopamine transporters in Parkinson's disease in various Hoehn & Yahr stages. *J. Neurol.* (2007). doi:10.1007/s00415-006-0322-9

13. Van der Perren, A., Toelen, J., Casteels, C., Macchi, F., Van Rompuy, A.-S., Sarre, S., Casadei, N., Nuber, S., Himmelreich, U., Osorio Garcia, M. I., Michotte, Y., D'Hooge, R., Bormans, G., Van Laere, K., Gijsbers, R. *et al.* Longitudinal follow-up and characterization of a robust rat model for Parkinson's disease based on overexpression of alpha-synuclein with adeno-associated viral vectors. *Neurobiol. Aging* **36**, 1543–1558 (2015).

14. Griggs, A. M., Ysselstein, D. & Rochet, J.-C. Role of Aberrant α-Synuclein–Membrane Interactions in Parkinson's Disease. *Bio-nanoimaging* 443–452 (2014). doi:10.1016/B978-0-12-394431-3.00039-0

15. Ysselstein, D., Dehay, B., Costantino, I. M., McCabe, G. P., Frosch, M. P., George, J. M., Bezard, E. & Rochet, J.-C. Endosulfine-alpha inhibits membrane-induced α-synuclein aggregation and protects against α-synuclein neurotoxicity. *Acta Neuropathol. Commun.* **5**, 3 (2017).

16. Pirc, K. & Ulrih, N. P. α-Synuclein interactions with phospholipid model membranes: Key roles for electrostatic interactions and lipid-bilayer structure. *Biochim. Biophys. Acta - Biomembr.* **1848**, 2002–2012 (2015).

17. Lee, H.-J., Choi, C. & Lee, S.-J. Membrane-bound α-Synuclein Has a High Aggregation Propensity and the Ability to Seed the Aggregation of the Cytosolic Form. *J. Biol. Chem.* **277**, 671–678 (2002).

18. Woods, W. S., Boettcher, J. M., Zhou, D. H., Kloepper, K. D., Hartman, K. L., Ladror, D. T., Qi, Z., Rienstra, C. M. & George, J. M. Conformation-specific Binding of -Synuclein to Novel Protein Partners Detected by Phage Display and NMR Spectroscopy. *J. Biol. Chem.* **282**, 34555–34567 (2007).

19. Kim, S. H. & Lubec, G. Brain alpha-endosulfine is manifold decreased in brains from patients with Alzheimer's disease: a tentative marker and drug target? *Neurosci. Lett.* **310**, 77–80 (2001).

20. Peyrollier, K., Héron, L., Virsolvy-Vergine, A., Le Cam, A. & Bataille, D. Alpha endosulfine is a novel molecule, structurally related to a family of phosphoproteins. *Biochem. Biophys. Res. Commun.* **223**, 583–6 (1996).

21. Liu, F., Nguyen, J. L., Hulleman, J. D., Li, L. & Rochet, J.-C. Mechanisms of DJ-1 neuroprotection in a cellular model of Parkinson's disease. *J. Neurochem.* **105**, 2435–2453 (2008).

22. Liu, F., Hindupur, J., Nguyen, J. L., Ruf, K. J., Zhu, J., Schieler, J. L., Bonham, C. C., Wood, K. V, Davisson, V. J. & Rochet, J.-C. Methionine sulfoxide reductase A protects dopaminergic cells from Parkinson's disease-related insults. *Free Radic. Biol. Med.* **45**, 242–55 (2008).

23. Siddiqui, A., Chinta, S. J., Mallajosyula, J. K., Rajagopolan, S., Hanson, I., Rane, A., Melov, S. & Andersen, J. K. Selective binding of nuclear alpha-synuclein to the PGC1alpha promoter under conditions of oxidative stress may contribute to losses in mitochondrial function: implications for Parkinson's disease. *Free Radic. Biol. Med.* **53**, 993–1003 (2012).

24. Gitler, A. D., Chesi, A., Geddie, M. L., Strathearn, K. E., Hamamichi, S., Hill, K. J., Caldwell, K. A., Caldwell, G. A., Cooper, A. A., Rochet, J.-C. & Lindquist, S. α-Synuclein is part of a diverse and highly conserved interaction network that includes PARK9 and manganese toxicity. *Nat. Genet.* **41**, 308–315 (2009).